THE MOLECULAR MECHANISM OF DUODENAL AND PLACENTAL IRON ABSORPTION DURING PREGNANCY

Thesis submitted by
Nita Shantilal Solanky

For the Degree of
Doctor of Philosophy in Biochemistry

University of London
University College London

Department of Biochemistry and Molecular Biology
Royal Free and UCL Medical School
Rowland Hill Street
London NW3 2PF

ProQuest LLC
789 East Eisenhower Parkway
P.O. Box 1346
Ann Arbor, MI 48106-1346

Abstract

During pregnancy duodenal iron absorption, placental transfer, and the release of iron from stores in the mothers liver, are increased to meet the requirements of the developing foetus. The regulatory mechanisms co-ordinating these events are for the first time illustrated here.

Various proteins, notably hepcidin and hfe, have been implicated as having a role in iron homeostasis. By quantitating the expression of *hepcidin* and the duodenal iron transporters: *DMT1, Tfr1, Dcytb* and *Ireg1,* in mice raised on iron-deficient and iron-loaded diets, this study confirms that *hepcidin* expression is positively regulated by body iron status and negatively regulates duodenal *DMT1*. A parallel study in hfe knockout mice, demonstrates inappropriately low *hepcidin* expression and elevated duodenal *DMT1* levels. This provides a possible explanation for the liver iron loading characteristic of hereditary haemochromatosis.

The expression of *hepcidin* is studied in pregnant rats and is shown to decrease during the final trimester when duodenal and placental iron transfer is maximal. This decrease is preceded by a reduction in liver iron stores and subsequent reduction in *hepcidin* expression. Iron supplementation to pregnant dams, increases liver iron status and *hepcidin* expression, this corresponds with a decrease in duodenal and placental *DMT1* expression, whilst iron deficiency during this period, increases both duodenal and placental uptake. This implies that the increase in duodenal iron absorption observed during pregnancy is, at least in part, a consequence of reduced liver iron stores.

Using an *in vitro* model of the placental syncytiotrophoblast, DMT1 is localised to endosomal compartments, but not co-localised with either Tfr1 or Ireg1. Hepcidin is demonstrated to bind to the plasma membrane of these cells and reduce the uptake of diferric-transferrin.

These results provide new insight into the molecular processes of iron homeostasis and implicate a regulatory role for hepcidin, not only in duodenal, but also in placental iron uptake.

For
Pappa, Mummy, Moona, Kalya, Pinku and Dhunya

Acknowledgments

The work reported in this thesis was carried out in the Department of Biochemistry and Molecular Biology at the Royal Free and University College School of Medicine, London, UK and at the Division of Development, Growth and Function, Rowett Research Institute, Aberdeen, Scotland, U.K.. I am grateful to the European Union for financial support, without which this work could not have been performed.

First and foremost, I would like to thank my supervisor Professor Kaila Srai for his supervision and critical review of this work.

I would like to thank fellow members of the Department of Biochemistry for their help and encouragement, specifically, Clare Turner, Monica Mascarenhas and Sachie Yamaji for their motivation, support and friendship. Special thanks go to Henry Bayele for enjoyable discussions and encouragement with the pursuit of new techniques, Tony Michael: the first person to not only make sense of statistical methods but also to make them interesting and to Christine Hall for her super efficiency.

This work would not have been possible without the help from various members of the Rowett Research institute in Aberdeen these include Professor Harry M^{c}Ardle who I would like to thank not only for his supervision of this project but also for helping me in the lab the first time I was left alone with ^{59}Fe and some duodenal rings, Dr Lorraine Gambling for her incredible organisational skills and for all the work she put into giving me the samples I required. Thanks also to Susan and Lyn who were so accommodating of me, and Cedric for helping with the calculations and the Gamma counter. Special thanks go to Ann White for picking me up from the airport, arranging my accommodation, and making my trips to the North run that little bit smoother.

I am grateful to Dr Roberta Ward who made a substantial contribution to this work by providing me with tissue samples, and to Dr Michael Garrick for his generosity and efficiency in providing the DMT1 constructs.

I would also like to thank Dr Edward Debnam for assistance with animal work and his valuable insights obtained by looking at my data from a different perspective. In addition, thanks go to Dr

Robert Simpson and Dr Abas Lafta, for quantification of iron levels and in the case of Abas as a welcome friendly face in the lab!

I received invaluable support from Dr Willem Rens, not only in the use of the super microscope but also for critical review of this thesis. A big Thank You also goes out to Kirty, Jay, Ted, Tricia and Henry for taking time to read the thesis and their encouraging, as well as critical, remarks.

I would also like to thank my friends for their encouragement over the past five years and making me laugh. Especial thanks in this respect goes to the jet-setting disgruntled Princess and Sakiba. I would like to thank Steve for opening the door, having a packed dinner and a smile whenever I finished from the lab at 10pm! To Gustavo for swapping shifts thus allowing me to have a social life and to Tasneem for convincing me to swap Cambridge for London.

Last but by no means least, my thanks go to Kirty for the roof over my head and masses of encouragement, Mita and Willem for their patience and invaluable support throughout the course of this thesis.

Collaborations

Chapter 3.2: Pregnant Wistar rats raised, tissues collected and haematological parameters and liver iron concentration assessed by Dr Roberta Ward[1].

Chapter 3.3.1: Placental RNA provided by Dr Lorraine Gambling[2].

Chapter 3.3.2: Rowett hooded lister rats raised and haematological parameters and liver iron concentration assessed by Dr Lorraine Gambling.

Chapter 3.4.1: Pregnant Wistar rats raised, tissues collected and haematological parameters and liver iron concentration assessed by Dr Roberta Ward.

Chapter 3.4.2: Rowett hooded lister rats raised and haematological parameters and liver iron concentration assessed by Dr Lorraine Gambling.

Chapter 3.4.3: Human Placental tissue collected by Wendy Hollands[3].

Chapter 3.6: DMT1 constructs provided by Dr Michael Garrick[4].

[1] Dr Roberta Ward, Universitè de Louvain, Louvain-la-Neuve, Belgium.

[2] Dr Lorraine Gambling, Rowett Research Institute, Greenburn Road, Bucksburn, Aberdeen, U.K.

[3] Wendy Hollands, Maternity Department of the Norfolk and Norwich University Hospital, Norwich, U.K.

[4] Dr Michael Garrick, University of Buffalo, NY, USA.

Contents

Title Page 1
Abstract 2
Dedication 3
Acknowledgments 4
Contents 7
List of Figures 13
List of Tables 15
Abbreviations 16
1 Background 19
1.1 Importance of iron in biological systems 20
1.1.1 Iron deficiency 20
1.1.2 Iron overload 21
1.1.3 Iron supplementation during pregnancy 21
1.1.3.1 Absorption of other micronutrients 22
1.1.4 Iron requirements 23
1.1.4.1 Iron requirements during pregnancy 23
1.1.4.2 Changes in haematological parameters during pregnancy 24
1.1.5 Distrbution of iron in adults 24
1.2 Duodenal Iron uptake 26
1.2.1 Structure of the duodenum 26
1.2.2 Duodenal Iron uptake: effect of dietary factors 28
1.2.3 The molecular mechanism of duodenal iron uptake 29
1.2.4 Integrin Mobiferrin Paraferritin Pathway 29
1.2.5 Dcytb 30
1.2.6 DMT1 31
1.2.7 Ferritin 35
1.2.8 Ireg1 36
1.2.9 Hephaestin 37
1.2.10 ZIRTL 38
1.3 Regulation of duodenal iron absorption 38

1.3.1 Duodenal iron uptake during pregnancy 38
1.3.2 Duodenal iron uptake in neonates 38
1.3.3 Regulation of iron uptake 39
1.3.4 Regulation by non-specific mechanisms 39
1.3.5 Regulation by dietary iron content and transferrin saturation 39
1.3.6 Regulation by hfe 41
1.3.7 Regulation by IRE-IRP interactions 43
1.3 Circulation of iron in the body 45
1.3.1 Transferrin 45
1.3.2 Tfr1 46
1.3.3 Tfr1 mediated iron uptake 47
1.3.4 Tfr2 49
1.4 Role of the liver in iron homeostasis 50
1.4.1 Ceruloplasmin 52
1.4.2 Hepcidin 52
1.5 Erythropoiesis 55
1.5.1 Erythropoietin 55
1.6 The Placenta 56
1.6.1 Comparison of human and rodent pregnancy 56
1.6.2 Placental structure 57
1.6.3 Placental Iron Transport 60
1.6.4 Regulation of iron transfer by gestational age 62
1.6.5 Regulation of placental iron transfer by maternal iron status 62
1.6.6 Regulation of placental iron transfer by cellular iron levels 63
1.6.7 Expression of Cytokines and Erythropoietin by the placenta 63
1.6.8 NTBI uptake by the placenta 63
1.6.9 Placental transferrin secretion 64
1.7 Aims 64
2 General Methods 66
2.1 Stocks, Solutions, Buffers and Gel Recipes 67
2.2 Methods 72

2.2.1 Animal models 72
2.2.2 Cell Culture 73
2.2.3 Iron uptake assays 74
2.2.3.1 *In vitro* Ferrous Iron Uptake in rat duodenum ('everted loop' method) .75
2.2.3.2 *In vitro* Ferric Iron Uptake in rat duodenum ('ring' method) 75
2.2.4 Protein Quantification 76
2.2.5 Quantitative gene expression 76
2.2.5.1 Tissue Collection and Storage 76
2.2.5.2 RNA extraction (QIAamp RNA Kit) 76
2.2.5.3 RNA extraction (TRIzol reagent) 77
2.2.5.4 Messenger RNA Quantification 77
2.2.5.4.1 Semi quantitative gene expression 78
2.2.5.4.2 Quantitative gene expression (real-time PCR) 81
2.2.5.4.3 cDNA synthesis 81
2.2.5.5 Agarose gel electrophoresis 88
2.2.5.6 Gel extraction of PCR products 88
2.2.5.7 DNA/RNA Quantification 88
2.2.6 SDS gel electrophoresis 89
2.2.7 Western Blotting 89
2.2.8 Iron quantification 90
2.2.9 Statistical analysis 90
2.2.9.1 Comparing two groups of data 90
2.2.9.2 Comparing more than two groups of data 91
3.1 Regulation of duodenal iron absorption 92
3.1.1 Duodenal & hepatic gene expression in C57blk/6 & $hfe^{-/-}$ mice 95
3.1.2 Gene expression in C57blk/6 & $hfe^{-/-}$ mice: effect of dietary iron levels 98
3.1.2.1 Effect of dietary iron deficiency 99
3.1.2.2 Effect of dietary iron loading 99
3.1.3 Duodenal localisation of DMT1: effect of dietary iron content 101
3.1.4 Dcytb protein expression: effect of dietary iron content 103
3.1.5 Discussion 104

3.1.5.1 Possible regulatory mechanisms for intestinal iron absorption 108
3.1.6 Conclusions 110
3.2 Iron metabolism during pregnancy 111
3.2.1 Expression of iron modulator & transporter genes during pregnancy 113
3.2.1.1 Haematological parameters 116
3.2.1.2 Duodenal gene expression during pregnancy 117
3.2.1.3 Hepatic gene expression during pregnancy 118
3.2.1.4 Liver non-haem iron levels during pregnancy 119
3.2.1.5 Placental gene expression during pregnancy 120
3.2.2 Discussion 121
3.2.2.1 Duodenal iron absorption during pregnancy 121
3.2.2.2 Liver iron stores during pregnancy 122
3.2.2.3 Placental iron transfer 123
3.2.3 Conclusions 124
3.3 Iron deficiency during pregnancy 125
3.3.1 Effect of iron deficiency on placental gene expression 126
3.3.2 Effect of iron deficiency on duodenal iron uptake during pregnancy 129
3.3.2.1 Haematological parameters 130
3.3.2.2 Duodenal iron uptake 131
3.3.2.2.1 Duodenal gene expression 132
3.3.2.2.2 Duodenal gene expression in dams at birth 133
3.3.2.2.3 Duodenal gene expression in pups at birth 133
3.3.2.2.4 Duodenal gene expression in 6 week old pups 133
3.3.3 Discussion 135
3.3.3.1 Effect of iron deficiency on duodenal and placental iron transfer 135
3.3.3.1 Neonatal iron absorption 137
3.3.4 Conclusions 138
3.4 Iron Supplementation During Pregnancy 139
3.4.1 Iron supplementation: Effect on gene expression 140
3.4.1.1 Haematological parameters 142
3.4.1.2 Liver Iron Concentration 144

3.4.1.3 Effect of iron supplementation on duodenal gene expression 145
3.4.1.3.1 Duodenal *Dcytb* mRNA expression 145
3.4.1.3.2 Duodenal *DMT1* mRNA expression 146
3.4.1.3.3 Duodenal *Ireg1* mRNA expression 147
3.4.1.4 Effect of iron supplementation on hepatic gene expression 148
3.4.1.4.1 Hepatic *DMT1* mRNA expression 148
3.4.1.4.2 Hepatic *hepcidin* mRNA expression 149
3.4.1.4.3 Hepatic *Ireg1* mRNA expression 150
3.4.1.5 Effect of iron supplementation on placental gene expression 151
3.4.1.6 Effect of iron supplementation on foetal liver gene expression 152
3.4.2 Effect of iron supplementation on duodenal iron uptake 153
3.4.3 Effect of dietary iron supplementation on placental iron transport 156
3.4.3.1 Haematological parameters 157
3.4.3.2 Placental mRNA Quantification 157
3.4.4 Discussion 158
3.4.4.1 The effect of iron supplementation to the foetus 160
3.4.5 Conclusions 162
3.5.1 The effect of maternal hepcidin levels on placental iron uptake 164
3.5.1.1 Iron uptake assay 164
3.5.1.2 Optimisation of assay conditions 165
3.5.1.2 Effect of apical hepcidin concentration on ^{59}Fe uptake 166
3.5.1.3 Time-specific response to hepcidin treatment 167
3.5.2 Effect of basolateral hepcidin on iron efflux from BeWo cells 168
3.5.2.1 Optimisation of efflux protocol 169
3.5.2.2 Effect of foetal hepcidin on iron efflux 170
3.5.3 Physical association of hepcidin with BeWo cells 172
3.5.4 Discussion 174
3.5.5 Conclusions 176
3.6 Molecular mechanism of placental iron transport 177
3.6.1 DMT1 localisation 183
3.6.1.1 DMT1 localisation with the ER lumen 184

3.6.1.2 DMT1 localisation with Tfr1 185
3.6.1.3 DMT1-ire localisation 186
3.6.1.4 DMT1+ire localisation 188
3.6.1.5 Loclisation of DMT1b 190
3.6.1.6 DMT1-G185R localisation 192
3.6.2 Ireg1 localisation 193
3.6.3 Copper oxidase localisation 195
3.6.4 Discussion 198
3.6.5 Conclusions 201
4 General Discussion 202
4.1 How is duodenal iron absorption increased during pregnancy? 203
4.2 How is duodenal iron absorption regulated? 205
4.3 How is hepcidin expression regulated? 206
4.3.1 Transferrin saturation 206
4.3.2 Body iron stores 207
4.3.4 Hormones 208
4.3.5 Dilutary effect of increased plasma volume 208
4.4 What is the molecular mechanism of placental iron transfer? 210
4.5 How is placental iron transfer regulated? 212
4.2 Conclusions 215
4.3 Future Studies 216
5 Bibliography 218
6 Appendices 255

List of Figures

Figure 1. 1 The distribution of iron in adults 25
Figure 1. 2 Structure of the duodenum 26
Figure 1. 3 Differentiation of the duodenal epithelia 27
Figure 1. 4 Duodenal iron transport 30
Figure 1. 5 Structural representation of DMT1 32
Figure 1. 6 Comparison of the 3' IRE of DMT1 + and - ire 33
Figure 1. 7 Comparison of exon 1a/ exon 1b of DMT1 34
Figure 1. 8 A ribbon representation of the structure of human hephaestin 37
Figure 1. 9 Iron acquisition by duodenal apical and crypt cells 40
Figure 1. 10 Structure of the hfe protein 41
Figure 1. 11 Post-translational regulation by IRE-IRP interactions 43
Figure 1. 12 Differential regulation of IRP1 and IRP2 44
Figure 1. 13 Ribbon representation of the transferrin molecule 45
Figure 1. 14 Structure of Tfr1 46
Figure 1. 15 Transferrin mediated iron uptake 48
Figure 1. 16 Electron-micrograph of a liver section 51
Figure 1. 17 Diagramatic representation of the structure of hepatic tissue 51
Figure 1. 18 Structural representation of hepcidin 53
Figure 1. 19 Structural comparison of the human and rodent placenta 59
Figure 1. 20 Hypothesised mechanism for placental iron transfer 61

Figure 2. 1 The Transwell model of the placental syncytiotrophoblast 74
Figure 2. 2 Cycle optimisation of gapdh amplification 78
Figure 2. 3 Melting peak of hepcidin gene products 85
Figure 2. 4 Effect of initial template concentration on PCR amplification 87
Figure 2. 5 Standard curve for mouse hepcidin-2 87

Figure 3.1. 1 Duodenal gene expression in the $hfe^{-/-}$ mouse 96
Figure 3.1. 2 Hepatic gene expression in the $hfe^{-/-}$ mouse 97
Figure 3.1. 3 Effect of diet on duodenal and hepatic gene expression 100
Figure 3.1. 4 Localisation of endogenous DMT1 in the rat duodenum 103
Figure 3.1. 5 Dcytb protein expression in the rat duodenum 104
Figure 3.1. 6 Hepcidin-1 & Duodenal DMT1 expression in C57blk/6 & $hfe^{-/-}$ mice. 107

Figure 3.2. 1 Estimated daily iron requirements during pregnancy 113
Figure 3.2. 2 Haematological parameters during pregnancy 116
Figure 3.2. 3 Duodenal *Dcytb, DMT1* & *Ireg1* mRNA expression during pregnancy 117
Figure 3.2. 4 Hepatic *Hepcidin-1, DMT1, Ireg1* & *Tfr2* mRNA expression 118
Figure 3.2. 5 Hepatic liver iron concentration during pregnancy. 119
Figure 3.2. 6 Placental *DMT1, Ireg1* & *Tfr1* mRNA expression during pregnancy. 120

Figure 3.3. 1 Placental gene expression in iron-deficient & control rats. 129
Figure 3.3. 2 Effect of maternal iron deficiency on duodenal iron uptake 132
Figure 3.3. 3 Duodenal expression of *DMT1, Dcytb, Ireg1* and *Tfr1* mRNA 134

Figure 3.4. 1 Effect of iron supplementation on haematological parameters 143
Figure 3.4. 2 Effect of iron supplementation on liver iron levels 144
Figure 3.4. 3 Effect of iron supplementation on duodenal *Dcytb* expression 145
Figure 3.4. 4 Effect of iron supplementation on duodenal *DMT1* expression 146
Figure 3.4. 5 Effect of iron supplementation on duodenal *Ireg1* expression 147
Figure 3.4. 6 Effect of iron supplementation on hepatic *DMT1* expression 148
Figure 3.4. 7 Effect of iron supplementation on *hepcidin* expression 149
Figure 3.4. 8 Effect of iron supplementation on hepatic *Ireg1* expression 150
Figure 3.4. 9 Effect of iron supplementation on placental gene expression 151
Figure 3.4. 10 Effect of iron supplementation on gene expression in the foetal liver 152
Figure 3.4. 11 Duodenal iron uptake in iron supplemented dams 155
Figure 3.4. 12 Placental gene expression following iron supplementation 158

Figure 3.5. 1 Iron uptake by BeWo cells 165
Figure 3.5. 2 Effect of hepcidin concentration on iron uptake in BeWo cells 166
Figure 3.5. 3 Effect of hepcidin treatment period on iron uptake in BeWo cells 167
Figure 3.5. 4 Iron efflux from BeWo cells 169
Figure 3.5. 5 Effect of hepcidin on the initial rate of iron efflux 171
Figure 3.5. 6 Effect of hepcidin on iron efflux from BeWo cells 172
Figure 3.5. 7 hepcidin binding to the plasma membrane 173

Figure 3.6. 1 Negative control 182
Figure 3.6. 2 DMT1 localisation 183
Figure 3.6. 3 DMT1 localised to the ER lumen. 184
Figure 3.6. 4 DMT1 did not co-localise with Tfr1. 185
Figure 3.6. 5 DMT1a-ire localisation 186
Figure 3.6. 6 DMT1a-ire localisation with clathrin and PDI. 187
Figure 3.6. 7 DMT1a+ire demonstrated some localisation to the ER. 188
Figure 3.6. 8 DMT1a+ire did not co-localise with clathrin. 189
Figure 3.6. 9 DMT1b-ire was localised near the plasma membrane. 190
Figure 3.6. 10 DMT1b-ire localisation with PDI and α-adaptin. 191
Figure 3.6. 11 G185R mutation in DMT1b-ire prevents localisation to endosomes. 192
Figure 3.6. 12 Subcellular localisation of Ireg1. 194
Figure 3.6. 13 Ceruloplasmin staining was speckled throughout the cytoplasm. 195
Figure 3.6. 14 Ireg1 localisation with the placental copper oxidase. 196
Figure 3.6. 15 DMT1 localisation with the placental copper oxidase. 197

Figure 4. 1 Duodenal iron absorption. 203
Figure 4. 2 Regulatory mechanism of iron homeostasis 209
Figure 4. 3 Proposed mechanism of placental iron transport 211
Figure 4. 4 Regulation of placental iron transfer 213

List of Tables

Table 1. 1 Proteins involved in iron transport and homeostasis 28
Table 1. 2 Comparison of human and mouse pregnancy 57

Table 2. 1 Primers used for Ready-To-Go™ RT-PCR. 80
Table 2. 2 Real-Time PCR primers 86

Table 3.4. 1 Parameters regulated by systemic iron deficiency 162

Table 3.6. 1 DMT1 contructs 179
Table 3.6. 2 Antibodies used in this study 181

Abbreviations

aa	Amino acid
APES	3-aminopropyl triethoxysilane
apo-Tf	Apotransferrin
APS	Ammonium persulphate
Arg	Arginine
β_2m	β_2-microgobulin
bbm	Brush border membrane
BCA	Bicinchoninic acid
blm	Basolateral membrane
bp	(Nucleotide) base pairs
BSS	Balanced salt solution
Cp	Ceruloplasmin
C-terminal	Carboxyl terminal
DAPI	4,6-di-amidino-2-phenyl indo
Dcytb	Duodenal cytochrome b*
dH_2O	Distilled water
DMT1	Divalent Metal Iron Transporter 1*
DMT1+ire	Divalent Metal Iron Transporter with an iron response element *
DMT1a	Divalent Metal Iron Transporter with exon 1a*
DMT1b	Divalent Metal Iron Transporter with exon 1b*
DMT1-ire	Divalent Metal Iron Transporter without an iron response element *
dsDNA	Double stranded deoxyribonucleic acid
ECL	Enhanced chemiluminescence system
Epo	Erythropoietin
er	Endoplasmic reticulum
Fe	Iron
Fe_2	Diferric
Fe^{2+}	Ferrous iron
Fe^{3+}	Ferric iron
FITC	Fluorescein isothiocyanate
gd	Gestational day
GI	Gastro intestinal tract
H-chain (ferritin)	Heavy chain*
$hfe^{-/-}$	Hfe knockout
HH	Hereditary haemochromatosis
HIF	Hypoxia inducable factor
HPRT	Hypoxanthine phosphoribosyltransferas
hpx	Hypotransferrinemic mice
hr	Hour
i.p.	Interperitoneal

IgG	Immuno globulin
IL-1	Interleukin 1
IL-6	Interleukin 6
IMP	Intergin mobiliferrin paraferritin pathway
IMS	Industrial methylated spirits
IRE	Iron response element
Ireg1	Iron regulatory like transporter 1*
IRP	Iron response protein
kDa	Kilo dalton
kg	Kilo gram
L-chain (ferritin)	Light chain*
Leu	Leucine
mA	Milli amps
mg	Milli grams
MHC	Major histo compatability
min	Minute
mL	Milli liter
mRNA	Messenger ribonucleic acid
n	Sample size
N_2	Nitrogen
NHS	Normal horse serum
NTA	Nitrilotriacetate
NTBI	Non transferrin bound iron
N-terminal	Amino terminal
o/n	Over night (12-18 hours)
PBS	Phosphate buffered saline
PBS-T	Phosphate buffered saline containing 0.05% Tween-20
PDI	Protein disulfide isomerase
PHZ	Phenyl hydrazine
PLIF	Placental immunomodulatoryferritin
PIT	Plasma iron turnover
pmol	Pico mole
ppm	Parts per million
RE	Reticulo endocyte
RNA	Ribonucleic acid
rt	Room temperature (20°C $\pm$ 2°C)
S.E.M.	Standard error of the mean
SDS-PAGE	Sodium dodecyl sulphate Polyacrylamide Gel Electrophoresis
SD	Standard deviation
S.E.M.	Standard error of the mean
sla mouse	Sex linked anaemia
TBS	Tris buffered saline
Tf	Transferrin*
Tfr1	Transferrin receptor 1*

TIBC	Total iron binding capacity
TNF-α	Tumour necrosis factor-α
UTR	Untranslated region of a mRNA transcript
UV	Ultra violet
μg	Micro gram
3'	3 prime terminal
5'	5 prime terminal
WHO	World Health Organisation
ZIRTL	Zinc Iron Regulatory Transporter Like

*if written in *italics* name refers to the gene or mRNA transcript

1 Background

1.1 Importance of iron in biological systems

The plentitude of iron in the environment and the redox properties of this element are the likely reasons for its role in many essential functions in both eukaryotic and prokaryotic organisms. It forms the active center of key enzymes including ribonucleotide reductase (Uppsten *et al.*, 2004) and aconitase (Jordanov *et al.*, 1992). As the center of haem-containing proteins, including the cytochromes of the electron transport chain and haemoglobin, iron plays an important role in energy metabolism and oxygen delivery to tissues (Winfield, 1965).

Alterations in body iron stores are associated with various human diseases, including neurodegenerative diseases (Wang *et al.*, 1995), microbial infections (Weinberg, 1985), diabetes mellitus (Bomford & Williams, 1976), cardiomyopathy (Salonen *et al.*, 1992), arterioscleroses (Smith *et al.*, 1992) and cancer (Nelson *et al.*, 1995).

1.1.1 Iron deficiency

Iron deficiency is the most common form of nutritional deficiency worldwide (World Health Organisation, 2003). A recent estimate based on criteria set by the WHO indicated that as many as 4-5 billion people, 66-80% of the world's population, may be iron deficient and around 600-700 million people worldwide have iron deficiency anaemia[1] (DeMaeyer & Adiels-Tegman, 1985; World Health Organisation, 2003). Due to the increased iron requirements during growth the prevalence of iron deficiency is highest amongst young children and pregnant women. Maternal iron deficiency present before conception results in a decrease in placental capillary surface area (Lewis *et al.*, 2001). During pregnancy iron deficiency can increase the frequency of premature births (Lieberman *et al.*, 1988), cause severe foetal growth retardation (Crowe *et al.*, 1995;Godfrey *et al.*, 1996) and increase blood pressure (Gambling *et al.*, 2003), which in turn affects normal brain function and the immune system (Hallquist *et al.*, 1992;Kwik-Uribe *et al.*, 2000). Complications caused by iron deficiency *in utero* and during early development can persist into adulthood (Crowe *et al.*, 1995;Godfrey & Barker, 1995;Kwik-Uribe *et al.*, 2000;Gambling *et al.*, 2003). In children, iron deficiency causes increased risk to infections, developmental delays and behavioural disturbances (World Health Organisation, 2003). In adults the symptoms of iron deficiency are in part explained by the presence of anaemia: pallor, fatigue, poor exercise tolerance and decreased work performance (Leventhal & Stohlman, Jr., 1966).

[1] A reduction in erythrocytes or in their heamoglobin content due to a lack of iron.

1.1.2 Iron overload

The consequences of iron overload are evident in hereditary haemochromatosis (HH) patients. Sufferers of HH absorb inappropriate levels of iron from their diet (Cox & Peters, 1978). This results in increased plasma iron levels, tissue iron overload, and in more advanced cases the development of liver cirrhosis, diabetes, hypogonadism, arthropathy and skin pigmentation (Trousseau, 1865; Feder *et al.*, 1996).

The iron homeostatic mechanism of the body ensures that Fe^{2+} levels are maintained at a minimum as these react with unsaturated fatty acids in the presence of O_2 and can initiate a lipid perioxidation cascade in biological membranes and lipoproteins by the production of highly reactive $OH^{\bullet}$. Many of the aldehydes produced through lipid perioxidation can also damage DNA by acting as free radicals.

1.1.3 Iron supplementation during pregnancy

Duodenal iron absorption increases during pregnancy (DeMaeyer & Adiels-Tegman, 1985), although not enough to prevent anemia in approximately 50% of the world's pregnant women (World Health Organisation, 2003). For this reason, iron supplementation during pregnancy is commonplace. Pregnant women treated with iron have greater iron reserves, higher haemoglobin levels, and a lower prevalence of iron deficiency anaemia (Sood *et al.*, 1975;Blot *et al.*, 1981;Makrides *et al.*, 2003). Furthermore, children born to iron-treated mothers have higher serum ferritin levels (Buytaert *et al.*, 1983; Dommisse *et al.*, 1983). However the efficacy of supplementation is not uniform with up to 35% of iron supplemented pregnant women showing iron deficiency (Makrides *et al.*, 2003). This is influenced by several factors, including the dose, iron stores of the recipient and whether iron is consumed alone or in combination with a vitamin-mineral supplement (Sandstrom, 2001). Iron absorption is higher in individuals who have either low iron stores or iron deficiency erythropoiesis and those with iron deficiency anaemia (Benito *et al.*, 1998). Additionally, supplemented iron is absorbed almost twice as well when taken between rather then with meals. However, unregulated supplementation is also not without risk both to the mother, with increased oxidative stress in the gastrointestinal tract (Lund *et al.*, 2001), alteration to macrophage function (Aldieri *et al.*, 2001) and interference in the metabolism of other micronutrients such as zinc and copper (Burns & Paterson, 1993;O'Brien *et al.*, 2000), and to the child causing increased risk of prematurity and poor outcome (Jameson, 1976).

Iron supplementation during pregnancy is commonplace due to the high incidence of iron deficiency in this population group. A study by Viteri *et al.* (1995) shows that dietary iron supplementation can restore liver iron levels within 3 days, however previously iron deficient individuals continue to accumulate liver iron to levels above those of the control, non-iron deficient, group. This raises the possibility that iron deficient pregnant women may be particularly susceptible to excessive iron accumulation and oxidative stress following iron supplementation. This is of concern as during pregnancy, the risk of pre-term delivery follows a U shaped relationship, increasing with high as well as low haemoglobin (Hb) concentration (Lu *et al.*, 1991;Garn *et al.*, 1981).

The risk of oxidative stress is also increased during pregnancy due to the presence of the placenta. Initially the placenta has a hypoxic environment, but as it matures vascularisation develops and it changes to an oxygen and mitochondrial rich environment. As about 5% of all electrons in the mitochondrial respiratory chain leak out of the mitochondria (Fridovich, 1979), this favours the production of reactive oxygen species (ROS), which increases free iron liberated from iron-sulfur clusters (Liochev & Fridovich, 1997). The placenta also produces nitric oxide (NO) this together with other reactive nitrogen species contributes to the potential oxidative stress in the presence of transition metals.

1.1.3.1 Absorption of other micronutrients

Iron metabolism cannot be considered in isolation, as iron status has effects on the absorption of other micronutrients. 100 mg iron supplements have been shown to depress zinc absorption in pregnant women (Simmer & Thompson, 1985), with teenage pregnancies a similar effect is apparent with daily 18 mg iron supplements (Dawson *et al.*, 1989).

In addition, iron supplementation may prevent a benefical fall in haematocrit and haemoglobin concentration during pregnancy and result in increased blood viscosity due to the development of macrocytosis (Taylor & Lind, 1976), which may alter placental exchange.

1.1.4 Iron requirements

Neonates are born with a total body iron of about 250 mg (Bothwell *et al.*, 1979). This is adequate to meet the developmental requirements for the first 4-6 months of life (European Communities, 1993). During the growth and developmental years iron absorption must exceed loss by about 0.5 mg daily in order to maintain a body iron concentration of about 60 ppm (Bothwell *et al.*, 1979).

The average 70 kg man has a total body iron of about 4 g which remains constant throughout adult life, and loses approximately 0.9 mg per day by non-specific mechanisms such as cell desquamation and intestinal secretions (DeMaeyer, 1989). Pre-menopausal women lose approximately 1.2 mg per day due to menses (DeMaeyer, 1989). Usually the non-specific sources of loss contain iron in proportion to the body iron stores and as there is no physiological mechanism for iron excretion in mammals, absorption by the intestine is assumed to have a primary role in regulating body iron levels (Cavell & Widdowson, 1964). Adult males absorb about 1 mg of iron daily from a diet containing 10-20 mg of iron. Women eat less food then men and must absorb about 1.2 mg of iron daily in order to avoid becoming iron deficient.

1.1.4.1 Iron requirements during pregnancy

Iron requirements increase during pregnancy (Svanberg *et al.*, 1975). However, due to the cessation of menstruation, iron requirements are reduced to approximately 0.8 mg per day in the first trimester of pregnancy. During the second trimester, the expansion of the red blood cell mass and the transfer of increasing amounts of iron to the placental structure results in an increase in daily iron requirements to 4-5 mg. During the final trimester, iron transfer to the foetus is in line with foetal growth, at this point the daily iron requirement of the mother increases to 6-7 mg. In addition to loss to the neonate, iron is also lost in maternal blood and lochia at parturition. A review by Bothwell published in 2000, estimates the total gestational requirement of a 55 kg women to be approximately 1000 mg, this is greater than can be absorbed from even an optimal diet, therefore a women must enter pregnancy with iron stores greater then 300 mg (serum ferritin > 8 μg/L) if she is to meet her requirements fully.

1.1.4.2 Changes in haematological parameters during pregnancy

After an initial decrease in the total red blood cell mass during the first trimester of pregnancy, the cell mass increases in the second and third trimesters (Beguin *et al.*, 1991). Despite the presence of the placenta and the frequent occurrence of iron deficiency, serum transferrin receptor (sTfr) levels, a measure of erythropoetic activity, remain low in the first trimesters and do not increase until the third trimester (Beguin *et al.*, 1991;Bianco *et al.*, 2000;Khatun *et al.*, 2003). This correlates with serum erythropoietin (Epo)[2], which is also decreased at the onset of pregnancy and later shows a gradual increase until term (Bianco *et al.*, 2000;Akesson *et al.*, 2002).

1.1.5 Distrbution of iron in adults

In the adult, on average, about 1800 mg of iron is incorporated into haemoglobin in erythrocytes circulating in the blood and 300 mg in erythroid precursors in the bone marrow (Figure 1.1). A further 300 mg is located in muscle fibers as myoglobin and in other tissues in enzymes and cytochromes. Most of the remaining iron is stored in the liver (1000 mg) and in reticuloendothelial (RE) macrophages (600 mg). These ingest senescent erythrocytes, breakdown haemoglobin and release iron into the plasma where it is loaded onto transferrin (Tf). Free non-transferrin-bound-iron (NTBI) is rapidly bound onto Tf and thus circulates around the body (Sahlstedt *et al.*, 2002). Under normal circumstances Tf is 20-35% saturated (Daniel, Jr. *et al.*, 1975). At any one time approximately 3 mg of iron is in this form. The erythron has a daily requirement of about 20 mg of iron (Cook *et al.*, 1973) therefore the function of RE macrophages is indispensable.

Iron homeostasis is maintained by strict control at the sites of uptake: the duodenum, storage: the liver, recycling: RE macrophages and use: mainly the erythroid, and during pregnancy: the placenta. In this section we address each site in turn, discussing in detail the various transporters and modulators involved in iron homeostasis and transport.

[2] Erythropoietin: a hormone, produced in the adult kidney, which stimulates the production of red blood cells.

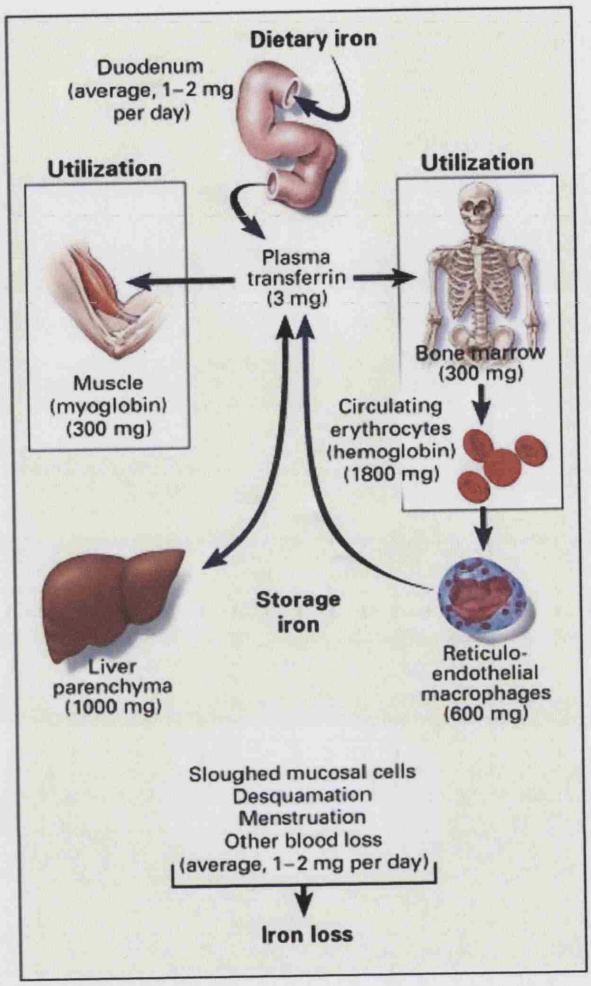

Figure 1. 1 The distribution of iron in adults

Iron enters the body by absorption through the duodenum. It circulates around the body bound to transferrin. This is taken up by the bone marrow and incorporated into haemoglobin and is recycled by reticulo-endothelial macrophages during the catabolism of senescent red blood cells. Iron is also utilised for the synthesis of myoglobin and various enzymes. Excess iron is stored predominantly in the parenchymal tissues of the liver. There is no physiological mechanism for iron excretion. Non-specific losses occur through cell desquamation and mestruation (Andrews, 1999).

1.2 Duodenal Iron uptake

Various anatomical and physiological adaptations occur in the maternal gastro-intestinal (GI) tract during pregnancy to accommodate the nutritional requirements of the feto-placental unit. The maternal GI tract increases in both mass and surface area (Burdett & Reek, 1979;Hammond, 1997) which potentially increases the absorption capacity of the gut. In addition, progesterone produced during pregnancy relaxes smooth muscle, decreasing the intestinal motility, delaying gastric emptying and prolonging GI transit time (Frederiksen, 2001). These modifications facilitate the breakdown and digestion of food thereby increasing the absorption of micronutrients.

1.2.1 Structure of the duodenum

The duodenum received its name from being approximately equal in length to the breadth of twelve fingers (25cm), and in mammals is the primary site of iron uptake (Duthie, 1964;Wheby *et al.*, 1964;Johnson *et al.*, 1983). The wall of the duodenum is covered in finger-like projections known as villi, these increase the absorptive surface of the duodenum. A single-layer of epithelial cells cover the villi, these cells have a microvillus membrane, known collectively as the brush border and is the site of iron absorbtion (Figure 1.2).

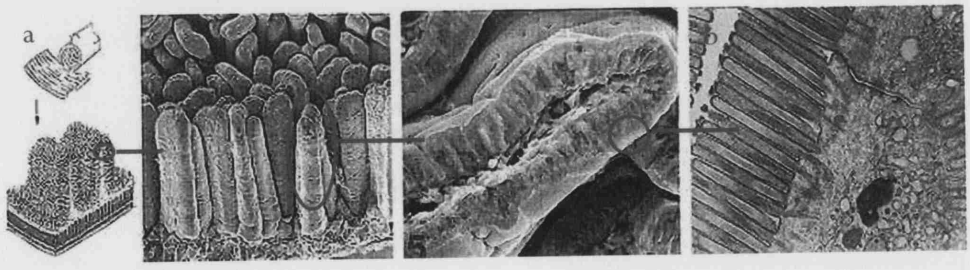

Figure 1. 2 Structure of the duodenum

(a) The duodenal epithelia is folded into villi, this increases the absorptive surface. (b) The apical membrane of absorptive cells is covered in microvilli, this brush border surface further increases the absorptive surface of the duodenum. Diagram adapted from (http://em-bioimage.iwate-med.ac.jp/duodenum-s.JPG, 2004).

Duodenal absorptive cells (enterocytes) originate from undifferentiated cells in the crypts of Lieberkuhn (Ito & Terao, 1994) (Figure 1.3). From here, they migrate up the villus over a period of 5-6 days in humans (MacDonald & Pechat, 1964) and 2-3 days in rodents (Messier & Leblond, 1960). During migration the cells differentiate, accumulating cell specific components (Cheng & Leblond, 1974;Potten & Loeffler, 1990). With respect to iron absorption this involves the expression and targeting of a number of proteins to specific cell membranes and to intracellular sites, as summerised in table 1.1. When the epithelial cells reach the villus tips they are lost by apoptosis and exfoliation into the gut lumen (Potten & Allen, 1977;Gavrieli *et al.*, 1992).

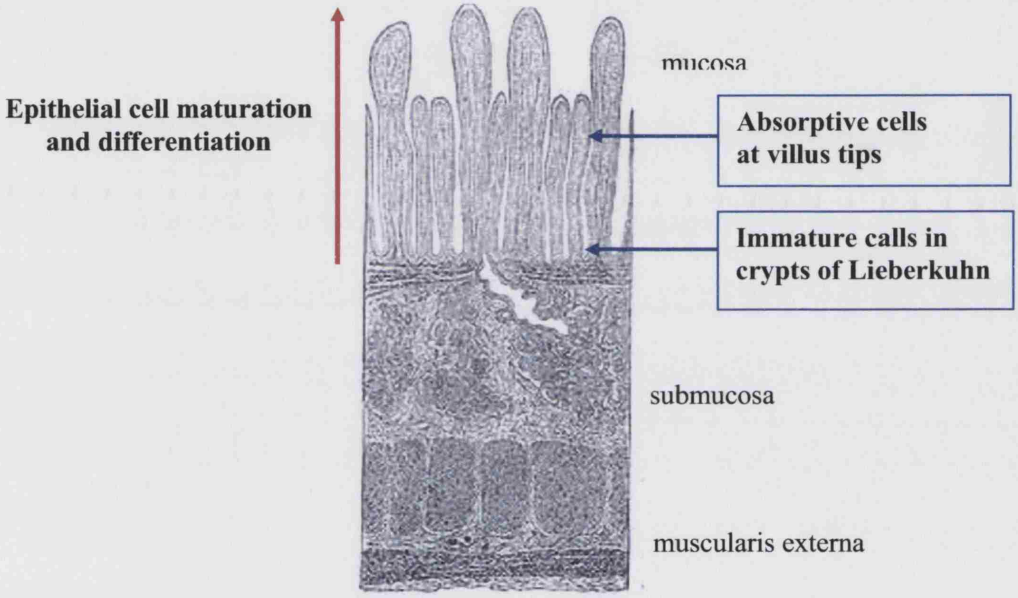

Figure 1. 3 Differentiation of the duodenal epithelia

Enterocyte stem cells in the crypts of Lieberkuhn divide. These cells acquire plasma diferric iron via Tfr1 displayed on the basolateral membrane. Enterocytes mature whilst migrating up the villi axis. Fully mature enterocytes absorb luminal ferrous iron by DMT1 expressed on the brush border membrane. Diagram adapted from (http://www.bartleby.com/107/Images/small/image1058.jpg, *2004).*

Protein	Function	Expression			Effect of iron depletion
		Site			
		Crypt	Villus	Other cells	
DMT1	Fe(II) transporter	–	+	+ (many)	Increase
Ferroportin *	Fe(II) transporter	–	+	+	Increase
Dcytb	Ferrireductase	–	+	–	Increase
Hepaestin	Ferroxidase	–	+	+	No Change
Ferritin	Iron storage	+	+	+ (many)	Decrease
HFE	Regulator	+	–	+	No Change
Hepcidin	Regulator	–	–	Liver	Decrease
TfR1	Transferrin endocytosis	+	+	+ (many)	Increase
TfR2	Transferrin endocytosis **	?	?	Liver	No Change
Transferrin	Iron transport	–	–	Liver	Increase
IRP1	Regulator	+	+	+ (many)	Increase
IRP2	Regulator	+	+	+ (many)	Increase

Table 1. 1 Proteins involved in iron transport and homeostasis

(+) Gene and/or protein localised
(-) Gene and/or proteinexpression not present
(?) Gene and/or protein expression not yet investigated or not yet conclusive
* *Ferroportin also known as Ireg1*
** *Tfr2 additionally functions in regulation*
From (Morgan & Oates, 2002)

1.2.2 Duodenal Iron uptake: effect of dietary factors

Dietary iron compounds can be divided into two groups, haem and non-haem. In humans haem iron is more readily absorbed than non-haem iron (Bothwell *et al.*, 1979). The mechanism for haem uptake is thought to differ from that of non-haem iron only for the initial step of transport across the brush border membrane (bbm) of the enterocyte, where it is thought to enter the cell as an intact iron-protoporphyrin complex (Figure 1.4) (Parmley *et al.*, 1981;Wyllie & Kaufman, 1982). Within the cell iron is released from the porphyrin ring by haem oxygenase (Raffin *et al.*, 1974). From then on the released iron probably enters the same iron pool as non-haem iron.

Non-haem ferric iron is highly insoluble at physiological pH and the efficiency of its uptake is dependent on a number of factors. The composition of the meal greatly enhances or inhibits inorganic iron uptake. Enhancers of iron uptake include reducing substances, in particular ascorbic acid, which keep iron in the reduced form (Van Campen, 1972;Sayers *et al.*, 1973). Organic acids such as citric acid, fermented vegetables, as well as meat, fish and seafood (which have been shown to also enhance haem iron uptake), increase non-haem iron uptake, although the nature of this enhancement has yet to be determined (Conrad & Schade, 1968).

Inhibitors of non-haem iron uptake include phytates. These are inositol hexaphospate salts, a storage form of phosphates and minerals found in grains, seeds, nuts, root vegetables and fruit. Phytates bind inorganic iron and form a complex that is not well absorbed. They inhibit iron absorption in a dose dependent manner, although even small amounts have been shown to have a marked effect (Gillooly *et al.*, 1983;Hallberg *et al.*, 1989;Brune *et al.*, 1992). Phenolic compounds containing galloyl groups have also been shown to inhibit iron uptake (Brune *et al.*, 1989), these are found in almost all plants as part of their defense system against insects and animals. Polyphenols, also present in plants, particularly tea, coffee and cocoa, bind iron and have a marked negative effect on absorption (Disler *et al.*, 1975;Derman *et al.*, 1977;Hallberg & Rossander, 1982;Morck *et al.*, 1983). Calcium also interferes in a dose-dependent fashion with the absorption of both haem- and non-haem iron, as it is thought to inhibit a process within the mucosal cell and unlikely to inhibit transfer of iron across the apical membrane (Hallberg, 1998).

1.2.3 The molecular mechanism of duodenal iron uptake

1.2.4 Integrin Mobiferrin Paraferritin Pathway

Ferric iron is bound to mucin in the acid pH of the stomach and kept soluble and available for absorption at the higher pH of the duodenum (Conrad *et al.*, 1991). Ferric iron is transported across the apical membrane of the gut mucosa by integrin (Figure 1.4). Integrin is a 90/150 kD protein expressed on the apical membrane of the duodenum. Integrin donates the iron to mobiliferrin, a 56 kD iron binding protein, present in the enterocyte cytosol, which acts as the shuttle protein for iron in the cytoplasm. Mobiliferrin associates with other proteins to form a large protein complex called paraferritin which serves as a ferrireductase. Paraferritin solublises iron binding proteins and reduces iron to make iron available for the cellular iron pool.

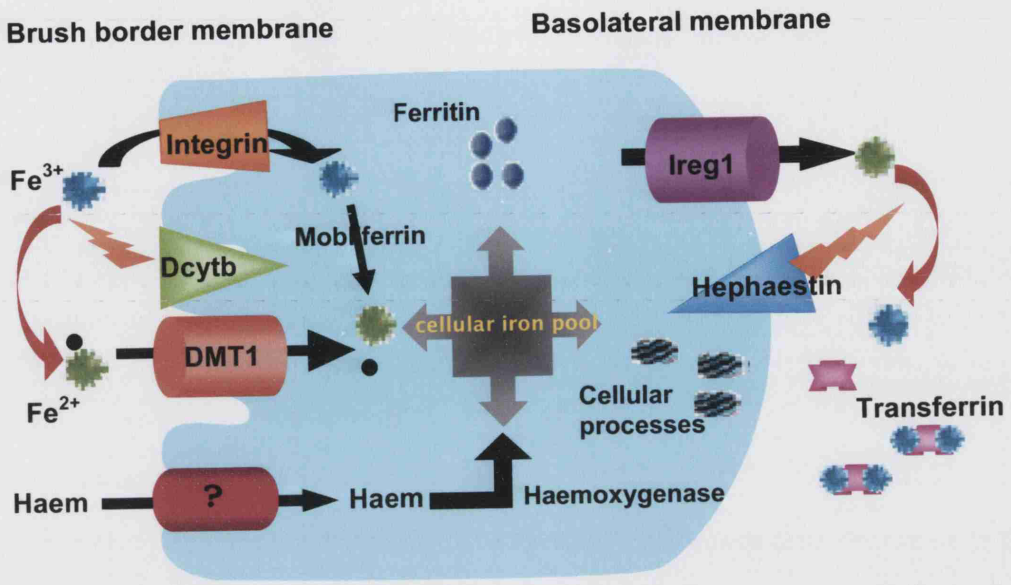

Figure 1. 4 Duodenal iron transport

Ferric iron bound to mucin is transported across the brush border membrane via the IMP pathway. However, the major pathway for ferric iron uptake involves reduction to the ferrous form by Dcytb, and transport across the brush border membrane via a proton symport mechanism by DMT1. Haem iron is transferred across the brush border membrane as an intact iron-protoporphyrin complex, which is broken down within the enterocyte by haemoxygenase before entering the cellular iron pool. Within the enterocyte iron is either used for cellular processes or stored in ferritin. Iron may also be transported across the basolateral membrane by Ireg1 coupled to hephaestin which converts ferrous iron to the ferric form at the site of iron efflux. Iron is circulated in the plasma bound to transferrin.

1.2.5 Dcytb

Dietary iron is predominately in the ferric form, which is reduced to the ferrous form by Dcytb (duodenal cytochrome b) before transportation across the brush border membrane (bbm). Dcytb is a di-haem plasma membrane protein (Pountney *et al.*, 1999). It has six membrane spanning regions and putative binding sites for ascorbate and dehydroascorbic acid (McKie *et al.*, 2001). The rabbit Dcytb homologue stimulates ascorbate driven iron and copper reduction *in vitro* (Knopfel & Solioz, 2002). *In vivo* the protein shuttles electrons from ascorbate to dehydrascorbate using metal as a oxidant (Pountney *et al.*, 1999;Knopfel & Solioz, 2002). Dcytb shares 45-50% homology with the cytochrome b561 family of plasma membrane reductases (McKie *et al.*, 2001). These also reduce dehydroascorbate to ascorbate in chromaffin granule membranes of the adrenal medulla (Srivastava *et al.*, 1984;Fleming & Kent, 1991;Kobayashi *et al.*, 1998).

In the mouse, Dcytb has been localised to the duodenum and the placenta (McKie *et al.*, 2001). It has also been identified in several intestinal cell lines: HuTu80, CaCo-2 and HL-60, in which plasma membrane ferric reductase activities have also been described. In these cells Dcytb is localised to the plasma membrane and to cytoplasmic vesicles (Latunde-Dada *et al.*, 2002).

Dcytb expression is highest in the proximal duodenum and decreases laterally down the GI tract (McKie *et al.*, 2001). It is predominately expressed on the enterocyte bbm and to a lesser extent in the cytoplasm of the upper villous regions of the duodenal villi, and is absent from crypt cells (Latunde-Dada *et al.*, 2002). This pattern of expression is similar to that of reductase activity in the gut (Raja *et al.*, 1992).

In the mouse, mucosal Fe^{3+} reduction rates, though quantitatively higher than uptake rates, correlate to iron uptake rates when induced by iron deficiency (Raja *et al.*, 1992). *Dcytb* mRNA levels are regulated by duodenal iron levels, increasing with deficiency and hypoxia (McKie *et al.*, 2001;Frazer *et al.*, 2002). Increased expression is also observed in hypotransferric mice (McKie *et al.*, 2001), these mice have a mutation linked to the Tf locus, this causes severe deficiency of Tf (Trenor, III *et al.*, 2000).. The regulation of Dcytb expression by iron status in the intestine is therefore similar to that of ferric reductase activity measured in intestinal fragments.

1.2.6 DMT1

Once reduced by Dcytb, ferrous iron is transported across the bbm by the divalent metal transporter 1 (DMT1), (also known as DCT1 for Divalent Cation Transporter 1 and Nramp2, for Natural resistance mediated protein 2) (Gruenheid *et al.*, 1995;Gunshin *et al.*, 1997). The DMT1 protein consists of 12 membrane spanning helices (Figure 1.5). It accepts a broad range of transition metals with substrates including Fe^{2+}, Cd^{2+}, Co^{2+}, Ni^{2+}, Cu^{2+}, Zn^{2+} and Ca^{2+}, although of these iron is preferentially transported (Tandy *et al.*, 2000). Transport across the apical membrane by DMT1 is energised by a proton electrochemical gradient (Gunshin *et al.*, 1997).

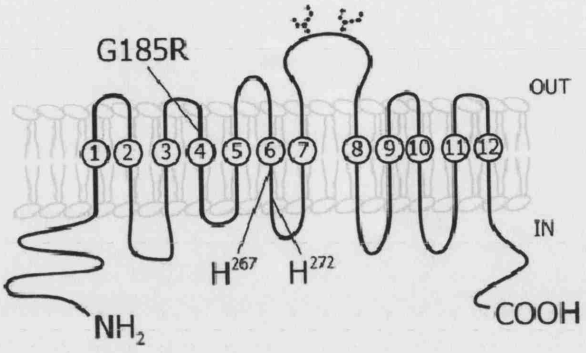

Figure 1. 5 Structural representation of DMT1

Cartoon of DMT1 demonstrating its 12 trans-membrane helices, and the position of the G185R mutation in helix 4. From (Tabuchi et al., 1999).

The biological importance of DMT1 is highlighted in two naturally occurring animal mutants of iron metabolism: microcytic anaemia in mice and the Belgrade phenotype in rats, both of which have severe defects in intestinal and reticulocyte iron absorption (Fleming *et al.*, 1997;Fleming *et al.*, 1998). In both species the G185R[3] mutation in DMT1 prevents correct localisation of the mature protein to the plasma membrane, resulting in the formation of high molecular weight aggregates in the golgi (Canonne-Hergaux *et al.*, 2000).

DMT1 is ubiquitously expressed, although most notably in the bbm and the microsomal compartments of duodenal upper villi (Canonne-Hergaux *et al.*, 1999;Tandy *et al.*, 2000). Expression is highest in the proximal duodenum and decreases laterally down the GI tract (Gunshin *et al.*, 1997). In tissues other then the duodenum and kidney, DMT1 is localised within recycling endosomes which have a key role in iron accumulation from the Tf cycle (Su *et al.*, 1998).

To date, four alternative splice variants of DMT1 have been characterised. Alternate splicing of the C-terminal generates two alternative transcripts, one with (*DMT1+ire*) and one without (*DMT1-ire*) an iron response element (IRE) (Figure 1.6)(Gunshin *et al.*, 1997;Fleming *et al.*, 1997;Lee *et al.*, 1998). Iron response proteins (IRPs) bind to IREs and protect the mRNA transcript from endocytic cleavage, increasing the half-life and thereby translation efficiency (Casey *et al.*, 1988). As the activity of IRPs are dependent on cellular free iron levels, DMT1+ire translation is regulated by cellular iron levels (Zoller *et al.*, 1999;Byrnes *et al.*, 2002), this has

[3] Glycine to Arginine mutation at amino acid position 185

been demonstrated in humans (Rolfs *et al.*, 2002), rats (Gunshin *et al.*, 1997) and mice (Fleming *et al.*, 2001).

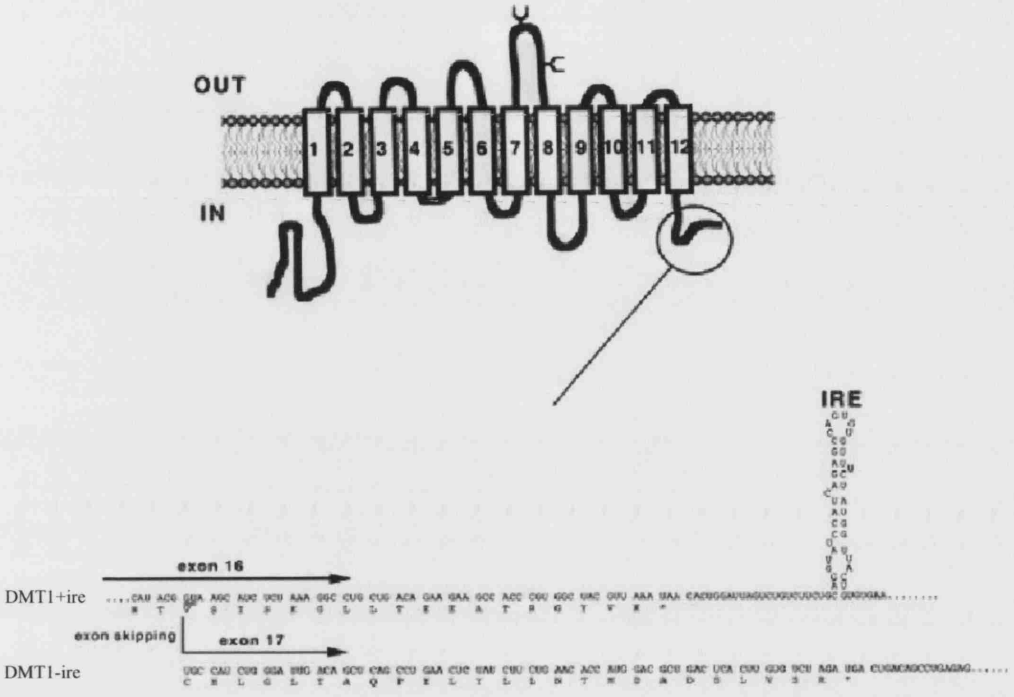

Figure 1. 6 Comparison of the 3' IRE of DMT1 + and - ire

Alternative splicing of the DMT1 transcript produces 2 splice variants: one with (DMT1+ire), and one without (DMT1-ire) an IRE. From (Tabuchi et al., 2002).

In contrast, the expression of *DMT1-ire* is not responsive to cellular iron levels (Canonne-Hergaux *et al.*, 1999;Gunshin *et al.*, 2001;Hubert & Hentze, 2002). The *DMT1-ire* transcript encodes a protein that is 7aa longer at the C-terminal then the +ire protein (Tabuchi *et al.*, 2000), never-the-less, alternative splicing of the C-terminal has not been shown to affect the ability to transport iron (Gunshin *et al.*, 2001). Both DMT1 isoforms are expressed in most organs (Hubert & Hentze, 2002) and are expressed in the plasma membrane and late endosomal compartments (Wardrop & Richardson, 1999).

DMT1 proteins also have two alternative N-termini. The expression of these proteins are regulated transcriptionally by two separate promoters, one of which recognizes an AUG initiation codon 99 nucleotides upstream of the other. This results in the synthesis of two alternative transcripts with differing exon 1 sequences (Tabuchi *et al.*, 2002) (Figure 1.7). The longer transcript DMT1a, bearing exon 1A, is highly expressed in the duodenum and the kidney (Hubert & Hentze, 2002). In the polarised cells of these tissues DMT1 is localised to the apical membrane (Canonne-Hergaux *et al.*, 1999;Griffiths *et al.*, 2000;Trinder *et al.*, 2000). Therefore the N-terminal peptide sequence encoded by exon 1A is predicted to target DMT1 to the apical membrane (Hubert & Hentze, 2002). The shorter transcript, DMT1b bearing exon 1B, is ubiquitously expressed (Hubert & Hentze, 2002) and may therefore encode for DMT1 localised in endosomal compartments.

In total four distinct DMT1 species have so far been identified: DMT1a+ire, DMT1b+ire, DMT1a-ire and DMTb-ire. The splicing of exon 1A determines cellular localisation and is regulated by promoter activity, this allows DMT1 localisation to be regulated by translation. Alternative C-terminal splicing allows post-translational regulation by cellular iron levels.

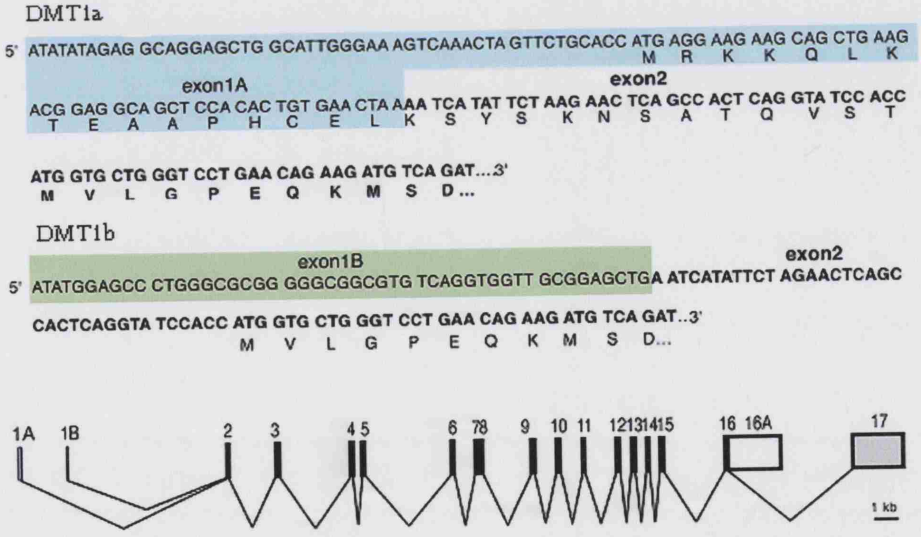

Figure 1. 7 Comparison of exon 1a/ exon 1b of DMT1

Sequence of the alternative exon 1 (a and b) of DMT1. Expression is regulated by different promoters and leads to a longer (DMT1a) transcript. In addition, alternative splicing in exon 16 produces a DMT1+ire (exon 16A) or DMT1-ire (exon 17). From (Hubert & Hentze, 2002).

1.2.7 Ferritin

The intracellular iron pool within the enterocyte is utilised for the metabolic requirements of the cell and any iron that is surplus to immediate needs is transported across the blm or stored in the enterocyte as ferritin (Theil, 1987). Ferritin has the capacity to sequester vast quantities of iron in a soluble, non-toxic and biologically useful form. It acts as a buffer against normal physiological variations in the iron requirements of tissues.

Ferritin is formed as an approximately spherical protein shell of 24 subunits. In the central cavity up to 4500 iron atoms are stored as polynuclear hydrous Fe^{3+} oxide phosphate (Mann *et al.*, 1986;Theil, 1987). The subunits of ferritin have two forms, termed heavy (H) and light (L) chains. These share 50% sequence identity and a similar 3D structure, but differ in the surface charges which gives the two subunits different properties (Arosio *et al.*, 1978;Harrison & Arosio, 1996). The H-chain has a ferrioxidase activity essential for the incorporation of iron (Levi *et al.*, 1988) and the L-chain is involved in core formation and mineralisation of iron (Levi *et al.*, 1994).

Ferritin mRNA contains IREs in the 5' untranslated region (UTR) (Huang *et al.*, 1999). IRPs bind to these sites in iron deficient conditions and block translation. A decline in ferritin levels increases the cellular availability of iron. This is either utilised within the cell or transported across the blm into circulation.

Due to the plasticity of duodenal enterocytes, iron stored in ferritin is lost into the gut lumen when mature enterocytes at the villus tips are sloughed off. As the expression of both DMT1 and Dcytb, required for the uptake of lumenal iron, is restricted to the proximal regions of the GI tract, this iron is lost in the faeces.

1.2.8 Ireg1

The basolateral transfer of iron requires two components: a copper-containing iron oxidase known as hephaestin and the membrane transport protein Ireg1. Ireg1 (for Iron REGulatory like transporter 1) also known as SLC11A3, Mtp1 (for metal transporter protein-1) and ferroportin1, is the putative basolateral iron transporter. It is highly expressed in mature duodenal enterocytes but its function as an iron efflux pathway is not restricted here as it is also present in the syncytiotrophoblast of the placenta, liver, spleen and RE macrophages (McKie *et al.*, 2000;Donovan *et al.*, 2000).

Mutations in Ireg1 cause an autosomal dominant form of hereditary haemochromatosis (HH) (Arden *et al.*, 2003;Pietrangelo, 2004). These patients show extensive hepatic iron loading, suggesting that Ireg1 is involved in the release of iron from hepatic cells (Montosi *et al.*, 2001;Njajou *et al.*, 2002). These patients also show extensive iron accumulation in RE macrophages (Pietrangelo, 2004) suggesting a role for Ireg1 in the release of iron from the RE system.

The 5'UTR of the *Ireg1* mRNA contains a functional IRE (McKie *et al.*, 2000;Abboud & Haile, 2000;Lymboussaki *et al.*, 2003). In other genes bearing an IRE in the 5'UTR, such as *ferritin*, the binding of cellular IRPs under low iron conditions causes a block in translation and decreased protein synthesis. Hepatic Ireg1 protein is increased in iron-loaded HH liver without any increase in mRNA (Adams *et al.*, 2003). This is consistent with iron-mediated translational regulation through the 5'IRE in the mRNA. Conversely, duodenal Ireg1 expression is increased in conditions of iron deficiency and decreased in conditions of iron loading (Zoller *et al.*, 2001;Anderson *et al.*, 2002; Dupic *et al.*, 2002;Martini *et al.*, 2002;Rolfs *et al.*, 2002;Chen *et al.*, 2003). This suggests that factors other then IRP binding also regulate Ireg1 expression.

1.2.9 Hephaestin

The second component of basolateral iron transport is a membrane bound multicopper oxidase, hephaestin. Mice with sex-linked anemia (*sla*) have a defect in hephaestin (Bannerman, 1976;Vulpe *et al.*, 1999). As a result iron accumulates in the enterocyte as ferritin and is lost during turnover of the intestinal epithelia (Edwards *et al.*, 1977).

Hephaestin is homologous to ceruloplasmin (Cp), a member of the family of 'blue' copper oxidases (Syed *et al.*, 2002). Cp exhibits ferrioxidase activity and facilitates iron egress from the RE system and various parenchymal cells (Harris *et al.*, 1995;Morita *et al.*, 1995). In contrast to Cp, hephaestin has a N-terminal leader peptide and 85 additional residues at the C-terminus which contain a predicted trans-membrane domain and a short cytoplasmic tail (Figure 1.8). Hephaestin is therefore considered to be a membrane bound homologue of Cp (Vulpe *et al.*, 1999;Syed *et al.*, 2002). Unlike Cp which is highly expressed in the liver, hephaestin expression is highest in intestinal villi and to a lesser extent in the kidney and lung (Vulpe *et al.*, 1999). In cultured cells, hephaestin is located exclusively to a supranuclear compartment, although in intestinal enterocytes it is also present on the blm (Chen *et al.*, 2003;Kuo *et al.*, 2004).

Hephaestin expression is regulated by both systemic and dietary iron levels (Sakakibara & Aoyama, 2002;Chen *et al.*, 2003). However, unlike the expression of *Dcytb, DMT1* and *Ireg1, hephaestin* mRNA expression is not increased in hfe knockout ($hfe^{-/-}$) mice (Dupic *et al.*, 2002).

Figure 1. 8 A ribbon representation of the structure of human hephaestin

A molecular representation of hephaestin demonstrating the putative iron binding site, and C-terminal membrane anchor by which it differs from ceruloplasmin. From (Syed et al., 2002).

1.2.10 ZIRTL

ZIRTL, for Zinc-Iron-Regulated-Transporter-Like protein, is a member of a family of divalent metal iron transporters (Eide *et al.*, 1996;Zhao & Eide, 1996). In humans the open reading frame encodes approximately 324 aas, and is predicted to be an integral membrane protein with eight transmembrane domains and contains a potential metal binding motif. The murine homologue has been demonstrated to be widely expressed in many tissues including the kidney, salivary glands and placenta (Lioumi *et al.*, 1999). Mutations in this gene was first postulated to be the cause of juvenile haemochromatosis, although this has since been proved wrong (Roetto *et al.*, 2000). *ZIRTL* expression is developmentally regulated, and appears relatively late in development when most cell types are undergoing terminal differentiation.

1.3 Regulation of duodenal iron absorption

1.3.1 Duodenal iron uptake during pregnancy

To satisfy the increased maternal and foetal iron requirements during pregnancy, duodenal iron uptake increases from gestational day (gd) 15, the start of the third trimester, in pregnant mice (Raja *et al.*, 1987) and rats (Batey & Gallagher, 1977). This is concurrent with a rise in *DMT1* expression (Leazer *et al.*, 2002). The mechanism which drives this increase is unknown.

1.3.2 Duodenal iron uptake in neonates

Although neonates have substantial body iron stores at birth, intestinal iron absorption is greater than in the adult (Loh & Kaldor, 1971;Mills & Davies, 1979;Srai *et al.*, 1988). This is due to various adaptations: increased uptake along both the duodenal axis (Debnam *et al.*, 1991) and the intestinal length (Chowrimootoo *et al.*, 1992), and decreased L-ferritin expressin (Kozma *et al.*, 1994). Although, It has also been suggested that the increased iron uptake potential maybe due to "leakiness" if the neonatal gut which is not yet fully developed. Possibly it is for these reasons, during early infancy neonates are unable to down-regulate intestinal iron transporters or iron absorption in response to iron supplementation (Leong *et al.*, 2003). In the guinea pig the increased absorption in the neonate falls to adult levels by about 10 days after birth (Srai, 1984).

1.3.3 Regulation of iron uptake

Although the amount of iron absorbed from the diet is small in comparison to the total body iron pool, the regulation of intestinal iron uptake is critical as there is no physiological pathway for excretion in mammals (Cavell & Widdowson, 1964;Canonne-Hergaux *et al.*, 1999). Duodenal iron absorption is regulated by various parameters that respond to dietary iron content, body iron stores and the erthyropoietic demand for iron (Duthie, 1964;Cook *et al.*, 1973;Bothwell *et al.*, 1979;Muir & Hopfer, 1985;Finch, 1994;Gunshin *et al.*, 1997).

1.3.4 Regulation by non-specific mechanisms

Duodenal uptake can be modulated by gross changes in anatomy. Pregnancy (Hammond, 1997), iron deficiency and hypoxia cause a gross increase in duodenal villus length, this increases the absorptive surface of the duodenum, increasing iron uptake (Burdett & Reek, 1979;Smith *et al.*, 2000). Interestingly, hypoxia also increases the membrane potential of the duodenual bbm by restricting sodium transport. This significantly increases iron absorption without a significant increase in the expression, either at the RNA or protein level, of iron transporters (O'Riordan *et al.*, 1997). Previous studies also underlined the dependence of iron uptake on a membrane potential (Raja *et al.*, 1989), which is possibly due to transport *via* DMT1 which is driven by a proton gradient.

1.3.5 Regulation by dietary iron content and transferrin saturation

A large oral dose of iron has been demonstrated to reduce the absorption of a subsequent smaller dose of iron (Frazer *et al.*, 2003). It is thought that this is due to an initial increase in dietary iron uptake and transfer across the blm into the plasma, leading to an increase in Tf saturation in the portal vein.

Developing enterocytes in the duodenal crypts take up Fe_2-Tf by the transferrin receptor (Tfr1) pathway (Figure 1.9). The amount taken up is determined in part by the degree of Tf saturation (Cazzola *et al.*, 1985). Thus, high Tf saturation increases the amount of chelatable iron in these cells. This decreases IRP1 activity, reducing IRP binding to IREs on *DMT1+ire* and *ferritin* mRNA transcripts. Endocytic action reduces *DMT1* mRNA levels, decreasing translation and consequently iron uptake. The converse, increased *DMT1* expression and absorption, is evident in conditions of iron deficiency (Gunshin *et al.*, 1997;Gunshin *et al.*, 2001;Rolfs *et al.*, 2002).

Reduced IRP binding to *ferritin* mRNA releases the block on translation, increasing ferritin protein levels. Iron transfer across the blm is reduced as iron accumulates within ferritin. This iron is lost from the body when the mature enterocyte is sloughed off into the gut lumen. This allows iron uptake and transfer to be inversely correlated with dietary iron levels and Tf saturation.

In addition, as Tf saturation is correlated to the iron requirement of the erythron, this allows iron uptake to increase in response to erythropoeitic demand, even in the setting of systemic iron overload. Indeed *DMT1* expression is inversely correlated to Tf saturation, blood haemoglobin and serum ferritin (Wheby & Jones, 1963;Duthie, 1964;Muir & Hopfer, 1985;Byrnes *et al.*, 2002; Rolfs *et al.*, 2002).

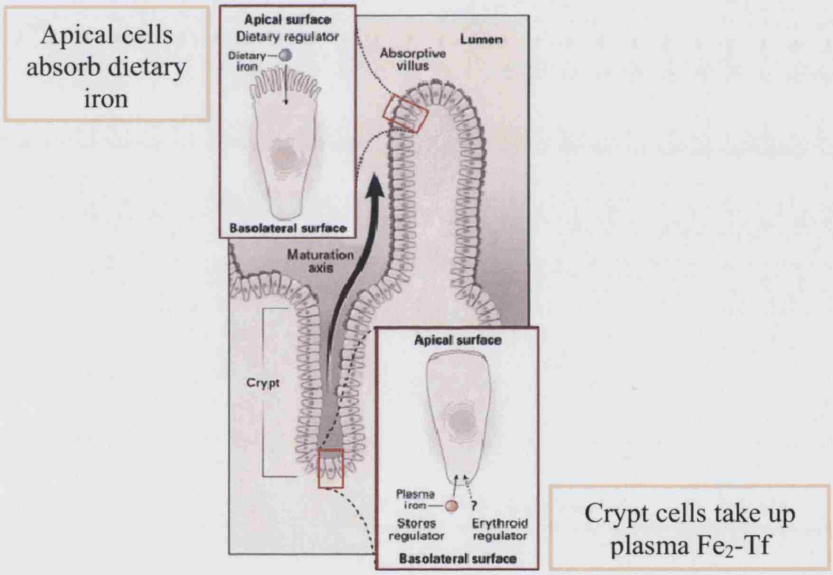

Figure 1. 9 Iron acquisition by duodenal apical and crypt cells

Developing enterocytes take up Fe_2-Tf which then enters the cellular labile iron pool. The amount taken up is dependent in part on Tf saturation in the portal vein. As these cells migrate up the villus axis they express iron transport proteins: DMT1, Dcytb and Ireg1. The expression of these genes is modulated by the size of the cellular iron pool. Figure adapted from Andrews (1999).

1.3.6 Regulation by hfe

The mechanism by which duodenal crypt cells sense Tf saturation levels is thought to involve the interaction of the hfe protein and Tfr1, as mice and patients with mutated hfe show inappropriate iron absorption.

The hfe protein is a 343 aa integral membrane protein, similar to major histocompatability (MHC) class 1 molecules, consisting of 3 extracellular loops (α1, α2, and α3), a transmembrane region and a short cytoplasmic tail (Waheed *et al.*, 1997) (Figure 1.10). The C282Y mutation in the hfe gene alters a critical disulfide bridge required for binding of the hfe protein to β_2-microglobulin (Feder *et al.*, 1997). This is required for late golgi processing and trafficking of the mature hfe protein to the cell surface (Waheed *et al.*, 1997). β_2-microglobulin knockout mice show iron loading similiar to hfe associated HH patients (Santos *et al.*, 1996).

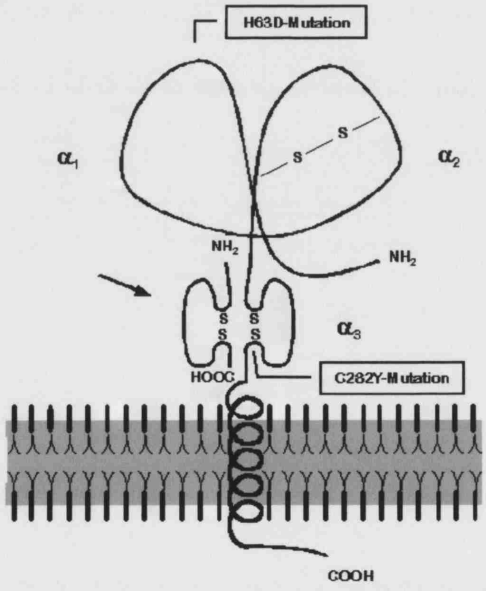

Figure 1. 10 Structure of the hfe protein

The bulk of the hfe molecule consists of a trans-membrane helix, a short cytoplasmic tail and 3 extracellular loops named α-1, α-2 and α-3. β_2-microglobulin attaches adjacent to the α-3 loop. Binding of β_2-microglobulin is inhibited by the C282Y mutation, which destroys the di-sulfide bond in the α-3 loop. (http://www.ikp.unibe.ch/lab2/Pp/pp5/img015.JPG , 2004).

Hfe protein is predominately expressed in liver hepatocytes (Zhang *et al.*, 2004) and is present in intracellular and perinuclear compartments in the enterocytes of the duodenal villus crypts (Parkkila *et al.*, 1997a). In other parts of the GI tract and in tissue culture models, hfe is expressed on the cell surface (Parkkila *et al.*, 1997a). Hfe is also highly expressed on the apical membrane of the placental syncytiotrophoblast, where it is physically associated with both β_2-microglobin and Tfr1 (Parkkila *et al.*, 1997b).

Hfe does not bind or transport iron, but physically interacts with Tfr1 (Parkkila *et al.*, 1997a;Feder *et al.*, 1998;Lebron *et al.*, 1998; Waheed *et al.*, 1999;Levy *et al.*, 2000). Cells transfected with hfe demonstrate decreased cellular Fe_2-Tf uptake. This is probably due to the binding of hfe to Tfr1, which consequently lowers its affinity for Fe_2-Tf (Feder *et al.*, 1998). However, studies by Waheed *et al.* (2002), have demonstrated that co-expression of hfe and β_2m increased Tfr1-Fe_2-Tf uptake.

HH is usually due to mutations in the hfe gene (Feder *et al.*, 1996). The most common mutation, found in individuals of Caucasian descent, is the C282Y[4] mutation found in 83% of Hfe associated HH patients (Feder *et al.*, 1996). Several other polymorphisms have also been identified including the H63D[5] mutation which can be deleterious when it is present as a second allele in persons who are heterozygous for C282Y (Bacon *et al.*, 1999;Olynyk *et al.*, 1999).

The current hypothesis to explain the elevated iron uptake in HH patients is that the hfe protein regulates plasma Fe_2-Tf uptake in the developing enterocytes present in the duodenal crypts. This is abrogated in $hfe^{-/-}$ mice which show decreased uptake of Fe_2-Tf (Trinder *et al.*, 2002b). Due to lower cellular iron levels in these cells IRP binding activity is increased (see Chapter 1.8.4). This is thought to stabilise *DMT1+ire* mRNA transcripts and inhibit the translation of *ferritin*, whilst cells migrate to form the absorptive epithelia, thus increasing iron absorption from the gut lumen. Studies investigating the expression of DMT1 and Ireg1 in the duodenum of $hfe^{-/-}$ mice are conflicting, with some studies demonstrating an increase in the expression of these transporters (Fleming *et al.*, 1999) whilst others show no change (Herrmann *et al.*, 2004). The probable reasons behind these inconsistencies may be related to inter-individual variations, the background strains of the mice, as well as differences in diet and age (Fleming *et al.*, 2001;Dupic *et al.*, 2002).

[4] Cysteine to Tyrosine mutation at amino acid position 282

1.3.7 Regulation by IRE-IRP interactions

Iron response elements are palindromic lengths of mRNA that fold into stem-loop structures (see Figure 1.6) (Hentze *et al.*, 1987;Casey *et al.*, 1988). These interact with IRPs to modulate translation or mRNA stability, allowing the translation of mRNA transcripts to adjust to the level of soluble iron atoms present in the cell (Beinert & Kennedy, 1993;Schalinske *et al.*, 1997;Muckenthaler *et al.*, 1998). IRE motifs have been identified in the 5'UTR of the erythroid specific *δ-aminolevulinic acid synthase* gene which is the first enzyme of the haem biosynthetic pathway and the 5' UTR of *ferritin* (Cox *et al.*, 1991;Dandekar *et al.*, 1991). When the IRP is bound to the IRE, the translation of the RNA sequence downstream is repressed by abrogating the recruitment of the small ribosomal subunit (Muckenthaler *et al.*, 1998) (Figure 1.11).

In addition, IRE motifs are present in the 3'UTR of *DMT1+ire* (Gunshin *et al.*, 1997) and *Tfr1* (Casey *et al.*, 1988). Unlike the IRE present in the 5'UTR of the *ferritin* gene which is equally sensitive to IRP1 and IRP2, the IRE motifs in *Tfr1* and *DMT1+ire* have a slightly modified structure which inhibits tight binding of IRP2, although IRP1 binding is unaffected (Butt *et al.*, 1996;Gunshin *et al.*, 2001). This suggests that the regulation of *DMT1+ire* and *Tfr1* are more dependent on IRP1 than IRP2. Binding of IRPs to the 3'UTR stabilises the mRNA transcript from RNAse degradation, thus increasing its half-life and translation efficiency (Weiss *et al.*, 1997) (Figure 1.11).

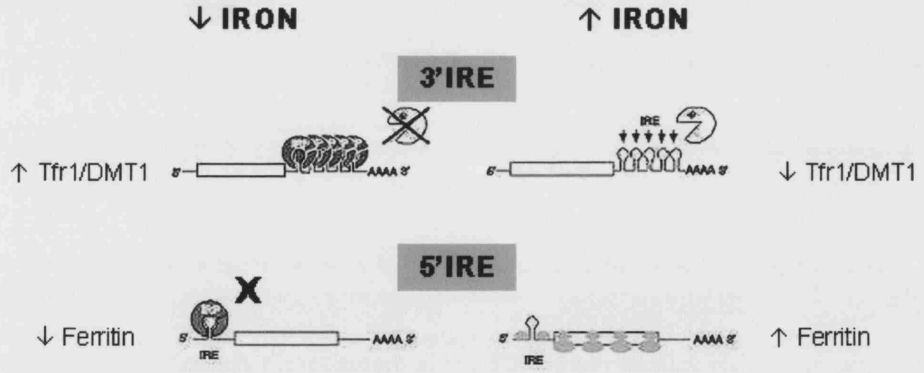

Figure 1. 11 Post-translational regulation by IRE-IRP interactions

Under low iron conditions IRPs are activated and bind to IREs in the 3'UTR of DMT1 and Tfr1 mRNA, this increases the half-life of the transcript by protecting it from RNAse degradation. Binding of IRPs to the 5'IRE of ferritin inhibits the formation of the pro-initiation complex inhibiting translation. Figure adapted from (http://www.uclm.es/inabis2000/symposia/files/138/fig2abc.jpg, 2004)

[5] Histidine to Aspartic acid mutation at amino acid position 63

To date, two distinct IRPs have been identified: IRP1 and IRP2 (Figure 1.12). IRP1, the predominant form in the liver, kidney and intestine (Henderson *et al.*, 1993;Samaniego *et al.*, 1994), exhibits two mutually exclusive functions as an RNA binding protein or as the cytosolic isoform of mitochondrial aconitase (Kaptain *et al.*, 1991;Rouault *et al.*, 1991;Rouault *et al.*, 1992). Mitochondrial aconitase catalyses the dehydration and rehydration reactions that convert citrate to isocitrate *via* the *cis*-aconitase intermediate in the citric acid cycle (Rouault *et al.*, 1991). When the iron status of the cell is low cytosolic aconitase loses its iron sulphur cluster (4Fe-4S) to become IRP1 (Beinert & Kennedy, 1993;Philpott *et al.*, 1994). Removal of the 4Fe-4S cluster creates a more open structure which is able to bind IREs (Schalinske *et al.*, 1997). The modulation of IRP1 activity by iron is reversible and thus does not involve permanent alterations to the integrity of the protein (Constable *et al.*, 1992). Unlike IRP1, IRP2 does not possess any aconitase activity and is regulated according to cellular iron levels as it is degraded by the proteosome in the presence of iron and preserved in the absence of iron (Guo *et al.*, 1995).

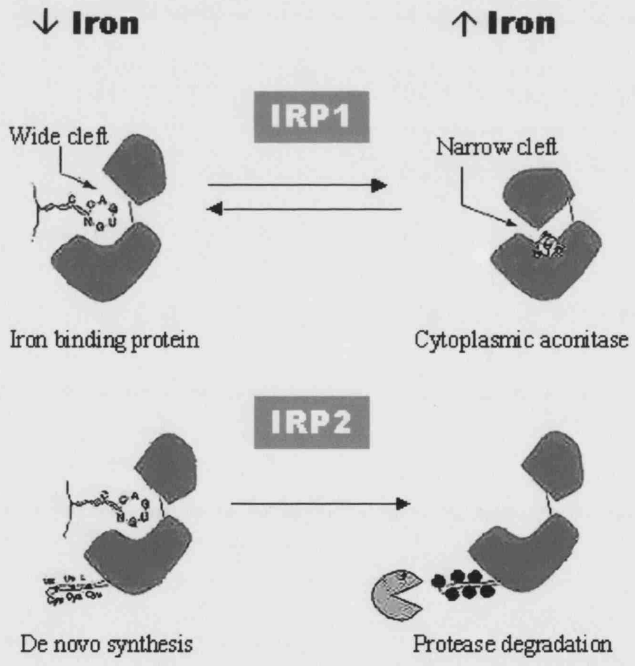

Figure 1. 12 Differential regulation of IRP1 and IRP2

IRP1 is reversibly regulated by cellular iron levels. Under low cellular iron conditions cytoplasmic aconiatse loses its iron sulpher cluster and converts to IRP1. IRP2 is degraded under high iron and stabilised under low iron conditions. Figure adapted from (http://www.uclm.es/inabis2000/symposia/files/138/fig2abc.jpg, 2004)

IRP1 and IRP2 are also differentially regulated by hypoxia (Hanson & Leibold, 1998;Hanson *et al.*, 1999). Iron homeostasis is regulated in two phases during hypoxia: an early phase where IRP1 RNA-binding activity decreases and a late phase where IRP2 RNA-binding activity increases (Schneider & Leibold, 2003).

1.3 Circulation of iron in the body

1.3.1 Transferrin

Iron circulating in the blood is bound to Tf. Tf is a plasma glycoprotein with a molecular mass of 80 kDa (as reviewed by Aisen & *Brown*, 1975). The liver is the main source of Tf, although it is also synthesised in small amounts in the brain, lymph nodes and mammary glands (McKnight *et al.*, 1980a;McKnight *et al.*, 1980b;Galbraith & Galbraith, 1981). Levels are regulated by the status of iron stores i.e. Tf production increases with iron deficiency and decreases with iron loading (McKnight *et al.*, 1980a;McKnight *et al.*, 1980b). Each Tf molecule has two high affinity binding sites for Fe^{3+}, one on the NH_2-terminal domain and another on the COOH-terminal domain of the protein (Figure 1.13)(Bailey *et al.*, 1988;Anderson *et al.*, 1989).

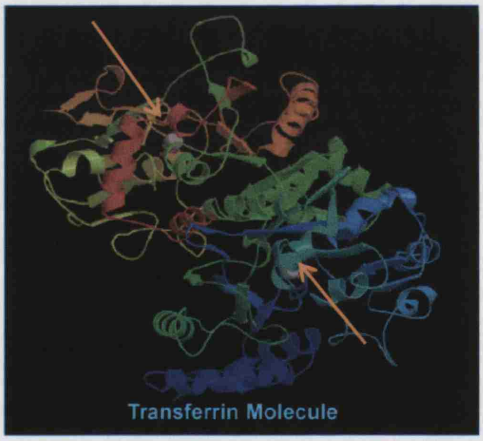

Figure 1. 13 Ribbon representation of the transferrin molecule

*Iron is circulated in the blood bound to transferrin. This glycoprotein has 2 high affinity binding sites for ferric iron. These are shown by arrows. (*http://www.umass.edu/karbon13/people/dmitry/tfn.gif, *2004).*

Tf plays two major functions in iron metabolism: by binding to iron it minimises the amount of free iron in the plasma, reducing the possibility of toxic oxygen radical formation and, it directs

iron to cells that express Tfr1. The importance of Tf is underscored by the effects seen with Tf deficiency: hereditary atransferrinemia caused by a mutation in the *Tf* gene results in severe life threatening anemia (Goya *et al.*, 1972;Bernstein, 1987; Hayashi *et al.*, 1993). Surprisingly, in the absence of Tf iron is absorbed often to excessive levels by a variety of tissues (Levy *et al.*, 1999). This observation is the most striking demonstration that a Tf independent iron transport mechanism exists.

1.3.2 Tfr1

Cells requiring iron display transferrin receptors (Tfr1) on their cell surface in quantities equivalent to their individual needs (Iacopetta *et al.*, 1982). Tfr1 is therefore ubiquitously expressed, especially in highly metabolic tissues such as the placenta and in the erythroid marrow.

Tfr1 is a glycosylated integral membrane protein that exists as a disulfide-linked homodimer of 90 kDa (Kanevsky *et al.*, 1997) (Figure 1.14). Tfr1 is up-regulated by iron starvation and down-regulated by iron loading (Louache *et al.*, 1984;Mattia *et al.*, 1984). This regulation is performed at the post-transcriptional level by IRP binding to IREs in the 3'UTR of the *Tfr1* transcript in an iron dependent manner (Casey *et al.*, 1988;Casey *et al.*, 1989; Kuhn & Hentze, 1992). Expression of Tfr1 is also regulated at the transcriptional level through the status of cell proliferation and oxygen saturation (Miskimins *et al.*, 1986;Lok & Ponka, 1999;Tacchini *et al.*, 1999), and by agents which signal mitogenesis (Tsuji *et al.*, 1991).

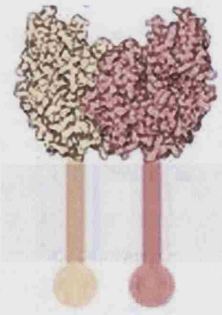

Figure 1. 14 Structure of Tfr1

The transferrin receptor is formed by two identical units (highlighted in yellow and pink). (http://www.chatham.edu/undergraduate/bio/lambert/transferrin/Receptors_files/image002.jpg , 2004).

1.3.3 Tfr1 mediated iron uptake

Circulating Fe_2-Tf binds to the Tfr1 displayed on the plasma membrane. The affinity of this binding increases with the ferric saturation of Tf at the physiological pH of 7.0 (Huebers *et al.*, 1978;Dautry-Varsat *et al.*, 1983). The affinity is also modulated by the hfe protein, which is thought to competitively bind to Tfr1 (Feder *et al.*, 1996;Waheed *et al.*, 1999;West, Jr. *et al.*, 2000).

Once bound to the receptor, the Fe_2-Tf-Tfr1-hfe complex is internalised by invagination of the plasma membrane to form a clathrin coated vesicle (Killisch *et al.*, 1992). Membrane-bound, ATPase dependent, proton pumps lower the internal pH of the vesicle causing a conformational change in the complex. This enables the dissociation of iron from Tf, whilst Tf remains bound to the Tfr1 (Dautry-Varsat *et al.*, 1983;van Weert *et al.*, 1995). Protons also activate DMT1, shown to localise to these recycling endosomes (Gunshin *et al.*, 1997;Fleming *et al.*, 1998;Gruenheid *et al.*, 1999), which actively transports free iron into the cytosol. After the release of iron, the endosome is recycled back to the cell surface (van Weert *et al.*, 1995). Due to the alkaline pH here apo-transferrin is released from Tfr1 (Dautry-Varsat *et al.*, 1983) (Figure 1.15).

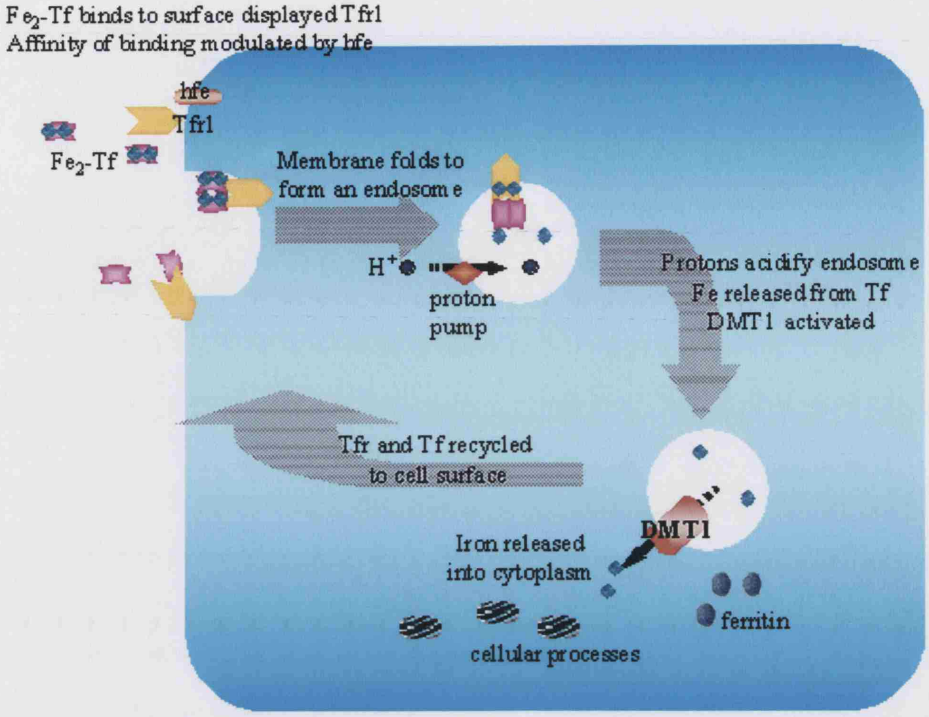

Figure 1. 15 Transferrin mediated iron uptake

Fe_2-Tf binds to Tfr1 displayed on the cell membrane. Once bound the complex is internalised by membrane invagination and formation of a clathrin coated vesicle. This is acidified by proton pumps on the endosomal membrane. Low lumenal pH releases iron from transferrin and increased membrane potential activates DMT1 also present in the endosomal membrane. This transports the released iron into the cytosol where it is utilised for cellular processes or stored in ferritin. The Tf-Tfr1 complex is recycled to the cell membrane where the higher pH releases Tf from Tfr1.

1.3.4 Tfr2

A second form of Tfr1, named Tfr2, is highly expressed in the liver (Kawabata *et al.*, 1999). This is in contrast to Tfr1 which is ubiquitously expressed but at a lower level in the liver (Kawabata *et al.*, 2001). The expression of Tfr2 in the intestine is controversial; a study by Griffiths and Cox (2003) points to the co-localisation of Tfr2 with hfe in intestinal crypt enterocytes, whereas Kawabata *et al.* (2001) showed no expression of the mRNA transcript in this location. In the embryo, hepatic Tfr2 expression increases, whilst Tfr1 levels decrease, with hepatic development (Kawabata *et al.*, 2001).

Tfr2 codes for at least 2 alternatively spliced transcripts: the alpha (α) form approximately 2.9 kbp long (AF067864) and the beta (β) form, approx 2.5 kbp long (AF053356) (Kawabata *et al.*, 1999). In the liver and the erythroid marrow, the α-transcript is highly expressed (Kawabata *et al.*, 1999). The β-form, coded from a start site in exon 4 of the α, has a low and ubiquitous expression (Kawabata *et al.*, 1999). Tfr2-α is a type II trans-membrane protein with high similarity to Tfr1 (Kawabata *et al.*, 1999). Tfr2-β lacks the amino terminal portion, which includes the putative transmembrane domain and part of the extracellular domain. It is therefore thought to be an intracellular form of the receptor (Kawabata *et al.*, 1999). The putative extracellular domain of the Tfr2-α protein is highly homologous to Tfr1 and is able to bind Tf and mediate iron uptake, although the binding affinity of Fe_2-Tf is lower for Tfr2 then Tfr1 (West, Jr. *et al.*, 2000).

Unlike *Tfr1*, *Tfr2* mRNA transcripts do not have any IRE motifs and are therefore unlikely to be regulated by cellular iron levels (Fleming *et al.*, 2000). The Tfr2 promoter contains 2 typical GATA-1 (an erythroid-specific transcription factor) consensus sequences, putative C/EBP binding sites and several CACCC sequences (which could be EKLF consensus sequences involved in the transcriptional control of genes required for erythropoiesis) (Kawabata *et al.*, 2001). Indeed, Tfr2-α mRNA is detected at high levels in the erythroid precursor cells and is down-regulated during erythropoietin induced differentiation *in vitro* (Kawabata *et al.*, 2001). Cell cycle status also regulates *Tfr2* mRNA synthesis, with maximal levels reached during the late G1 phase (Kawabata *et al.*, 2000).

The precise function of Tfr2 is not yet understood, however it is distinct from that of Tfr1. It is possible that cells control iron influx by having two different receptors for Tf: Tfr1, a high affinity receptor that is controlled by cellular iron levels, and Tfr2α, a low affinity transporter whose expression depends on the cell cycle rather than on iron status. A recent study has demonstrated a possible role for Tfr2 in the monitoring of Tf saturation as Fe_2-Tf was demonstrated to increase the half-life of the protein (Johnson & Enns, 2004).

Mutations in Tfr2 result in HH, with clinical symptoms that are very similar to those of hfe related HH, i.e. iron loading in the liver and low iron concentration in the spleen (Camaschella *et al.*, 2000;Roetto *et al.*, 2001). For this reason it is thought that Tfr2 modulates iron homeostasis, possibly in a pathway with the hfe protein.

1.4 Role of the liver in iron homeostasis

The liver is the main site at which nutrients, that have been absorbed from the gut and then transferred to the blood, are processed for use by other cells in the body. It receives a major part of the blood supply directly from the intestinal tract *via* the portal vein. Liver hepatocytes are arranged in folded sheets. These are covered by a single layer of flattened endothelial cells which face into blood filled spaces known as sinusoids (Figure 1.16-1.17). The liver plays an important role in iron homeostasis: it takes up NTBI from the blood, stores excess iron and modulates intestinal iron uptake by the secretion of hepcidin. It also hosts RE macrophages, which play an important role in iron delivery to plasma Tf through phagocytosis of senescent red blood cells, haem-catabolism and recycling of iron. Iron egress from macrophages is probably mediated by Ireg1 as patients with heterozygous Ireg1 mutations develop progressive iron overload in liver macrophages (Wallace *et al.*, 2002).

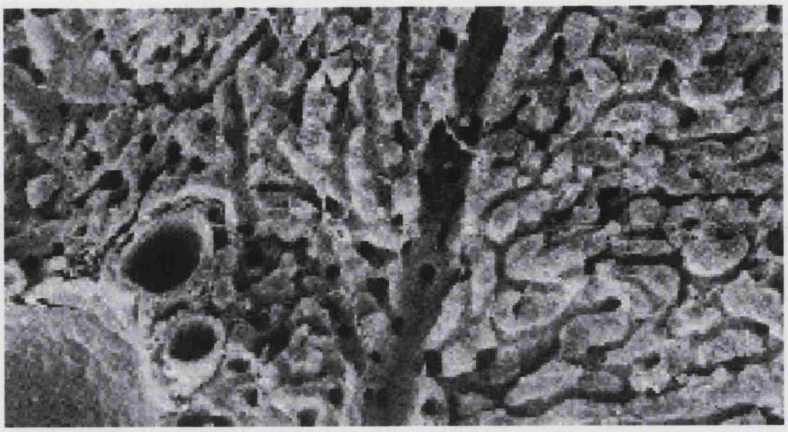

Figure 1. 16 Electron-micrograph of a liver section

Scanning electron micrograph demonstates the hepatocytes arranged in irregular sheets, blood flows through the small channels. The large channel running through the center of the micrograph is a vessel that distributes and collects the blood that flows through the sinusoids, (Alberts et al., 1989).

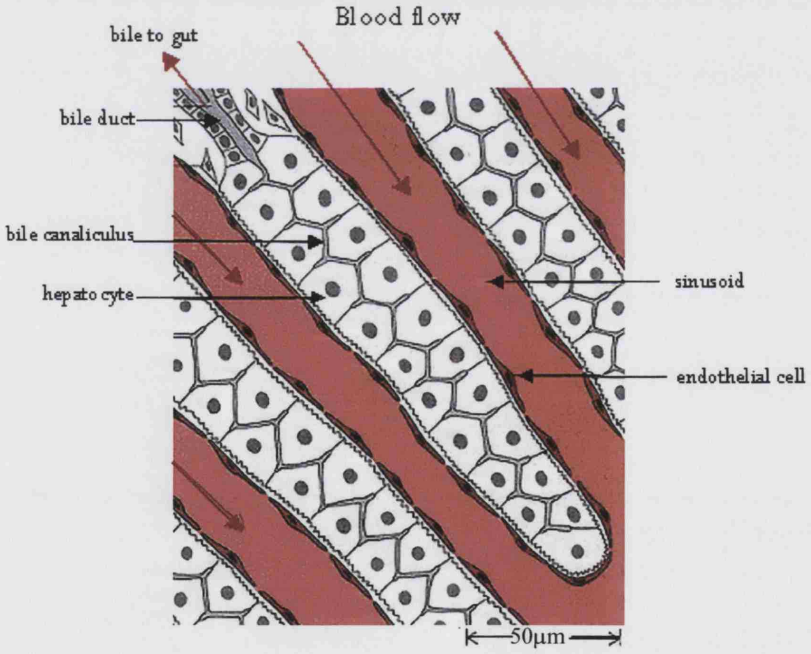

Figure 1. 17 Diagramatic representation of the structure of hepatic tissue

Hepatocytes are arranged in sheets, lined with a single layer of sinusoidal endothelial cells. Blood flows directly over these. The hepatocytes form a system of bile canals. Adapted from Alberts et al., (1989).

Iron in excess of immediate requirements is stored in the liver as ferritin (Loreal *et al.*, 2000;Philpott, 2002). When body iron levels are low, iron is released from the hepatic stores. It is thought that Ireg1, expressed in hepatocytes, releases iron into circulation. This is subsequently oxidised by serum Cp to facilitate binding to circulating apo-Tf.

1.4.1 Ceruloplasmin

Ceruloplasmin (Cp) is a copper-dependent oxidase with roles that include mobilisation of iron from hepatocytes (Osaki & Johnson, 1969), participation in the acute-phase response to inflammation (Bingle *et al.*, 1992), and antioxidant systems (Cranfield *et al.*, 1979). Due to its copper binding ability, Cp is also postulated to have a role as a copper transport vehicle (Frieden & Hsieh, 1976). The secreted form of Cp is produced by the liver and is abundant in serum. A role for Cp in iron metabolism is suggested by its ferroxidase activity and by the tissue iron overload in hereditary Cp deficiency patients. In addition, plasma Cp increases markedly in several conditions of anaemia, e.g. iron deficiency, haemorrhage, renal failure, sickle cell disease, pregnancy and inflammation (Letendre & Holbein, 1984). Cp levels are regulated at the transcriptional level by the binding of hypoxia-inducible factors (HIF) to the three pairs of hypoxia-inducible enhancer sequences located in the 5'UTR of the Cp gene. This binding triggers the Cp promoter to transcribe Cp mRNA (Mukhopadhyay *et al.*, 2000). The activity of HIF is modulated by hypoxia and iron deficiency, as discussed previuosly. Cp is also regulated developmentally, possibly by thyroid hormone and glucocorticoids (Fitch *et al.*, 1999).

1.4.2 Hepcidin

Hepcidin, for HEPatic bacteriCIDal proteIN, is an antimicrobial peptide synthesised in the basolateral membrane of liver hepatocytes (Park *et al.*, 2001;Pigeon *et al.*, 2001;Kulaksiz *et al.*, 2004). It is a cysteine rich peptide, containing eight cysteine residues connected by disulfide bonds (Hunter *et al.*, 2002) (Figure 1.18). It is produced as an 84 aa propeptide (Pigeon *et al.*, 2001), but is found in the plasma and the urine in three forms with different amino terminal truncation. The two most common forms are hepc20 and hepc25, containing 20 and 25 aa respectively. A less common 22 aa form is also detected in the plasma (Park *et al.*, 2001).

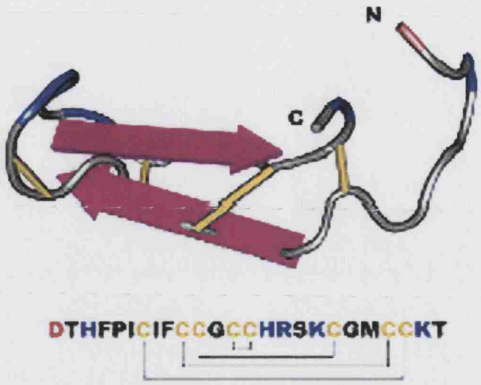

Figure 1. 18 Structural representation of hepcidin

The hepcidin molecule is a short 25 aa peptide consisting of 2 β-sheets. The structure of this peptide is due to the position of 4, highly conserved di-sulphide bonds (Park et al., 2001).

There are numerous lines of evidence linking hepcidin expression to the regulation of iron homeostasis. Over-expression of hepcidin has been linked to reduced duodenal iron uptake: (a) transgenic mice over-expressing hepcidin are severely iron deficient due to decreased duodenal iron uptake (Nicolas *et al.*, 2001); (b) mice showing hepatic iron loading, either by placing on a high iron diet or loading with carbonyl iron or iron dextran, induced hepcidin gene expression in the liver (Pigeon *et al.*, 2001). Additionally decreased expression of hepcidin has been linked to increased duodenal iron uptake: (a) mice lacking the hepcidin gene develop iron loading in the liver, heart and pancreas (Nicolas *et al.*, 2001); (b) dietary iron deficient rats show increased iron absorption accompanied by an increase in duodenal Dcytb, DMT1 and Ireg1, these changes correlate with decreases in hepcidin expression and Tf saturation (Frazer *et al.*, 2002). (c) Mutations in the hepcidin gene cause a severe form of juvenile HH (Roetto *et al.*, 2003).

Expression of hepcidin has also been correlated with Tf saturation and hepatic Tfr2 expression and is inversely correlated with plasma NTBI and erythopoeitin levels (Nicolas *et al.*, 2002a). It therefore appears that hepcidin expression is induced by liver iron loading and that the peptide negatively regulates duodenal iron uptake.

Hepcidin has been demonstrated to specifically depress duodenal bbm iron uptake in Caco-2 cells by down-regulating DMT1 expression (Yamaji *et al.*, 2004). Studies determining the influence of hepcidin levels on duodenal Ireg1 expression have shown conflicting results. Many groups find that changes in hepcidin levels, either due to dietary modifications or to deletion of the hfe gene,

have no effect on Ireg1 levels (Bridle *et al.*, 2003). Other groups however, report that circulating hepcidin influences Ireg1 expression in the mature villus enterocytes of the duodenum, thereby regulating iron absorption in response to body iron requirements (Frazer & Anderson, 2003).

Ireg1 is down-regulated in macrophages in mice with acute inflammation (Yang *et al.*, 2002). This is thought to prevent iron release from the RE system and thereby withhold iron to infectious agents. The mechanism for this may also involve hepcidin, which is up-regulated during acute inflammation. A recent study demonstrated the ability of hepcidin to bind to Ireg1 (Nemeth *et al.*, 2004). This led to internalisation and degradation of Ireg1, inhibting the iron efflux pathway (Nemeth *et al.*, 2004).

In contrast to the human genome the mouse contains two genes encoding hepcidin (Nicolas *et al.*, 2001). The processed 25 aa hepcidin-2 peptide shares 68% identity with hepcidin-1 with perfect conservation of the eight cystine residues (Ilyin *et al.*, 2003). Both have similar genomic organisation, with three exons and two introns and probably arise due to duplication of chromosome 7 (Ilyin *et al.*, 2003). Both isoforms are highly expressed in the liver and to a much lesser extent in the heart although, unlike hepcidin-1, hepcidin-2 is also highly expressed in the pancreas (Ilyin *et al.*, 2003). The expression of both hepcidin genes is thought to respond coordinately to dietary iron content; increasing with high iron and decreasing with low iron diet, suggesting that the expression of both transcripts is regulated by iron status (Ilyin *et al.*, 2003;Mazur *et al.*, 2003). However, hepcidin-1 and hepcidin-2 have distinct roles as transgenic mice over-expressing hepcidin-1 show severe iron-deficient anemia. In contrast the hematological parameters of transgenic hepcidin-2 mice are similar to non-transgenic littermates (Lou *et al.*, 2003). This suggests that only hepcidin-1 modulates duodenal iron absorption.

Antimicrobial peptides have an important role in the innate immune system of most species including plants, insects, fish, amphibians and mammals (Andreu & Rivas, 1998). Their antimicrobial activity is mainly due to the disruption of the microbial cytoplasmic membrane which increases its permeability (Ganz & Lehrer, 1995; Hancock, 1997;Ganz, 1999). Because of this rather non-specific mechanism, antimicrobial peptides are active against a broad spectrum of agents including bacteria: *Escherichia coli, Staphylococcus epidermidis,* and group *B Streptococcus*, yeasts, fungi: *Candida albicans, Apergillus fumigatus* and Aspergillus niger and viruses. Hepcidin-20 has more potent anti-fungal activity then hepcidin-25 (Park *et al.*, 2001). Hepcidin is synthesised in response to bacterial infection and inflammation (Park *et al.*, 2001;Pigeon *et al.*, 2001;Shike *et*

al., 2002). It is therefore thought to play a role in defense against infection by depriving microorganisms of a ready source of iron.

Hepcidin expression is therefore modulated by Tf saturation, erthryopoeitin levels, NTBI and Tfr2 expression. Most of these factors are primarily dependent on erythropoietic demand. How the liver senses erythropoietic demand and body iron levels, thus adjusting hepcidin expression accordingly, is not yet known.

1.5 Erythropoiesis

Erythropoiesis requires 20 mg of iron per day, therefore iron and erythropoiesis are inextricably linked. Erythropoiesis is triggered by a lack of oxygen or a shortage of erythrocytes (Mendel, 1961;Tribukait, 1963). The principal factor in the regulation of erythropoiesis is a glycoprotein hormone named erythropoietin (Epo) (Napier *et al.*, 1977).

1.5.1 Erythropoietin

Erythropoietin is a 51 kDa highly glycosylated protein, which structurally belongs to a family of cytokines (Manavalan *et al.*, 1992). It is produced primarily by the kidney in response to a lack of oxygen or a shortage of erythrocytes (Jacobson *et al.*, 1957). It binds to erthropoietin receptors expressed on erythrocyte colony forming cells and stimulates the maturation and release of new erythrocytes (Mayeux *et al.*, 1993;Pharr *et al.*, 1993). The production of new erythrocytes requires a large amount of iron, and possibly for this reason erythropoietin negatively regulates hepcidin expression (Nicolas *et al.*, 2002a).

Serum Epo levels are negatively correlated to the haematocit (Schrezenmeier *et al.*, 1994). Regulation of Epo gene expression occurs mainly at the transcriptional level. A hypoxia-inducible enhancer, similar to those present in the 5'UTR of Cp, is present in the 3' flanking region of the Epo gene (Dube *et al.*, 1988;Blanchard *et al.*, 1992;Mukhopadhyay *et al.*, 2000). Hypoxia-inducible factor 1 (HIF-1) binds to this region and triggers the Epo promoter to transcribe *Epo* mRNA (Huang *et al.*, 1997;Kvietikova *et al.*, 1997).

HIF complexes contain two proteins, HIF-α and HIF-ß. A hydroxyl (-OH) group is added to proline 564, located within the oxygen-dependent degradation domain of HIF-1, in an iron- and oxygen-dependent manner. The product of the von Hippel-Lindau tumour suppressor gene pVHL, binds to the modified region on the HIF-α and targets it for degradation (Hoffman *et al.*, 2001;Ivan *et al.*, 2001). Therefore the HIF-α is degraded rapidly under normal oxygen concentrations, but is stabilised under hypoxia. This increases serum Epo levels in the presence of anaemia (Takeichi *et al.*, 1988;Schrezenmeier *et al.*, 1994).

Interestingly, in young mice, from the age of 10 day to weaning at 20 day, iron also induces Epo production. This is not seen in adult mice (Bechensteen & Halvorsen, 1996).

1.6 The Placenta

The placenta is a complex and dynamic organ whose structure and function changes throughout pregnancy. It is the first organ to form and function in development and is central to vivaparity. It allows the embryo to implant into the uterus, mediates nutrient, gas and waste exchange between the foetus/embryo and the mother, and directs maternal metabolism, ovarian function, growth and blood supply to the uterus.

1.6.1 Comparison of human and rodent pregnancy

Rodents are extremely attractive models in which to study development and physiology because gestation is short and it is possible to control both genetic and environmental influences. A number of features of pregnancy are similar between humans, rats and mice. They show similar gestation stage-dependent changes in maternal blood pressure, such that during a normal pregnancy blood pressure actually falls during late gestation (Wong *et al.*, 2002). Despite some differences in gross anatomy and physiology, humans and rodents share considerable cellular and molecular features (Table 1.2) (Figure 1.19). Both have hemochorial placentae i.e. ones in which maternal blood directly irrigates the feto-placental epithelium (Hemberger & Cross, 2001;Rossant & Cross, 2001). However there are two main differences between rodents and humans. First, in rats gestation lasts approx 20 days, with implantation occurring on gestation day (gd) 4.5 and formation of the beating heart and vascularised placenta completed by gd 10. Therefore, the events of later development that take the last 8 months of gestation in humans occur in only the last 9 days in rats and mice. The second major difference is that rats and mice are a litter bearing species.

	Human	Mouse
Length of gestation	9 months	20 days
Timing of implantation (post-fertilisation)	7 days	4.5 days
Initiation of foetal heartbeat	21 days	8.5 days
Vascularisation of placental villi	25 days	10 days
Hemochorial blood flow through placenta	yes	yes
Chorionic villi lined by syncytiotrophoblast	yes	yes
Invasive trophoblast entering uterine spiral arteries	extravillous cytotrophoblast	trophoblast giant cells

Table 1. 2 Comparison of human and mouse pregnancy

From (Cross, 2003).

1.6.2 Placental structure

In rats and mice there are three types of trophoblast cells (Figure 1.19). The first to differentiate, known as trophblast giant cells, are polyploid cells which surround the conceptus and direct contact and implantation with the maternal decidua. These have a crucial role in remodeling the embryonic cavity, avoiding maternal immune rejection and promoting blood flow to the implantation site. The equivalent cells in human placenta are known as extravillous cytotrophoblast cells. Both cell types lie on the outermost edge of the placenta, have inherent invasive behavior and express othologous genes, e.g. the matrix-degrading enzyme metalloproteinase 9 (Bany *et al.*, 2000;Isaka *et al.*, 2003) and cell adhesion molecule α,β integrin (Downs, 2002;Hanashi *et al.*, 2003). However, the human extravillous cytotrophoblast cells are not polyploidal and do not produce hormones similar to those produced by the trophoblast giant cells of the rodent.

The spongiotrophoblast and trophoblast giant cells form the ectoplacental cone in the mouse. This is equivalent to the cytotrophoblast cell columns in humans which produces othologous genes e.g. Mash-2 (mammalian achaete/solute homologue-2) required for the maintenance of the trophoblast stem cell population (Guillemot *et al.*, 1994).

The bulk of the mature rodent placenta is a densely branched, villous tree-like structure, termed the labyrinth. In mid gestation, chorion trophoblast cells interact with the extraembryonic mesoderm of the allantois to fold into the villus tree-like labyrinth. Blood vessels form within the mesoderm to create the feto-placental capillary network. The surface of the labyrinth is covered by a single layer of mononuclear trophoblast cells and two layers of syncytotrophoblast. The murine labyrinth is functionally analogous to floating chorionic villi in humans, in having a large villus-tree like structure and in being covered by syntial (syncytiotrophoblast) layers, reviewed in (Cross, 2000).

Human cytotrophoblast differentiate into either floating or anchoring chorionic villi. During generation of the floating villi, cytotrophoblast stem cells detach from the underlying basement membrane and fuse to form a multinucliate syncytium that encase the villi that float in maternal blood. Cytotrophoblast stem cells also detach from the basement membrane and form aggregates of unpolarised cells. These are called columns and adhere to the uterine wall. Cells emanating from these columns invade the entire endometrium and the first third of the myometrium this anchors the placenta to the uterus. These cells also breach and enlarge the maternal spinal arterioles, and to a lesser extent, veins. Blood in these vessels bathe the floating villi before it returns to the maternal circulation *via* the uterine veins.

The outermost cells of the rodent placenta are trophoblast giant cells, which are analogous to extravillous cytotrophoblast cells in the human placenta. As in humans a specialised subset invades the uterine wall in close proximity to the spiral arteries and replaces the endothelial lining of the arteries. This promotes the transition from endothelial lined artery to trophoblast-lined {hemochorial} blood space. These distinct trophoblast cell subtypes in humans and mice share common gene expression patterns (Hemberger & Cross, 2001). Rats and mice therefore make useful models in which to study placental transport and the effect of pregnancy on iron homeostasis.

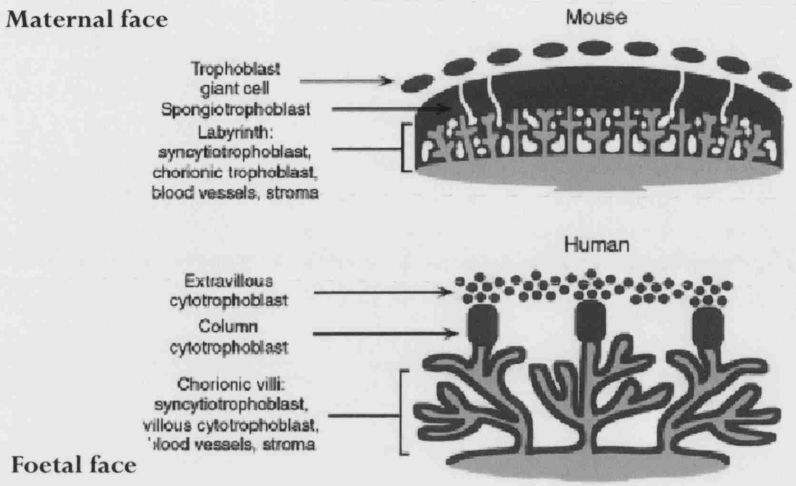

Figure 1. 19 Structural comparison of the human and rodent placenta

Humans, rats and mice have hemochorial placenta, i.e. the mothers blood is separated from the foetal blood by a single (syncytiotrophoblast) epithelial layer. The placenta, in all three species, consist of 3 cell types. In the humans these are termed the extravillous- column- cytotrophoblast and the choronic villi which are lined with the syncytiotrophoblast. The analogous layers in mice consist of the Trophoblast, Spongiotrophoblast and the chorionic trophoblast, from (Cross, 2003).

Various placental cell lines are available and are a useful tool in which to elucidate placental transport mechanisms. One such cell line, BeWo derived from a human malignant gestational choriocarcinoma, shows many characteristics of trophoblastic epithelial cells. When fully differentiated these cells secrete placental hormones, including gonadotrophin, lactogen and steroid hormones, and express transferrin receptor on both apical and basolateral cell surfaces (Cerneus & van der, 1991).

1.6.3 Placental Iron Transport

The mechanisms involved in placental iron transport are highly efficient, since foetal serum iron concentrations normally exceed those in maternal circulation (Okuyama *et al.*, 1985). Iron uptake by the placenta is through Tfr1 (Galbraith *et al.*, 1980;McArdle & Morgan, 1982;Baker *et al.*, 1983;McArdle *et al.*, 1984;McArdle *et al.*, 1985;van der *et al.*, 1987;Bergamaschi *et al.*, 1990). These are highly expressed on the microvillous surface of syncytiotrophoblast in immature and term placentae (Galbraith *et al.*, 1980;King, 1976;Okuyama *et al.*, 1985;Bierings *et al.*, 1991). Fe_2-Tf binds to Tfr1 and is internalised in clathrin coated pits (McArdle *et al.*, 1985). Hfe is also expressed in coated pits along the syncytiotrophoblast apical plasma membrane (Parkkila *et al.*, 1997a;Leitner *et al.*, 2002) where it is physically associated with the Tfr1 and β_2-microglobin (Bergamaschi *et al.*, 1990;Parkkila *et al.*, 1997a). Endosomes containing the Fe_2-Tf-Tfr1-hfe complex, are acidified by proton pumps, which releases the iron from Tf (McArdle *et al.*, 1985). Iron crosses the endosomal membrane presumably *via* DMT1 (Figure 1.20) (Georgieff *et al.*, 2000;Tabuchi *et al.*, 2000). DMT1 is localised intracellularly and on the basal (foetal facing) membrane of the syncytotrophoblast as well as in the hofbauer (resident macrophage) cells, while Tfr1 is localised predominantly in the maternal (apical) side of the syncytiotrophoblastic membrane (Georgieff *et al.*, 2000). How DMT1 is brought together with the iron released from Tfr1 is not known.

Whilst the majority of iron is transported across the syncytiotrophoblast, a small amount remains within the cell. This iron accumulates and is stored in ferritin (Figure 1.20) (Okuyama *et al.*, 1985 Contractor & Eaton, 1986;Verrijt *et al.*, 1999).

Efflux of iron out of the syncytotrophoblast is probably as Fe^{2+} through Ireg1 (Donovan *et al.*, 2000b). In the mouse placenta Ireg1 is located on the blm (Abboud & Haile, 2000;Donovan *et al.*, 2000;McKie & Barlow, 2003). Before iron is incorporated into foetal Tf it is oxidised by a placental homologue of ceruloplasmin which is located in a perinuclear compartment (Figure 1.20) (Danzeisen *et al.*, 2000;Danzeisen *et al.*, 2002).

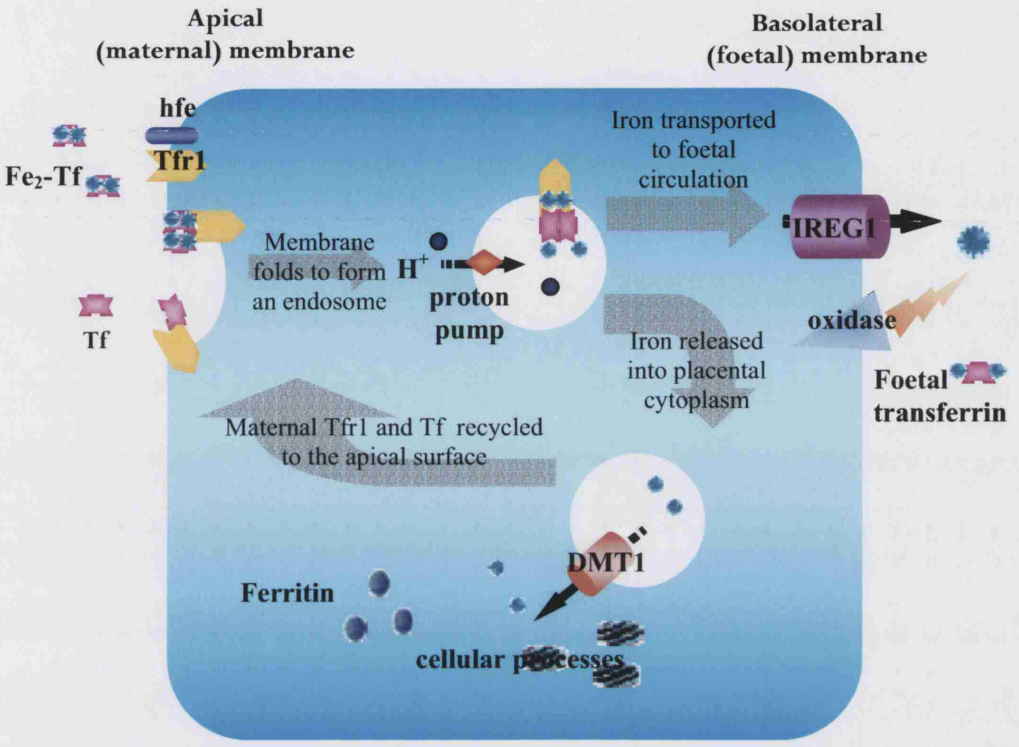

Figure 1. 20 Hypothesised mechanism for placental iron transfer

Fe_2-Tf attaches to Tfr1 displayed on the apical membrane of the placenta. Hfe protein also binds to Tfr1 and thereby affects its affinity for Fe_2-Tf. The Fe_2-Tf-Tfr1 complex is internalised within an endosome. Proton pumps lower the pH within the endosome, reducing the affinity of iron for Tf. Free iron is transported out of the endosome by DMT1. Tf and Tfr1 are subsequently recycled to the apical membrane. Iron is transported across the basolateral membrane of the placenta by Ireg1 coupled to an oxidase. Iron is subsequently transported in foetal circulation bound to foetal transferrin.

It is the placenta, and not the foetus, which regulates iron uptake, as the placenta continues to accumulate iron for at least 28 hours after foetalectomy (McArdle & Morgan, 1982). This indicates that placental iron uptake is does not receive continous feedback from the foetus.

1.6.4 Regulation of iron transfer by gestational age

The transfer of iron across the syncytiotrophoblast is not constant. By far the greatest amount is transferred during the final trimester when foetal requirements peak (McArdle & Morgan, 1982). The increase in iron transfer during pregnancy is a result of a number of modifications to the placental physiology as well as specific enhancement of the placental iron transport system. Morphological changes include the thinning of the syncytiotrophoblast and an increase in the placental blood flow as pregnancy progresses (Moll, 2003). At the molecular level a gradual increase in Tfr1 and DMT1 expression on the maternal surface of the placenta is observed (McArdle & Morgan, 1982;Leazer *et al.*, 2002). In addition the iron efflux mechanism matures during development (McArdle & Morgan, 1982).

1.6.5 Regulation of placental iron transfer by maternal iron status

During pregnancy maternal iron deficiency can induce anaemia in the developing foetus. However the severity tends to be less than that of the mother, as protective mechanisms ensure iron is preferentially available to the foetus (Harthoorn-Lasthuizen *et al.*, 2001). These protective measures respond to reduced placental non-haem levels, foetal and maternal iron deficiency, by enhancing placental iron transport (Bergamaschi *et al.*, 1990). These modifications involve stimulation of Tfr1 synthesis (Kroos *et al.*, 1996), redistribution of Tfr1 from intra-cellular pools to the cell surface (Starreveld *et al.*, 1993) and increased placental volume (Huang *et al.*, 2001). Iron deficiency also increases TNFα and TNFα receptor 1 levels in the placenta (Benyo *et al.*, 1997). This may be a part of the mechanism for placental restructuring, or a signal to modulate maternal iron homoeostatic mechanisms directly. Although, in Caco-2 cells TNFα decreased iron uptake by upregulating ferritin and downregulating DMT1 and Tfr1 (Johnson *et al.*, 2004). However, in many studies these modifications are not apparent and iron transport is not increased with low iron levels (Bergamaschi *et al.*, 1990;Starreveld *et al.*, 1996).

Iron deficiency prior to the onset of pregnancy however, results in decreased capillary surface area density, total capillary area and capillary length and increased endothelial cell volume (Lewis *et al.*, 2001).

The reverse of these cellular responses to iron deficiency is seen with iron loading, in that a reduction in Tfr1 expression on the apical membrane is evident and ferritin synthesis is enhanced (Bergamaschi *et al.*, 1990;Bierings *et al.*, 1991;Starreveld *et al.*, 1995).

1.6.6 Regulation of placental iron transfer by cellular iron levels

Placental iron homeostasis is regulated, in part, by coordinated stabilisation of *Tfr1* mRNA and translation inactivation of *ferritin* mRNA by IRP-1 and -2. IRP-1 activity inversely correlates with cord serum ferritin and placental non-haem iron concentration (Georgieff *et al.*, 1999). Placental cellular iron homeostasis is therefore probably regulated by IRE-IRP interactions, in much the same way as in other tissues.

1.6.7 Expression of Cytokines and Erythropoietin by the placenta

Cytokines are intercellular messenger proteins released by white blood cells. They facilitate communication between cells of the immune system and the rest of the body. The cytokines interleukin-6 (IL-6) and tumour necrosis factor-α (TNFα) also have a role in the modulation of *hepcidin* expression (Nemeth *et al.*, 2003). The placenta also produces various cytokines, which regulate growth and development. Production of TNFα, IL-6 and IL-1ß is highest in the first trimester and declines as cytotrophoblasts differentiate into syncytiotrophoblast, they are also present in term placenta (Kameda *et al.*, 1990;Chen *et al.*, 1991). TNFα production is elevated in response to hypoxia in placental cell lines (Benyo *et al.*, 1997). TNFα levels also increase in the trophoblast giant cells of the placenta during iron deficiency (Benyo *et al.*, 1997).

Epo is produced at very small levels by the trophoblast cells of the human placenta (Davis *et al.*, 2003). Expression is increased under hypoxic conditions (Davis *et al.*, 2003). Not much is known about the effect of Epo on the placenta, although a role for this hormone in the survival, proliferation, or differentiation of trophoblast cells has been proposed (Conrad *et al.*, 1996;Fairchild & Conrad, 1999;Kim *et al.*, 2001).

1.6.8 NTBI uptake by the placenta

In the placenta of the guinea pig, which is also haemochorial, the transfer of maternal iron to the syncytiotrophoblast is very fast, suggesting that NTBI may also be involved in placental iron transfer (Wessling-Resnick, 2000). Elevated NTBI levels are detected shortly after the ingestion of iron supplements in plasma and in umbilical cord blood (Breuer *et al.*, 2000). However no direct evidence has yet been seen for the transport of NTBI across the placenta.

1.6.9 Placental transferrin secretion

During pregnancy Tf plays a key role in iron transport across the placenta. It is also present in relatively high concentrations in amniotic fluid, though it has a different glycosylation pattern compared to maternal Tf (van Dijk *et al.*, 1993). Placental trophoblast cells also synthesise Tf with an identical carbohydrate structure to that of amniotic fluid Tf (Boockfor *et al.*, 1994;Streu *et al.*, 2000). This amniotic Tf modulates the endocrine function of trophoblast cells in culture by regulating progesterone production (Streu *et al.*, 2000). The secretion of placental Tf is therefore unlikely to modulate maternal iron homeostasis *via* a simple process of Tf displacement (Brown *et al.*, 1982).

During pregnancy numerous physiological modifications occur in order to meet the iron requirements of the developing foetus. These include increasing duodenal iron absorption. The mechanism of this increase has been demonstrated to involve the upregulation of *DMT1*. How *DMT1* is upregulated in this circumstance is not known but may involve decreased maternal or cellular iron status. Hfe and hepcidin may also be involved in this mechanism. Additionally placental, foetal or hormonal factors may influence this increase.

Iron efflux to the foetus is also not constant throughout pregnancy. Placental iron transfer is most substantial during the final trimester. The mechanism behind this is not yet known, but may also involve an increase in DMT1, Tfr1 and/or Ireg1 all of which have been localised to the placenta. Iron deficiency during pregnancy is less pronounced in the foetus than in the mother, this implies a compensatory mechanism of the placenta and the upregulation of the placental iron transport mechanism under maternal iron deficiency. This is possibly responsive to maternal transferrin saturation, iron stores and/or maternal serum hepcidin. The foetal liver may also produce and secrete hepcidin, adding further complexity to the regulatory mechanism.

1.7 Aims

To identify the mechanism by which duodenal and placental iron transport are regulated during pregnancy, the expression of iron transporter and modulator genes is quantified in the liver, gut and placenta. A $hfe^{-/-}$ mouse model is used to elucidate the role of hfe in the regulation of iron absorption under dietary iron deficiency and loading.

The molecular mechanism of placental iron transport will be elucidated in a cell culture model with the use of immunohistochemical techniques, and the role, if any, of hepcidin in placental iron transfer will be determined.

2 General Methods

2.1 Stocks, Solutions, Buffers and Gel Recipes

Balanced Salt Solution (BSS)

4 g NaCl

0.2 g KCl

0.1 g $MgCl_2$

2.1 g Hepes

450 mL H_2O, adjust pH to 7.4, top up with H_2O to 500 mL

DEPC water

1 mL Diethyl Pyrocarbonate (DEPC)

999 mL dH_2O

autoclave to destroy DEPC, incubate at 37°C o/n to remove CO_2 released from DEPC breakdown

$^{59}Fe_2$-Tf

40 µL BSS

50 µL of $NaHCO_3$ (7.5%)

25 mM apo-transferrin

$^{59}FeCl_3$ (50 nM) in 0.1 M HCl, added dropwise to the apo-transferrin

Hepes buffer

1 g Hepes

0.074 g KCl

0.027 g $Na_2HPO_4 \bullet 2H_2O$

1.6 g NaCl

0.2 g Dextrose

pH 7.5 with 0.5 M NaOH

Dilute to 100 mL with H_2O

Phosphate buffered saline (PBS) pH 7.5

11.5 g Na_2HPO_4

2.96 g NaH_2PO_4

5.84 g NaCl

Dilute to 1000 mL with distilled water. Adjust pH if necessary.

PBS-Tween (PBS-T)

100 µL Tween-20

100 mL PBS

RIPA buffer

8.6 g NaCl

1.6 g Tris HCl

0.4 g EDTA•$2H_2O$

10 mL NP40

5 mL 20% SDS

Dilute to 1L

Saline

9 g NaCl

dH_2O to 1L

50x TAE buffer

242 g Tris base

100 mL 0.5M EDTA pH 8.0

57.1 mL glacial acetic acid

dH_2O to 1L, dilute 1/10 for working solution

0.5M EDTA

18.6 g EDTA

dH_2O to 100 mL

pH 8.0 with NaOH

Tris buffered saline (TBS) pH 7.6

2.42 g Tris base

8 g NaCl

3.8 mL 1M HCl

Dilute to 1 L with distilled water. Adjust pH if necessary.

Western Blotting buffers

10% APS

0.1 g Ammonium persulphate

1 mL dH_2O

Electrophoresis buffer

10x Tris/Glycine/SDS buffer from BioRAD (Hertfordshire, U.K.)

dilute to 1x with dH_2O

2x Loading buffer

2.5 mL Tris-HCl pH 6.8

4 mL 10% SDS

2 mL Glycerol

2 mg Bromophenol blue

0.31 g dithothreitol (DTT)

make up to 10 mL with dH_2O and store at –20°C for 6 months

10% SDS PAGE gel

for 2 running gels:

5.2 mL dH_2O

4.3 mL 30% BIS Acrylamide

3.3 mL TRIS-HCl pH 8.8

130 µL 10% SDS

6.6 µL TEMED

66 µL 10% APS, freshly prepared- add last

Stacking gel buffer

3.0 g TRIS

40 mL dH_2O

pH to 6.8 with HCL

make up to 50 mL with dH_2O, wrap in foil and store in dark for up to 3 months

Stacking gel

For 2 stacking gels:

4.05 mL dH_2O

1005 µL 30% Bis Acrylamide

750 µL stacking gel buffer (Tris-HCl pH 6.8)

60 µL 10% SDS

6 µL TEMED

60 µL 10% APS, freshly prepared-add last

Transfer buffer

3.03 g Tris

14.41 g glycine

1.0 g SDS

100 mL methanol

make up to 1 litre, pH should be 8.2 to 8.4

<u>Agarose gel electrophoresis</u>

1% TAE agarose gel with ethidium bromide

1.5 g agarose (4.5 g for a 3% gel)

150 mL 1x TAE

ethidium bromide 0.5 g/mL

10x loading buffer for agarose gel electrophoresis

0.4 % bromophenol blue (w/v),

67 % glycerol

in 10x TAE buffer

DNA markers for agarose gel electrophoresis

100-1000 kb Hyperladder IV (Bioline, London, U.K.)

5 µL loaded per gel

Unless otherwise specified all reagents were purchased from Sigma (Poole, U.K.) and were of the highest grade available.

2.2 Methods

2.2.1 Animal models

A number of rodent models were used in this thesis:

1) Male Sprague-Dawley rats, C57blk/6 and hfe knockout (originally mixed 129/Ola-C57blk/6 background strain) mice were provided by the Comparative Biology Unit at the Royal Free and UCL Medical School, London. Experimental procedures were approved and conducted in accordance with the U.K. animals (Scientific Procedures) Act, 1986.

2) Material from Wistar rats, originally brought from Charles River, was kindly provided by Prof Robert Crichton and Dr Roberta Ward at the Unité de Biochimie, Université de Louvain, Louvain-la-Neuve, Belgium. Animals received humane care in compliance with the recommendations of EEC (86/609/CEF), the guidelines of the GSF-National Research Center for Environment and Health, Neuherberg, Germany, and the Belgian "projet de loi" (Moniteur Belge 19.92.1992).

3) Material from Rowett Hooded Lister rats was provided with collabaration with Prof Harry M^{c}Ardle and Dr Lorraine Gambling at the Rowett Research Institute, Aberdeen, U.K. Experimental procedures were approved and conducted in accordance with the U.K. animals (Scientific Procedures) Act, 1986.

All animals were reared in a 12 hour light/ 12 hour dark cycle and received food and water *ad libitum*.

4) Human placental samples were collected by Wendy Hollands from Maternity Department of the Norfolk and Norwich University Hospital, Norwich, U.K. The study was approved by the Norwich Local Ethics Committee and the East Norfolk and Waveney Research Governance Committee.

2.2.2 Cell Culture

BeWo cells were used as a model of the placental syncytiotrophoblast. This cell line, originally isolated by Pattillo and Gey in 1968, demonstrates many of the biochemical and morphological parameters associated with the placental syncytiotrophoblast. BeWo cells synthesise and secrete a number of placental hormones including estrogenic and progestational steroids, human placental lactogen, and human chorionic gonadotropin. Treatment with methotrexate or forskolin stimulates dramatic morphological changes, i.e., cell division is arrested but DNA synthesis and nuclear division continue, resulting in multinucleated cells resembling the syncytiotrophoblast of placenta (Speeg *et al.*, 1976; Friedman & Skehan, 1979;Wice *et al.*, 1990).

Transwells™ (Costar, London, U.K.) provide a physical but porous support for cells (Figure 2.1). When grown on these filters BeWo cells form a polarised monolayer and display directional transport features (Cerneus & van der, 1991;Cerneus *et al.*, 1993;Qian *et al.*, 1996;Danzeisen *et al.*, 2000). For these reasons BeWo cells are routinely used to study placental iron uptake and flux (van der *et al.*, 1987;van der *et al.*, 1989;van der *et al.*, 1990;Cerneus & van der, 1991;Cerneus *et al.*, 1993;Qian *et al.*, 1996;Danzeisen *et al.*, 2000;Danzeisen *et al.*, 2002).

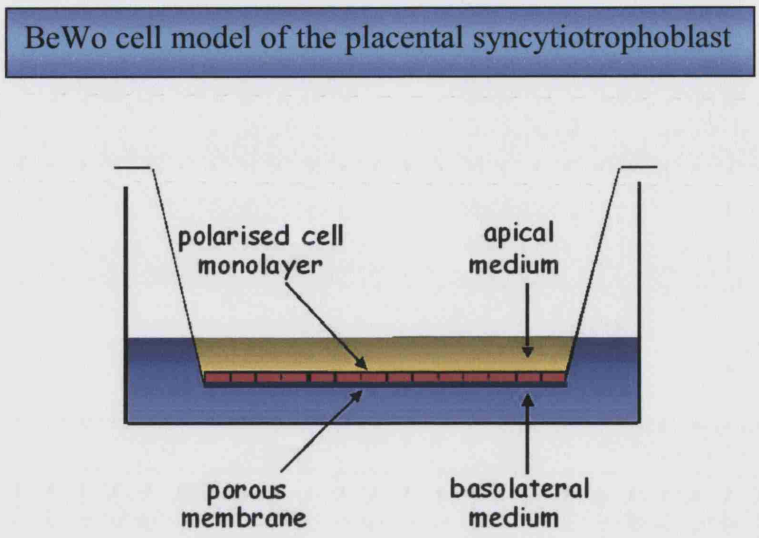

Figure 2. 1 The Transwell model of the placental syncytiotrophoblast

When grown on Transwells BeWo cells form a polarised monolayer. The apical membrane produces microvilli and is representative of the apical membrane of the syncytiotrophoblast. The Transwell format isolates the apical (maternal) and basolateral (foetal) systems, allowing the independent manipulation of each. Figure adapted from S. Yamaji (Royal Free & UCL Medical School, London).

BeWo cells were obtained from the European Collection of Animal Cell Cultures (Salisbury, Wilts., U.K.). Cells were routinely cultures in 70 cm^2 flasks and maintained in Ham's F-12 with L-Glutamine media (Invitrogen, Renfrew, Renfrewshire, U.K.) supplemented with 20% FBS (Sigma, Poole, U.K.), penicillin (200 units/mL) and streptomycin (200 μg/mL) (Sigma, Poole, U.K.), at 37°C in a 95% air/5% CO_2 mixture. The media was refreshed every 24 hours.

2.2.3 Iron uptake assays

The protocols used to quantify *in vitro* iron uptake from rat proximal duodenum were adapted from that outlined by Smith *et al.* (2000).

2.2.3.1 *In vitro* Ferrous Iron Uptake in rat duodenum ('everted loop' method)

Immediately following culling, a 2 cm section of proximal duodenum was removed and rinsed with oxygenated Hepes buffer. The tissue was everted on a Perspex rod and firmly secured by means of ligatures at both ends of the segment. The tissue was placed in oxygenated Hepes buffer at 37°C. After 5 minutes the rod was transferred to the oxygenated incubation buffer [200 μM $^{59}Fe^{2+}$, 4 mM ascorbic acid, Spec Act 14 μCi/mL, in Hepes buffer]. During both incubations, a rotating stir bar ensured adequate exposure of tissue surface to the solution by minimising the effects of unstirred water layers. Following incubation, the tissue was washed in excess non-radioactive Fe-ascorbate at 0°C to displace surface-bound iron. Two further washes in Hepes buffer and one wash in PBS were carried out at room temperature (rt, 20°C±2°C). ^{59}Fe content of tissue was counted on a Cobra 5003 Auto-Gamma Counter (Packard Instrument Co., Meriden, CT, USA). Tissue sections were blotted dry and weighed. ^{59}Fe uptake was expressed as μmole ^{59}Fe uptake per gram wet tissue weight per minute.

2.2.3.2 *In vitro* Ferric Iron Uptake in rat duodenum ('ring' method)

Immediately following culling of animal, proximal duodenum was collected, rinsed with oxygenated Hepes buffer and cut into approximately 5 mm rings. These were stored in oxygenated Hepes buffer at 15°C for a maximum of 3 hours this allowed the duodenal rings to spontaneously evert thus exposing the microvillus surface to the buffer. Before uptake, duodenal rings were placed in oxygenated Hepes buffer at 37°C for 5 minutes, and were then transferred to oxygenated uptake solution [500 μM Fe, 1 mM NTA, Spec Act 250 μCi/mL, in Hepes buffer] at 37°C for 5 minutes. The incubation period of 5 minutes was chosen on the basis of previous studies investigating iron entry into *in vitro* preparations of duodenum (Cox & Peters, 1979; Raja *et al.*, 1989), where uptake was found to be linear with time for up to 10 minutes. Uptake was terminated and surface bound ^{59}Fe displaced by incubating duodenal rings in ice cold wash buffer containing excess non-radioactive iron [1 mM Fe, 2 mM NTA, in Hepes buffer] for 3 x 5 minutes. Duodenal rings were finally washed with PBS and ^{59}Fe content of tissue quantified on a Cobra 5003 Auto-Gamma Counter (Packard Instrument Co., Meriden, CT, USA). Tissue sections were blotted dry and weighed. ^{59}Fe uptake was expressed as μmole ^{59}Fe uptake per gram wet weight tissue per minute.

2.2.4 Protein Quantification

Tissues were resuspended in RIPA buffer to extract proteins. The protein concentration of the lysate was determined using the Pierce BCA (bicinchoninic acid) Protein Assay (Pierce, Rockford IL, USA). 50 parts reagent A was combined with 1 part reagent B. 2 mL of the reaction mix was mixed with 0.1 mL of the cell homegenate. Reactions were incubated for 30 minutes at rt. The absorption of the reaction products was measured at 562 nm visible light using a Beckman Du®650 spectrophotometer (Beckman Coulter, Fullerton, CA. USA). Each sample and standard was tested in duplicate. A standard curve of duplicate BSA concentrations ranging from 25 to 2000 μg/mL was produced. Protein concentration of samples were back-calculated from this.

2.2.5 Quantitative gene expression

2.2.5.1 Tissue Collection and Storage

Tissue for RNA analysis was immediately collected from culled animals and snap frozen in liquid N_2. Long term storage of tissue was at –80°C. Tissues collected by collaborators in Aberdeen and Brussels were also snap frozen in liquid N_2 and shipped on dry ice.

2.2.5.2 RNA extraction (QIAamp RNA Kit)

Frozen tissue was ground to a fine powder using a mortar and pestle pre-cooled in liquid nitrogen. Powdered tissue was resuspended in QIAamp RLT buffer (Qiagen, Crawley, U.K.). RNA was extracted using the QIAamp RNA Blood Mini Kit (Qiagen, Crawley, U.K.) as follows: approximately 1 mg of tissue was homogenised in RLT buffer by centrifugation at 13,000 *g* for 2 minutes in a Qiamp shredder. An equal volume of ice-cold 70% ethanol was added to the supernatant and transferred to the QIAamp Spin column. This was centrifuged at 6,000 *g* for 20 seconds to bind RNA to the column membrane. RNA bound to the membrane was washed with RW1 buffer. Contaminating DNA was digested by incubation of the membrane with QIAamp RNAse-free DNAse Set (Qiagen, Crawley, U.K.) for 15 minutes at room temperature. Membranes were rewashed with RW1 buffer, followed by two washes in RPE buffer containing 80% ethanol to remove contaminants. Columns were centrifuged at 13,000 *g* for 2 minutes to remove all traces of ethanol. RNA was reconstituted into 30 μL of DEPC treated water, this was added onto the membrane and centrifuged at 6,000 *g* for 2 minutes to elute. RNA concentration was assessed and diluted to 1 mg/mL.

2.2.5.3 RNA extraction (TRIzol reagent)

Tissue was disrupted, by grinding to a fine powder using a mortar and pestle under liquid N_2. TRIzol reagent (Gibco Life Technologies, Paisley, U.K.) was added to the powdered tissue (90% v/v) and tissue homogenised by drawing up TRIzol mix through a 22 gauge needle and syringe. The homogenised samples were incubated at room temperature for 5 minutes to complete the dissociation of nucleotide/protein complexes. Chloroform (Sigma, Poole, U.K.) was added to the samples (20% v/v) and samples shaken vigorously for 20 seconds. These were incubated at room temperature for 5 minutes then centrifuged at 12,000 *g* for 15 minutes at 4°C. The mixture separated into a lower red phenol-chloroform phase which contained DNA and protein. A pale aqueous phase which contained the RNA sat on top, this was carefully removed with a pipette to prevent contamination with the phenol-chloroform phase. The RNA was precipitated in isopropyl alcohol (Sigma, Poole, U.K.) (30% v/v), by incubating sample for 10 minutes at room temperature and centrifuging at 7500 *g* for 5 minutes at 4°C. The supernatant was removed and the RNA pellet washed by resuspending in 70% ethanol and centrifuging at 7,500 *g* for 5 minutes at 4°C. The supernatant was removed and the RNA pellet air-dried for 10 minutes at room temperature. The RNA pellet was resuspended in DEPC treated water. The RNA concentration was assessed and diluted to 1 mg/mL.

RNA quality was assessed by running 2 µL on a 2% TAE agarose gel, stained with ethidium bromide and visualised under UV light, this method had several advantages in addition to quantification by spectrophotometry alone, as RNA integrity is evident as was the presence of contaminating DNA.

2.2.5.4 Messenger RNA Quantification

Messenger RNA levels can be quantified using a number of methods, these include Northern blotting, nucleotide protection assays and PCR based methods. PCR based methods have an advantage in that they require very little starting template, do not use radionucleotides, are less time consuming and can have better sensitivity compared to alternative methods. They work on the premise that the PCR product yield is directly related to the starting template concentration. Messenger RNA templates are amplified and the product concentration is measured. However, PCR amplification is an exponential process, therefore small changes in amplification efficiency can have a drastic effect on yield. In the latter stages of amplification, reaction components other then target concentration become limiting, in addition, reduced enzymatic activity and accumulation of product lead to decreased PCR efficiency. For this reason quantification of

starting template concentration is only possible during the initial exponential phase of amplification, although product concentration may be limiting due to sub-sensitive detection methods.

2.2.5.4.1 Semi quantitative gene expression (Ready-To-Go™ RT-PCR Beads)

To produce a quantitative PCR based RNA assay the cycle at which the product concentration is measured is optimised by running the PCR reaction over a number of cycle numbers, typically between 15 and 35, and detecting the amount of product after each consecutive cycle. When PCR product concentration is plotted against cycle number a sigmoidal curve is produced as demonstrated in figure 2.2. Two or three cycles after the product levels came above background levels was chosen as the optimal PCR cycle number for quantification. The cycle number varied for each gene: the housekeeping gene *gapdh* is highly expressed, and product levels were quantified after 20 cycles, whereas less highly expressed genes were quantified after further cycles, e.g. hfe mRNA levels were assessed after 32 cycles. It was also important to accurately quantify RNA concentrations and to dilute all samples to a similar concentration as the optimal cycle number is directly correlated to starting template concentration.

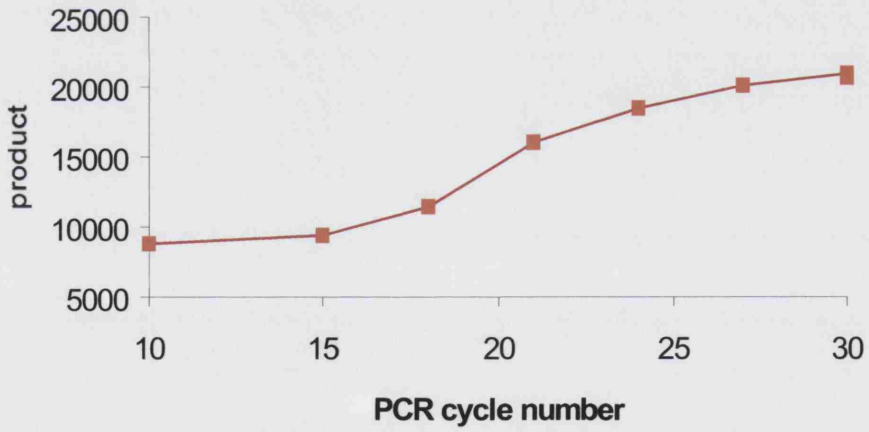

Figure 2. 2 Cycle optimisation of gapdh amplification

Product concentration increases exponentially between cycles 15 and 26. The slope is steepest between cycles 17 and 22. PCR products were therefore measured after 20 PCR cycles.

Reverse transcriptase PCR was performed using Ready-To-Go™ RT-PCR Beads (Amersham Pharmacia, Bucks., U.K.) on total RNA. Ready-To-Go™ RT-PCR Beads were re-suspended in 47 µL of DEPC treated H_2O, 5 pmol of each specific forward and reverse primer and 1 µg of total RNA was added to the reaction mix. The reaction mix was overlaid with oil.

Complementary DNA transcripts were produced by incubation at 42°C for 30 minutes. PCR was performed by denaturation at 94°C for 30 seconds, annealing for 2 minutes, extension at 72°C for 2 minutes, followed by a final extension at 72°C for 10 minutes in a PTC-100 Thermal cycler (MJ Research Inc., Reno, NV, USA). Conditions were optimised for individual primer pairs by adjusting the annealing temperature, annealing time and the number of PCR cycles (refer to Table 2.1 for optimised PCR conditions). Reverse transcriptase PCR products were separated on a 3% TAE agarose gel and visualised using a Fluor-S MultiImager (BIO-RAD, Hemel Hempstead, U.K.). Bands were analysed using MultiAnalyst (BIO-RAD, Hemel Hempstead, U.K.) image analysis software. The amount of mRNA was standardised to that of the housekeeper by dividing densitometry readings for the gene of interest by those for the housekeeper. Results were therefore expressed as arbitrary optical density units of (gene of interest)/ (housekeeper).

A housekeeper gene was used as an internal control of RNA concentration. A 'housekeeper' gene is one whose expression remains constant between the control and test groups. In the experiments conducted here either *glyceraldehyde-3-phosphate* (*gapdh*) or *actin* were utilised. Glyceraldehyde-3-phosphate catalyses the conversion of glyceraldehyde 3-phosphate into 1,3-bisphosphoglycerate during glycolysis. Actin is a cytoskeleton protein. Both actin (Mazur *et al.*, 2003) and gapdh (Bridle *et al.*, 2003) are regularly used as housekeeper genes, have relatively low overall variability within tissues (Szabo *et al.*, 2004) and as neither of these proteins is likely to be up- or down-regulated due to pregnancy or iron status they are ideal to use as internal controls in this study.

Primers were designed manually to mouse: *DMT1, Ireg1, hephaestin, TfR1, TfR2α, TfR2β,* membrane bound *hfe,* total (cytoplasmic and membrane bound) *hfe, haemoxygenase-1 (hox1), haemoxygenase-2 (hox2), ZIRTL* and the housekeeping gene *gapdh* and are outlined in table 2.1. Where possible, primers were designed to be specific for both mouse and rat homologous genes, BLAST search (http://www.ncbi.nlm.nih.gov/BLAST/) was conducted on all primers to ensure specificity to the gene of interest. Primers were between 19 and 26 bases, with a annealing temperature (T_m) between 54°C and 67°C and were designed to give products between 400 and 800 nucleotides. If possible, primers were designed so that products contained intron-exon boundaries. This ensured that amplification from genomic DNA would produce larger products then those amplified from mRNA templates and would therefore be easily detected. All primers were synthesised by Sigma Genosys Ltd. (Pampisford, Cambridge U.K.).

Gene	Primer	length	T_m	cycle
GAPDH NM017008	f. 5'-ATGTCGTGAGTCTACTGGT-3' r. 5'-CTGTAGCCGTATTCATTGTC-3'	681b	54	23
DMT1 AF008439	f. 5'-GGTGTTGTGCTTGGATGTTA-3' r. 5'-AGTACATGTTGATGGAGCAG-3'	400 b	54	27
Ireg1 AF231120	f. 5'-CTTGACTGTATCACTACAGGGTACGC'3' r. 5'-AATCAAAGGACCAAAGACCGATTC-3'	425 b	65	32
Tfr1 M58040	f. 5'-CCTCGTGAGGCTGGTCTCAA-3' r. 5'-TGGACCAGTTTACCAGTAACTT-3'	250 b	59	32
Tfr2a NM015799	f. 5'-ACCCTGGTCCAAGATATCCTCG-3' r. 5'-CCGATAAGGAGAGCCTGAGAGG-3'	651b	67	32
Tfr2b NM015799	f. 5'-TGCGAGTTGGAATTACTAGCTTCG-3' r. 5'-CCGATAAGGAGAGCCTGAGAGG-3'	353 b	67	32
Hfe total AF176535	f. 5'-CTAGAACACAGCTGGACCTAAC-3' r. 5'-TGGATGCAGAAAACGAAGGAT-3'	203 b	59	32
Hfe membrane AF176535	f. 5'-CTAGAACACAGCTGGACCTAAC-3' r. 5'-GGCAGAGAAGTCAGRGTAGTCA-3'	402 b	59	32
Hephaestin NM014799	f. 5'-CTGTGGGCCATGAAGGCAG-3' r. 5'-CACCTCAGCCTGTAACAGTG-3'	515 b	61	32
ZIRTL AJ243651	f. 5'-TCCAAGAGTCACCGAGTTATC-3' r. 5'-GGCCTCATCTATGGCAGCC-3'	521b	60	32
Haemoxygenase 1 NM010442	f. 5'-CCGAGAATCCTGAGTTCATG-3' r. 5'-AGATCAGCACTAGCTCATCCC-3'	709 b	54	32
Haemoxygenase 2 AF054670	f. 5'-GTACAGGAACTAGTCACGAC-3' r. 5'-CATAATGAGCTGCAGGCTAG-3'	580 b	54	32

Table 2. 1 Primers used for Ready-To-Go™ RT-PCR.

Table lists gene name and Genbank accession number, PCR product length in nucleotide bases, primer annealing temperature in °C [Tm], and number of PCR amplification cycles used.

2.2.5.4.2 Quantitative gene expression (real-time PCR)

During the course of this study real-time PCR technology became available for use. Real-time PCR quantifies the amount of PCR product after each PCR cycle, this method therefore does not require the initial production of a PCR cycle *vs* product curve to determine an optimal cycle number at which to quantitate product levels. This method has a higher sensitivity than that of Ready-To-Go beads and has been shown to detect down to two-fold changes in template concentrations (Singer-Sam *et al.*, 1990). For this reason real-time PCR was used whenever possible over RT-To-Go beads.

Real time PCR can be conducted either as a one- or a two-step reaction. In the one-step RT-PCR, RNA is used as a template. This is incubated with reverse transcriptase and gene specific primers. Immediately following the reverse transcriptase reaction in which cDNA is produced, the reaction mix also containing a DNA polymerase, is placed under PCR cycles. In two-step RT-PCR, cDNA is produced in a preliminary step, and used subsequently as a template for PCR. Two-step RT-PCR has several advantages over one step RT-PCR. The initial reverse transcriptase reaction produces enough product to perform several subsequent PCRs. This means that a single batch of cDNA can be used to quantitate the concentration of several genes, this eliminates variation in the results due to the reverse transcriptase reaction. Two-step RT-PCR is also advantageous, as cDNA is more stable then RNA, this not only reduces error due to RNA degradation, but is also easier to handle routinely. For these reasons, the two-step protocol for RT-PCR was used throughout this study.

2.2.5.4.3 cDNA synthesis

Complementary DNA was synthesised using the Abgene Reverse-iT 1st Strand Synthesis Kit. 1 µg of total RNA was used as a template and incubated with 500 nM oligo pT primer and H_2O for 5 minutes at 70°C to denature any secondary structure. 1st strand synthesis buffer, dNTPs and reverse transcriptase were added. Reaction components were incubated at 42°C for 60 minutes. Complementary DNA was stored at –20°C.

Real-time PCR

Real-time quantitative gene analysis was performed using a Lightcycler system II (Roche Diagnostics GmbH, Mannheim, Germany), with Lightcycler version 3.5 software (Roche Molecular Biochemicals, Mannheim, Germany), and QuantiTect SYBR Green PCR Kit (Qiagen, Crawley, UK). SYBR green, present in the PCR mix, binds to dsDNA, but not ssDNA, once bound it is excited at 494 nm and emits light at 521 nm. Monitoring of emissions at 521 nm, following excitation at 494 nm, allows indirect quantification of the dsDNA concentration within the reaction vial. Fluorescence at 521 nm is quantified within each reaction vial following the completion of every PCR extension step. The PCR cycle at which the fluorescence (product) reaches a threshold value is used as a measure of the original template concentration. When back calculated against a standard curve, the number of mRNA templates in the initial sample can be calculated. This is in contrast to quantification using Ready-To-Go beads, where the amount of product is quantitated after a set number of PCR cycles. SYBR green does not interfere with PCR cycling as it dissociates from the product DNA during the denaturation step of the following PCR cycle.

The second derivative maximal method was used to determine threshold values of fluorescence. The LightCycler software version 3.5 (Roche Molecular Diagnostics, Mannheim, Germany) was used to calculate the PCR cycle at which the maximal increase in fluorescence in the log/linear phase of cycling within each individual reaction vial. There was no requirement to set a noise band/threshold, reducing user data manipulation. The cycle number of maximal increase in fluorescence was compared to that of standards using RelQuant software (Roche Molecular Diagnostics, Mannheim, Germany).

All runs were performed in duplicate and each sample was run with the gene of interest alongside actin. Lightcycler RelQuant software version 1.01 (Roche Molecular Diagnostics, Mannheim, Germany) quantified the ratio of gene of interest to that of *actin* for all samples, using standard curves of the gene of interest *vs actin* to determine the PCR efficiency for each primer set.

Meltcurve analysis was performed after PCR cycling. This involved heating the PCR products at 65°C for 10 seconds, the temperature was then slowly increased to 95°C with a ramp rate of 0.2°C per second, whilst fluorescence was continually monitored. At 65°C all DNA in the PCR vial is double stranded, SYBR green binding and fluorescence is therefore maximal. As the temperature is raised, DNA products are denatured, SYBR green is unbound and fluorescence decreases. Plotting fluorescence against temperature produces a meltcurve. Very little change in fluorescence is detected until the temperature reaches that of the melting temperature of the PCR product (Figure 2.3); this is determined by the GC content as well as the length of the PCR transcript. Each specific PCR product displays a characteristic meltcurve. Primer dimer and other short non-specific products can be distinguished using this method as these melt at a lower temperature (as they are usually shorter and less specific) then the desired product. Increasing the fluorescence acquisition temperature used during PCR to above the melting temperature of primer-dimer and non-specific products eliminates any fluorescence due to the presence of these products.

The RT-PCR reaction conditions were as suggested by the manufacturers protocol, this included an initial hot-start at 95°C for 15 minutes, followed by PCR cycling of denaturation at 94°C for 15 seconds, annealing at 60°C for 20 seconds, extension at 72°C for 30 seconds, the temperature was increased to 2°C below the product melting temperature and held for 5 seconds before fluorescent acquisition. Each RT-PCR run was followed by meltcurve analysis.

Primers were designed using LightCycler Probe Design software version 1.01 (Roche Molecular Biochemicals, Mannheim, Germany).
BLAST (http://www.ncbi.nlm.nih.gov/BLAST/) searches were conducted on all primers to ensure specificity to the gene of interest, and if possible to be specific for analogues in other (rat, mouse, human) species. Suitability of primers was determined by producing a single product of the correct length, determined by agarose gel electrophoresis, after PCR cycling with the protocol described above. A single peak on the meltcurve analysis was also required to determine suitability of primers. Table 2.2 lists all primers used for real-time PCR.

Standard curves were produced of all primers. For this, purified DNA (from test PCR runs, purified with Geneclean (Biogene, Cambridge, U.K.)) was serially 10 fold diluted. These were used as templates for RT-PCR. Standards for the gene of interest were run in duplicate alongside actin standards. RT-PCR was performed and the range of standards adjusted to give a linear range between 20-25 cycles and covered a dynamic range of at least 5 logarithmic orders (Figures 2.5 – 2.6). Standard curves were analysed and saved in RelQuant software version 1.01 (Roche Molecular Biochemicals, Mannheim, Germany) for the relative quantification of gene of interest to *actin*.

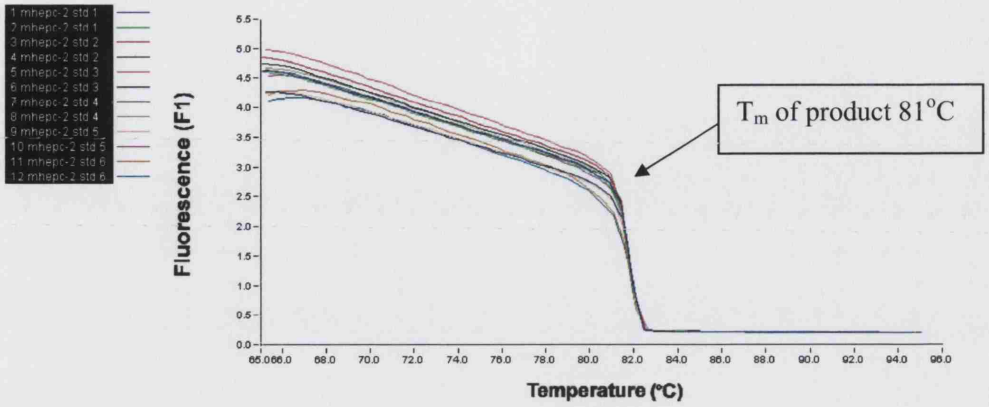

Figure 2. 3 Meltcurve anaysis of hepcidin PCR product

Fluorescence, measured on the Y axis is maximum at 65°C. Temperature (X-axis) is gradually increased to 95°C whilst fluorescence (Y-axis) is continually measured. Fluorescence in samples decreases dramatically at 81°C. A decrease in fluorescence is due to the denaturation of the product DNA and subsequant dissociation of SYBR green.

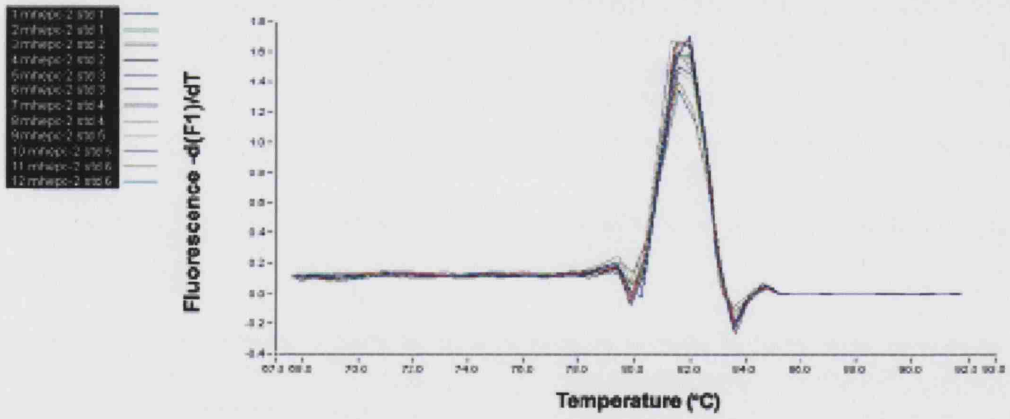

Figure 2. 4 Melting peak of hepcidin gene products

This plots the change in fluorescence (Y axis) against temperature (X axis). The sharp decrease in fluorescence at 81°C in figure 2.3 above is represented as a single peak at 81°C.

Gene	Primers	Product length
Rodent actin V01217	F: 5'-GACGTTGACATCCGTAAAG-3' R: 5'-CAGTAACAGTCCGCCT-3'	410 bp
Rat hepcidin NM053469	F: 5'-CCTATCTCCATCAACAGATG-3' R: 5'-AACAGATACCACACTGGGAA-3'	170 bp
Rodent DMT1 NM008732	F: 5'-GGCTTTCTTATGAGCTTGCCTA-3' R: 5'-GGAGCACCCAGAGCAGCTTA-3'	385 bp
Rodent Ireg1 NM016917	F: 5'-TTGCAGGAGTCATTGCTGCTA-3' R: 5'-TGGAGTTCTGCACACCATTGAT-3'	119 bp
Rodent Dcytb AF354666	F: 5'-GCAGCGGGCTCGAGTTTA-3' R: 5'-TTCCAGGTCCATGGCAGTCT-3'	98 bp
Mouse hepcidin-1 NM032541	F: 5'-ACCACCTATCTCCATCAAC-3' R: 5'-GGTCAGGATGTGGCTC-3'	205 bp
Mouse hepcidin-2 AY23284	F: 5'-CCTATCTCCAGCAACAGATG-3' R: 5'-AACAGATACCACAGGAGGGT -3'	170 bp
Human HPRT BT019350	F: 5'-TTGTAGCCCTCTGTGTGCTCAAG-3' R: 5'-GCCTGACCAAGGAAAGCAAAGTC-3'	269 bp
Human DMT1+IRE AF064484	F: 5'-GGACCTAGGGCATGTGGCAT-3' R: 5'-ACACAAGTGAGTCAGCGTGG-3'	179 bp
Human DMT1-IRE AF064484	F: 5'-AGTGGTTTATGTCCGGGACC-3' R: 5'-TTTAAGGTAGCCAGCGGTGG-3'	180 bp
Human Ireg1 NM014585	F: 5'-CGTCATTGATGCTAGAATCG-3' R: 5'-AGACTGAAATCAATACGAGC-3'	202 bp
Human Tfr1 BC001188	F: 5'-TGAACAAAGTGGCACGAGCA-3' R: 5'-CTCATGACACGATCATTGAGT-3'	291 bp

Table 2. 2 Real-Time PCR primers

Table lists primers used for real-time PCR, the Genbank accession number of the sequence used to produce the primers is listed, Sense and antisense primer sequences are given, and the PCR product length.

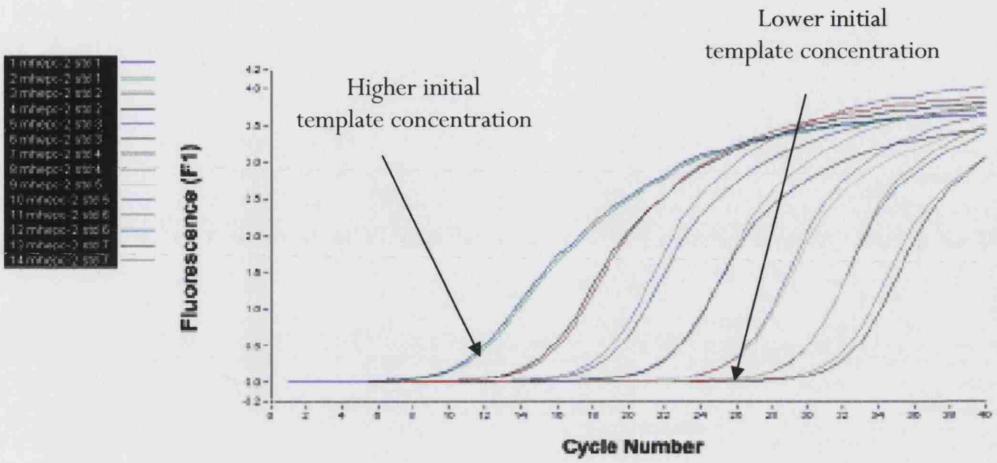

Figure 2. 5 Effect of initial template concentration on PCR amplification

The chart demonstrates the increase in fluorescence against PCR cycle number. An increase in fluorescence was detected in earlier cycles in reactions with higher initial template concentrations. Chart shows samples over 7 logarithemic dilutions.

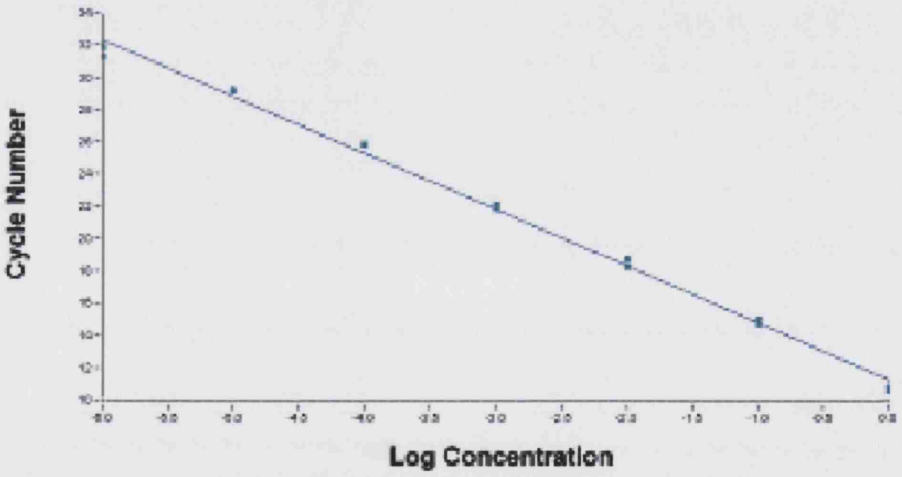

Figure 2. 6 Standard curve for mouse hepcidin-2

Chart demonstrating the linear relationship between cycle number at which fluorescence demonstrates maximum acceleration against log of initial template concentration. The slope of 3.5 calculates the number of cycles between standards differing in concentrations of x10. Under perfect conditions a 1/10 dilution results in a slope of ~3.2 (this is equivalent with an increase of 1 cycle for a doubling in template concentration).

2.2.5.5 Agarose gel electrophoresis

To visually analyse DNA and RNA, samples were run on 1% agarose/TAE gels (3% agarose gels were utilised for quantification of Ready-To-Go rtPCR products) alongside molecular weight markers (Bioline, London, U.K.) using a horizontal gel apparatus (BioRad, Hemel Hempstead, U.K.). The gels were prepared by dissolving 1.5 g agarose (4.5 g for a 3% gel) in 150 mL of 1 x TAE/ ethidium bromide 0.5 g/mL by microwaving. Cooled molten agarose was poured into a gel cast, a comb added and the gel allowed to set for approximately 30 minutes at room temperature. Prior to loading DNA/RNA was mixed with 0.1 volume of 10x loading buffer. Electrophoresis was typically carried out at 110 volts for 20 minutes. DNA/RNA was visualised using a Fluor-S MultiImager (BIO-RAD, Hemel Hempstead, U.K.).

2.2.5.6 Gel extraction of PCR products

The Geneclean kit (Biogene, Cambridge, U.K.) was used to purify PCR products from TAE gels. Approximately 300 mg of the product of interest were excised from the gel using a clean scalpel and placed in a 1.5 mL eppendorf with 400 µL of glassmilk, this was incubated at 55°C to dissolve. Glassmilk containing the DNA/gel mix was placed in the Geneclean spin filter column and centrifuged at 13,000 *g* for 1 minute to bind the DNA to the membrane and the glassmilk/gel in the supernatant was discarded. The membrane was washed twice with wash buffer, dried by centrifuging for 2 minutes and the bound DNA was resuspended in 10-25 µL H_2O by gentle pipetting. DNA was eluted into a clean eppendorf by centrifugation at 13,000 *g* for 1 minute. This procedure was repeated, the eluents pooled, and the DNA concentration quantified by spectrophotometry.

2.2.5.7 DNA/RNA Quantification

DNA concentration was determined by spectrophotometry at 260nm. Double stranded DNA concentration was determined by the formula below:

$$\text{DNA concentration } (\mu g/mL) = A_{260} \times \text{dilution} \times 20$$

2.2.6 SDS gel electrophoresis

3 mL of molten running gel was applied to the SDS glass plate assembly, this was overlaid with a layer of acetone (BDH Chemicals Ltd, Poole, U.K.) and allowed to set for 30 minutes at rt. Once set the acetone was discarded and the gel rinsed with dH_2O. Molten stacking gel was carefully applied to the gel cast and the comb carefully inserted. The gel was allowed to set for at least 30 minutes at rt. Once set the comb was removed and the wells rinsed with dH_2O. 10 µg of protein sample was combined with loading buffer and applied to the SDS polyacrylamide gel. The protein samples were seperated at 20 mA constant current for 1 hour.

2.2.7 Western Blotting

Protein transfer onto a PVDF membrane (Amersham Pharmacia Biotech UK Ltd, Berkshire, U.K.) was by semi-dry blotting for 2 hour at a constant current of 1 mA/cm^2 (Trans-blot semi-dry transfer cell, BioRAD, Hertfordshire, UK). Similar loading and transfer of proteins was verified by incubating the membrane in neat Ponceau S reagent (Sigma, Poole, U.K.) for 5 minutes at room temperature. This stained proteins attached to the membrane a bright pink. Equal loading and separation was noted in all lanes. Ponceau S reagent was removed by rinsing with dH_2O. To prevent non-specific antibody binding, the membrane was blocked with PBS-T containing 5% non-fat milk (Safeway, Middlesex, U.K.) for 1 hour at room temperature. Membranes were then incubated in Dcytb antibody (1:200)/1% non-fat milk/PBS-T for 16 hours at rt. Membranes were washed 3 x for 5 minutes in PBS-T. Primary antibody was probed with donkey anti-rabbit IgG horseradish peroxidase (1:5000) (Amersham Pharmacia, Bucks, U.K.) for 1 hour at room temperature. After washing 3x for 5 minutes in PBS, bound antibody was detected, with ECL (enhanced chemiluminescence system) plus kit (Amersham Pharmacia Biotech UK Ltd, Berkshire, U.K.) briefly, 4 mL of ECL solution A was mixed with 100 µl solution B. The reagent mix was applied to the membrane and the chemiluminescence measured for 4 minutes with a Fluor-S MultiImager System (BIO-RAD, Hertfordshire, U.K.).

2.2.8 Iron quantification

100 mg of fresh tissue was homogenised in 1 mL water, after which 300 µL was taken and digested with 1.5 mL nitric acid. After an overnight incubation, 1.2 mL water was added to the sample. A 0.3 mL portion of sample was wet-ashed with 1.5 mL of ultrapure 65% HNO_3 (Merck, Darmstadt, Germany). After 24 hours 1.2 mL H_2O was added and iron concentrations determined by ICP-AES by Dr Domineque Klien (Institute of Toxicology, GSF-Forschungszentrum fur Umwelt und Gesundheit GMBH Neuherberg, Germany).

2.2.9 Statistical analysis

Data points lying outside the 95% confidence intervals were discarded, this allowed outliers to be identified and removed from subsequent analyses.

The Kolmogorov-Smirnoff Test (Stevens M.A. & D'Agostino R.B., 2005) was used to determine the probability of a normal distribution for each group ($P \geq 0.05$). The KS statistic quantifies the similarity between the sample distribution and that of a Gaussian distribution. A large similarity between the two populations results in a large P value. In the data presented here a KS statistic of ≥ 0.05 was presumed to indicate a Gaussian distribution.

2.2.9.1 Comparing two groups of data

To test the significance between two groups of Gaussian distributed data, the F-test was performed to determine whether the variances for both groups was similar. For experiments where the F-test gave a P value above 0.05, i.e. both sets of data had equal variance, a Student's two-tailed unpaired *t*-test was used. For groups with unequal variance, i.e. an F-test $P \leq 0.05$, a Student's *t*-test with *Welch*'s correction was used to test for significance.

To test the significance of two groups where at least one of the groups did not follow a Gaussian distribution, the two-tailed Mann-Whitney test was used.

2.2.9.2 Comparing more than two groups of data

To test for statistically significant difference between groups in experiments with more than two groups ANOVA with Bonferoni *post hoc* test was used when all groups demonstrated a Gaussian distribution.

The Kruskal-Wallis with Bonferoni *post hoc* test was used when one or more of the groups did not follow a Gaussian distribution.

In all but the Kolmogorov-Smirnoff Test, a P value ≤ 0.05 was considered to demonstrate significant difference between the groups tested. All analysis were performed in Microsoft Excel version 9.0 with Analyse-It™ version 1.71 (Microsoft, Reading, U.K.). Data in charts are presented as mean + standard error of the mean (S.E.M) in all instances except those data supplied by collaborators.

S.E.M. values were quoted as opposed to standard deviation (SD), as this measure of variance took sample size into account.

3.1 Regulation of duodenal iron absorption: a study in non-pregnant mice

Introduction

The molecular mechanism of duodenal iron uptake is well understood, but how this is regulated is less well understood. Both hfe and hepcidin have been implicated to have a role in this, but, how or if ,they interact is not known. The experiments described in this chapter investigate the role of hfe and hepcidin in iron homeostasis. A mouse hfe knockout model is used, in which iron deficiency and iron loading is induced. The effect of this on the expression of duodenal and hepatic iron transporters and modulators is analysed.

Iron transport across the duodenal enterocyte can be considered in two steps: reduction of ferric iron to ferrous iron by Dcytb and transfer across the bbm by DMT1; followed by transfer across the basolateral membrane by Ireg1 linked to the membrane-bound ferroxidase hephaestin (Fleming *et al.*, 1997;Gunshin *et al.*, 1997;Vulpe *et al.*, 1999;Abboud & Haile, 2000 Donovan *et al.*, 2000;McKie *et al.*, 2000;McKie *et al.*, 2001) (Figure 1.4).

Regulation of iron absorption was originally hypothesised to occur in the crypt regions of the duodenum. Here immature enterocytes take up plasma Fe_2-Tf at their basolateral surface and were thought to receive signals from a 'stores regulator' which responds to body iron stores, and an 'erythroid regulator' which responds to the body's requirement for erythropoiesis. Crypt cells mature into absorptive cells whilst they migrate to the upper villus where they absorb dietary iron across the brush border surface. The expression of iron transporters in these cells was originally thought to be determined whilst in the crypts, see figure 1.9 (Frazer *et al.*, 2003).

Hfe homozygote knockout ($hfe^{-/-}$) mice are a useful tool to study the regulation of duodenal iron uptake as, similar to patients with HH, these mice exhibit inappropriately high duodenal iron absorption which leads to excessive tissue iron loading (Zhou *et al.*, 1998;Griffiths & Cox, 2000;Griffiths *et al.*, 2001;Lebeau *et al.*, 2002).

In the duodenum, hfe is confined to the crypt cells where it physically associates with Tfr1 (Parkkila *et al.*, 1997a), and is thought to determine the uptake of Fe_2-Tf by these cells (Feder *et al.*, 1998;Levy *et al.*, 1999). This mechanism is compromised in $hfe^{-/-}$ mice and in HH patients with defective hfe, whose duodenal crypt cells are consequently iron deficient and therefore programmed to over-express duodenal iron transporters (Simpson *et al.*, 2003). In the liver, hfe expression is predominantly in the hepatocytes, as shown by *in situ* analysis and Western blotting (Zhang *et al.*, 2004). However, immunohistochemical analysis identifies maximum hfe expression in Kupffer and endothelial cells (Bastin *et al.*, 1998), or sinusoidal endothelial cells and the bile duct (Parkkila *et al.*, 1997b). A possible reason for this discrepancy could be the similarity of hfe to other major histocompatibility class 1 molecules.

Similiar to $hfe^{-/-}$ mice and HH patients, $hepcidin^{-/-}$ mice develop severe iron overload (Nicolas *et al.*, 2001). Hepcidin is a 20-25aa peptide which is produced in the hepatocytes of the liver (Kulaksiz *et al.*, 2004;Zhang *et al.*, 2004) and is thought to inhibit duodenal iron absorption (Nicolas *et al.*, 2001;Park *et al.*, 2001). As $hepcidin^{-/-}$, $Hfe^{-/-}$ and HH patients all develop severe iron overload it is possible that hfe and hepcidin are components of the same iron homeostatic mechanism.

3.1.1 Duodenal & hepatic gene expression in C57blk/6 & $hfe^{-/-}$ mice

In the following set of experiments the regulation of iron homeostasis by hfe and hepcidin is tested by quantification the mRNA expression of iron transporter and regulatory genes in the liver and proximal duodenum of wild-type (C57blk/6) and $hfe^{-/-}$ mice.

Methods

Weanling $hfe^{-/-}$ (originally mixed 129/Ola-C57blk/6 background strain) (Bahram *et al.*, 1999) (n=6) and C57blk/6 males (n=6), reared in a 12 hour light/12 hour dark cycle, were fed a control diet (180 mg Fe/kg diet) (Altromin, Lage, Germany) and received distilled water *ad libitum*. At twelve weeks of age, following an overnight fast, mice were terminally anaesthetised with intraperitoneal pentobarbitone sodium (Sagatal, Rhone-Merieux, Harlow, UK, 90 mg/kg). The proximal duodenum was removed and rinsed with saline. The mucosa, collected by scraping with a clean glass slide, was snap frozen in liquid N_2 and stored at –80°C. The liver was also collected into liquid N_2 and stored at –80°C.

Total RNA, extracted from tissues using Trizol (Sigma, Poole, U.K.), was used as a template to transcribe cDNA using the ABgene Reverse-iT 1st Strand Synthesis Kit (ABgene, Surrey, U.K.). Messenger RNA expression of duodenal *DMT1, Ireg1* and *Dcytb*, and hepatic *DMT1, hepcidin-1, hepcidin-2* and *Ireg1* was quantified by real-time PCR. Gene expression levels were normalised to that of *actin*. Expression of duodenal *hfe* and *Tfr1*, and hepatic *Tfr2* was quantified using Ready-to-Go™ RT-PCR Beads (Amersham Pharmacia, Bucks.,U.K.) and normalised to *gapdh* levels. Each PCR run was performed in duplicate. Protocols were as described in chapter 2.2.

Students *t*-tests were used to compare data sets. Significance was assumed at $P < 0.05$. Expression levels of the C57blk/6 control group was given an arbitrary unit of 1 and all other groups were adjusted accordingly. Data are presented as means + S.E.M.

Results

Duodenal *DMT1* expression was increased in $hfe^{-/-}$ mice to twelve times the level in C57blk/6 mice ($P>0.001$) (Figure 3.1.1). In addition, duodenal *Ireg1* was increased in $hfe^{-/-}$ mice by 20%, ($P>0.05$). Duodenal *hfe* expression was increased two fold in the $hfe^{-/-}$ mice, but this did not reach statistical significance ($P=0.073$). Neither *Dcytb* nor *Tfr1* differed between the two mice strains ($P\geq0.05$). The expression of Tfr2 in the duodenum was below the sensitivity of the method used.

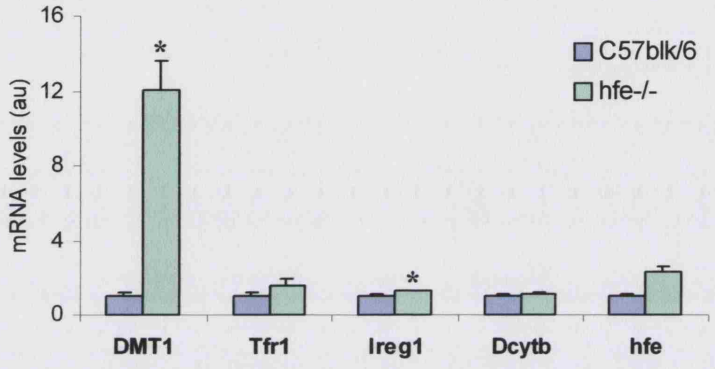

Figure 3.1. 1 Duodenal gene expression in the $hfe^{-/-}$ mouse

*Duodenal gene expression in $hfe^{-/-}$ mice compared to that in C57blk/6 mice. Expression of duodenal DMT1 and Ireg1 mRNA was increased in the $hfe^{-/-}$ mice. Bars depict mean + S.E.M. C57blk/6 expression levels were given an arbitrary value of 1 and the value for the corresponding $hfe^{-/-}$ group were adjusted accordingly. *Denotes significance difference from the C57blk/6 and $hfe^{-/-}$ group at $P\leq0.05$.*

Hfe$^{-/-}$ mice had significantly reduced liver *hepcidin-1* expression (Figure 3.1.2), approximately a fifth that of C57blk/6 ($P<0.05$), *hepcidin-2* expression was increased in hfe$^{-/-}$ mice but this was not statistically significant ($P=0.055$). Neither hepatic *DMT1* nor *Tfr2* expression differed between the two mice strains ($P\geq0.05$). Expression of hepatic Tfr1 was undetectable with the method used. All means + S.E.M. and P values are tabulated in appendix I.

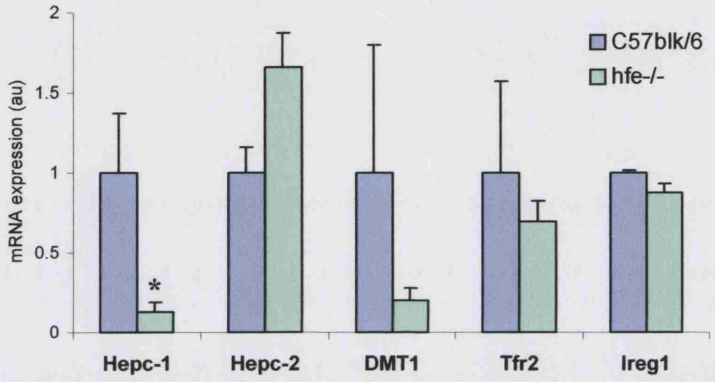

Figure 3.1. 2 Hepatic gene expression in the hfe$^{-/-}$ mouse

*Hepatic gene expression in hfe$^{-/-}$ mice compared to that of C57blk/6 mice. Expression of hepcidin-1 was significantly decreased in the hfe$^{-/-}$ group. Bars show mean + S.E.M. C57blk/6 expression levels were given an arbitrary value of 1 and the value for the corresponding hfe$^{-/-}$ group was adjusted accordingly. *Denotes significance difference from the C57blk/6 group at $P\leq0.05$.*

3.1.2 Gene expression in C57blk/6 & hfe$^{-/-}$ mice: effect of dietary iron levels

In the following set of experiments the mechanism by which the duodenal mucosa adapts to body iron status was studied. Messenger RNA expression was quantified in mice placed on control, iron deficient or iron loaded diets. The role of hfe in this mechanism was also examined in a parallel experiment using hfe$^{-/-}$ mice.

Experimental protocol

Hfe$^{-/-}$ and C57blk/6 male mice were placed onto an iron deficient, iron loaded, or control diet for five weeks, after which duodenal and liver tissues were collected for mRNA analysis. The expression of duodenal *DMT1, Dcytb, Ireg1, Tfr1, hfe,* and hepatic *hepcidin-1, hepcidin-2, DMT1, Ireg1 and Tfr2* were compared between the C57blk/6 and hfe$^{-/-}$groups, and their response to iron loading and deficiency was investigated.

Methods

Weanling hfe$^{-/-}$ and C57blk/6 males were reared as described previously (Chapter 3.1.1). At seven weeks of age mice were randomised into three groups and placed onto either an iron deficient (6 mg Fe/kg diet), iron loaded (20 g/kg diet added carbonyl iron) or remained on the control (180 mg Fe/kg diet) diet. After five weeks, mice were culled and the proximal duodenal mucosa and liver were collected and stored as described previously (Chapter 3.1.1). Quantification of mRNA expression was as described previously (Chapter 3.1.1).

Results

Tissue iron levels and haematocrit data demonstrate that the deficient diet caused systemic iron deficiency (decreased liver iron and Hb) and the iron loaded diet caused systemic iron loading (increased liver iron and Hb) in both hfe$^{-/-}$ and C57blk/6 mice, (Simpson *et al.*, 2003a). Duodenal non-haem iron content correlated with liver iron stores and did not depend on dietary iron levels in both C57blk/6 and hfe$^{-/-}$ mice. However, duodenal iron content was reduced in hfe$^{-/-}$ mice for any given content of liver iron (Appendix V)(Simpson *et al.*, 2003).

3.1.2.1 Effect of dietary iron deficiency

Duodenal *DMT1* demonstrated a seven-fold increase in C57blk/6 mice when placed on an iron deficient diet ($P<0.01$) (Figure 3.1.3a). Duodenal *Tfr1* expression also increased under iron deficient conditions ($P<0.01$) (Figure 3.1.3a), a finding in agreement with immunohistochemistry data (Barisani & Conte, 2002).

Hepcidin-1 expression decreased with iron deficiency in C57blk/6 mice (Figure 3.1.3b), this has since been confirmed by Frazer and colleagues (2002). Expression of hepatic *hepcidin-2, DMT1, Ireg1* or *Tfr2* did not alter due to iron deficiency in C57blk/6 mice (Figure 3.1.3b). With the exception of hepatic *DMT1* expression (Figure 3.1.3b), gene expression in the duodenum and the liver was identical in $hfe^{-/-}$ mice raised on a control and those raised on an iron deficient diet (Figure 5.1.3). In addition, as control diet
$hfe^{-/-}$ mice had expression levels similar to that of the iron deficient C57blk/6 mice, the expression profile were similar in both mouse genotypes raised on the iron deficient diet.

3.1.2.2 Effect of dietary iron loading

C57blk/6 mice did not respond to iron loading, maintaining *hepcidin-1, DMT1* and *Ireg1* at levels similar to that on control diet (Figure 3.1.3). *Hepcidin-1* expression in either strain on an iron-loaded diet was similar to that of the C57blk/6 control diet group (Figure 3.1.3).

In $hfe^{-/-}$ mice dietary iron loading caused an increase in *hepcidin* expression and a decrease in duodenal *DMT1* ($P<0.001$), *Ireg1* ($P<0.001$) and *Tfr1* ($P<0.05$) expression (Figure 3.1.3). Consequently, these mice had a gene expression pattern similar to that of C57blk/6 mice on a control diet. The decrease in both *DMT1* and *Tfr1* on a high iron diet is consistent with the regulation of these mRNA transcripts *via* IRE-IRP interactions. A decrease in both iron uptake (DMT1) and iron efflux (Ireg1) has been demonstrated to effectively reduce iron absorption (Nicolas *et al.*, 2002b;Oates *et al.*, 2000).

Surprisingly, when placed on a high iron diet C57blk/6 mice increased *hepcidin-2*. This did not increase under similar conditions in $hfe^{-/-}$ animals (Figure 3.1.3). Hepatic *Ireg1* levels did not fluctuate between dietary regimes. This has also subsequently been confirmed by Bridle *et al.* (2003), and could suggest that rather than depleting existing stores, the body responds to iron deficiency by increasing duodenal iron uptake.

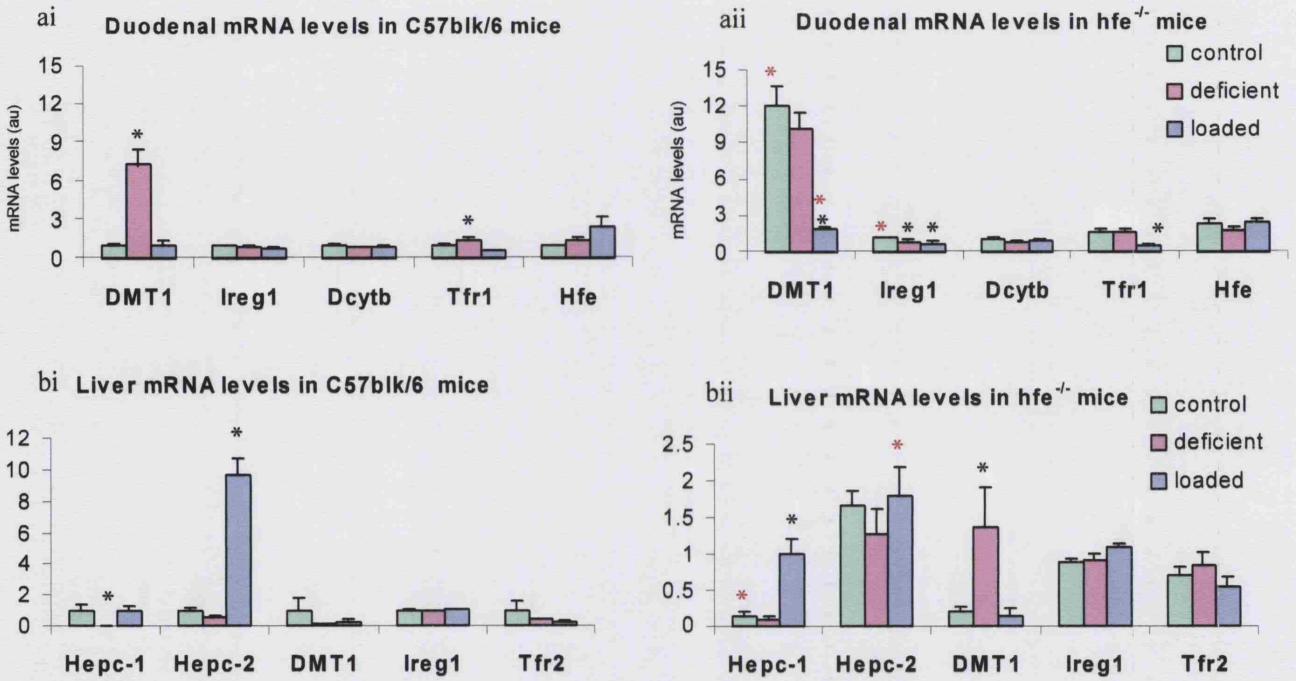

Figure 3.1.3 (a) Duodenal and (b) hepatic gene expression in $hfe^{-/-}$ (ii) and C57blk/6 (i) mice raised on control (green bars), iron deficient (pink bars) or iron loaded (blue bars) diets. C57blk/6 mice respond to an iron deficient diet by decreasing hepcidin-1 levels and increasing duodenal DMT1. In contrast $hfe^{-/-}$ mice respond to iron loaded diet by increasing hepcidin expression and reducing duodenal DMT1, Ireg1 and Tfr1. Data is normalised to give an arbitrary value of 1 to the C57blk/6 control diet group. Values for all other groups are adjusted according to this. The bars represent mean + S.E.M. * denotes significant different from the control diet group ($P<0.05$), * denotes significant difference from the equivalent C57blk/6 group ($P<0.05$).

3.1.3 Duodenal localisation of DMT1: effect of dietary iron content

DMT1 is present both on the cell membrane and within the cytoplasm in endocytic vesicles (Gunshin *et al.*, 1997;Fleming *et al.*, 1998;Su *et al.*, 1998). DMT1 transports lumenal iron into the enterocyte when present on the apical bbm of the duodenum. The amount of DMT1 expressed, and the proportion present on the bbm therefore significantly affects the iron uptake potential of the duodenal mucosa (Gunshin *et al.*, 1997). In this experiment the localisation of duodenal DMT1 was examined in iron deficient, control and iron loaded conditions.

Methods

Male Sprague-Dawley rats (initial mass 230-250 g) were placed on either a control (109 mg Fe/kg diet. RMI, SDS, Witham, Essex, U.K.), iron deficient (7 mg Fe/kg diet. ICN Pharmaceuticals, Basingstoke, Hants, U.K.), or iron replete (20 g/kg diet added carbonyl iron) diet for 5 weeks. Animals were terminally anaesthetised with intraperitoneal sodium pentobarbitone (Sagatal, Rhone-Merieux, Harlow, U.K., 90 mg/kg).

Duodenal biopsies were collected and rinsed in saline. These were embedded in OCT cryoprotectant (BDH, Poole, U.K.) and frozen in isopropanol (Sigma, Poole, U.K.) chilled over liquid N_2. Once the OCT turned opaque, sections were transferred directly into liquid N_2. Tissues was stored at –80°C until required. Sections of duodenum (6 μm) were cut on a cryostat at -20°C onto APES coated slides and dried for 1 hour followed by 10 minutes fixing in acetone (Sigma, Poole, U.K.). Sections were washed in TBS and blocked with 10% normal horse serum (NHS) in TBS for 20 minutes. Sections were incubated with DMT1 antibody for 1 hour. Unbound antibody was removed with 3x5 min TBS washes. Sections were incubation with anti-rabbit Cy3/Rhodamine conjugated antibody (Jackson Immunochemicals, Stratech Scientific, Soham, Cambridgshire, U.K., 1:200 TBS), and finally washed 3x5 min with TBS and mounted with Vectashield + 4,6-Diamidino-2-phenylindole (DAPI) (Vector Labs, Burlingame, CA, USA). Immunofluorescence was analysed with an Olympus BX40 fluorescence microscope with x40, x60 and x100 objectives, equipped with filters specific to DAPI and Cy3 using CytoVision software (Applied Imaging Ltd, Newcastle Upon Tyne, U.K.). Immunolocalisation of DMT1 was identified in 3 animals per diet group. All procedures were carried out at ambient temperature unless otherwise specified.

Apes coated slides

Glass slides (BDH Chemicals Ltd, Poole, U.K.) were washed with detergent, rinsed in hot running water and finally rinsed in industrial methylated spirits. Slides were air dried for a minimum of 1 hour, then immersed in freshly prepared 2% 3-aminopropyl triethoxysilane (APES) (Sigma, Poole, U.K.)/acetone (BDH Chemicals Ltd, Poole, U.K.) solution for 2 minutes in a fume hood. Coated slides were washed in dH_2O for 1 minute, drained on paper towels and dried at 37°C o/n. Slides were stored at room temperature until required.

DMT1 antibody

DMT1 antibody was raised in rabbit against a synthetic peptide, produced by Dr Bala Ramesh, corresponding to amino acids 310-330 of the human DMT1 (Genbank accession BAA24933). Antisera was collected and affinity purified by passage through a column of peptide immobilised on Sulfollink gel as per manufacturers instructions (Pierce, Chester, U.K.) followed by elution and dialysis into PBS. DMT1 antibody cross-reacted with rat DMT1. Pre-immune sera was used as a negative control to identify specific immunoreactivity.

Results

DMT1 expression in the control rat duodenum was predominantly in the upper to mid-sections of the villi, here bbm staining was distinct (Figure 3.1.4 control). Staining was reduced at the villus tips. This is supported by previous *in situ*, Western blotting and immunolocalisation studies (Gunshin *et al.*, 1997;Fleming *et al.*, 1998;Su *et al.*, 1998). Comparisons with sections incubated in pre-immune sera demonstrated weak staining within the enterocyte cytoplasm of sections stained with DMT1 (Figure 3.1.4 pre-immune). Iron loaded mice demonstrated negligible staining of the brush border (Figure 3.1.4 iron loaded), although staining of the enterocyte was more intense than that of the control diet sections. Iron deficient animals had little staining of the cytoplasm but demonstrated intense brush border staining (Figure 3.1.4 iron deficient), which was most notable at the villi tips, these findings are in agreement with similar immunohistochemical studies by Trinder *et al.* (2000).

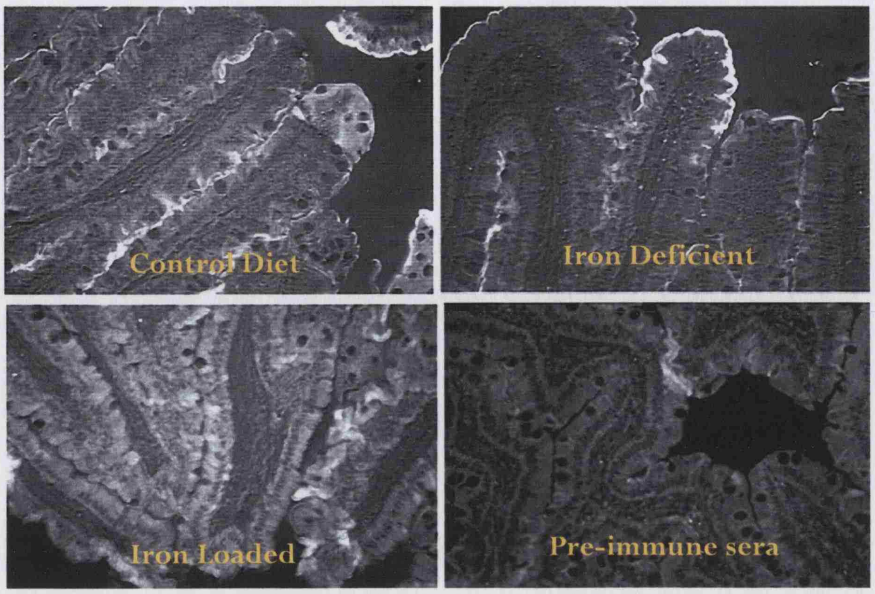

Figure 3.1. 4 Localisation of endogenous DMT1 in the rat duodenum

Duodenal sections from rats raised on control, iron deficient and iron loaded diet and stained for DMT1 expression. The negative control tissue was a duodenal section from a rat raised on a control diet and was incubated with pre-immune sera in place of affinity purified DMT1 antibody. Plates show representative sections from 3 experiments. Original magnification x10.

3.1.4 Dcytb protein expression: effect of dietary iron content

In addition to DMT1 expression, iron uptake across the brush border membrane is modulated by Dcytb activity (Raja *et al.*, 1992; M^{c}Kie *et al.*, 2001). In this experiment, duodenal Dcytb protein expression was quantified in iron replete, deficient and loaded mice.

Methods

Nine weaning C57blk/6 males were raised on a control diet (180 mg/kg diet) until 7 weeks old. Mice were randomised into 3 groups (n=3) and placed on iron deficient (6 mg Fe/kg diet), iron loaded (20 g/kg diet added carbonyl iron), or remained on the control diet. All diets were purchased from Altromin (Lage, Germany). After 5 weeks mice were killed by sodium pentobarbitone overdose (Sagatal, Rhone-Merieux, Harlow, U.K., 90 mg/kg) and cervical dislocation. The proximal duodenum was quickly removed and flushed with saline. The mucosa was collected, mixed with 500 µl of protease inhibitor (Sigma, Poole, U.K.), snap frozen in liquid N_2 and stored at –80°C. Duodenal proteins were extracted from the mucosal scrape as

described previously and the expression of Dcytb assessed by SDS-PAGE separation and Western blotting, as described previously in chapter 2.2.

Antiserum against mouse Dcytb (DAESSSEGAARKRTLGLADSGQRSTM), corresponding to amino acids 223-COOH of mouse Dcytb (Genbank accession: XP130253) as described in (McKie *et al.*, 2001) was a kind gift from Dr Andrew M^{c}Kie, pre-immune rabbit serum was also provided for use as a negative control.

Results

Dcytb was expressed in all samples (Figure 3.1.5). Dietary iron deficiency increased expression, however, iron loading had negligible effect on Dcytb expression.

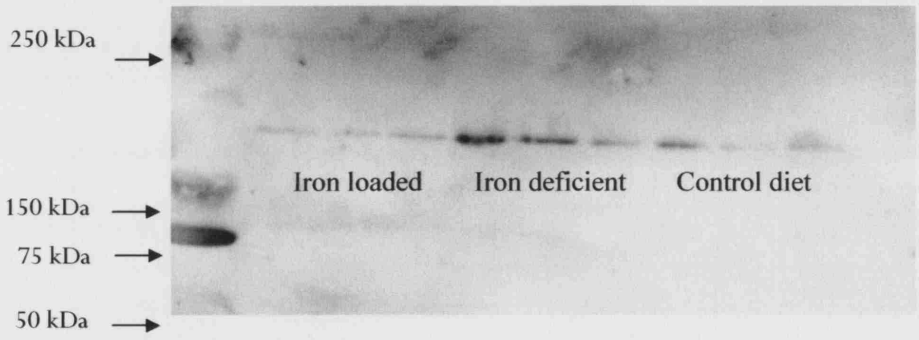

Figure 3.1. 5 Dcytb protein expression in the rat duodenum

Lane 1 shows molecular weight markers. Lanes 2-4 correspond to duodenal mucosa isolated from iron-loaded mice, lanes 5-7 correspond to iron deficient and lane 8-10 to control diet mucosa, probed with antibody raised against Dcytb.

3.1.5 Discussion

The major findings presented here are; (1) Dcytb protein, but not mRNA, expression is regulated by body iron status; (2) Duodenal DMT1 localisation to the bbm is regulated according to body iron status; (3) $Hfe^{-/-}$ mice have increased duodenal *DMT1* mRNA expression when on a control diet; (4) $Hfe^{-/-}$ mice retain the ability to regulate the expression of duodenal iron transporters; (5) *Hepcidin-1* demonstrates an inverse relationship with that of duodenal *DMT1*, this relationship is maintained over a range of body iron levels both above and below the norm and is maintained in $hfe^{-/-}$ mice.

Brush border iron absorption is in part regulated by *Dcytb* expression (Raja *et al.*, 1992;McKie *et al.*, 2001). Various studies in rats have identified changes in *Dcytb* mRNA in iron deficient juveniles or following dietary supplementation with a large bolus of iron (Frazer *et al.*, 2003;Collins *et al.*, 2005). However, this was not identified in this study. Instead an increase in Dcytb protein was identified under iron deficient conditions. This correlates with the increase in reductase activity documented by Simpson *et al.* (2003), and implies a post-translational mechanism for the regulation of Dcytb protein expression.

$Hfe^{-/-}$ mice had significantly higher expression of duodenal *DMT1* and *Ireg1* mRNA compared to the C57blk/6 mice (Figure 3.1.1). Changes in the mRNA expression of *DMT1* and *Ireg1* have previously been demonstrated to be mirrored in the expression of their respective protein (Yamaji *et al.*, 2004;Chua *et al.*, 2004). Protein levels, as well as mRNA expression levels of DMT1 are correlated to iron uptake by duodenal enterocytes (Gunshin *et al.*, 1997;Su *et al.*, 1998;Tandy *et al.*, 2000). Ireg1 protein expression is correlated with iron efflux (Abboud & Haile, 2000;McKie & Barlow, 2003). An increase in both the uptake (DMT1) and efflux (Ireg1) components of the duodenal iron uptake mechanism is probably the cause of the iron overload observed in phenotypic HH. Indeed studies have demonstrated that compound mutations in hfe and DMT1 do not show an iron-loaded phenotype (Levy *et al.*, 2000) supporting a role for DMT1 in the pathology of this disease. Elevated *DMT1* expression is also characteristic in individuals who are iron deficient (Gunshin *et al.*, 2001;Frazer *et al.*, 2003). The gene expression pattern of $hfe^{-/-}$ mice therefore resembles that of an iron deficient phenotype suggesting that hfe has a role in monitoring elevated body iron levels.

Hepcidin-1 demonstrated an inverse relationship with duodenal *DMT1*, this was irrespective of dietary iron content and was maintained in $hfe^{-/-}$ and wildtype C57blk/6 mice (Figure 5.1.2). This has since been confirmed by various groups working with mice and untreated HH patients (Frazer *et al.*, 2002). A number of independent studies also implicate hepcidin as a negative regulator of the iron absorption, these include; (i) $hepcidin^{-/-}$ mice developed severe iron overload similar to that observed in HH and in $hfe^{-/-}$ mice; (ii) transgenic mice over-expressing hepcidin exhibit severe body iron deficiency and microcytic hypochromic anaemia, and; (iii) hepcidin is increased in patients with infections, or inflammatory diseases (Nicolas *et al.*, 2001;Nicolas *et al.*, 2002c;Nemeth *et al.*, 2003).

Changes in *hepcidin* expression are detected prior to that of intestinal iron uptake and precede the decline in transferrin saturation seen in rats in which the acute-phase response was experimentally induced (Anderson *et al.*, 2002). This suggests that a change in *hepcidin* expression is the primary event to changes to iron absorption. Therefore, decreased hepcidin expression probably causes increased iron absorption in HH patients rather than *vice versa*. Taken together these data suggest that hepcidin may indeed be the 'master negative regulator' of duodenal iron uptake.

Hfe is expressed in the hepatocytes (Zhang *et al.*, 2004), hepcidin is also produced in hepatocytes and is probably secreted from the basolateral (sinusoidal) membrane into hepatic sinusoids (Kulaksiz *et al.*, 2004). As $hfe^{-/-}$ mice have iron deficient duodenum (Appendix V) (Simpson *et al.*, 2003) and depressed *hepcidin-1* expression, it is probable that the functional iron deficiency in $hfe^{-/-}$ mice is not limited to the crypt enterocytes but is also present in hepatocytes. This hypothesis is supported by studies which demonstrate that when C282Y HH patients are transplanted with non HH livers they do not go on to express the HH phenotype, and also, normal recipients of C282Y livers develop phenotypic HH (Wigg *et al.*, 2003). These studies indicate that the increased duodenal iron uptake characteristic of HH is caused by the mis-sensing of iron levels by the hepatocytes, which produce hepcidin-1, rather than solely a direct effect of iron deficiency in the duodenal crypt enterocytes as put forward by the mucosal block theory (Chapter 1.3.5).

The ability of $hfe^{-/-}$ mice to increase *hepcidin-1* expression when placed on a high iron diet implies that disruption of the hfe protein does not fully obliterate the iron homeostatic mechanism. The present finding that *hepcidin-1* levels are regulated in
$hfe^{-/-}$ mice although the amount of iron required to elicit a certain amount of *hepcidin-1* expression is higher than in the C57blk/6, supports previous studies with HH patients (McLaren *et al.*, 1991). This suggests that hfe has a small role in the iron homeostatic mechanism and that alternative signaling pathways exist that can bypass hfe when it is defective. It is not surprising that a number of signaling/modulating pathways exist given the number of stimuli (body iron levels, erythopoeisis, Tf saturation, infection) that modulate iron absorption.

A novel finding of this work was that *hepcidin-1* expression is either high (as with C57blk/6 mice on a control diet) or low (as with mice on an iron-deficient diet) , with no intermediate expression levels. This may be due to the experimental protocol which did not include intermediate loaded or deficient groups. In C57blk/6 mice, expression of *hepcidin-1* is within the higher range and decreased with iron deficiency. In $hfe^{-/-}$ mice *hepcidin-1* mRNA expression was

within the lower range and increased with iron loading. The regulation of *hepcidin-1* is therefore analogous to a switch: a threshold value flicking it from the high to low. In this case, the set point of the threshold is higher in the $hfe^{-/-}$ then in the C57blk/6 mice, i.e. a higher iron concentration is required by the $hfe^{-/-}$ mice to switch *hepcidin-1* expression to the higher (loaded) level (Figure 3.1.6).

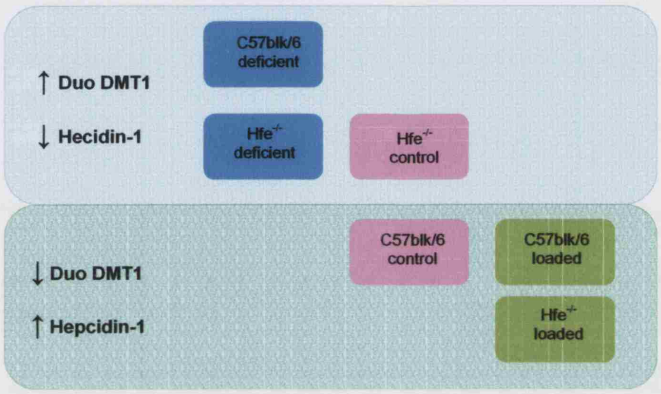

Figure 3.1. 6 Hepcidin-1 & Duodenal DMT1 expression in C57blk/6 & $hfe^{-/-}$ mice.

On the iron deficient diet, both genotypes have high duodenal DMT1/low hepcidin. On the iron loaded diet, both genotypes have low DMT1/high hepcidin. C57blk/6 mice on control diet have a phenotype similar tothat in the iron loaded mice, whereas $hfe^{-/-}$ mice on a control iron diet have a phenotype similar to the iron deficient groups.

Hepcidin-1 expression is inversely correlated to that of duodenal but not hepatic *DMT1*. Duodenal tissue is unique in that the expression of DMT1a is higher than that of DMT1b (Hubert & Hentze, 2002). As *hepcidin* expression does not show any correlation with *DMT1* expression in any other tissues to date it is possible that hepcidin suppresses the expression of the DMT1a isoform specifically.

The function of hepcidin-2 is not known. A study by Lou *et al.* (2003) using transgenic mice demonstrated distinct roles for hepcidin-1 and hepcidin-2 in iron metabolism; transgenic mice over-expressing hepcidin-1, showed severe iron deficient anaemia, probably due to decreased duodenal *DMT1* expression. Whilst, transgenic mice over-expressing hepcidin-2, did not suffer from anaemia and had normal haematological parameters. This suggests, as with the results presented here, that hepcidin-2 does not

regulate duodenal *DMT1* levels. However, two further studies looking specifically at iron overload demonstrated a coordinated increase in *hepcidin-1* and *hepcidin-2* under similar conditions (Ilyin *et al.*, 2003). Whilst this demonstrates an effect of iron status on *hepcidin-2* expression it does not necessarily imply that hepcidin-2 modulates duodenal iron absorption (Mazur *et al.*, 2003). The results of these two studies contrast with those presented here which demonstrate that *hepcidin-2* expression is independent to that of *hepcidin-1*. The reason underlying the discrepancies is not clear. However, Courselaud *et al.* (2004), have demonstrated that the expression of *hepcidin-1* and *hepcidin-2* differs between mouse strains: C57blk/6 mice expressed predominantly *hepcidin-1* mRNA, whereas in DBA/2 mice *hepcidin-2* mRNA was predominantly expressed. Gender related influences were also documented with higher *hepcidin-2* expression in females compared to males (Courselaud *et al.*, 2004).

Hepatic DMT1 is required for the uptake of plasma Fe_2-Tf and accumulation into liver stores (Chua *et al.*, 2004). Hepatocytes respond to systemic iron deficiency by decreasing DMT1 expression and *vice versa* (Trinder *et al.*, 2000). This redistributes the supply of Fe_2-Tf from the liver for storage to erythroid precursors. However, in this study $hfe^{-/-}$ mice responded to iron deficiency by increasing hepatic *DMT1* expression. This is an interesting observation and requires further investigation.

The function of Tfr2 is not known. In this study, *Tfr2* expression was identical between genotypes and dietary regimes. This is supported by data from various groups which demonstrated that cellular iron levels do not regulate *Tfr2* mRNA expression (Kawabata *et al.*, 2001;Johnson & Enns, 2004), although Fe_2-Tf has been demonstrated to increase the half-life of the Tfr2 protein in HepG2 and HuH7 cells (Johnson & Enns, 2004). It is therefore possible that Tfr2 may monitor Tf saturation.

3.1.5.1 Possible regulatory mechanisms for intestinal iron absorption

To date, several mechanisms have been proposed for the regulation of duodenal iron absorption. Waheed *et al.* (2002) demonstrated that hfe increased Fe_2-Tf uptake in CHO cells. This may be representative of the function of hfe in duodenal crypt cells and suggests that dysfunctional hfe reduces Fe_2-Tf uptake, causing iron deficiency in these cells. This is consistent with Trinder *et al.* (2002), who showed decreased Fe_2-Tf uptake in $hfe^{-/-}$ duodenal crypt cells and Simpson *et al.* (2003) who showed the ratio of duodenal iron levels to body iron stores was decreased in $hfe^{-/-}$

mice (Appendix V). Both *DMT1* and *Tfr1* contain IREs in the 3'UTR, these are stablised under iron deficient conditions. Therefore, the increase in both *DMT1* and *Tfr1* mRNA levels in $hfe^{-/-}$ duodenum supports the hypothesis of iron deficiency in the intestinal crypts.

However, whilst *DMT1* expression showed a 12-fold increase, this was mirrored by less than a 2-fold increase in *Tfr1*, suggesting the influence of additional, possibly systemic, regulatory mechanisms in addition to IRE-IRP interactions alone. This is consistent with a subsequent study by Anderson *et al.* (2002), which demonstrated an increase in duodenal *DMT1* mRNA and a decrease in *hepcidin* mRNA expression in response to changes in body iron status within 6 hours. As enterocytes in the villus crypts take approximately 3 days to reach maturity, the signal to increase uptake probably has an (additional) effect on *DMT1* expression in mature absorbative enterocytes. A study by Yamaji *et al.*, (2004), demonstrated decreased iron absorption by fully differentiated Caco-2 cells treated with hepcidin, which was due to a decrease in duodenal DMT1 mRNA and protein. Decreased iron absorption is also evident in mice treated with hepcidin (Appendix VII) (Laftah *et al.*, 2004). Together these studies suggest that depressed hepcidin levels cause an increase in duodenal *DMT1* mRNA in $hfe^{-/-}$ mice. High duodenal *DMT1* mRNA causes an increase in protein expression and therefore iron absorption. As a consequence, the iron load in $hfe^{-/-}$ mice is increased.

A study by Frazer *et al.* in 2002, demonstrated that *hepcidin* expression correlated positively with Tf saturation. Changes in both were detected before any changes in liver iron or haematological status were evident. As Tf is the acceptor for iron absorbed from the diet and supplies iron to most cell types (reviewed by Conrad & Barton, 1981), Tf saturation is rapidly affected by both dietary intake and body iron usage. This makes it an ideal indicator of body iron requirement and dietary supply. How transferrin saturation is monitored by hepatocytes, which express limited Tfr1, is not known. Although studies demonstrating that Fe_2-Tf increases the half-life of Tfr2, suggest a role for Tfr2 in this monitoring mechanism (Johnson & Enns, 2004). Intriguingly, mice with mutations in hfe (Zhou *et al.*, 1998;Levy *et al.*, 2000), β_2-microglobulin (Santos *et al.*, 1996), Tfr2 (Fleming *et al.*, 2002) and hepcidin (Nicolas *et al.*, 2001) show almost identical phenotypes with increased Tf saturation, periportal hepatic iron loading and RE iron sparing. This suggests that hfe and Tfr2 may function together to regulate *hepcidin* expression.

Additionally, hepcidin may be regulated at the post-translational level. This possibility could not be investigated because reliable antibodies against hepcidin were not available. However, post-translational regulation seems unlikely due to the tight inverse correlation between *hepcidin* and duodenal *DMT1* mRNA expression shown here.

The fact that hfe, like hepcidin, is highly expressed in the liver (Frazer *et al.*, 2001;Zhang *et al.*, 2004) and that disruption of either molecule leads to iron loading, raises the possibility that these molecules function together or as part of the same regulatory pathway. In addition, it suggests that the liver and not the intestine plays the central role in body iron homeostasis.

3.1.6 Conclusions

The data presented here demonstrate that duodenal *DMT1* expression is negatively correlated to that of *hepcidin-1* across all dietary regimes and in both the C57blk/6 and the $hfe^{-/-}$ genotype. $Hfe^{-/-}$ mice maintain the ability to regulate iron absorption according to body iron status. The iron-loaded phenotype of $hfe^{-/-}$ mice is due to inappropriately low *hepcidin-1* expression, this causes a increase in duodenal *DMT1*. The reason for this is probably due to the mis-sensing of body iron status by the hepatocytes which produce and secrete hepcidin-1. This disagrees with the original hypothesis which predicted the role of the hfe protein in sensing iron levels was limited to the duodenal crypts.

The data presented here suggests that the increased iron absorption characteristic of pregnancy may also be regulated at the hepatic level *via* modulating *hepcidin* expression. This hypothesis is tested in the following chapter.

3.2 Iron metabolism during pregnancy

Introduction

The previous chapter highlighted the role of hepcidin in the regulation of duodenal iron absorption in non-pregnant animals. In this chapter we investigate how iron homeostasis is modulated during pregnancy. The gene expression of iron transporters and modulators in the duodenum, liver and placenta are quantified.

Iron requirements during pregnancy are not constant (Figure 3.2.1). Initially, the requirements of the mother decrease to about 0.8 mg/day due to the cessation of menstruation. During the second trimester, an increase in oxygen consumption by both the mother and the foetus is associated with major haematological changes. In women total blood volume can increase by ~45%, plasma volume by ~50%, red blood cell mass by ~35% and haemoglobin by ~30% (De Leeuw *et al.*, 1966;Bonnar & Goldberg, 1969;Bothwell *et al.*, 1979). This expansion of the red blood cell mass and the transfer of increasing amounts of iron to the placental structures increase iron requirements to between 4-5 mg per day. During the final trimester, iron transfer to the foetus is in line with foetal growth, at this point the daily iron requirement of the mother is 6-7 mg/day (McArdle & Morgan, 1982;Hallberg, 1992;Viteri, 1998). This is in part acquired by an increase in duodenal absorption (Burdett & Reek, 1979;Hammond, 1997;Frederiksen, 2001;Leazer *et al.*, 2002), but this amount is in excess of what can be absorbed from even an optimal diet and the difference is compensated from the mothers iron stores (Bothwell *et al.*, 1979).

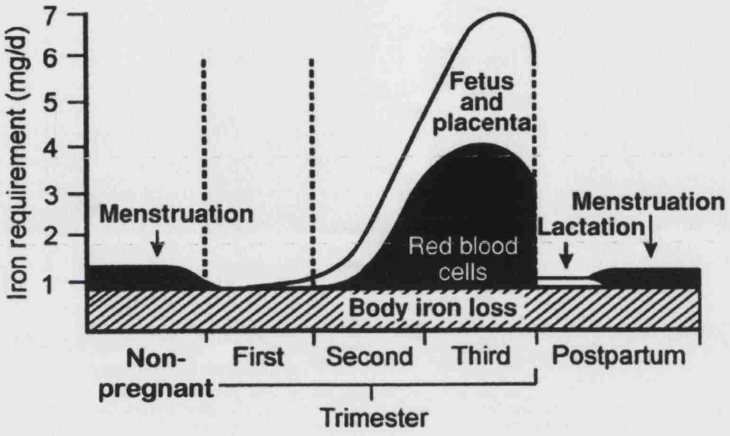

Figure 3.2. 1 Estimated daily iron requirements during pregnancy

Iron requirements, shown for an average 55 kg woman, during pregnancy are not constant. During the first trimester iron requirements decrease due to the cessation of menstruation. Iron requirements peak during the third trimester, due to an increase in the red blood cell mass and increased iron accumilation in the foetus and placenta. Adapted from Bothwell (2000).

3.2.1 Expression of iron modulator & transporter genes during pregnancy

As the primary sites of iron uptake, storage and usage, the duodenum, liver and placenta, respectively, are the sites at which iron homeostasis is regulated. By determining the expression of iron transport and modulator genes in these tissues the effect of pregnancy on iron homeostasis can be determined. In this preliminary study the expression of *DMT1, Ireg1, Dcytb, hepcidin, Tfr1* and *Tfr2* in the gut, liver and placenta during the second and third trimester of pregnancy was quantified, and compared to expression levels in non-pregnant dams.

Experimental design

Female rats were divided into three groups. One group was culled at the onset of the experiment, the remaining animals were allowed to mate and were sacrificed during the second or the third trimester as shown in the scheme below. Duodenal, liver and placental tissues were collected for quantification of mRNA and liver iron levels.

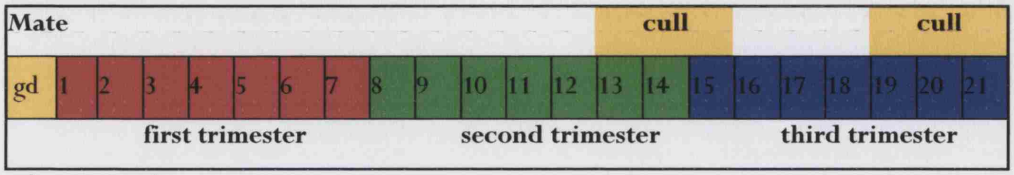

gd: gestation day

Animals

Wistar rats (Charles River, Sulzfeld, Germany) were fed a commercial diet (Altromin, Lage, Germany) and received tap water *ad libitum*. Animals were reared in a 12 hour light/12 hour dark cycle to assure regular oestrous cycles. Female, age matched virgin rats mated with males of the same strain. Pregnancy was confirmed by the presence of sperm in the vagina. This was taken to be day 1 of gestation. Dams were anaesthetised with Nembutal, 0.5 mL/kg and killed by stunning and cervical dislocation at gd 13-15 (the second trimester), or between gd 19-21 (the third trimester).

Duodenal, hepatic and placental tissue was collected, snap frozen in liquid N_2, stored at –80°C and shipped on dry ice. Blood was removed by cardiac puncture for the analysis of haematological parameters. Animals were reared and tissue collected at the Unité de Biochimie, Université de Louvain, Louvain-la-Neuve, Belgium by Dr Roberta Ward. All animals received humane care in compliance with the recommendations of EEC (86/609/CEF), the guidelines of the GSF-National Research Center for Environment and Health, Neuherberg, Germany, and the Belgian "projet de loi" (Moniteur Belge 19.92.1992).

mRNA Quantification

Total RNA was extracted from tissues using Trizol (Sigma, Poole, U.K.). This was used as a template to transcribe cDNA using the ABgene Reverse-iT 1st Strand Synthesis Kit (ABgene, Surrey, U.K.). Expression of duodenal *DMT1, Ireg1* and *Dcytb*, Hepatic *DMT1, hepcidin* and *Ireg1* and placental *DMT1* and *Ireg1* was quantified by real-time PCR, Gene expression levels were normalised to that of *actin*. Each PCR run was performed in duplicate. Protocols are as described in chapter 2.2.

Semi quantitative PCR using Ready-to-Go™ beads (Amersham Pharmacia, Bucks., U.K.) were used to quantify hepatic *Tfr2* and placental *Tfr1* levels, expression levels of these genes were normalised to that of *gapdh*, as described in chapter 2.2.

Quantification of haematological parameters

Liver iron levels were quantified by Dr Roberta Ward at the Unité de Biochimie, Université de Louvain, Louvain-la-Neuve, Belgium. Using the following method: maternal livers were removed, an aliquot of 100 mg was homogenised in 1 mL water, after which 300 µL was taken and digested with 1.5 mL nitric acid. After an overnight incubation, 1.2 mL water was added to the sample. A 0.3 mL portion of sample was wet-ashed with 1.5 mL of ultrapure 65% HNO_3 (Merck, Darmstadt, Germany). After 24 hours 1.2 mL of ultrapure water was added and the iron concentration determined by ICP-AES by Dr Dominik Klein (Institute of Toxicology, GSF-Forschungszentrum fur Umwelt und Gesundheit, GMBH, Neuherberg, Germany).

Blood was removed by cardiac puncture for the analysis of haematological parameters by routine haematological methods (Laboratoire medical du Sud, Namur, Belgium).

Statistical analysis

Statistical analysis was carried out by one-way ANOVA on Gaussian distributed data (KS statistic $P<0.05$) or two-tailed Mann-Whitney test on non-parametric data. The control group mean was given an arbitrary value of 1 and the test group means were adjusted accordingly. Each group consisted of 4-8 dams.

Results

3.2.1.1 Haematological parameters

Haemoglobin concentration was significantly decreased by the second trimester (Figure 3.2.2a). Significant changes in serum iron, TIBC and Tf saturation were not evident until the final trimester (Figure 3.2.2b-d).

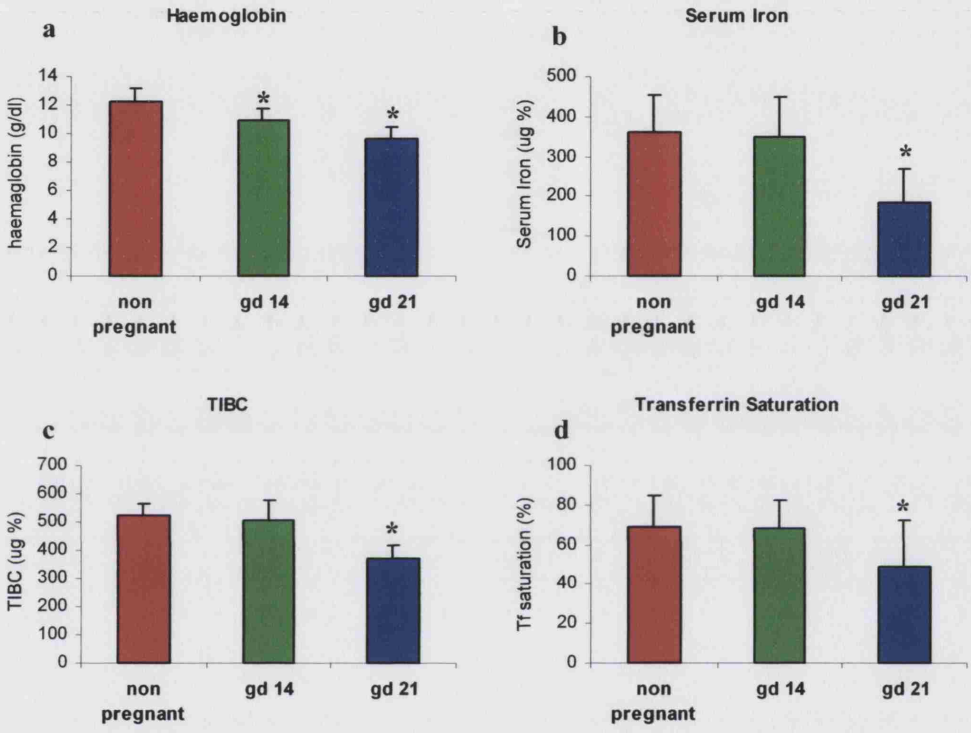

Figure 3.2. 2 Haematological parameters during pregnancy

*(a) Haemoglobin, (b) Serum Iron, (c) Total Iron Binding Capacity and (d) Transferrin saturation in non-pregnant (red bars), second trimester (green bars) and third trimester (blue bars) rats. Data is presented as means + SD of 6-8 animals. * denotes significant difference from the non-pregnant group at $P<0.05$.*

3.2.1.2 Duodenal gene expression during pregnancy

The expression of duodenal *Dcytb, DMT1* and *Ireg1* mRNA transcripts did not differ between the non-pregnant and the second trimester pregnant females [P=0.647, P=0.328 and P=0.619, respectively] (Figure 3.2.3).

During the third trimester, there was a significant change in the expression of *DMT1* [P=0.006], which increased. *Dcytb* increased five fold during this period, however due to a large degree of variation between individuals in the third trimester group, this did not reach significance at the 5% confidence limit [P=0.055]. Duodenal *Ireg1* mRNA expression was not significantly altered during pregnancy [P=0.213].

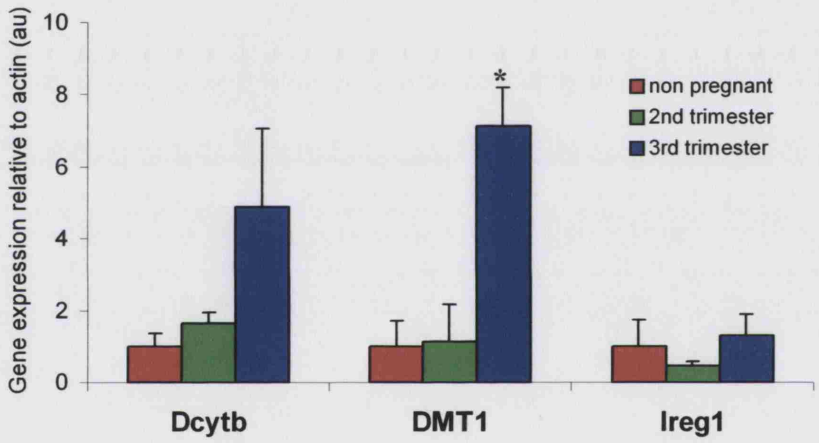

Figure 3.2. 3 Duodenal *Dcytb, DMT1* & *Ireg1* mRNA expression during pregnancy

The expression of duodenal transporters did not change significantly during the first two trimesters. During the final trimester Dcytb expression increased but this was not statistically significant, the increase in DMT1 was significant. Ireg1 mRNA expression did not alter between groups. Data is presented as mean + S.E.M. of 3-7 animals.

3.2.1.3 Hepatic gene expression during pregnancy

The mRNA expression profile for *hepcidin* was analysed: compared to the non-pregnant group *hepcidin* levels remained unchanged until the third trimester [P=0.839 second trimester] when expression plummeted to less than a tenth of that observed in the non-pregnant group [P=0.029] (Figure 3.2.4). The mRNA expression of hepatic *DMT1* was altered significantly in the second trimester [P=0.013], to less than a fifth that of the non-pregnant group (Figure 3.2,4), this decrease was sustained throughout the course of pregnancy [P=0.021 third trimester compared to the non-pregnant group]. Conversely, *Ireg1* mRNA expression increased two-fold by the third trimester [P=0.030 third trimester compared to the non-pregnant group]. *Tfr2* expression did not show a statistically significant change in expression although expression in the third trimester was less then half that of the non-pregnant group [P=0.414 second and P=0.103 third trimester].

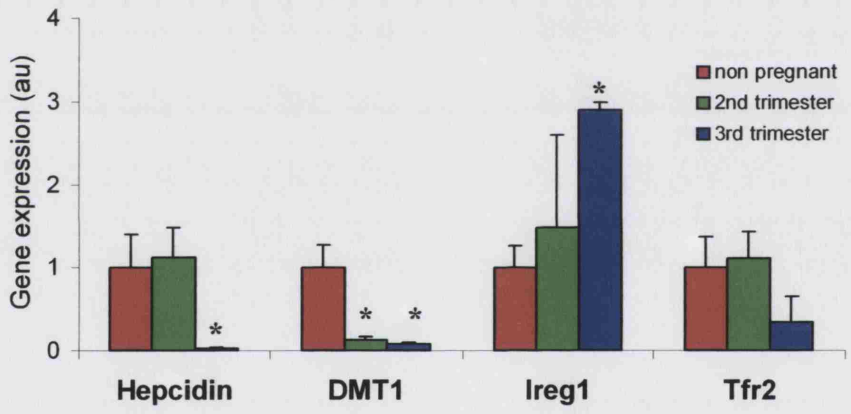

Figure 3.2. 4 Hepatic *Hepcidin-1, DMT1, Ireg1* & *Tfr2* mRNA expression

Hepcidin expression did not change until the final trimester when levels fell. This was preceded by a decrease in DMT1, which was significantly reduced in the second trimester. Ireg1 expression increased during the final trimester. During this period hepatic Tfr2 expression decreased but did not reach significance at the 5% confidence level. Data is presented as mean + S.E.M. of 3-7 animals.

3.2.1.4 Liver non-haem iron levels during pregnancy

By the second trimester maternal liver iron levels were reduced from 311 ± 13.4 μg Fe/g (mean + SD) in non-pregnant, age matched female rats to 247 ± 30.6 μg Fe/g (Figure 3.2.5). This reduction was significant at $P \leq 0.05$. There was a further significant reduction in maternal liver iron to 135 ± 56.2 μg Fe/g during the third trimester.

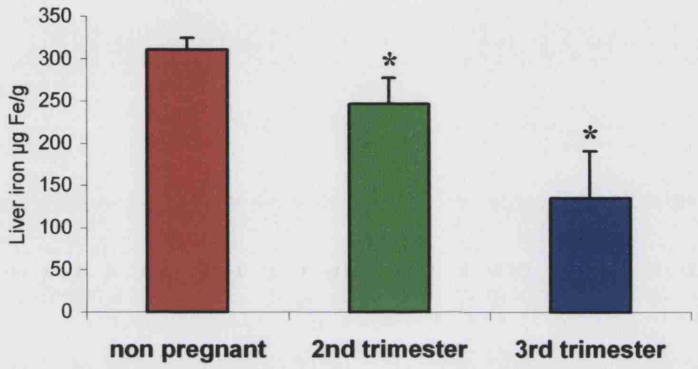

Figure 3.2. 5 Hepatic liver iron concentration during pregnancy

Liver iron content decreased during gestation, this was significant at the 5% confidence limit during the second trimester. The drop in iron levels was greatest between the second and third trimester. Data is presented as mean + SD of 4-7 animals. Liver iron concentrations were quantified and data analysed by Dr Roberta Ward at the Unite de Biochimiè, Universitè de Louvain, Louvain-la-Neuve, Belgium.

3.2.1.5 Placental gene expression during pregnancy

The expression of iron transporter genes were quantified in the placenta collected from dams in the second trimester. These were compared with gene expression levels quantified in placenta collected during the final trimester. The mRNA expression of placental *DMT1* increased between the second and third trimester [P=0.004] (Figure 3.2.6). However, *Tfr1* and *Ireg1* did not increase significantly during this period [P=0.289 and P=0.197 respectively].

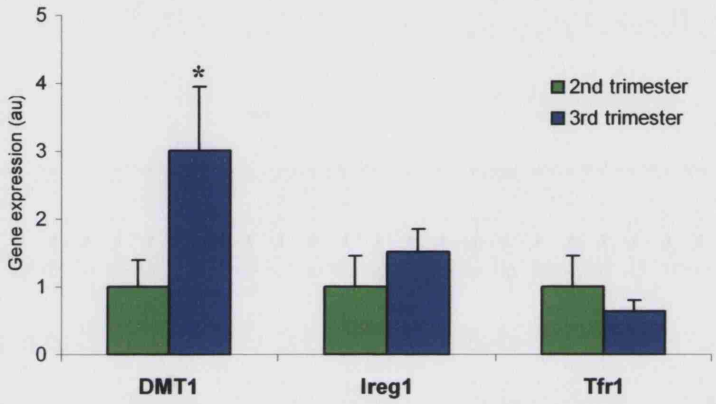

Figure 3.2. 6 Placental *DMT1, Ireg1* & *Tfr1* mRNA expression during pregnancy

Expression of placental DMT1, Ireg1 and Tfr1 was quantitated at the end of the second and end of the third trimester. During this period the expression of DMT1 increased. Ireg1 expression also increased but did not reach significance at $P \leq 0.05$. Data is presented as mean + S.E.M. of 4-6 animals.

3.2.2 Discussion

3.2.2.1 Duodenal iron absorption during pregnancy

This study demonstrates that during the final trimester duodenal *DMT1* mRNA levels were elevated, whereas *Ireg1* mRNA levels did not change (Figure 3.2.3). This is supported by a study conducted by Leazer *et al.* (2002), which demonstrated a sharp increase in *DMT1* mRNA expression from gd 15 in rats and is consistent with studies demonstrating an increase in iron uptake during the third trimester in human subjects (Svanberg *et al.*, 1975;Whittaker *et al.*, 1991).

The increase in duodenal iron absorption from gd 15 may be due to systemic iron deficiency as, data from iron deficient non-pregnant rats demonstrated an increase in absorption due to elevated *DMT1* and *Dcytb* expression, also without an increase in *Ireg1* mRNA (Frazer *et al.*, 2003). Indeed, systemic iron deficiency is observed in this study by a decrease in all the haematological parameters measured (Hb, serum iron, liver iron and Tf saturation). Iron deficiency is linked to increased duodenal *DMT1+ire* expression, as systemic iron deficiency also causes reduced iron levels in duodenal enterocytes of non-pregnant mice (Appendix V) (Simpson *et al.*, 2003).

Once within the enterocyte, absorbed iron may be sequestered into ferritin and lost from the body when the cell is sloughed off. Increased iron absorption has been associated with a reduction in iron incorporation into ferritin and *vice versa* (Batey & Gallagher, 1977). Ferritin translation, under the influence of *IREs* in the 5'UTR, is increased under high iron conditions and lowered under iron deficiency (Huang *et al.*, 1999). Studies in pregnant gd 21 rats have demonstrated a decrease in iron incorporation into ferritin compared to non-pregnant controls (Batey & Gallagher, 1977).

Despite the increase in iron absorption demonstrated during pregnancy (DeMaeyer & Adiels-Tegman, 1985), an increase in *Ireg1* mRNA was not observed during pregnancy. A recent study by Nemeth *et al.* (2004) demonstrated that hepcidin may bind to Ireg1 localised to the blm, and cause its internalisation and subsequent degradation. This would reduce the capacity for basolateral iron transfer. If this is correct, a reduction in hepcidin expression during the final trimester would increase basolateral iron transfer through Ireg1. This in turn would reduce the free iron pool within the enterocyte, increasing IRP activity and *DMT1+ire* translation, and consequently increase duodenal iron uptake. As this study quantified mRNA levels only, we were unable to test whether Ireg1 protein was increased in the pregnant dams. However, taking into

account the increase in uptake, decrease in ferritin and decreased mucosal plasticity, the availability of iron for transfer across the blm is increased, and it is probable that basolateral iron transfer is increased during pregnancy with or without an increase in Ireg1 protein levels.

3.2.2.2 Liver iron stores during pregnancy

The data presented here demonstrates that, during pregnancy, maternal liver iron levels fall (Figure 3.2.5). This is supported by data from a number of other groups which also report depressed hepatic iron accumulation during pregnancy (Svanberg *et al.*, 1975;Wilms & Batey, 1983;Howells *et al.*, 1986). Depletion of liver iron occurred before a reduction in any serum iron parameter assessed, with the exception of Hb (Figure 3.2.2). This is consistent with data presented by Heinrich (1975). The decrease in Hb concentration may therefore serve as a signal to trigger the mobilisation of maternal iron stores during pregnancy.

Tfr2 mRNA expression did not change during pregnancy. This is consistent with the data presented in chapter 3.1, which demonstrated that *Tfr2* mRNA expression was independent of changes in body iron status.

Our findings demonstrate a concurrent decrease in liver iron stores and hepatic *DMT1* mRNA expression during pregnancy (Figure 3.2.4). A decrease in hepatic DMT1 would decrease both NTBI and Fe_2-Tf uptake into hepatic iron stores and would increase iron availability for erythropoiesis and uptake by the placenta. The decrease in hepatic *DMT1* is consistent with a decrease in iron status, as *in vivo* studies also demonstrate a decrease in DMT1 protein expression in the hepatic sinusoidal plasma membrane under iron deficient conditions (Trinder *et al.*, 2000). Our data is contrary to data presented by Leazer *et al.* (2002) who did not detect any change in hepatic *DMT1* mRNA during pregnancy in Sprague-Dawley rats. The reason for this discrepancy may be due to differing genetic backgrounds of the rats, as in mice the genetic background has been shown to affect the ability to modulate *DMT1* expression (Fleming *et al.*, 2001;Dupic *et al.*, 2002).

In addition to decreasing uptake, existing liver iron stores are mobilised by increased iron efflux. Iron is thought to efflux from hepatocytes through Ireg1 (Montosi *et al.*, 2001;Njajou *et al.*, 2001;Njajou *et al.*, 2002) followed by oxidation by Cp before loading onto circulating apo-Tf (Liu *et al.*, 2002). However, *Ireg1* mRNA levels do not significantly increase until the third trimester (Figure 3.2.4), although a decrease in iron stores is evident from as early as the second trimester

(Figure 3.2.5). It is likely that the decrease in liver iron levels without a change in *Ireg1* expression is due to the increase in serum Cp during pregnancy (Chmielnicka & Sowa, 2000). The fall in liver iron levels accelerated during the final trimester (a 20% decrease over the initial two trimester, compared to a 55% decrease over the final trimester). This may be due to a reduction in hepcidin expression, which may increase hepatic Ireg1 protein during this period (Nemeth *et al.*, 2004).

It is plausible that the reduction in *hepcidin* expression during pregnancy demonstrated here is due to increased erythropoeisis, which is maximal in the third trimester (Figure 3.2.1). This is supported by a number of studies linking increased erythropoiesis with reduced *hepcidin* expression (Nicolas *et al.*, 2002). Alternatively it may is due to iron deficiency and/or the reduction in liver iron stores. To distinguish between these two factors, in chapter 3.4, a parallel experiment is conducted in which pregnant dams are supplemented with iron to maintain their iron stores and the expression of duodenal iron transporters is quantified.

3.2.2.3 Placental iron transfer

Placental iron transfer increases several fold over the final trimester of pregnancy (McArdle & Morgan, 1982). By quantifying the expression of iron transporters at the end of the second and towards the end of the third trimester the mechanism by which placental iron transfer is regulated was elucidated.

In the placenta no significant difference in placental *Tfr1* expression was observed between the second and third trimester. This is supported by immuno-localisation data which demonstrated no difference between the first and final trimester regarding placental Tfr1 staining (Khatun *et al.*, 2003). As *Tfr1* expression is regulated primarily by local iron concentrations (Louache *et al.*, 1984;Mattia *et al.*, 1984), this suggests that placental iron levels remain constant throughout pregnancy. *DMT1* expression increased between the second and third trimester. This is consistent with previous data which demonstrated a gradual increase in DMT1 expression on the maternal surface of the placenta during the final trimester (McArdle & Morgan, 1982;Leazer *et al.*, 2002).

Ireg1 expression did not increase between the second and third trimester. This suggests that Ireg1 is not a limiting for iron transfer across the placenta, however, as discussed earlier, it is possible that protein expression was increased without a detectable increase in mRNA levels.

The data presented here suggests that the increase in placental iron transfer during the final trimester is due to an increase in *DMT1* expression. Additionally, placental iron transfer may increase due to non-specific mechanisms such as the thinning of placental membranes and an increase in placental blood flow during the final stage of pregnancy. Coincidental, evidence for this is provided by Southon *et al.* (1989), who demonstrated a positive correlation between foetal weight and placental iron absorption. As an increase in foetal weight would require an increase in all nutrients required for growth, not specifically iron, this suggests that non-specific factors, such as increased blood flow over the placenta, may be the primary mechanism influencing the increase in placental iron transfer during the final trimester.

3.2.3 Conclusions

To compensate for the additional iron requirements of pregnancy, hepatic *DMT1* decreases and *Ireg1* expression increases during pregnancy. This mobilises liver iron stores. *Hepcidin* expression decreases during pregnancy, and interestingly, corresponds with an increase in both duodenal and placental *DMT1* expression. Various parameters may modulate *hepcidin* expression including iron deficiency and liver iron levels. The effect of these during pregnancy are addressed in the following two chapters.

3.3 Iron deficiency during pregnancy

Introduction

Although iron absorption is increased and stores mobilised (Chapter 3.2), iron deficiency is common during pregnancy (World Health Organisation, 2003). The consequences of this, both on the mother and her developing foetus, have been extensively studied and demonstrate that anaemia during pregnancy results in an increased risk of mortality and morbidity (reviewed by Allen, 2000 and Rush, 2000). The cloning and characterisation of DMT1, Dcytb and Ireg1 now allow us to demonstrate how iron homeostasis is regulated. Chapter 3.2 demonstrated that during pregnancy duodenal *DMT1* is increased and maternal stores are mobilised as a consequence of the increased requirements of pregnancy.

In this set of experiments the effect of iron deficiency on the two organs central to iron uptake during this period: the duodenal mucosa (3.3.2) and the placenta (3.3.1) is studied to elucidate the regulatory mechanisms underlying iron absorption at these sites.

3.3.1 Effect of iron deficiency on placental gene expression

Iron deficiency is usually less severe in the foetus then the mother (Appendix VI) (Gambling *et al.*, 2003). This suggests that there is a protective mechanism in place which ensures that the foetus receives an adequate iron supply, and during periods of iron deficiency this is at the expense of the mother. As all micronutrients must cross the placenta to enter the foetal circulation it is probable that the protective mechanism is located here.

To identify this mechanism, the expression of the placental genes postulated to be involved in iron transfer were quantified in pregnant rats placed on a low iron diet. Samples were collected at gd 21 since this is the period of greatest iron transfer (McArdle & Morgan, 1982) and any changes induced by iron deficiency would be expected to be maximally expressed.

The dietary regime used induces a mild but significant iron deficiency in the mother (Gambling *et al.*, 2002) and is therefore more representative of the human condition. Dams were placed on the low iron diet prior to mating to represent the human condition as a significant proportion of women are on the borderline of iron deficiency prior to conception, reviewed by Allen (2000).

Experimental design

Experiments were performed using rats of the Rowett Hooded Lister strain. They were group housed in cages, under constant temperature and humidity. Controlled illumination with a 12 hour light-dark cycle was maintained. All animals were provided with food and distilled water *ad libitum*.

16 female weanling rats were fed control diet for two weeks, before being randomly assigned to control or iron-deficient diets. They were fed this diet for 4 weeks prior to mating with males of the same strain. Mating was confirmed by the detection of a vaginal plug. Female rats were maintained on the same experimental diet until gd 21, when they were killed by stunning and cervical dislocation, see scheme below. Placentas associated with healthy foetuses were frozen in liquid N_2 before longer term storage at –80°C. All experimental procedures were carried out by Dr Lorraine Gambling at the Rowett Research Institute, Aberdeen, U.K.

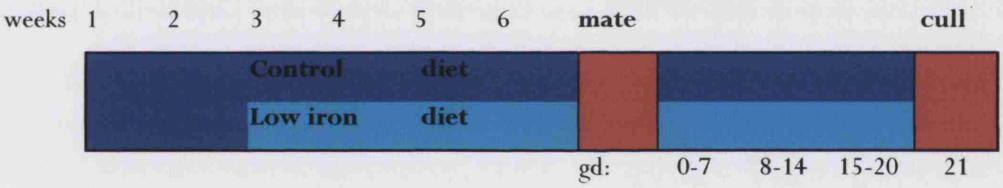

The experimental diets used were based on a dried egg albumin diet (Williams & Mills, 1970) and conformed to American Institute of Nutrition guidelines for laboratory animals (American Institute of Nutrition, 1980). $FeSO_4$ was added to achieve iron levels of 50 mg/kg (control diet) and 12.5 mg/kg (iron deficient diet). Dietary ingredients were purchased from Mayjex Ltd (Chalfont-St Peter, U.K.), BDH Chemicals (Poole, U.K.) or Sigma (Poole, U.K.).

Placental RNA was extracted from tissues using Trizol (Sigma, Poole, U.K.) by Dr Lorraine Gambling (Rowett Research Institute, Aberdeen, U.K.) as previously described (Chapter 2.2). RNA was stored at –70°C and shipped on dry ice.

Placenta RNA samples from 8 rats on a control diet and from 7 rats on a low iron diet were analysed and expression of *DMT1, Ireg1, Tfr1, Tfr2α, Tfr2β, hephaestin, ZIRTL* and *haemoxygenase-1* and *-2* was quantified and normalised to that of *gapdh* using Ready-to-Go™ RT-PCR beads (Amersham Pharmacia, Bucks., U.K.). Each PCR run was performed in duplicate. Protocols were as described previously in chapter 2.2.

The control (diet) group mean was given an arbitrary value of 1 and the test (low iron) group mean was adjusted accordingly. All results are presented as mean + S.E.M. of 7-8 animals. Statistical analysis was carried out by Students *t*-tests on Gaussian distributed data (Kolmogorov-Smirnoff $P>0.05$) with similar variance (F-test $P<0.05$). Significance was accepted at $P< 0.05$.

Results

Significant up-regulation of genes involved in iron uptake: *DMT1* [control 1.00 ± 0.08, deficient 1.99 ± 0.18, $P=0.002$], *Tfr1* [control 1.00 ± 0.09, deficient 1.94 ± 0.13, $P=0.007$] and *ZIRTL* [control 1.00 ± 0.46, deficient 3.02 ± 0.23, $P=0.026$] was observed in the placenta of iron deficient dams (Figure 3.3.1). This is consistent with Northern blot analysis using these samples by Gambling *et al.* (2001)(Appendix IV), which demonstrated an increase in *Tfr1* expression and *DMT1*, +ire isoform specifically, in iron deficient placenta. A complementary rise in protein expression was also identified.

The expression of genes involved in iron efflux: *Ireg1* [control 1.00 ± 0.20, deficient 1.00 ± 0.19, $P=1.00$] and *hephaestin* [control 1.00 ± 0.05, deficient 1.08 ± 0.17, $P=0.68$] did not alter in iron deficient placenta. Again consistent with Northern and Western blot analysis published by Gambling *et al.* (2001)(Appendix IV).

Messenger RNA levels of *haemoxygenase* was analysed to provide an indication of the extent of hypoxia due to iron deficiency. *Haemoxygenase* expression [*hox-1* control 1.00 ± 0.17, deficient 0.85 ± 0.17, $P=0.51$; *hox-2* control 1.00 ± 0.04, deficient 1.19 ± 0.07, $P=0.07$] did not alter in the placenta due to iron deficiency. This demonstrated that the effects of iron deficiency in the placenta were not due to hypoxia. *Tfr2α* and *Tfr2β* mRNA levels were below the sensitivity of the method used in both the control and iron-deficient placenta samples.

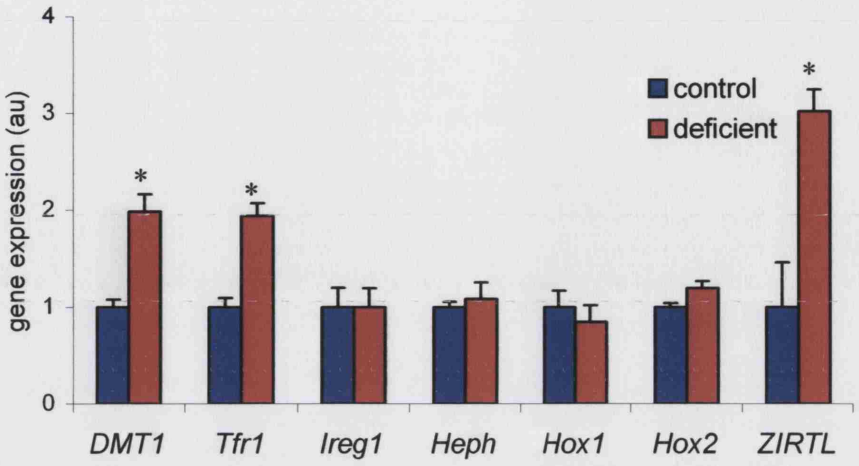

Figure 3.3. 1 Placental gene expression in iron-deficient & control rats

Iron deficiency caused an increase in placental DMT1, Tfr1 and ZIRTL expression and had no effect on Ireg1, hephaestin or haemoxygenase mRNA expression. Bars show mean of 8 control and 7 iron deficient animals + S.E.M., (*) denotes significance at $P \leq 0.05$.

3.3.2 Effect of iron deficiency on duodenal iron uptake during pregnancy

Recent figures show that worldwide up to 50% of pregnant women may be iron deficient (World Health Organisation, 2003). As demonstrated in section 3.2 duodenal iron uptake is enhanced during pregnancy, which is probably mediated by a decrease in hepcidin levels. Increased duodenal iron uptake, with a concurrent decrease in *hepcidin*, is also noted during iron deficiency (Chapter 3.1).

Whether the increase in duodenal uptake characteristic of pregnancy is at the maximum rate, or whether dietary iron deficiency leads to an further increase in iron uptake is investigated here. In addition, the long-term effects of iron deficiency in the neonate are not known. Here the effect of iron deficiency during pregnancy on the mechanism of duodenal iron uptake in the pups is studied at various time points postpartum. The iron concentration in rat milk is related to the iron status of the dam (Anaokar & Garry, 1981;O'Connor *et al.*, 1988). Therefore, by cross fostering newborn pups with dams on a control diet, this study isolated the effects of iron deficiency during pregnancy from additional confounding effects due to lactation by iron-deficient mothers.

Experimental design

Experiments were performed using weanling female rats of the Rowett Hooded Lister strain, as previously described (Chapter 3.3.1). However dams were not sacrificed until after birth, at which point 8 mothers from each group were culled and duodenal tissue was collected.

At birth, one male and one female pup from each litter was also culled and duodenal tissue collected. All remaining pups were cross-fostered to control diet dams. One male and one female pup from each litter were culled at 6 and 15 weeks after birth and duodenal tissue collected for iron uptake and gene expression analysis. Proximal duodenal tissue was collected, rinsed in PBS and stored, for a maximum of 20 minutes in oxygenated Hepes buffer at 15°C to assay for ^{59}Fe uptake assay, or rinsed with PBS and snap frozen in liquid N_2 and stored at –70°C for gene expression analysis. All animal procedures were conducted by Dr Lorraine Gambling at the Rowett Research Institute, Aberdeen, U.K.

3.3.2.1 Haematological parameters

Maternal and neonatal blood and liver samples were analysed by Dr Lorraine Gambling. Haematocrits were measured by drawing blood into heparinised capillary tubes, which were then centrifuged and read in a microhaematocrit reader. Tissue iron levels were determined by graphite furnace atomic-spectrophotometry (Gambling *et al.*, 2002).

Results, presented in appendix VI, show iron deficiency reduced the maternal haematocrit, Hb and liver iron levels significantly. Pups born to iron deficient dams were smaller, had significantly lower liver iron levels and were anaemic. Both the iron deficient and the control 6-week old postnatal groups had similar liver iron levels. However, the anaemia in the iron deficient pups was not reversed and persisted in the 16-week postnatal group.

3.3.2.2 Duodenal iron uptake

Duodenal ^{59}Fe uptake was measured *in vitro* using duodenal biopsies. These were exposed to an oxygenated ^{59}Fe (500 mM) solution for 5 minutes and were then washed in 10 x cold Fe solution to displace surface bound ^{59}Fe. Uptake was expressed as µmoles Fe uptake per gram wet weight tissue (protocol as described in chapter 2.2). Ferric iron uptake was measured in mothers and pups immediately after birth and in 15 week old pups. Ferrous iron uptake was quantified in pups at 6 weeks after birth, (method as described in chapter 2). Iron uptake was expressed as µmole Fe uptake/min/gram tissue. Each duodenal tissue section was divided into three approximately equal parts and each sub-section was assayed independently. In this manner duodenal iron uptake by each animal was tested in triplicate. Statistical analyses were carried out by Students *t*-tests on Gaussian distributed data (Kolmogorov-Smirnoff $P>0.05$) with similar variance (F-test $P<0.05$). Significance was accepted at $P<0.05$.

Results

Iron deficiency during pregnancy increased iron uptake in the duodenum of the mother [control 7.05 ± 0.88, deficient 39.56 ± 8.43 µmoles Fe (NTA)/min/gm, $P=0.005$] and the pups at birth [control 36.64 ± 5.85, deficient 114.28 ± 18.62 µmoles Fe (NTA)/min/gm, $P=0.002$] (Figure 3.3.2).

In the 6-week old pups the uptake of ferrous iron was quantified. It was decided to quantify ferrous rather then ferric iron uptake in this age group as iron uptake was expected to be reduced (Chowrimootoo *et al.*, 1992). As ferrous iron uptake is considerably higher then that of ferric iron, this provided a more sensitive assay. The increased duodenal iron uptake observed in pups of iron deficient mothers was reversed within six weeks of nursing to control diet dams [control 6485.25 ± 929.77, deficient 7179.75 ± 1630.35 µmoles Fe (ascorbate)/min/gm, $P=0.697$].

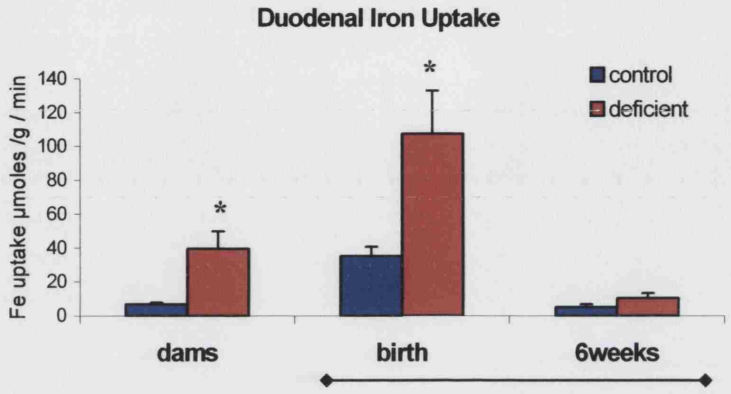

Figure 3.3. 2 Effect of maternal iron deficiency on duodenal iron uptake in dams and pups at birth and at 6 weeks postpartum

Duodenal ferric iron uptake was quantified in dams and pups immediately after birth. After nursing for 6 weeks with dams on a control diet, ferrous iron uptake was measured in pups. At birth uptake was significantly higher in the dams ($P \leq 0.01$) raised on iron deficient diet and their pups ($P \leq 0.01$). At six weeks of age no significant difference was observed between the two groups ($P \leq 0.05$). Data is presented as mean + S.E.M. of 8 animals, (*) denotes significance at $P \leq 0.01$.

3.3.2.2.1 Duodenal gene expression

Pups

Duodenal tissue was also collected for the quantification of gene expression. Tissues were rinsed with saline. Total RNA was extracted from tissues using Trizol (Sigma, Poole, U.K.). This was used as a template to transcribe cDNA using the ABgene Reverse-iT 1st Strand Synthesis Kit (ABgene, Surry, U.K.) and expression of *Dcytb*, *DMT1* and *Ireg1* was quantified by real-time PCR, levels were normalised to those of *actin* (protocol as described in chapter 2.2). Semi quantitative PCR using Ready-to-Go™ beads (Amersham Pharmacia, Bucks., U.K.) were used to quantify *Tfr1* levels, which was normalised to that of *gapdh*, as described in chapter 2.2.

Each sample was tested in duplicate. Statistical analysis was carried out by Students *t*-tests on Guassian distributed data (Kolmogorov-Smirnoff $P<0.05$) with similar variance (f-test $P>0.05$). Significance was accepted at $P \leq 0.05$. The control group mean was given an arbitrary value of 1 and the test group was adjusted accordingly. All data is presented as mean + S.E.M. of 4-6 animals.

Results

3.3.2.2.2 Duodenal gene expression in dams at birth

In the dams immediately after birth no difference in the gene expression of *DMT1* [control 1.00 ± 0.34 n=6, deficient 1.28 ± 0.20 n=6, P=0.503], *Dcytb* [control 1.00 ± 0.12 n=6, deficient 1.23 ± 0.24 n=7 P=0.438], or *Iregl* [control 1.00 ± 0.06 n=6, deficient 0.81 ± 0.11 n=4, P=0.172] was evident between the control and the iron deficient group (Figure 3.3.3a).

3.3.2.2.3 Duodenal gene expression in pups at birth

Dietary iron deficiency during pregnancy caused an increase in *DMT1* expression [control 1.00 ± 0.40 n=9, deficient 4.76 ± 0.75 n=5 P=0.0004] in pups at birth (Figure 3.3.3b). *Iregl* also increased in the iron deficient group [control 1.00 ± 0.40 n=7, deficient 2.91 ± 0.52 n=4 P=0.017]. In the iron deficient group *Dcytb* was also increased but, due to the large variation between individual animals within the deficient group, the difference between groups was not significant at the 5% confidence level [control 1.00 ± 0.33 n=7, deficient 60.61 ± 43.88 n=4 P=0.092]. *Tfr1* expression was identical between the two groups [control 1.00 ± 0.04 n=7, deficient 0.95 ± 0.03 n=4 P=0.380].

3.3.2.2.4 Duodenal gene expression in 6 week old pups

After nursing with control diet dams for 6 weeks no significant difference in the expression of *DMT1* [control 1.00 ± 0.53 n=7, deficient 0.35 ± 0.20 n=7, P=0.26], *Dcytb* [control 1.00 ± 0.19 n=8, deficient 0.61 ± 0.13 n=8, P=0.11], *Iregl* [control 1.00 ± 0.22 n=8, deficient 0.72 ± 0.13 n=8, P=0.44], or *Tfr1* [control 1.00 ± 0.05 n=8, deficient 0.92 ± 0.06 n=8, P=0.51] was evident between the iron deficient and control groups (Figure 3.3.3c).

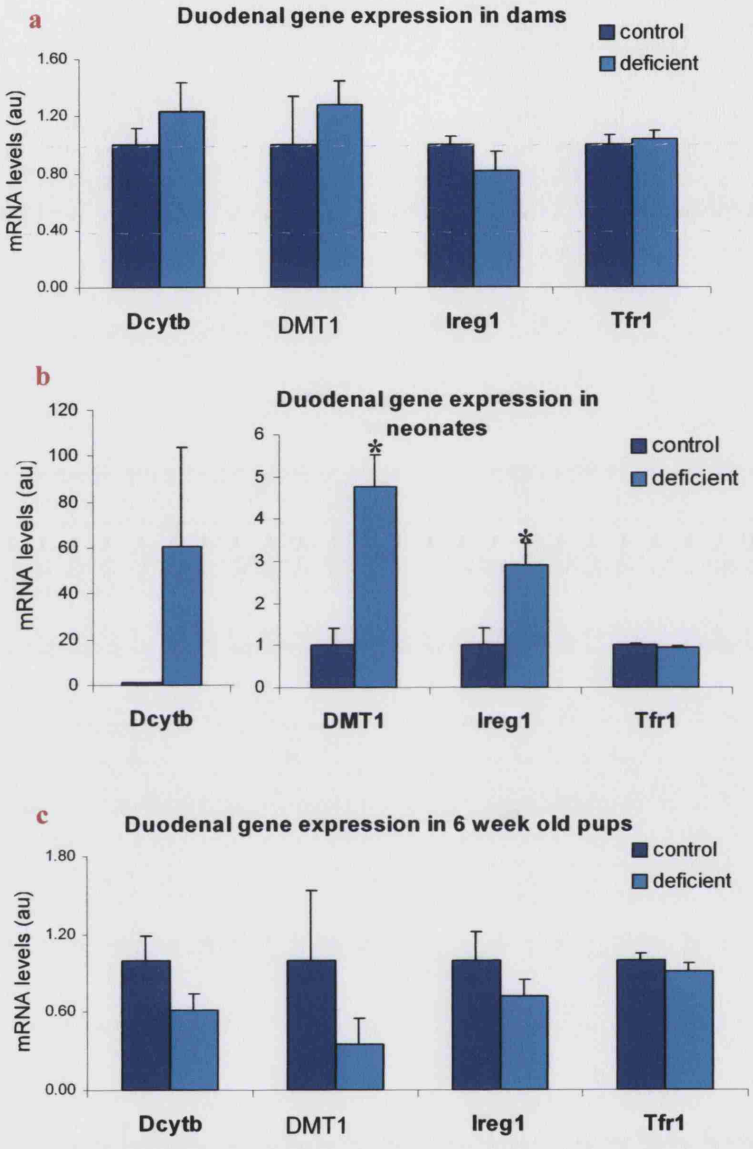

Figure 3.3. 3 Duodenal expression of *DMT1, Dcytb, Ireg1* and *Tfr1* mRNA in (a) dams, (b) newborn, and (c) six week old pups, raised on a low iron diet

Expression of DMT1 ($P \leq 0.001$) and Ireg1 ($P \leq 0.02$) was increased in the neonates at birth, this was not evident in either the dams or the 6 week old neonates. Dcytb and Tfr1 did not change significantly. Data is presented as mean + S.E.M. of 4-6 animals. (*) denotes significance at $P \leq 0.05$.

3.3.3 Discussion

3.3.3.1 Effect of iron deficiency on duodenal and placental iron transfer

In non-pregnant animals, iron deficiency, whether due to increased erythropoeisis, decreased dietary availability or inflammation, leads to a decrease in *hepcidin* expression and consequently an increase in duodenal *DMT1* and iron uptake (Anderson *et al.*, 2002;Frazer *et al.*, 2002; Nicolas *et al.*, 2002;Nemeth *et al.*, 2003;Laftah *et al.*, 2004; Yamaji *et al.*, 2004). The previous chapter demonstrated that *hepcidin* levels are low and duodenal *DMT1* expression is elevated during pregnancy. This study demonstrates that duodenal iron uptake increases further in pregnant dams raised on an iron deficient diet.

Iron deficiency increases iron uptake in both the duodenum (Chapter 3.3.2) and the placenta (Chapter 3.3.1). In the placenta *DMT1+ire* and *Tfr1* mRNA and protein are increased (Figure 3.3.1, appendix VI). In the gut, although uptake is increased, this is not a consequence of an increase in transporter mRNA levels (Figures 3.3.2-3). Instead, it is likely to be due to a relocalisation of DMT1 and Dcytb protein from intracellular vesicles to the brush border membrane as demonstrated in chapter 3.1.

The expression of placental *ZIRTL* is also increased as a consequence of iron deficiency. This study demonstrates *ZIRTL* expression in the rat placenta for the first time. *ZIRTL* expression is developmentally regulated, and appears relatively late in development when most cell types are undergoing terminal differentiation, therefore the expression of *ZIRTL* in term placenta is not surprising. Increased expression in the face of iron deficiency as demonstrated here, is also characteristic of the homologous gene in plants, where, as an iron transporter in roots, it is induced by iron deficiency (Eide *et al.*, 1996). The mechanism of placental iron transfer is not well understood, however preliminary data by Lioumi *et al.* (1999) showed ZIRTL to localise in the endosomal lysosomal pathway. The significance of this compartment in placental iron transport is discussed further in chapter 3.6.

Interestingly, *Ireg1* mRNA expression was not increased under iron deficient conditions in either the duodenum or the placenta. This may again be due to an increase in translation but not mRNA levels, as discussed previously, or may be indicative that iron transfer across the blm is not the limiting step to either duodenal or placental iron transfer. The latter is probably true in iron deficient conditions. Iron deficiency in these circumstances is due to insufficient iron in the gut lumen. By increasing expression of brush border Dcytb and DMT1 the mucosa has the potential to absorb a greater percentage of the dietary iron available. This should compensate for the reduced availability of iron and ensure the required amount is absorbed into the enterocyte. As iron requirements for the animal have not changed, subsequent basolateral transfer (*via* Ireg1) remains constant.

The same is probably true for placental iron transfer. Reduced iron levels in the maternal serum do not affect the iron requirements of the foetus. This means that the placental transfer rate remains constant. However due to reduced serum iron levels apical Tfr1 and DMT1 expression is increased to compete more effectively for Fe_2-Tf. The increase in both *Tfr1* and *DMT1* mRNA and protein suggests that this may be due to increased IRP activity within the cell. Continued iron efflux from the placental tissue but reduced uptake, due to reduced serum iron, would result in cytosolic iron depletion. This would cause an increase in IRP activity, increase binding to *DMT1+ire* and *Tfr1* mRNA increasing its half-life and therefore translational efficiency. In support of this hypothesis, an increase in placental *DMT1+ire* without a change in *DMT1-ire* has been demonstrated in these iron deficient rat placenta (Appendix IV) (Gambling *et al.*, 2001).

However, the increase in apical transport is not sufficient to compensate completely for the iron deficiency as both dams on iron deficient diet and their pups are iron deficient. This is not surprising, if the compensation was complete, placental iron levels would return to control levels, this would lead to a decrease in IRP activity and decreased *DMT1* and *Tfr1* expression to control levels and a lower iron uptake than controls since maternal Tf saturation/ lumenal iron concentration would be lower.

3.3.3.1 Neonatal iron absorption

Studies by Chowrimootoo *et al.* (1992) using guinea pigs, have demonstrated the higher capacity of the neonatal gut to absorb iron compared to the adult. This is also evident here, where iron uptake in the neonate at birth was ~4 times greater then that of the control dams, and ~2.5 times higher in the iron deficient dams and neonates. In rats this may be due to hypertrophy of the villi, increased absorption in lower crypt regions and in the distal small intestine (Debnam *et al.* 1991;Chowrimootoo *et al.* 1992).

Duodenal iron uptake is increased in neonates of iron deficient mothers. This corresponds to an increase in *DMT1, Dcytb* and *Ireg1* mRNA suggesting that *de novo* synthesis of these gene products drive the increase in uptake. Quantification of liver iron levels reveal that the neonates of iron deficient mothers have significantly lower iron stores, although the difference between the neonates is not as extensive as between the dams (Appendix VI). These findings are in keeping with those of Rodrigues-Matas *et al.* (1998) and are due to increased placental *DMT1* and *Tfr1* which upregulates iron transport due to iron deficiency in the mother. As the neonates had not been fed, dietary influences were eliminated. The increase in *DMT1, Dcytb* and *Ireg1* mRNA is therefore due to systemic iron deficiency generated *in utero*.

Little data is available at present concerning the expression of hepcidin in the neonate. In the foetal liver, *hepcidin* expression is low and, in one study, has been demonstrated to increase transiently shortly after birth (Courselaud *et al.*, 2002). Whether this transient increase is functionally significant, possibly due to increased stress during pregnancy, or due to maturation of the foetal liver is not clear. However, due to the increased expression of duodenal *DMT1, Dcytb* and *Ireg1* in iron-deficient pups, and the decrease in *hepcidin* expression exhibited in supplemented pups (Chapter 3.4), it is possible that foetal hepcidin may have an active role in modulating duodenal gene expression at birth in a mechanism analogous to that of the adult.

Alternatively, hepcidin secreted by the mother, may cross the placenta and enter foetal circulation. To date, there is no data confirming or contesting this, however hepcidin is a small peptide that is readily filtered through the kidney and could potentially transverse the polarised cells of the placenta. It is possible that maternal hepcidin enters foetal circulation and supresses the expression of duodenal iron transporters in the neonatal gut. However, although iron uptake was increased in the maternal gut, this was not due to a change in the expression of *DMT1, Dcytb*

and *Ireg1* mRNA and it does not seem plausible that maternal hepcidin would supress neonatal but not maternal duodenal gene expression.

Within 6 weeks of fostering with control diet mothers the difference between the control and iron deficient groups, in respect to duodenal iron uptake, had been abrogated. This was further supported by similar expression levels of *Dcytb, DMT1* and *Ireg1* mRNA in the duodenum. At this age, liver iron levels were similar between the two groups, demonstrating that although mothers milk had very little iron, upregulation of the iron transporters was an effective mechanism by which to regulate iron homeostasis. This data demonstrates that iron uptake is regulated to liver iron stores in neonates.

3.3.4 Conclusions

This chapter has demonstrated that although iron absorption is increased during pregnancy, iron deficiency further enhances duodenal iron uptake. Iron deficiency also increases placental iron uptake, reducing the extent of iron deficiency in the neonate. However the neonate is not entirely protected from iron deficiency as neonatal liver iron levels are reduced, and surprisingly, duodenal iron uptake is increased. The increased capability of the duodenum and placenta to transport iron could lead to iron overloading when pregnant animals are given iron supplements. The possibility of this is addressed in the following chapter.

3.4 Iron Supplementation During Pregnancy

To test whether the increase in iron absorption associated with pregnancy is driven by iron deficiency, pregnant dams were administered an iron supplement. This limited the decrease in iron status associated with pregnancy. Various parameters were subsequently quantified and compared to those in pregnant non-supplemented animals. These parameters included:

Experiment 3.4.1: mRNA levels of iron transporters and regulators in the duodenum, liver, placenta and foetal liver

Experiment 3.4.2: duodenal iron absorption

Experiment 3.4.3: placental gene expression in humans

3.4.1 Iron supplementation: Effect on gene expression

The consequence of iron supplementation on the mRNA expression of iron transporters and modulators was assessed in non-pregnant animals and during the second and third trimester in pregnant dams.

Experimental design

Wistar rats, reared in a 12 hour light/12 hour dark cycle, were fed a commercial diet (Altromin, Lage, Germany) and received tap water *ad libitum*. Male rats were housed with female, age-matched virgin rats overnight after which males were removed. Pregnancy was confirmed by the presence of a vaginal plug. This was taken to be day 0 of gestation. 10 mg iron as iron dextran (Vifor Pharmaceuticals, St. Gallen, Switzerland) or an equal volume of saline was administered intramuscularly on day 0 of pregnancy. The pregnancy proceeded for 14 or 21 days, after which the rats were anaesthetized with Nembutal (0.5 g/kg, Abbott Laboratories, Chicago, USA) and killed by stunning and cervical dislocation. Duodenal, liver and placental tissue was collected, snap frozen in liquid N_2, stored at –80°C and shipped on dry ice.

In a parallel experiment (see scheme below), age matched Wistar females were administered 10 mg iron as iron dextran (Vifor Pharmaceuticals, St. Gallen, Switzerland) intramuscularly, for use of non-pregnant, iron-supplemented controls. After 14 or 21 days the rats were culled and tissue collected as with the pregnant groups. All animals were reared and tissue collected at the Unité de Biochimie, Université de Louvain, Louvain-la-Neuve, Belgium by Dr Roberta Ward.

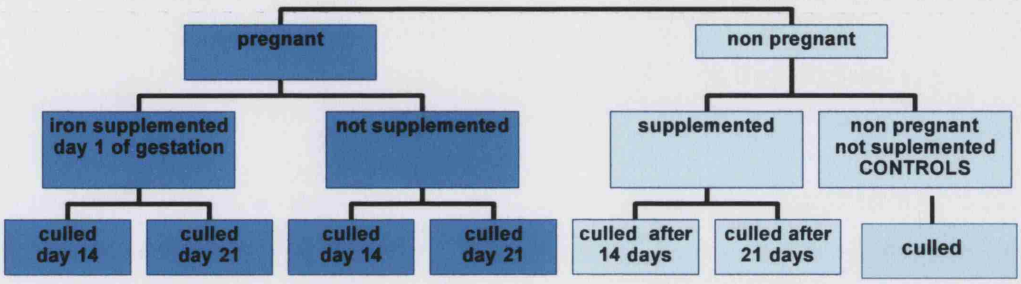

mRNA Quantification

Total RNA was extracted from tissues using Trizol (Chapter 2.2). This was used as a template to transcribe cDNA (Chapter 2.2). Duodenal *DMT1, Ireg1* and *Dcytb*, Hepatic *DMT1, hepcidin* and *Ireg1* and placental *DMT1* and *Ireg1* expression was quantified by real-time PCR and normalised to that of *actin* (Chapter 2.2). Each PCR run was performed in duplicate.

Semi quantitative PCR using Ready-To-Go beads were used to quantify hepatic *Tfr2* and placental *Tfr1* levels, expression levels of these genes were normalised to that of *gapdh* (Chapter 2.2).

Quantification of iron levels

Iron levels were quantified by Dr Roberta Ward at the Unite de Biochimiè, Universitè de Louvain, Louvain-la-Neuve, Belgium, as described in chapter 2.2. Blood was removed by cardiac puncture for the analysis of serum iron concentration, Tf saturation, TIBC and Hb concentration by routine haematological methods (Laboratoire medical du Sud, Namur, Belgium).

Statistical analysis

Statistical analysis was carried out by one-way ANOVA on Gaussian distributed data (Kolmogorov-Smirnoff $P>0.05$) or by two-tailed Mann-Whitney on non-parametric data, with *Bonferoni* posthoc tests. Significance was set at $P\leq0.05$ for all statistical tests. Each group consisted of 4-8 dams.

Gene expression data is presented as mean + S.E.M. The control group mean was given an arbitrary value of 1 and the test groups were adjusted accordingly. Liver iron levels, and serum iron parameters (Hb, TIBC, Tf saturation and serum iron), quantified by Dr Roberta Ward, are presented as mean + SD.

Results

3.4.1.1 Haematological parameters

Non-pregnant rats supplemented with a single 10 mg iron dose showed no significant changes in the haematological parameters tested (Figure 3.4.1). Significant reduction in Hb, serum iron, TIBC and Tf saturation was evident in non-supplemented dams during the final trimester. Iron supplementation increased all haematological parameters tested at gd 21, although none reached values approaching that of the non-pregnant group.

3.4.1.1 Haematological parameters

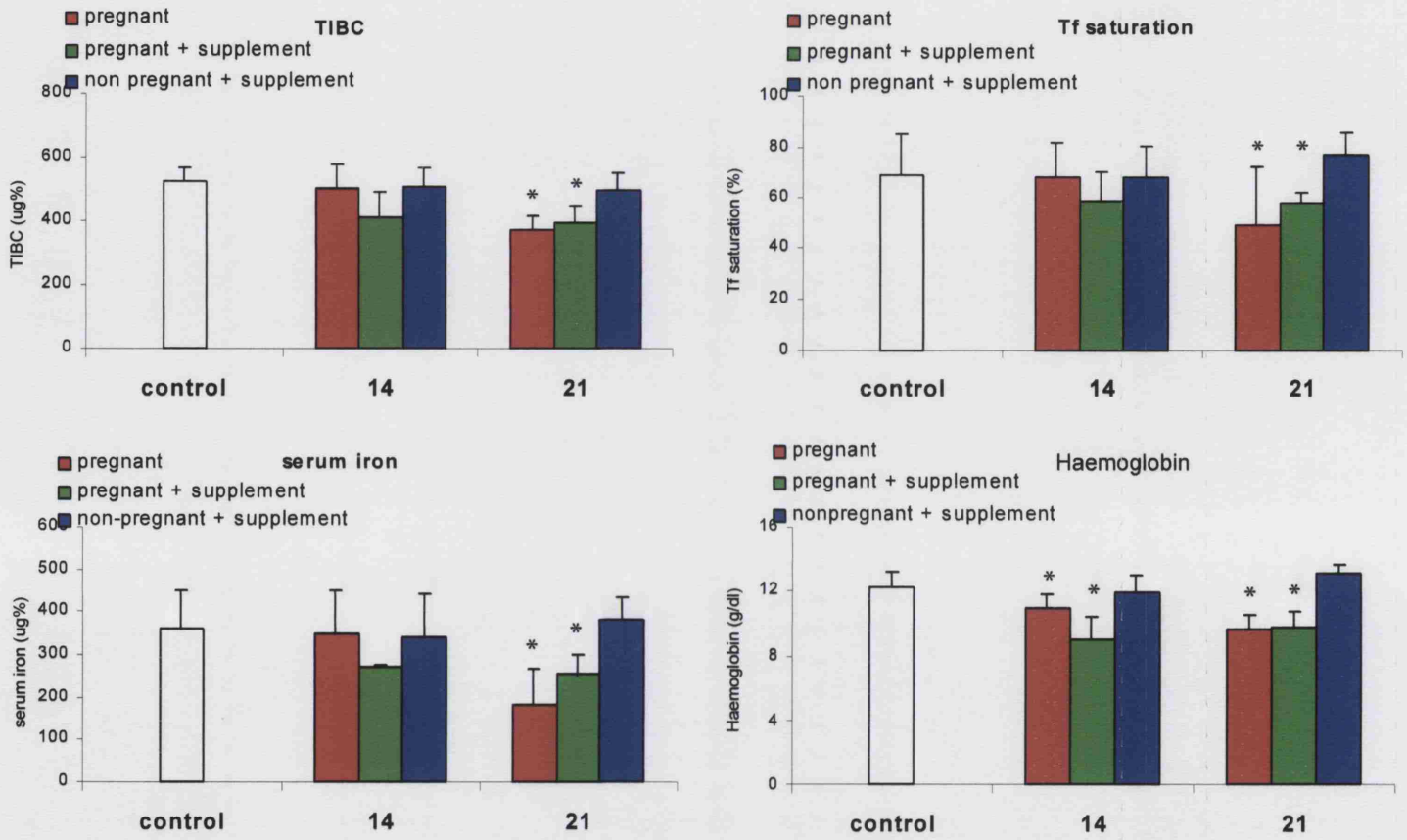

Figure 3.4.1 Effect of iron supplementation on haematological parameters during pregnancy

*Pregnant (gd 1) and non-pregnant rats were supplemented with a single 10 mg dose of iron dextran. Animals were culled 14 and 21 days after supplement. (a) TIBC, (b) Tf saturation, (c) serum iron, and (d) haemoglobin concentration was quantified by Dr R. Ward. Data is presented as mean + SD. Statistical analysis was by ANOVA. Asterix denote significance at * $P<0.05$ all groups were compared to the control non-pregnant group.*

3.4.1.2 Liver Iron Concentration

In non-pregnant animals, iron supplementation increased hepatic iron stores (Figure 3.4.2). By 14 days post-supplementation iron levels were 153%, and by 21 days 174%, that of the non-supplemented group. During pregnancy hepatic iron levels fell, by gd 14 iron levels were 55% that of the non-pregnant animals, this droped further to 28% by gd 21. In pregnant rats supplemented with 10 mg of iron dextran on gd 0, hepatic iron levels increased by 20% by gd 14, compared to a drop to a 55% in the non supplemented group. However, in both supplemented and non-supplemented groups, hepatic iron levels fell approximately 50% between gd 14 and gd 21. As the supplemented group had higher reserves at gd 14, the hepatic iron concentration was higher in the supplemented cohort compared to the non supplemented group (55% compared to 28% that of the non pregnant group) at term. Means, SD and P values are tabulated in appendix II.

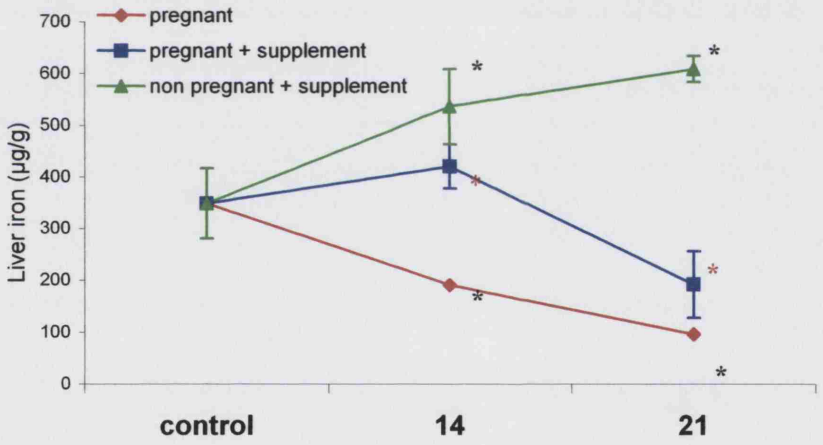

Figure 3.4. 2 Effect of iron supplementation on liver iron levels

Pregnant (gd 0) and non-pregnant rats were supplemented with a single 10 mg dose of iron dextran. Animals were culled 14 and 21 days after supplement, after which liver iron concentration was quantified. A single 10 mg of dose of iron dextran administered at gd 0 did not fully compensate for the iron requirement of pregnancy. Data is presented as mean ± SD. Statistical analysis was by ANOVA. (*) denotes significant difference at P<0.05 from the control group. (*) denotes significant difference at P≤0.05 from the corresponding non-supplemented pregnant group.

3.4.1.3 Effect of iron supplementation on duodenal gene expression

3.4.1.3.1 Duodenal *Dcytb* mRNA expression

In non-pregnant animals, iron supplementation reduced duodenal *Dcytb* expression (Figure 3.4.3), this was evident up to 21 days post administration. However, this change in expression was not statistically significant at either time-point.

In the pregnant cohort, iron-supplementation also caused a reduction in *Dcytb* expression, but again, this did not reach statistical significance at $P \geq 0.05$.

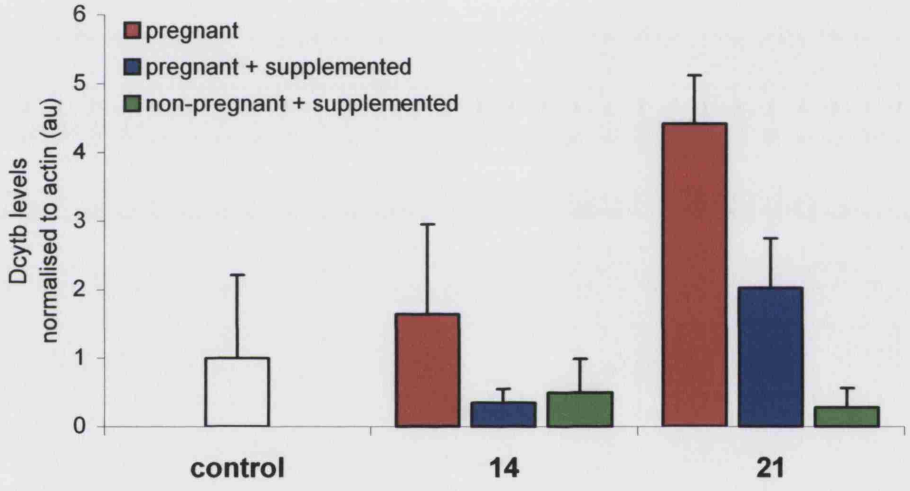

Figure 3.4. 3 Effect of iron supplementation on duodenal *Dcytb* expression

Duodenal Dcytb levels were quantified and normalised to that of actin in iron supplemented and control rats during the second and third trimester. Non-pregnant rats were also supplemented and Dcytb expression quantified after 14 and 21 days. Data is presented as mean + S.E.M.

3.4.1.3.2 Duodenal *DMT1* mRNA expression

Iron supplementation had no effect on *DMT1* expression 14 days post administration in either pregnant or non-pregnant groups (Figure 3.4.4). Quantification of *DMT1* levels 21 days post administration demonstrated a decrease in *DMT1* expression in both groups. Iron supplementation therefore reversed the increase in duodenal *DMT1* expression characteristic of pregnancy.

As demonstrated previously in chapter 3.1, duodenal *DMT1* mRNA expression was correlated to iron status in C57blk/6 mice, increasing with iron deficiency and decreasing with supplementation. A reduction in *DMT1* expression upon iron supplementation in pregnant rats demonstrates that this mechanism is also functional during pregnancy.

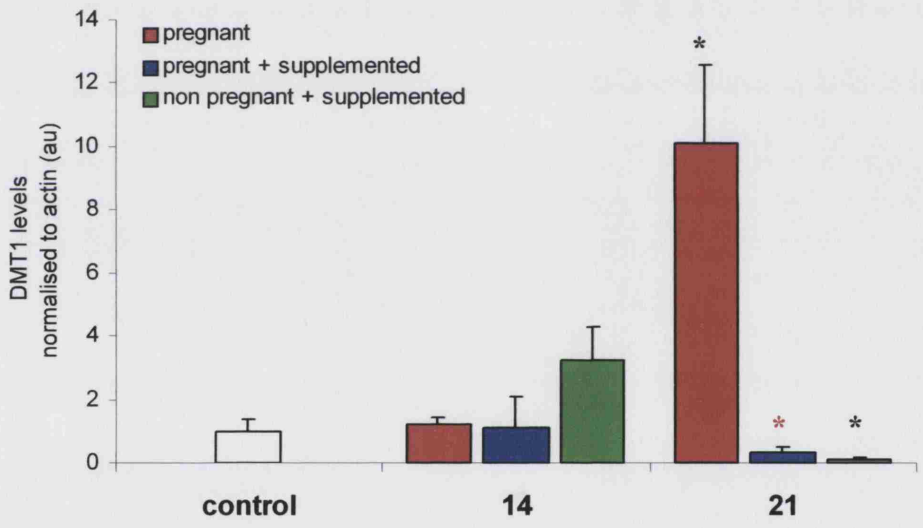

Figure 3.4. 4 Effect of iron supplementation on duodenal *DMT1* expression

Duodenal DMT1 levels were quantified and normalised to that of actin in iron supplemented and control rats during the second and third trimester. Non-pregnant rats were also supplemented and DMT1 expression quantified after 14 and 21 days. Data is presented as mean + S.E.M. (*) denotes significance difference at P≤0.05 from the control group. (*) denotes significant difference (P≤0.05) from the corresponding non-supplemented pregnant group.

3.4.1.3.3 Duodenal *Ireg1* mRNA expression

In non-pregnant animals, iron supplementation caused a small non-significant increase in duodenal *Ireg1* mRNA expression at 14 days post supplementation (Figure 3.4.5 green bars). This increase continued and reached significance by 21 days post supplementation. During pregnancy, *Ireg1* demonstrates a small, though non-significant, increase in expression (Figure 3.4.5 red bars). The combination of iron supplementation and pregnancy led to slightly higher expression of this gene. However, this did not reach statistical significance due to variation between individuals in the third trimester group (Figure 3.4.5 blue bars).

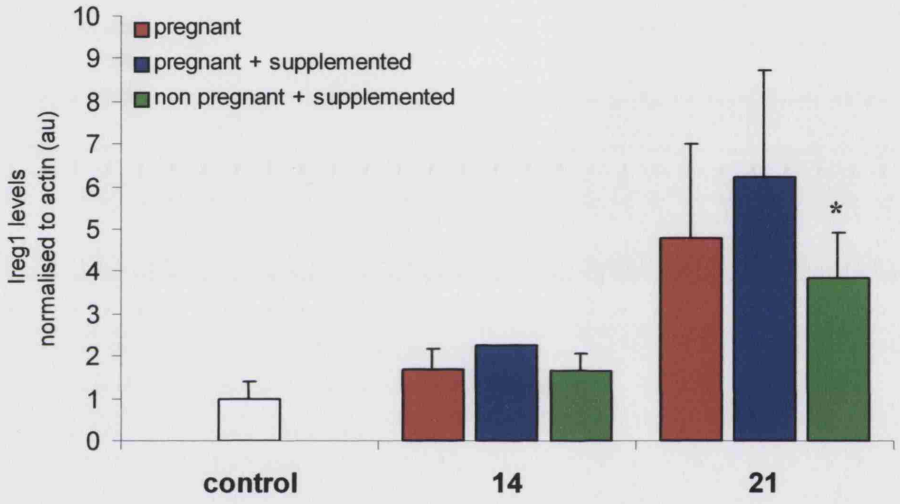

Figure 3.4. 5 Effect of iron supplementation on duodenal *Ireg1* expression

Pregnant and non-pregnant rats were administered iron. Duodenal Ireg1 expression was quantified at 14 and 21 days post supplementation. Data is presented as mean + S.E.M. (*) denotes significant difference from the control group at $P \leq 0.05$.

3.4.1.4 Effect of iron supplementation on hepatic gene expression

3.4.1.4.1 Hepatic *DMT1* mRNA expression

During pregnancy hepatic *DMT1* expression decreased, this was evident during the second and third trimester (Figure 3.4.6). Iron supplementation possibly reversed the decrease during the final trimester, as there was no significant difference between the non pregnant and the pregnant supplemented group at gd 21, this however may be due to the large variation between individuals in the pregnant iron supplemented group. Iron supplementation had no effect on *DMT1* expression in the non-pregnant group. These data are consistent with those of C57blk/6 mice, (Chapter 3.1), where dietary iron variability also showed no effect on hepatic *DMT1* mRNA levels. This illustrates that rat and mouse data are comparable.

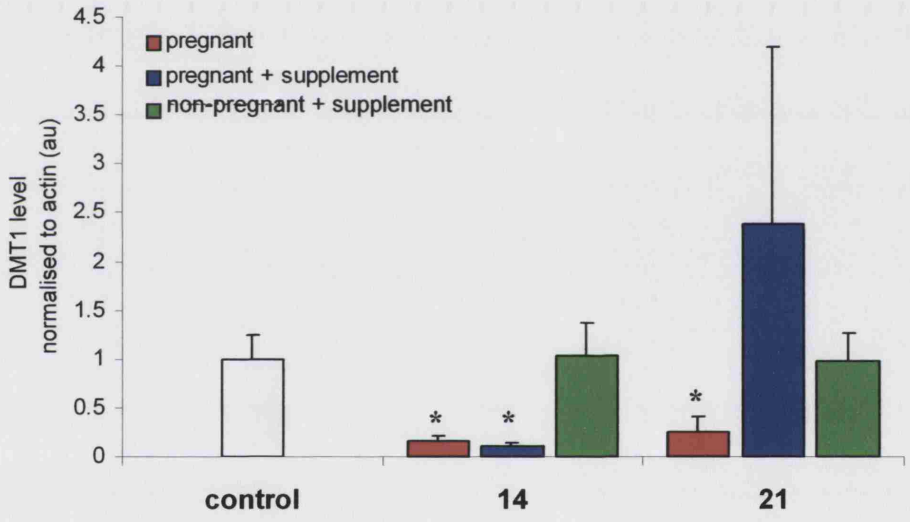

Figure 3.4. 6 Effect of iron supplementation on hepatic *DMT1* expression

Hepatic DMT1 levels were quantified and normalised to that of actin in iron supplemented and control rats at gestational day 14 and 21. Non-pregnant rats were also supplemented and DMT1 expression quantified during the second and third trimester. Data is presented as mean + S.E.M. (*) denotes significant difference from the control group at $P<0.05$.

3.4.1.4.2 Hepatic *hepcidin* mRNA expression

Iron supplementation increased *hepcidin* expression measured 14 days after administration (Figure 3.4.7). This is consistent with studies in C57blk/6 mice, where iron supplementation increased *hepcidin-1* expression. In rats, this increase was transient as levels were reduced to normal levels within 21 days. An increase in *hepcidin* expression was not detected in iron supplemented pregnant rats during the second trimester.

Hepcidin expression decreased during the third trimester of pregnancy. Iron supplementation, increased *hepcidin* levels in this group but was unable to restore expression levels to that of non-pregnant animals. Unlike the situation in mice (Figure 3.1) rats demonstrate more than two levels of *hepcidin* expression, although this may be due to the combination of variables (pregnancy and iron supplementation) in this study.

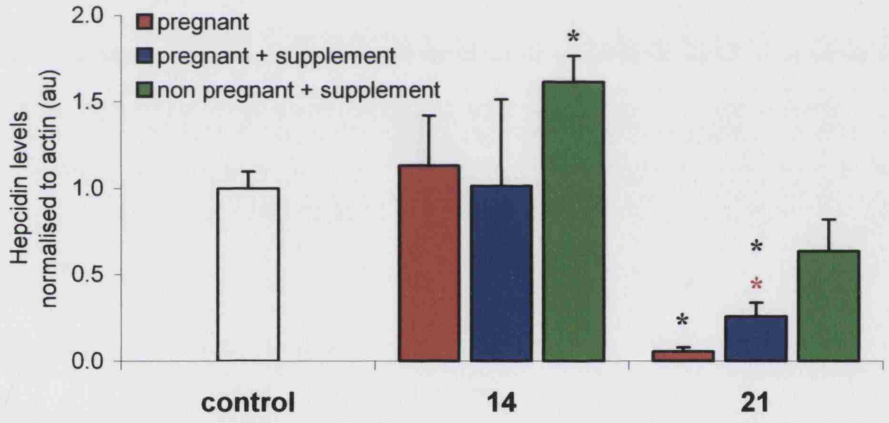

Figure 3.4. 7 Effect of iron supplementation on *hepcidin* expression

Hepatic hepcidin levels were quantified and normalised to that of actin in iron supplemented and control rats during the second and third trimester. Non-pregnant rats were also supplemented and hepcidin expression quantified after 14 or 21 days. Data is presented as mean + S.E.M. (*) denotes significance difference from the control group at $P<0.05$, (*) denotes significant difference from the non-supplemented group at $P\leq 0.05$.

3.4.1.4.3 Hepatic *Ireg1* mRNA expression

Ireg1 mRNA expression decreased following supplementation in non-pregnant animals (Figure 3.4.8), however, this did not reach significance with the model and n numbers used in this study. *Ireg1* expression increased during pregnancy. However, this data was unable to conclusively determine the effect of iron supplementation during pregnancy due to the large variation in this group.

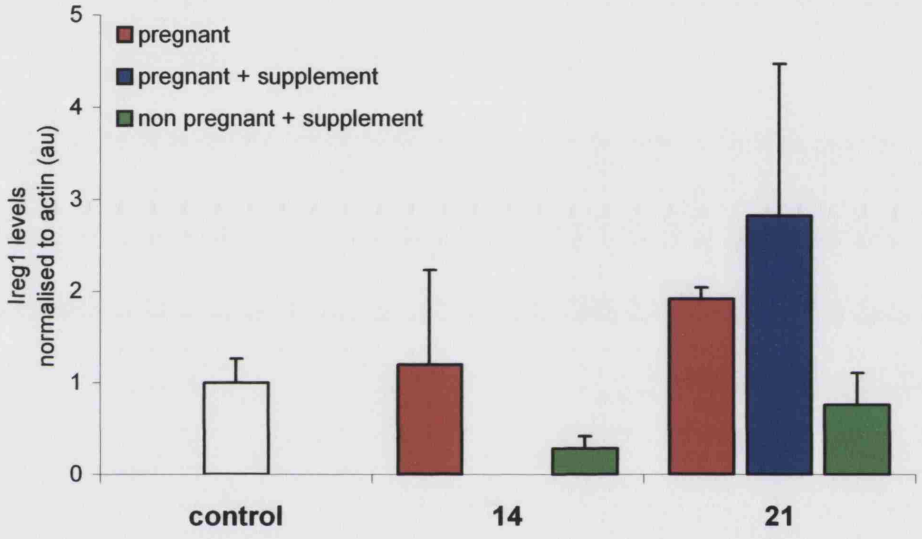

Figure 3.4. 8 Effect of iron supplementation on hepatic *Ireg1* expression

Hepatic Ireg1 levels were quantified and normalised to that of actin in iron supplemented and control rats during the second and third trimester. Non-pregnant rats were also supplemented and Ireg1 expression quantified after 14 or 21 days. Data is presented as mean + S.E.M.

3.4.1.5 Effect of iron supplementation on placental gene expression

A single 10 mg dose of iron dextran administered at day 1 of gestation had no effect on the expression of placental iron transporters, *DMT1* (all isoforms combined), *Tfr1* or *Ireg1* in rats (Figure 3.4.8).

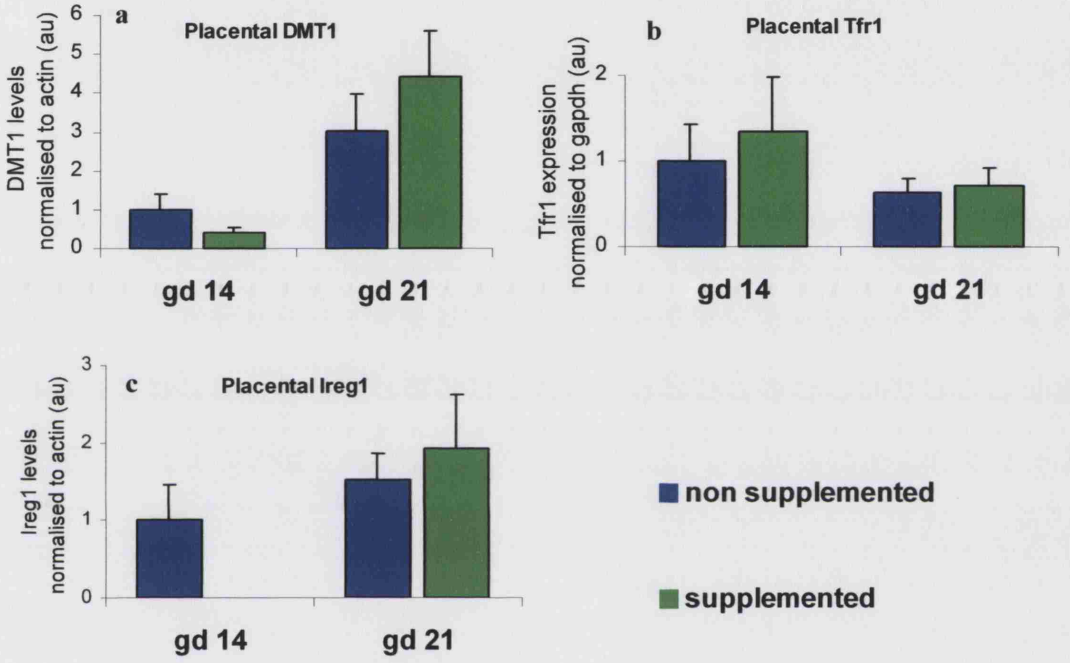

Figure 3.4. 9 Effect of iron supplementation on placental gene expression

Placental (a) DMT1, (b) Tfr1, and (c) Ireg1 expression: effect of iron supplementation.
Placental mRNA levels were quantified in iron supplemented and control rats at gestational day 14 and 21.
Data is presented as mean + S.E.M.

3.4.1.6 Effect of iron supplementation on foetal liver gene expression

A significant increase ($P \leq 0.05$) in hepatic *DMT1* (Figure 3.4.9) and *hepcidin* expression was demonstrated at term in foetuses of iron-supplemented dams. *Ireg1* mRNA expression was not modified.

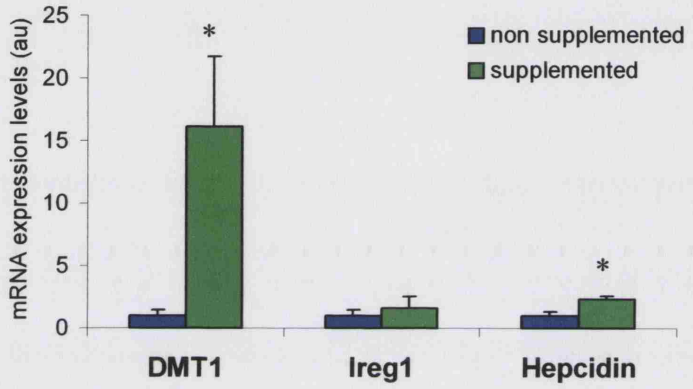

Figure 3.4. 10 Effect of iron supplementation on gene expression in the foetal liver

The foetal liver was removed at term and the expression of DMT1, Ireg1 and hepcidin was quantified and normalised to that of actin. In a parallel experiment dams were supplemented with 10 mg iron dextran at gd 1. Data is presented as mean + S.E.M. (*) denotes significant difference from the non-supplemented group at $P \leq 0.05$.

3.4.2 Effect of iron supplementation on duodenal iron uptake

The previous set of experiments demonstrated that iron supplementation decreased duodenal *DMT1* expression during the final trimester (Figure 3.4.4). The consequence of this on duodenal iron absorption is evaluated in this experiment.

Pregnant rats raised on a control diet were administered an iron supplement at gd 0.5. Duodenal iron uptake was quantified at gd 21. As the decrease in *DMT1* was concurrent with a slight, though statistically non-significant, decrease in *Dcytb* expression, the absorption of both ferric and ferrous iron uptake was quantified.

Experimental design

Experiments were performed using weanling female rats of the Rowett Hooded Lister strain, which were group housed in cages, under constant temperature and humidity. Controlled illumination with a 12 hour light-dark cycle was maintained. All animals were provided with distilled water and control diet (50 mg Fe/kg diet) *ad libitum*.

24 female rats were mated with males of the same strain. Mating was confirmed by the detection of a vaginal plug, this day was denoted at gd 0. Animals were randomised into 3 groups and administered either 2 mg or 20 mg Fe/kg, as iron gluconate (Sigma, Poole, U.K.) intraperitoneally. The control group were administered an equal volume of saline. Dams were killed by stunning and cervical dislocation on gd 21, see scheme overleaf. All animal experimental procedures were carried out by Dr Lorraine Gambling at the Rowett Research Institute, Aberdeen, U.K.

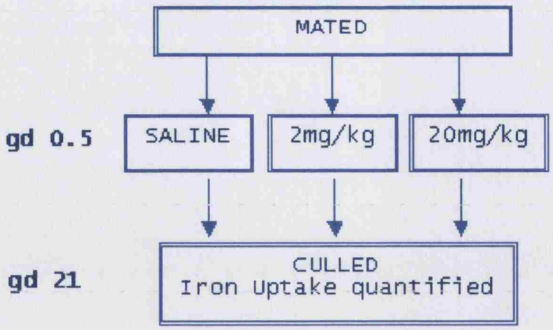

The proximal duodenum was collected, rinsed with PBS and stored in oxygenated Hepes buffer for a maximum of 20 minutes before commencement of the iron uptake assay. Both ferrous (Fe-ascorbate) and ferric (Fe-NTA) iron uptake was assessed *in vitro* using the duodenal ring method as described in chapter 2.2. Iron uptake was expressed as μmole Fe uptake/min/gram tissue. Data is presented as mean + S.E.M. of 8 animals, each performed in triplicate. One-way ANOVA was used to test for differences between groups. Significant difference from the mean was considered at $P \leq 0.05$.

Results

Duodenal iron uptake, either ferric and ferrous, at day 21 of gestation was not affected by iron supplementation of 2 mg Fe/kg [ferric: 2.21 $\pm$ 0.27 μmole Fe/min/gm, P=0.500; ferrous: 3492 $\pm$ 272.66 μmole Fe/min/gm, P=0.11] (Figure 3.4.10). A 20 mg/kg iron supplement reduced iron uptake of both ferric and ferrous iron at day 21, but was not statistically significant [ferric: 1.81 $\pm$ 0.17 μmole Fe/min/gm, P=0.70; ferrous: 2860.38 $\pm$ 218.82 μmole Fe/min/gm, P=0.29] compared to saline supplemented controls at day 0.5 of pregnancy [ferric: control group= 1.92 $\pm$ 0.28 μmole Fe/min/gm; ferrous: 3233.61 $\pm$ 287.14 μmole Fe/min/gm].

Although the uptake of ferrous iron was over a 1000 fold higher then that of ferric iron across all groups, the relationship between groups was identical, demonstrating that Dcytb activity was unaffected by iron supplementation.

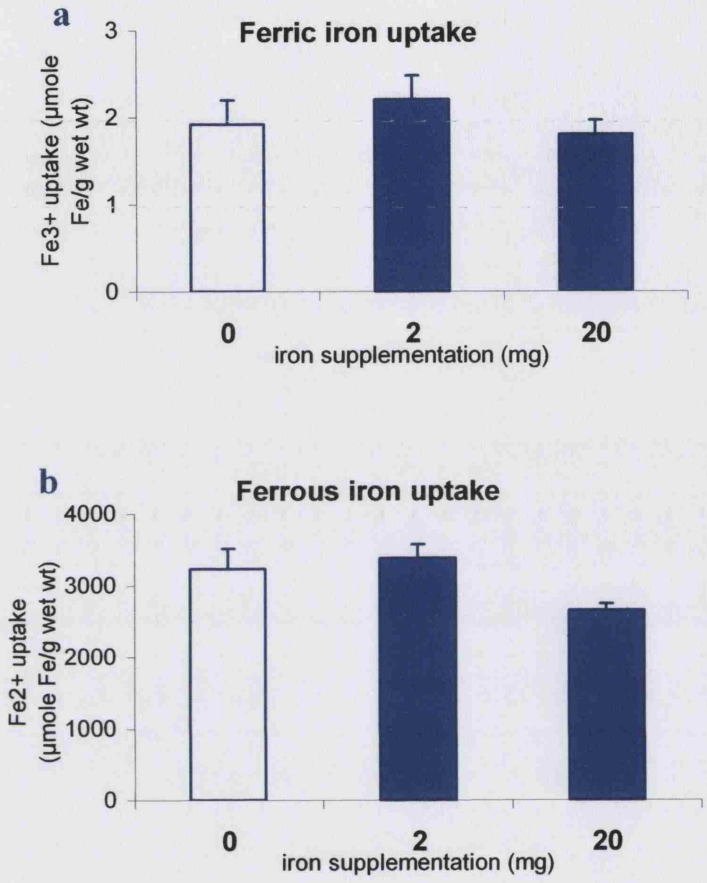

Figure 3.4. 11 Duodenal iron uptake in iron supplemented dams

Duodenal (a) ferric and (b) ferrous iron uptake at term in dams supplemented with saline (open bars), 2 or 20 mg/kg iron (blue bars) on day 0.5 of gestation. No significant change in iron uptake was observed in the supplemented groups. Data are presented as mean + S.E.M. of 8 dams.

3.4.3 Effect of dietary iron supplementation on placental iron transport

Section 3.4.1 demonstrated that in rats the expression of placental iron transporters was not modulated by parenteral iron supplementation. In the following experiment, conducted in human subjects, the effect of daily oral iron supplementation, on placental gene expression was investigated.

Experimental design

12 matched pregnant volunteers, received 100 mg of ferrous gluconate, or a placebo folate supplement, in a tablet form daily, from the first trimester of pregnancy until birth. At birth the placenta was collected and snap frozen in liquid N_2 and stored at –70°C. Samples were shipped on dry ice. Placentae were collected by Wendy Hollands (Maternity Department of the Norfolk and Norwich University Hospital, Norwich, U.K.). The study was approved by the Norwich Local Ethics Committee and the East Norfolk and Waveney Research Governance Committee.

RNA was extracted from the placenta from a region selected at random. Real-time PCR was used to quantitate the expression of *DMT1+ire, DMT1-ire, Ireg1* and *Tfr1*. Values were normalised to that of the housekeeping gene hypoxanthine phosphoribosyltransferase (HPRT). Primers for human genes and their corresponding standard curves were kindly donated by Sachie Yamaji (Royal Free & UCL Medical School, London). PCRs were repeated in duplicate. Students *t*-test was used to assess significant difference between Gaussian distributed data with similar variances or with *Welch*'s correction.

Maternal and neonatal blood was also collected to quantify serum iron concentration, Tf saturation and soluble Tfr levels.

Results

3.4.3.1 Haematological parameters

Serum iron concentration and Tf saturation decreased during the course of pregnancy in both the supplemented and the control group, but the decline was greater in the control group. Soluble Tfr levels remained stable in the supplemented group. In the control group levels rose slightly between weeks 16 and 24, and rose sharply between weeks 24 and 34. Neonatal serum ferritin, sTfr and Tf saturation did not change following iron supplementation of the mother. Placental iron levels were similar between the control and supplemented groups. All haematological parameters were analysed by Professor Susan Fairweather-Taits group (Institute of Food Research, Norwich, U.K.).

3.4.3.2 Placental mRNA Quantification

Placental *DMT1-ire* expression was significantly reduced in the iron-supplemented group [control 1.00 $\pm$ 0.13 n=6, supplemented 0.52 $\pm$ 0.01 n=5, P=0.013] (Figure 3.4.12), however *DMT1+ire* was not reduced [control 1.00 $\pm$ 0.06 n=6, supplemented 0.68 $\pm$ 0.23 n=5, P=0.15]. In addition neither *Tfr1* [control 1.00 $\pm$ 0.18 n=6, supplemented 0.84 $\pm$ 0.40 n=4, P=0.77) nor *Ireg1* [control 1.00 $\pm$ 0.31 n=6, supplemented 0.55 $\pm$ 0.27 n=5, P=0.34] differed between the supplemented and control groups. The expression of *DMT1+ire, Tfr1* and *Ireg1*, all of which are regulated by IRE-IRP interactions, is consistent with placental iron concentration data, which were not affected by iron supplementation.

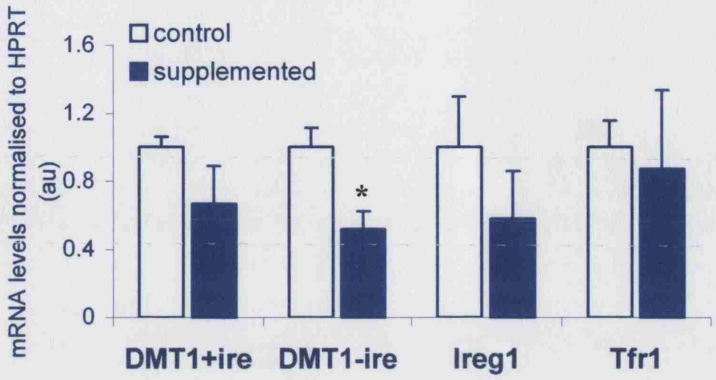

Figure 3.4. 12 Placental gene expression following iron supplementation

Expression of *DMT1+ire*, *DMT1-ire*, *Ireg1* and *Tfr1* in iron supplemented human placenta at birth. *Placentae were collected at birth. mRNA levels of DMT1+ and –ire, Ireg1 and Tfr1 were compared to those in non supplemented placentae.* Data is presented as mean + S.E.M. of 4-6 placenta. * $P \leq 0.05$.

3.4.4 Discussion

During pregnancy iron absorption increased and liver iron levels decreased (Chapter 3.2). It is possible that this was due to systemic iron deficiency. In the experiments presented here animals were supplemented with iron at the onset of pregnancy; this reduced the iron deficiency characteristic of pregnancy, and identified those mechanisms which were responsive to factors other than iron deficiency.

Following supplementation, liver iron levels rose due to the accumulation of supplemented iron (Figure 3.4.2). At gd 14 hepatic iron accumulation was less than that in non-pregnant rats (120% , compared to 154% in the non-pregnant iron-supplemented group), this was partly due to decreased hepatic *DMT1* expression. This decrease in expression was not alleviated by iron supplementation, suggesting that hepatic *DMT1* levels were not responsive to local (liver) iron stores. This is also suggested by the predominance of DMT1-ire over DMT1+ire expression at this location (Hubert & Hentze, 2002), and is substantiated by data from iron -deficient and -loaded C57blk/6 mice in chapter 3.1 where hepatic *DMT1* expression did not respond to changes in iron status. Plasma iron turnover (PIT) is increased by gd 14 and Hb concentration was decreased (Figure 3.2.1), it is therefore possibly a combination of these changes that cause the decrease in hepatic *DMT1* expression. Hb levels at gd 14 were not responsive to iron

supplementation, confirming that the reduction in Hb at this stage was primarily due to an increase in plasma volume rather then iron deficiency.

Iron supplementation at the onset of pregnancy has no effect on *hepcidin* expression during the second trimester. However, as the requirements of the foetus and the erythroid increase, in the final trimester, maternal liver iron levels continue to fall. This fall caused a 50% decrease in liver iron stores between gd 14 and 21 in both supplemented and non-supplemented dams. Due to an initial rise in liver iron stores following iron supplementation, these dams had higher iron stores at term. Probably due to this, *hepcidin* expression was higher than in their non-supplemented counterparts, although expression remained significantly lower than that of the non-pregnant group. Not surprisingly, the elevated *hepcidin* expression in these iron-supplemented dams was reflected by a decrease in duodenal *DMT1* expression at gd 21.

Interestingly, the gene expression data did not correlate with duodenal absorption data. There was no difference in iron uptake between the two groups, indicating that the decrease in liver iron reserves was not solely responsible for the increase in iron uptake during pregnancy. Iron uptake is dependent on a number of factors in addition to mRNA levels. It is possible that the expression of iron transporters was reduced without a decrease in transporter activity due to increased localisation of DMT1 to the bbm. If iron levels are higher within the mucosal cells of the iron supplemented group, the stability of the *DMT1+ire* transcript would be reduced, causing the drop in mRNA expression as observed here. By trafficking a greater proportion of DMT1 to the brush border membrane, the enterocyte is able to maintain an uptake rate in line with the requirements of the erythroid which remain high during this period. The cellular localisation of DMT1 is thought to be regulated at the level of transcription, by differential expression of exon 1A or 1B (Hubert & Hentze, 2002). The mechanism for the transcriptional regulation of those two splice variants is not known, and may be regulated by hepcidin. This theory of increased localisation to the bbm following iron supplementation is not consistent with data presented in chapter 3.1.3 or that of Trinder *et al.* (2000), which demonstrate that bbm localisation of DMT1 is increased under iron deficient and not iron loaded conditions. A major difference between these studies is that in this experiment iron loading was not attained by dietary means.

Additionally the discrepancy between the uptake and the gene expression data may be due to the different genetic background of the animals used in each experiment. Although not yet identified in rats, in mice, many studies have demonstrated the influence of the genetic background on the regulation of iron transport proteins and uptake (Fleming *et al.*, 2001;Dupic *et al.*, 2002). These findings are supported by a number of studies which demonstrate little correlation between iron absorption during the third trimester and Hb concentration, liver iron concentration or total liver iron (Southon *et al.*, 1989). Indeed *hepcidin* expression is negatively correlated to erythropoietin levels despite adequate liver iron stores (Nicolas *et al.*, 2002b;Latunde-Dada *et al.*, 2004;Kulaksiz *et al.*, 2004). This finding implies that iron-supplementation has the beneficial effect of maintaining iron stores at least until the final trimester. This is important not only for the mother and subsequent pregnancies, but also for the neonate if the mother is lactating.

The data presented here demonstrate that the rat model used may not have been appropriate, because at the dosage used, we were unable to fully compensate for the decrease in hepatic iron levels or alleviate reduced Tf saturation or serum iron levels. In future studies it may be beneficial to supplement dams at gd 14 in addition to gd 1 to prevent a reduction in liver iron stores during the final trimester. Alternatively, the formulation and/or the dosage of the iron supplement could be modified.

3.4.4.1 The effect of iron supplementation to the foetus

Under iron deficient conditions, the placenta increases DMT1 and Tfr1 levels in order to acquire more iron (Chapter 3.31). Under dietary iron supplementation a decrease in placental *DMT1-ire* expression was observed in humans, although this did not reach statistical significance in the rat model where dams were supplemented with a single dose of iron dextran (Figure 3.4.8).

The regulation of placental *DMT1* and *Tfr1* is not as simple as originally hypothesised, when it was thought that these were regulated *via* IRE-IRP interactions (Chapter 3.3). However, the data here demonstrates a decrease in *DMT1-ire* expression, whilst *Tfr1* and *DMT1+ire* expression remain constant, suggesting that placental iron concentration is unchanged during iron supplementation. It is possible that placental *DMT1* expression is additionally regulated by hepcidin. The role of hepcidin in the foetus and the neonate is not yet known. Preliminary data from our lab demonstrates an increase in foetal *hepcidin* expression during the final trimester in rats and mice (unpublished data). As the *hepcidin* 5'UTR contains C/EBP elements which regulate transcription to cell cycle parameters (Courselaud *et al.*, 2002), the developmental regulation of *hepcidin*,

increasing between the second and third trimester is not surprising, although the role of hepcidin during foetal development is not known. It is the placenta, and not the foetal gut, which is the primary site of iron absorption. Therefore, it is possible that foetal hepcidin may regulate placental iron uptake in a mechanism parallel to that of adult hepcidin and duodenal absorption. In support of this we find a 50% increase in *hepcidin* expression in the liver of iron supplemented foetuses. However, it is unlikely that foetal hepcidin negatively regulates placental iron transfer as both foetal *hepcidin* and placental iron uptake increases during pregnancy (McArdle & Morgan, 1982;Viteri, 1998).

In the uterus the foetal gut is not functional for iron acquisition, as iron is supplied to the foetus from the placenta *via* the uterine artery. Iron is stored mainly within the foetal liver. At term the foetal liver contributes to less then 10% of foetal weight/mass, but contains approximately 50% of the foetal iron (Finch *et al.*, 1983).

This data demonstrates that iron-supplementation to dams which are not iron deficient, resulted in increased *DMT1* expression in the foetal liver at gd 21. *DMT1* expression in the foetal liver may be regulated by a mechanism similar to that of the adult, in which raised iron levels increase hepatic *DMT1* expression in order to clear the plasma of NTBI thereby protecting other tissues from oxidative stress. A study by Zhou *et al.* (2001) reported increased postnatal oxidative damage to liver DNA in neonates exposed to higher amounts of dietary iron during pregnancy. Together these data suggest that under iron loading the foetus responds by a similar mechanism to that of the adult by sequestering excess iron into liver stores.

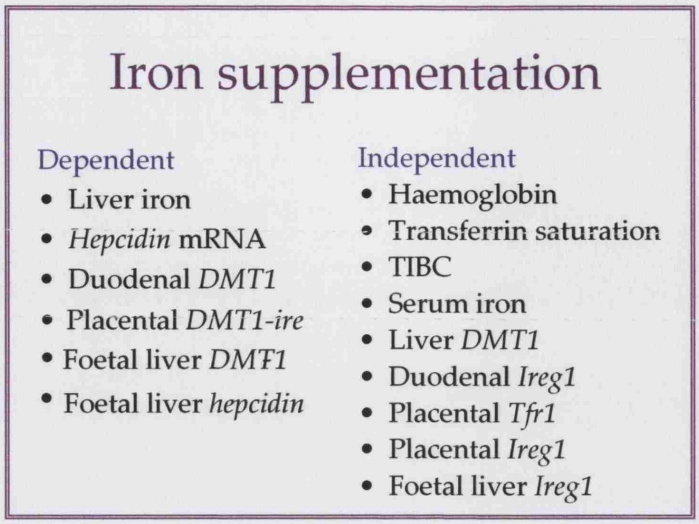

Table 3.4. 1 Parameters regulated by systemic iron supplementation

Summary of iron parameters investigated, the first column lists the parameters which are modified following iron supplementation in rats and/or humans, the second column lists parameters which were not modified.

3.4.5 Conclusions

Iron supplementation during pregnancy reduces iron loss from maternal stores and leads to an increase in *hepcidin* expression, this in turn reduces the upregulation of duodenal *DMT1* during the final trimester. The findings presented here imply that iron deficiency has a role in the mobilisation of liver iron stores and the increase in iron absorption associated with pregnancy. Iron-supplementation also causes a decrease in placental *DMT1-ire* expression in humans. This provides evidence that the foetus is protected from potential iron over-loading. The regulation of placental iron uptake is studied further in the following chapter.

3.5 The regulation of placental iron transport by hepcidin

The role of hepcidin in the regulation of duodenal iron absorption has been demonstrated in chapter 3.1 and 3.2, however, a regulatory role on placental iron transport has yet to be investigated. In similarity with duodenal absorption, placental iron transport increases during the final trimester of pregnancy (McArdle & Morgan, 1982;Viteri, 1998). In both organs this increase is due, at least in part, to an increase in *DMT1* expression. This is consistent with *hepcidin* expression, hypothesised as a negative regulator of iron uptake, which decreases during this period. In addition, an inverse correlation between maternal iron status and placental *DMT1* gene expression was noted in chapter 3.3 and 3.4, therefore it is feasible that hepcidin may modulate placental iron transport in a mechanism parallel to that of the duodenum. To investigate this possibility the effect of synthetic hepcidin on iron uptake and efflux in placental cariocarinoma (BeWo) cells was determined.

3.5.1 The effect of maternal hepcidin levels on placental iron uptake

The effect of maternal hepcidin on placental iron transfer was investigated here. BeWo cells were cultured in Transwells and the apical chamber, representative of the maternal circulation, was supplemented with hepcidin. Subsequently, the uptake of iron, applied as $^{59}Fe_2$-Tf to the apical chamber, was examined.

Methods

3.5.1.1 Iron uptake assay

BeWo cells were grown on Transwell filters, and were differentiated by addition of 10 μM forskolin when approximately 70% confluent. Hepcidin (hepcidin-25 DTHFPICIFCCGCCHRSKCGMCCKT) was synthesised by Dr Bala Ramesh, as described in Appendix VII (Laftah *et al.*, 2004). This was diluted in PBS and applied to the apical chamber of the Transwell. Control cells were incubated with an equal volume of PBS.

To initiate iron uptake, media from the apical chamber was removed and replaced with media containing 10 µg/mL $^{59}Fe_2$-Tf , at time 0. The uptake assay was performed at room temperature. Iron uptake was stopped by washing filters 3x5 minutes with ice cold BSS. The cellular contents were harvested by incubating Transwell filters in 1 M NaOH for 5 mins and collecting the supernatant. ^{59}Fe uptake was quantified using a Cobra 5003 Auto-Gamma Counter (Packard Instrument Co., Meriden, CT, USA). The protein concentration was used as a measure of the number of cells. Iron uptake was expressed as µmole Fe uptake/g protein/ minute.

3.5.1.2 Optimisation of assay conditions

The time course for iron uptake was determined by incubating BeWo cells for 2, 5, 10, and 20 minutes in the uptake buffer containing $^{59}Fe_2$-Tf. As demonstrated in figure 3.5.1, iron accumulated at a steady rate over the entire time period. In subsequent assays, uptake was measured for 10 minutes as iron uptake was not saturated at this time point and it allowed the cells a brief period to acclimatise to the assay conditions.

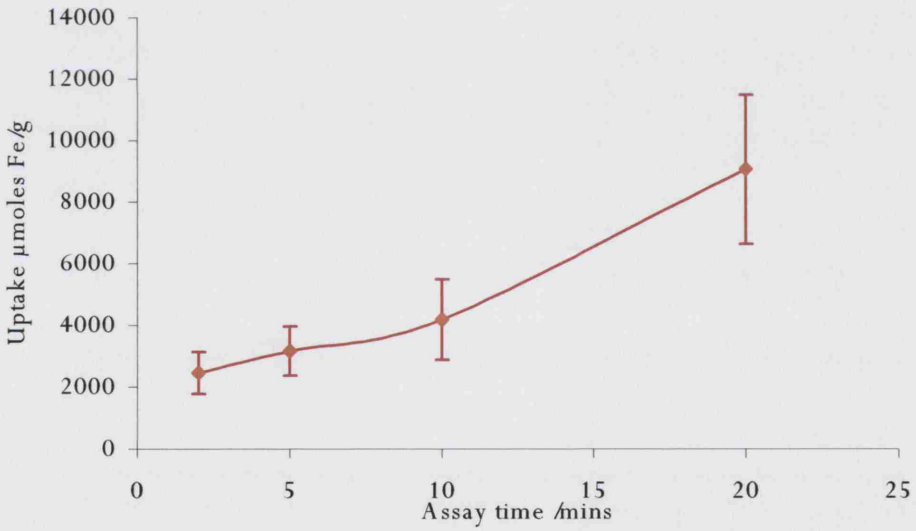

Figure 3.5. 1 Iron uptake by BeWo cells

^{59}Fe uptake demonstrated a steady increase over the initial 20 minute uptake period.

Results

3.5.1.2 Effect of apical hepcidin concentration on ^{59}Fe uptake

To determine the effect of hepcidin on iron uptake, BeWo cells were treated with PBS or PBS containing 1, 10 or 100 μM of hepcidin on the apical face for 24 hours before the commencement of the iron assay. This mimics exposure of the placenta to maternal serum hepcidin. An exposure time of 24 hours was considered to be sufficient to induce a response, as 24 hour incubation with hepcidin was previously shown to significantly decrease apical iron uptake in Caco-2 cells (Yamaji *et al.*, 2004).

Exposure of BeWo cells to 1 μM hepcidin on the apical face for 24 hrs had no significant effect on iron uptake (Figure 3.5.2). However, exposure to higher concentrations of hepcidin decreased apical iron uptake. This was significant in cells treated with 10 and 100 μM hepcidin over a 24 hour period (0 μM: 530.82 ± 20.57, 1 μM: 419.66 ± 131.50 P=0.45, 10 μM: 183.17 ± 38.58 P=0.001, 100 μM: 125.63 ± 28.12 P=0.0003).

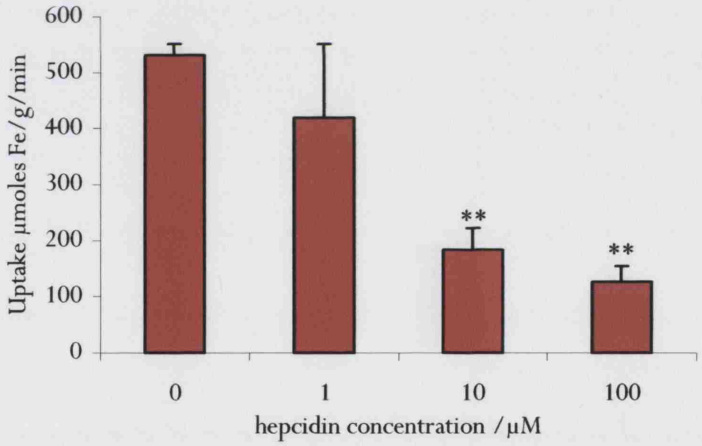

Figure 3.5. 2 Effect of hepcidin concentration on iron uptake in BeWo cells

BeWo cells were treated with PBS or PBS containing 1, 10 or 100 μM hepcidin in the apical chamber for 24 hours. Iron uptake was assayed in these cells and compared to that of the control (PBS treated) group. A dose specific response to hepcidin was evident. Iron uptake is expressed as μM iron uptake per minute per gram protein. Bars show mean of 3 observations + S.E.M. (**) denote significant difference from the control P≤0.01.

3.5.1.3 Time-specific response to hepcidin treatment

To determine whether the period of hepcidin treatment influenced the extent by which iron uptake was inhibited, cells were treated with 10 μM hepcidin for 1, 24 or 48 hours in the apical chamber prior to the commencement of the uptake assay. A hepcidin concentration of 10 μM was used as this fell within physiological levels (Park *et al.*, 2001;Dallalio *et al.*, 2003) and was shown to induce a reduction in iron uptake in cells treated for 24 hours. To ensure that nutrient depletion was consistent across all groups, cells treated with hepcidin for 48 hours, were refreshed with fresh media containing 10 μM hepcidin after 24 hours.

As demonstrated in figure 3.5.3, incubation with 10 μM of hepcidin on the apical face reduced apical iron uptake in BeWo cells. This was evident in cells treated for 1 hour (374.67 ± 20.42 μmole Fe/gm/min), 24 hour (320.34 ± 24.97 μmole Fe/gm/min) and 48 hour (294.94 ± 10.98 μmole Fe/gm/min) prior to assay, compared to cells treated with PBS for 24 hrs (530.82 ± 20.57 μmole Fe/gm/min). However, no significant differences ($P \geq 0.05$) were evident between the hepcidin treated groups suggesting that treatment times above 1 hour had a negligible effect in further reducing iron uptake.

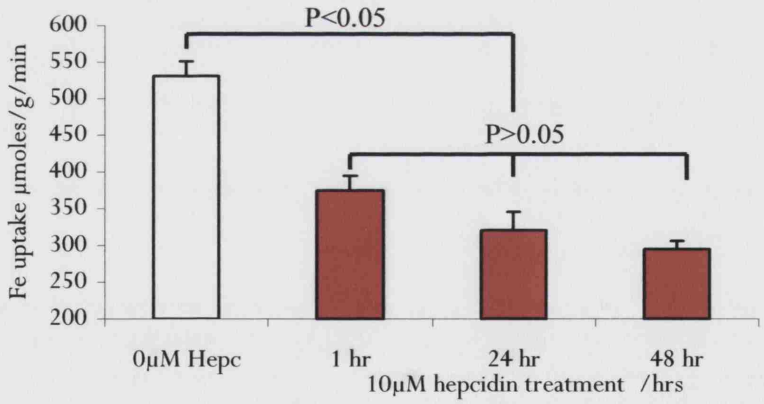

Figure 3.5. 3 Effect of hepcidin treatment period on iron uptake in BeWo cells

BeWo cells were treated with PBS (open bar) or 10 μM hepcidin for 1, 24 or 48 hrs prior to the uptake assay (red bars). Apical iron uptake was reduced in cells treated with hepcidin for 1 hr. Bars show mean uptake (μmoles Fe per gram protein per minute) of 3 observations + S.E.M.

3.5.2 Effect of basolateral hepcidin on iron efflux from BeWo cells

Although the amount of hepcidin produced by the foetal liver during the second trimester is almost undetectable, expression increases dramatically during the final trimester when placental iron transfer is maximal. Foetal hepcidin, if secreted into foetal circulation, would have direct contact with the basolateral surface of the placental syncytiotrophblast where iron efflux takes place. In this set of experiments the role of foetal hepcidin on iron efflux from the syncytiotrophoblast into foetal circulation was investigated.

Experimental protocol

Cell culture

BeWo cells were grown and differentiated as described in the previous section. Hepcidin was applied to the basolateral chamber (representative of foetal circulation). Cells were pre-loaded with ^{59}Fe prior to the efflux assay.

Iron loading

To load BeWo cells with ^{59}Fe, the apical chamber was refreshed with media containing $^{59}Fe_2$-Tf 18 hours prior to the onset of the efflux assay. This time period is routinely used to load BeWo cells with iron (Danzeisen *et al.*, 2000).

Efflux assay

Cells were rinsed with BSS to remove residual ^{59}Fe. The apical chamber was refreshed with complete media containing no hepcidin, iron or Tf. The basolateral chamber was refreshed with media containing 10 μg/mL apo-Tf at time 0 and incubated at 37°C. 10 μl aliquots were removed from the basolateral media to quantitate ^{59}Fe levels. To terminate the assay, cells were harvested with 1M NaOH and the remaining efflux media collected for ^{59}Fe quantification.

Statistical Analysis

As the amount of ^{59}Fe taken up by cells may have varied between individual populations and treatment groups, this would affect the amount and rate of iron efflux. For this reason, iron efflux was expressed as a percentage of the total cellular ^{59}Fe content at time 0.

3.5.2.1 Optimisation of efflux protocol

Iron efflux was studied over time in untreated BeWo cells to optimise the efflux protocol. Cells were pre-loaded with ^{59}Fe, and the appearance of ^{59}Fe in the efflux media was quantitated at 2, 5, 10, 20, 60 and 120 minutes. At the final time-point the cells were harvested and the remaining efflux media was collected to calculate the total ^{59}Fe content of the cells at the onset of the assay.

Approximately 10% of the total cellular iron was released during the initial 2 hours (Figure 3.5.4). This is consistent with previous studies which demonstrate BeWo cells efflux 50% of the total iron content in 15 hours (van der Ende *et al.*, 1987). The efflux rate however, was not constant over the entire period. 5% of the total iron content was released into the basolateral solution within 20 minutes. The subsequent 5% took over 100 minutes to efflux. Therefore, iron efflux was measured at 10 minutes to calculate the initial efflux rate and again after 2 hours to calculate total iron efflux in subsequent assays.

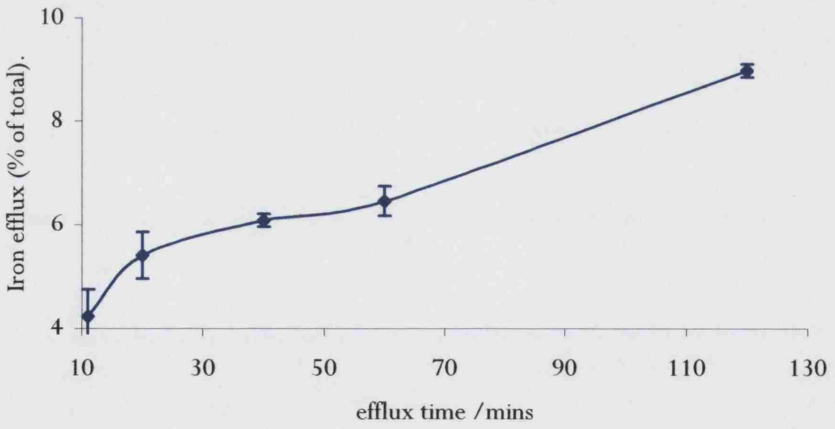

Figure 3.5. 4 Iron efflux from BeWo cells

BeWo cells were pre-loaded with ^{59}Fe and iron efflux into the basolateral chamber measured for 2 hours subsequently. The rate of iron efflux was highest during the initial 20 minutes of the assay. During the following 100 minutes the iron efflux rate was constant. Chart shows ^{59}Fe efflux into the basolateral chamber at 10, 20, 60 and 120 minutes. Error bars show S.E.M. of 3 observations.

3.5.2.2 Effect of foetal hepcidin on iron efflux

To determine the effect of foetal (basolateral) hepcidin on placental iron efflux, BeWo cells were grown on porous filters. Once fully differentiated, the basolateral chamber was refreshed with media containing synthetic hepcidin. Cells were incubated with hepcidin (either 0, 1, 10 or 100 μM) for either of 1, 24 or 48 hours, before the commencement of the efflux assay. To maintain the nutrient reserves of the media, the basolateral media of the cells treated for 48 hours was refreshed after 24 hours. The apical chamber contained no hepcidin. This was similar to the situation during pregnancy where very little hepcidin is present in the maternal circulation during the final trimester.

Cells were pre-loaded with ^{59}Fe and the basolateral media was replaced with complete media containing 10 μg/mL apo-Tf and PBS or PBS containg hepcidin at the concentration of the pre-treatment. A control cell group received no hepcidin pre-treatment, but the efflux media was supplemented PBS or 0, 1, 10 or 100 μM hepcidin. Cells were incubated in the efflux buffer for 120 minutes. 10 μL samples of efflux media were removed at 10 and 120 minutes and ^{59}Fe content quantified. At the final time point (120 minutes) the cells were harvested and the remaining efflux media collected for ^{59}Fe quantification.

BeWo cells were pre-treated with PBS, 1, 10 or 100 μM hepcidin for 48, 24, 1 hour or only during the assay. This had no effect on the initial iron efflux rate of these cells compared to cells treated with PBS (Figure 3.5.5) ($P \geq 0.05$, means, S.E.M. and P values tabulated in appendix III).

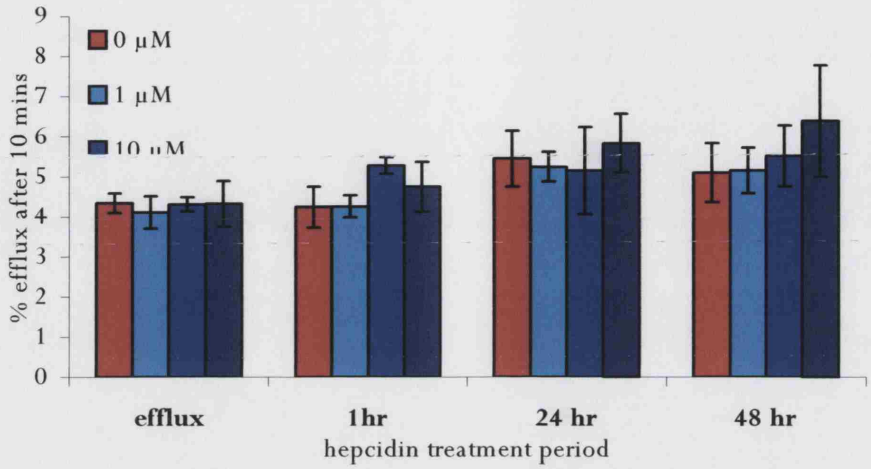

Figure 3.5. 5 Effect of hepcidin on the initial rate of iron efflux

BeWo cells were incubated with hepcidin in the basolateral chamber for the duration of the efflux assay, 1, 24 or 48 hours. ^{59}Fe efflux into the basolateral chamber was measured for 10 minutes. Hepcidin treatment had no effect on the initial rate of iron efflux. Bars show mean ± S.E.M. of three observations. Statistical analysis by ANOVA.

BeWo cells were pre treated with PBS, 1, 10 or 100 μM hepcidin for 48, 24, 1 hour or only during the assay. Iron efflux into the basolateral chamber was quantified after 2 hours. Hepcidin treatment did not affect iron efflux in BeWo cells ($P>0.05$) (Figure 3.5.6), except for cells treated with 10 μM hepcidin for 1 hour prior to the efflux assay. In these cells efflux was increased compared to cells incubated with PBS (1 hour hepcidin pre-treatment, 0 μM: 8.98 ± 0.13, 10 μM: 11.79 ± 0.87 $P=0.03$, $n=3$) ($P>0.05$, means, S.E.M. and P values tabulated in appendix III).

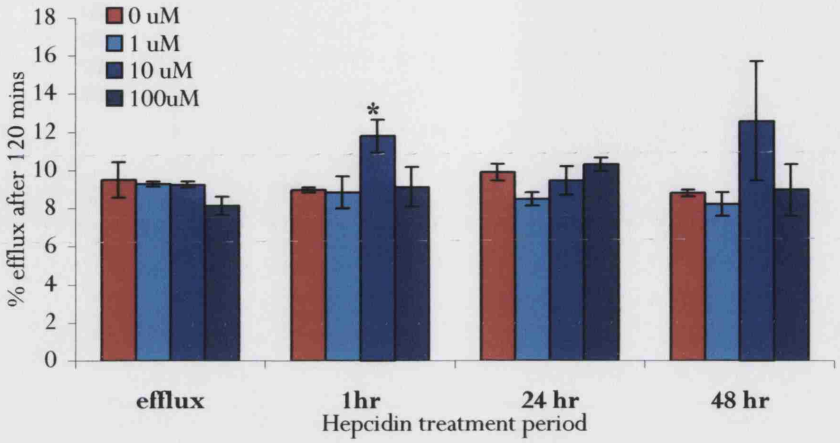

Figure 3.5. 6 Effect of hepcidin on iron efflux from BeWo cells

Except for 1 hour pre-treatment with 10μM hepcidin which caused an increase in Fe^{59} efflux, foetal hepcidin had no effect on iron efflux into the basolateral chamber over a concentration range of 0 to 100 μM. Cells either received no pre-treatment (efflux buffer group) or 1, 24 or 48 hours hepcidin pre-treatment. Iron efflux was assessed at 120 minutes. Bars show mean ± S.E.M. of three observations. (*) denotes significance at $P \leq 0.05$. Statistical analysis by ANOVA with bonferoni posthoc test.

3.5.3 Physical association of hepcidin with BeWo cells

The previous experiments demonstrated a negative effect of maternal hepcidin on placental iron uptake and a possible positive effect of foetal hepcidin on iron efflux. In this experiment, the physical association of hepcidin with the placental syncytiotrophoblast was determined in BeWo cells with the use of synthetic FITC-tagged hepcidin.

Experimental protocol

BeWo cells were grown on glass coverslips (BDH Chemicals, Dorset, U.K.), when approximately 60% confluent, cells were treated with 10 μM forskolin (Sigma, Poole, U.K.) for 48 hours to stimulate cells to differentiate. The media was refreshed with media containing 10 μM FITC-tagged hepcidin and cells incubated for 1 hour at 37°C. A control set of cells were incubated with 10 μM unconjugated-FITC for 1 hour at 37°C. Cells were gently washed with warm PBS (3x2 minutes) to remove unbound hepcidin/ FITC. Cells were fixed in fresh 4% v/v paraformaldehyde/PBS (Sigma, Poole, U.K.), mounted with Vectasheild containing DAPI (Vector Laboratories, Burlingame, CA, USA) and visualised with a Leica DMRXA fluorescence

microscope with filters specific for FITC and DAPI. Leica CW4000 image capture and image analysis software was used to capture images.

Synthetic hepcidin

Hepcidin (hepc25 Fluorescein-DTHFPICIFCCGCCHRSKCGMCCKT) was synthesised by Dr B. Ramesh as described in appendix VII (Laftah *et al.*, 2004). This was diluted in sterile water and applied to the cell media.

Results

In BeWo cells incubated with FITC-hepcidin for 1 hour, FITC fluorescence was visible on the plasma membrane. Some areas of the plasma membrane demonstrated a greater accumulation then others, see arrows (Figure 3.5.7). Scanning through the Z-plane of the cell revealed a clear cytoplasm and nucleus. As demonstrated in figure (b), a duplicate cell sample in which cells were incubated with unbound FITC, no FITC fluorescence was visible, demonstrating that the FITC tag alone did not bind to the plasma membrane of BeWo cells.

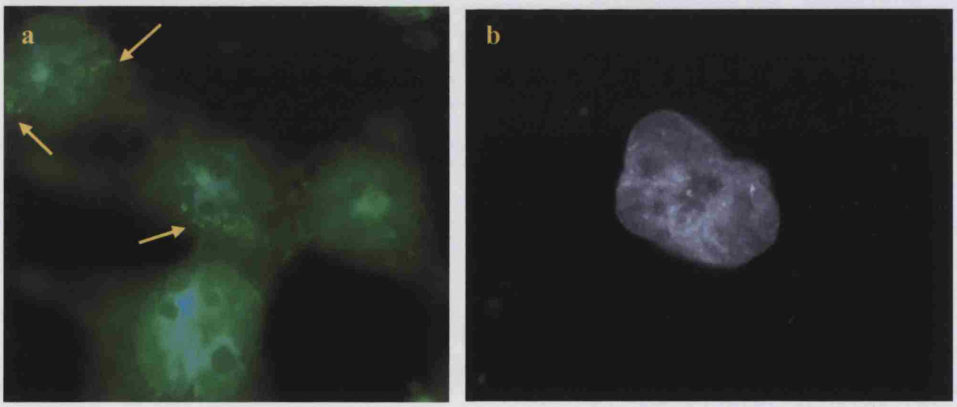

Figure 3.5. 7 hepcidin binding to the plasma membrane

BeWo cells were incubated with (a) 10 μM FITC-hepcidin, or (b) 10 μM FITC for 1 hour. Unbound FITC ± peptide was removed with PBS washes. Cells were fixed and nuclei were stained with DAPI. Figure (a) demonstrates FITC-hepcidin bound to the plasma membrane of BeWo cells, signal is absent within the cytoplasm and nuclei. Figure (b) demonstrates no FITC binding to the plasma membrane of BeWo cells. Original magnification x60.

3.5.4 Discussion

The regulation of hepcidin levels is central to iron homeostasis (Chapter 3.1, 3.2, 3.4). Upstream, hepcidin levels respond to numerous parameters of iron status including anaemia, Tf saturation, dietary iron levels, iron stores, plasma NTBI and erythropoietin levels (Nicolas *et al.*, 2002b;Gehrke *et al.*, 2003), and downstream hepcidin regulates duodenal iron transfer (Anderson *et al.*, 2002;Frazer *et al.*, 2002).

During pregnancy maternal hepcidin levels fall, resulting in an increase in duodenal iron absorption (Chapter 3.2). The placenta has many similarities to the duodenum. One being that placental iron transport is also increased during pregnancy (McArdle & Morgan, 1982), and also that DMT1 is involved in iron uptake (Georgieff *et al.*, 2000). Various lines of evidence point to the regulation of placental iron transfer by maternal iron status: placental *DMT1* is decreased with iron loading (Chapter 3.4), placental *Tfr1, ZIRTL* and *DMT1* are increased with iron deficiency (Chapter 3.3). These may be due to intracellular mechanisms such as IRE/IRP interactions, or may be due to extracellular stimuli such as hepcidin.

The placenta receives hepcidin signals from both the maternal and the foetal liver. The signals from these two sources are not combinatory as maternal hepcidin decreases, whereas foetal hepcidin increases, during the course of gestation. These two sources were differentiated in this study with the use of BeWo cells grown in Transwells, which allowed the isolation of the apical (maternal) and the basolateral (foetal) solutions.

This study demonstrates that maternal hepcidin negatively regulates placental iron uptake. This is consistent with the decrease in *hepcidin* expression observed during the second-third trimester and the rise in placental iron transfer during this period (Chapter 3.2). A similar response to hepcidin is observed in intestinal CaCo2 cells which demonstrate a decrease in iron uptake in cells incubated with synthetic hepcidin in the basolateral chamber of the Transwell (Yamaji *et al.*, 2004) and in experiments in which the direct injection ofhepcidin into mice decreased the apical uptake step of duodenal iron absorption (Appendix VII)(Laftah *et al.*, 2004). A recent study has demonstrated that hepcidin may down-regulate duodenal iron uptake by causing the internalisation and degradation of Ireg1 (Nemeth *et al.*, 2004); this would reduce iron efflux and increase cellular iron levels, which in turn reduce *Tfr1* and *DMT1* expression and iron uptake. However this study and those by Yamaji *et al.* (2004), have demonstrated that hepcidin decreases apical iron uptake but does not modulate basolateral efflux. The study by Nemeth *et al.* (2004)

was conducted in cells over-expressing Ireg1 and incubated in 10 μM ferric ammonium citrate, expression of Ireg1 on the plasma membrane of these cells would be far greater than that of the models used in the present study and in the experiments conducted by Yamaji *et al.* (2004). It is therefore possible that the effect of hepcidin in internalising Ireg1, as demonstrated by Nemeth *et al.* (2004), may have been over represented and that hepcidin may additionally inhibit iron uptake *via* an alternative mechanism.

Iron efflux was increased in cells pre-treated with 10 μM (foetal) hepcidin for 1 hour. This effect was not apparent in cells pre-treated for either 24 or 48 hours, suggesting that the synthetic hepcidin molecule may degrade over time. When applied to the apical chamber hepcidin decreased iron uptake, and this effect was sustained in both the 24 and 48 hour treatment groups. This could be explained if hepcidin had a transient effect on iron efflux but a sustained effect on iron uptake. However, taking into account that when applied to the efflux buffer without any pre-treatment, and at concentration both above (100 μM) and below (1 μM) 10 μM, hepcidin had no effect on iron efflux, the bulk of the data presented here argues against a real effect of foetal hepcidin on placental iron efflux.

Constitutive *hepcidin* expression in transgenic mice during embryogenesis and development causes severe anaemia and death around birth (Nicolas *et al.*, 2002c). This suggests that foetal hepcidin may inhibit placental iron transfer. A recent study examining the placenta of these mice at gd 16.5 demonstrate decreased *Tfr1* mRNA levels (Martin *et al.*, 2004). Surprisingly, this was independent of placental iron content and IRE/IRP activity (Martin *et al.*, 2004) and therefore suggests the regulation of Tfr1 transcriptionally. Tfr1 is transcriptionally regulated when resting cells become proliferative (Enns, 2002) and during erythroid differentiation (Martin *et al.*, 2004). The results of this present study demonstrate that maternal hepcidin reduced iron uptake which could be due to a reduction in Tfr1, however the role of foetal hepcidin on placental iron uptake was not assessed here. The study by Martin *et al.* (2004) contradicts physiological data which demonstrates that placental iron transfer increases during gestation in line with foetal hepcidin secretion (McArdle & Morgan, 1982; Viteri, 1998; Kelley-Loughnane *et al.*, 2002).

To identify the mechanism by which hepcidin regulates placental iron transfer FITC- tagged hepcidin was localised in BeWo cells. Following 1 hour incubation with FITC-hepcidin, FITC fluorescence was localised to the plasma membrane. However fluorescence was absent from the cytosol and nucleus. There are a number of explanations why hepcidin was not internalised within

the cell: (i) another substrate, not present in the cell culture media, is required for hepcidin uptake, however this is unlikely as synthetic (unconjugated) hepcidin reduces iron uptake under similar conditions, (ii) the FITC-tag interfered with the binding and/or internalisation of the protein. This was not addressed in this study, but could be assessed by duplicating the $^{59}Fe_2$-Tf uptake assay and comparing the effect of tagged and un-tagged hepcidin, (iii) the binding of hepcidin to the plasma membrane/ Tfr1 causes stoichiometric inhibition of iron uptake. Consistent with this, hepcidin inhibition demonstrated a dose responsive effect, however in the duodenum, where hepcidin also inhibits iron uptake across the apical membrane, serum hepcidin is administered from the basolateral membrane (Laftah *et al.*, 2004;Yamaji *et al.*, 2004). If the mechanism of hepcidin inhibition is *via* binding to iron transporters and inhibiting internalisation, an alternative mechanism would be required in the duodenum. It is possible that hepcidin binding induces a signal transduction pathway which blocks further iron uptake without the requirement of hepcidin internalisation, (iii) recently Nemeth *et al.*, demonstrated that hepcidin was internalised by Ireg1 in HEK293 cells over-expressing Ireg1 (Nemeth *et al.*, 2004). Data from unpolarised BeWo cells demonstrate an intracellular localisation for Ireg1 (Chapter 3.6). If Ireg1 is required for hepcidin internalisation then it explains the hepcidin-free cytoplasm displayed here, and also demonstrates the binding of hepcidin to plasma membrane proteins other then Ireg1.

3.5.5 Conclusions

Maternal serum hepcidin reduces placental iron uptake in a dose-dependent manner. Foetal serum hepcidin probably has no effect on placental iron transfer. The mechanism by which hepcidin decreases placental iron uptake is not known. In this chapter fluorescently tagged hepcidin was demonstrated to bind to the plasma membrane of BeWo cells, although in the timescale studied internalisation was not evident. This raises the question of how hepcidin inhibits iron uptake. It is possible that hepcidin binding induces a signal transduction pathway which blocks further iron uptake or binding itself inhibits internalisation of the Fe_2-Tf-Tfr1 complex into the placenta. It is known that Tfr1 is highly expressed on the apical brush border membrane of the syncytiotrophoblast, and that DMT1 and Ireg1 are probably also involved in the mechanism of iron transport. However, the precise molecular mechanism of placental iron transfer is not known; this is studied in the following chapter.

3.6 Molecular mechanism of placental iron transport

Introduction

Although widely studied in other tissues, the mechanism by which iron is transported across the placenta into the foetal circulation is incompletely understood. The process is initiated by the binding of maternal serum Fe_2-Tf to Tfr1 which is highly expressed on the apical plasma membrane of the syncytiotrophoblast (Faulk & Galbraith, 1979;Loh *et al.*, 1980). It is thought that as with erythroid cells, the Tfr1-Tf-Fe_2 complex is then internalised into a clathrin coated vesicle (McArdle & Morgan, 1982). Acidification of the endosome releases iron from Tf. DMT1, of which both the +ire and –ire isoform are expressed (Chapter 3.4), is probably involved in the export of iron out of the endosome (Fleming *et al.*, 1998;Georgieff *et al.*, 2000). The mechanism by which DMT1 enters this compartment is not known; it is presumed that DMT1 is present on the apical surface and is internalised with Tfr1 into the endosomal membrane (Touret *et al.*, 2003).

The universal iron exporter Ireg1 has been localised to the syncytiotrophoblast (Donovan *et al.*, 2000), as has a placental-specific Cp homologue. This oxidase has been localised to the perinuclear region (Danzeisen *et al.*, 2000), however the subcellular localisation of Ireg1 is so far unknown.

In this study BeWo cells were utilised to model the placental syncytiotrophoblast. With the use of immunofluorescent-techniques Tfr1, DMT1, Ireg1 and the copper oxidase are localised and a mechanism by which iron is transported across the placenta is postulated.

Methods

Cell culture

BeWo cells were obtained from the European Collection of Animal Cell Cultures (Salisbury, Wilts., U.K.). Cells were maintained in Ham's F-12 with L-Glutamine (Invitrogen, Paisley, U.K.) supplemented with 20% foetal bovine serum (Sigma, Poole, U.K.), penicillin (200 units/mL, Invitrogen, Paisley, U.K.) and streptomycin (200 μg/mL, Invitrogen, Paisley, U.K.), at 37°C in a 95% air/5% CO_2 mixture. The cell culture media was replaced every 24 hours. Cells were split 1:2 into 70 cm^2 flasks when 80-90% confluent.

DMT1 constructs

Antibodies which recognise the individual DMT1 isoforms were not available. Therefore, in order to localise each specifically, constructs encoding tagged isoforms were utilised. The DMT1 constructs used were all derived from rat sequences and are tabulated below (Table 3.6.1). These constructs were a kind gift from Prof. Michael Garrick (University of Buffalo, NY, USA) and are as described by Roth *et al.*, (2000).

Insert	Tag	Tag position	Vector
DMT1 exon 1A+IRE	FLAG	N-terminal	pcDNA3.2
DMT1 exon 1A-IRE	FLAG	N-terminal	pDEST12.2
DMT1 exon 2-IRE	FLAG	C-terminal	pDEST12.2
DMT1 exon 2-IRE with G185R mutation	FLAG	N-terminal	pDEST12.2

Table 3.6. 1 DMT1 contructs

To amplify plasmids, the constructs were transfected into DH5 competent cells (Invitrogen, Poole, U.K.) using manufacturer's protocol. Briefly, cells were thawed on ice and 30 μl of these were transferred into a 15 mL falcon tube and incubated with 1 μL (100 ng) plasmid DNA for 30 minutes on ice. Cells were transferred to a 42°C water bath for 30 seconds and incubated on ice for a further 2 minutes. 500 μL of antibiotic-free nutrient broth was added and the mixture incubated in a shaking incubator at 37°C for 1 hour. Cells were transferred to LB plates containing 100 μg/mL ampicillin and incubated overnight at 37°C. Single bacterial colonies were picked and inoculated into 5 mL LB broth containing 100 μg/mL ampicillin overnight in a shaking incubator at 37°C.

Plasmid DNA was extracted from 3 mL bacterial cultures using the NucleoSpin Plasmid Kit (BD Biosciences, CloneTech, Palo Alto, CA, USA) as instructed by the manufacturer. Plasmid DNA was eluted by centrifugation with 50 µL of elution buffer. The DNA concentration was determined by spectrophotometry (Chapter 2.2).

Cell Transfection

Differentiated BeWo cells at ~70% confluence were transfected with the above plasmids using FuGENE 6 (Roche, Lewes, Sussex, U.K.) according to the manufacturer's instructions. Briefly, ~200 ng of plasmid DNA was complexed with 1 µg of FuGENE 6 in OptiMEM I media (Gibco, BRL, Life Technologies Ltd, Paisley, U.K.) to a final volume of 100 µL. The mixture was incubated for 15 minutes at room temperature for complex formation. Fresh medium was added to the BeWo cells before addition of the FuGENE 6/ plasmid complexes. Cells were incubated for 24-36 hours at 37°C in 5% CO_2, after which the localisation of the transfected protein was determined by indirect immunofluorescence.

Indirect immunofluorescence microscopy

BeWo cells were grown on glass coverslips (BDH, Poole, U.K.) until approximately 60% confluent. Differentiation was initiated by addition of forskolin, final concentration 10 µM, to the culture media, as outlined by Wice *et al.* (1990). Cells were rinsed in PBS and fixed for 15 minutes in freshly prepared 4% v/v paraformaldehyde/ PBS, pH 7. Cells were washed 3 times in PBS before permeabilisation for 20 minutes with 0.05% Triton/ PBS. Cells were washed 3 times in PBS then blocked with 10% serum/ PBS for 20 minutes. The blocking serum was of the same species from which the secondary antibody was produced. The block was shaken off and cells incubated in primary antibody/ 10% block/ PBS for 1 hour. Cells were washed 3 x 5 minutes in PBS. The fluorescent conjugated secondary antibody was applied for 1 hour at room temperature. Cells were washed 3 times in PBS and mounted with Vectorshield containing DAPI (Vector Laboratories, Burlingame, CA, USA). Unless otherwise specified all reagents were purchased from Sigma (Sigma, Poole, U.K.). A complete list of antibodies and dilutions used is tabulated below (Table 3.6.1). Cells were visualised using a Leica DMRXA fluorescence microscope with filters specific for FITC, Cy3 and DAPI. Leica CW4000 image capture software was used for the analysis of images. Results show fluorescence staining of a typical cell (~15-50 cells were analysed).

	conjugate	produced in	supplier
Primary antibodies			
anti-Nramp2 human		rabbit	Alpha Diagnostic
anti-human CD71 (Tfr1)		mouse	Sigma
anti-Ireg1		rabbit	Alpha Diagnostic
anti-Ceruloplasmin*		goat	Sigma
anti-clathrin		goat	Sigma
anti-Protein Disulfide Isomerase		rabbit	Sigma
anti-alpha-Adaptin (AP-2)		mouse	Sigma
anti-FLAG Ms		mouse	Sigma
Secondary antibodies			
anti-mouse IgG	TRITC	rabbit	Sigma
anti-rabbit IgG	TRITC	goat	Sigma
anti-goat IgG	Cy3	rabbit	Sigma
anti-rabbit IgG	FITC	goat	Sigma
Blocking serum			
		Rabbit serum	Sigma
		Mouse serum	Sigma
		Goat serum	Sigma

Table 3.6. 2 Antibodies used in this study

**Anti-ceruloplasmin antibody recognises the placental copper oxidase (Danzeisen et al., 2000).*
(Alpha Diagnostics, San Antonia, Texas, USA; Sigma, Poole, U.K.)

Results

No staining was demonstrated in cells in which the primary antibody was replaced with 10% serum /PBS, murine, rabbit or goat serum (Figure 3.6.1). This confirmed that the signal detected using antibodies was not due to non-specific binding of the fluorescent antibody.

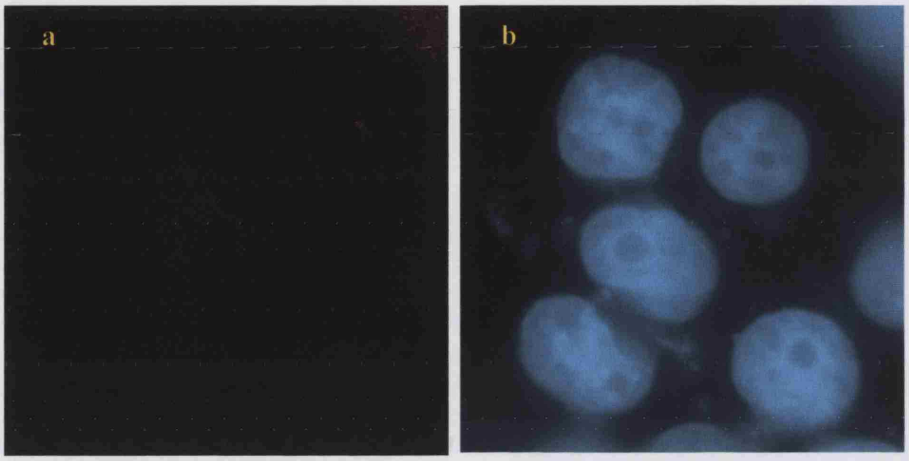

Figure 3.6. 1 Negative control

BeWo cells incubated with rabbit serum and anti-rabbit-FITC antibody.
No FITC signal (green), a, *was detected. Nuclei, counterstained with DAPI (blue), are identified in* b. *Similar results were obtained when cells were incubated with goat serum and detected with anti-goat-Cy3 antibody. Original magnification x40.*

3.6.1 DMT1 localisation

The cell periphery was distinct in cells stained for endogenous DMT1 due to expression throughout the cytoplasm (Figure 3.6.2). Punctate DMT1 staining of the cytoplasm indicated localisation within vesicles. Expression was pronounced in the perinuclear region.

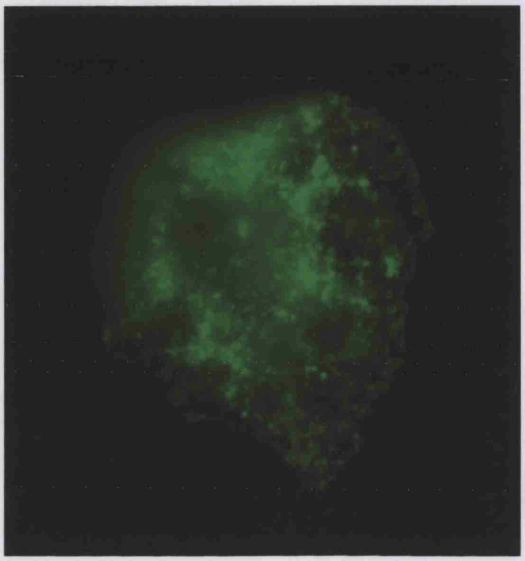

Figure 3.6. 2 DMT1 localisation to the perinuclear region and punctate structures within the cytoplasm.

Unpolarised BeWo cells grown on glass microscope slides were incubated with anti-DMT1 antibody. Bound antibody was visualised using a FITC-conjugated secondary antibody. The figure shows a typical cell with prominent localisation of endogenous DMT1 to the nuclear/perinuclear region and punctate staining of the cytoplasm. Intense staining of the plasma membrane was not visible. Original magnification was x60.

3.6.1.1 DMT1 localisation with the ER lumen

To identify the perinuclear compartment to which DMT1 was located, BeWo cells were labelled for both DMT1 and PDI (protein disulfide isomerase, a marker for the ER) simultaneously. Anti-PDI antibody demonstrated a characteristic perinuclear staining. Dual staining with DMT1 demonstrated that the perinuclear localisation of DMT1 was due to localisation within the ER lumen (Figure 3.6.3).

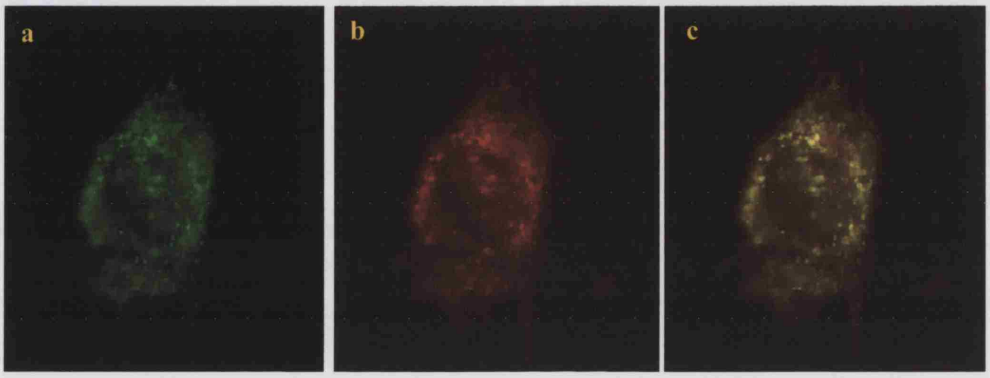

Figure 3.6. 3 DMT1 localised to the ER lumen

To identify the subcellular localisation of DMT1 BeWo cells were stained for endogenous DMT1 (shown in green, a) this demonstrated the characteristic punctate staining with prominent perinuclear localisation, and PDI (shown in red, b) a marker for the ER, demonstrated extensive staining of the perinuclear region. An overlay in DMT1 and PDI (c) demonstrated overlapping (yellow regions) in the expression of both proteins in the ER. Original magnification was x60.

3.6.1.2 DMT1 localisation with Tfr1

Cells were dual stained for endogenous DMT1 and Tfr1. Very little colocalisation was demonstrated between these two proteins (Figure 3.6.4). Clathrin was expressed close to the cell periphery whereas DMT1 demonstrated localisation further within the cell.

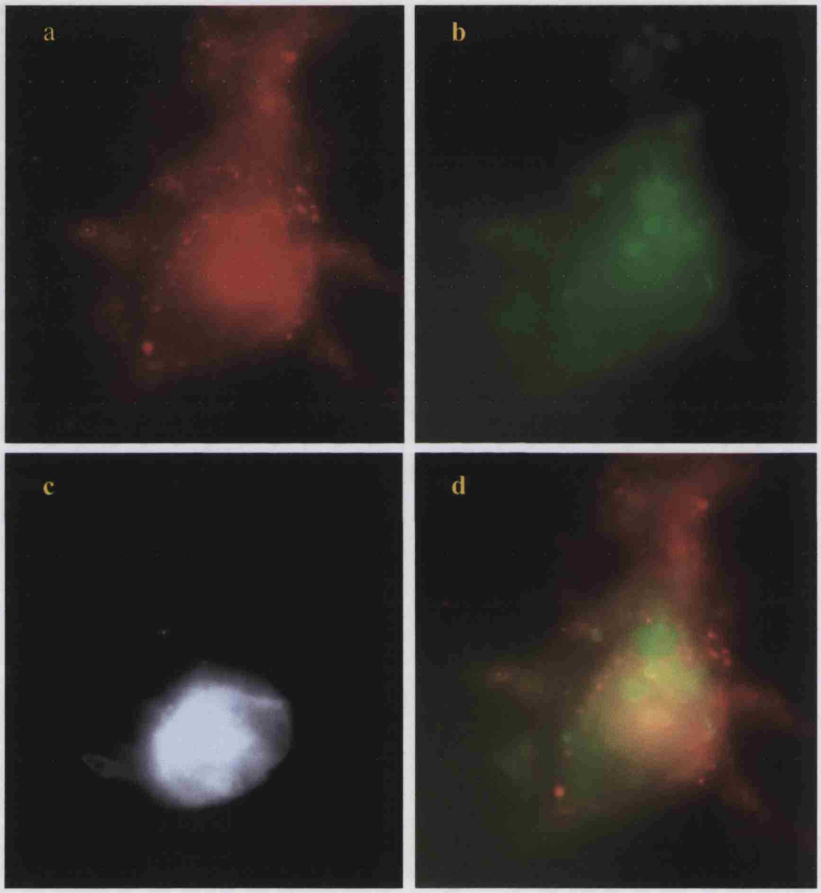

Figure 3.6. 4 DMT1 did not co-localise with Tfr1

BeWo cells were dual-stained for DMT1 and Tfr1. DMT1 represented in green was prominent in the cytoplasm in punctate compartments and towards the perinuclear region (b). Tfr1 was also present in punctate cytoplasmic structures (a). However the structures were not identical and dual staining revealed very little (yellow) overlap between the two proteins (d). Position of cell nucleus identified with DAPI staining in plate (c). Original magnification x60.

3.6.1.3 DMT1-ire localisation

The placenta expresses both isoforms of DMT1: those containing IREs (DMT1+ire) and those that do not (DMT1-ire). To determine whether these two isoforms co-localised to the same subcellular compartment, BeWo cells were transfected with FLAG tagged constructs encoding these proteins. These were subsequently detected by staining with fluorescent anti-FLAG antibodies.

DMT1a-ire demonstrated similar localisation to that of endogenous DMT1 in that the nuclear and perinuclear regions were highly stained with little staining towards the cell periphery. Expression in perinuclear region was more pronounced than that of the endogenous protein (Figure 3.6.5).

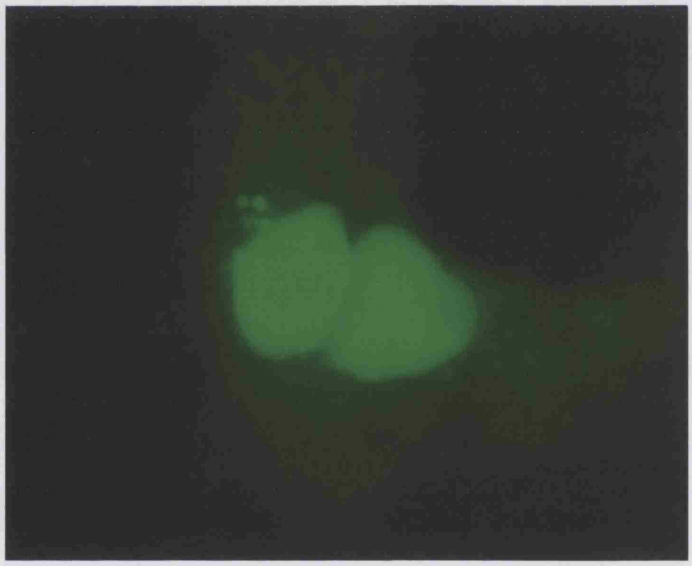

Figure 3.6. 5 DMT1a-ire localisation to the perinuclear region and not to the plasma membrane

To identify the role of the 3'IRE in DMT1, BeWo cells were transfected with tagged DMT1-ire. *Once expressed, the protein localised to the nuclear and perinuclear region. Very little localisation was present at the cell periphery. Original magnification x60.*

Dual staining of transfected DMT1a-ire with clathrin demonstrated some, but not complete, colocalisation (Figure 3.6.6 a-d). Dual staining for the transfected protein with PDI demonstrated that this is due to localisation of DMT1-ire to the ER lumen (Figure 3.6.6 e-g). However, the colocalisation is not complete with puntate staining of DMT1-ire in the cytoplasm.

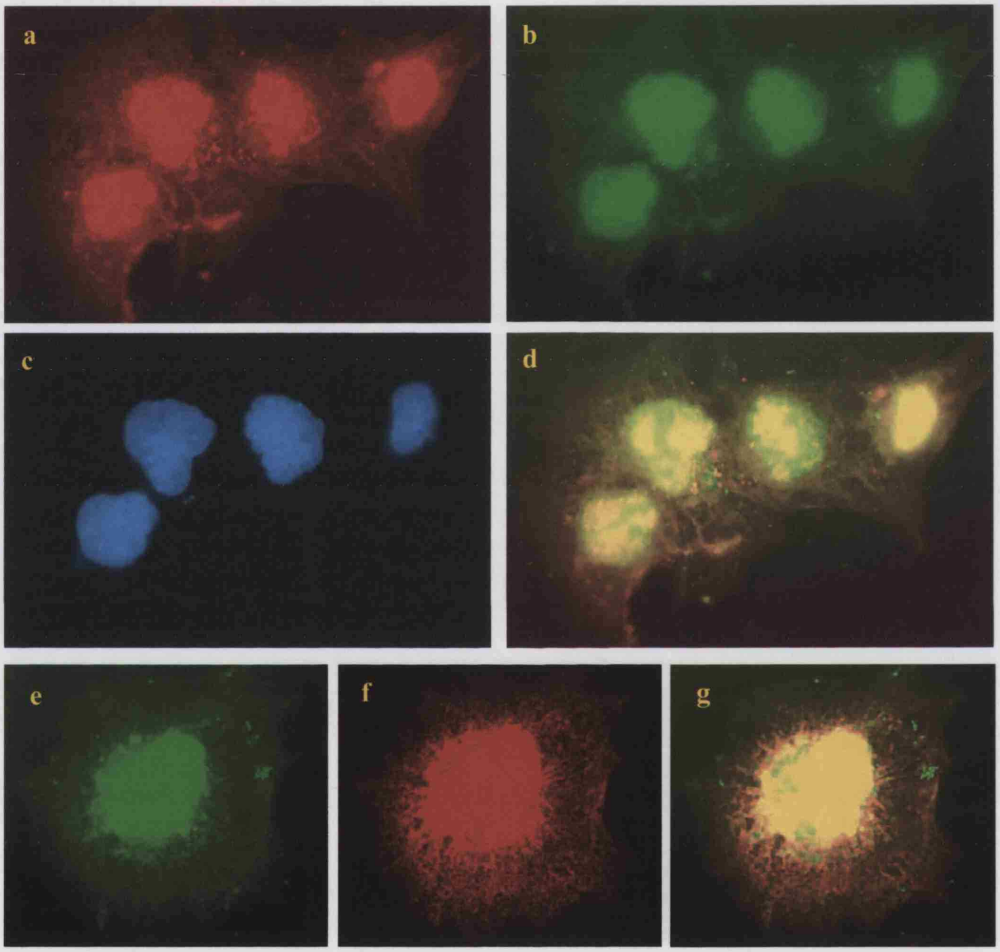

Figure 3.6. 6 DMT1a-ire localisation with clathrin and PDI

DMT1a-ire transfected BeWo cells were labelled for clathrin, a marker for early endosomes. Clathrin demonstrated characteristic punctate staining towards the cell periphery (b). This was similar to that of DMT1a-ire which additionally stained the perinuclear region (a). Colocalisation between the two proteins, demonstrated by yellow regions (c), was not evident in the cytoplasm or on the plasma membrane. The position of the nuclei are shown in (c). DMT1-ire *transfected cells were alternatively stained for PDI. DMT1a-ire demonstrated characteristic staining in the perinuclear region (f). PDI also demonstrated a similar pattern (e). Both proteins demonstrated extensive localisation; however DMT1a-ire also showed faint punctate staining of the cytoplasm, this did not co-localised with PDI (g). Original magnification x60.*

3.6.1.4 DMT1+ire localisation

To determine the role of the DMT1 iron response element, the subcellular localisation of DMT1+ire was identified. This was found to be identical to that of the non-ire isoform, demonstrating extensive overlap with PDI expression (Figure 3.6.7) and little overlap with clathrin (Figure 3.6.8). As both episomally-expressed proteins were tagged with a FLAG epitope and antibodies specific for DMT1+ire or –ire were not available, dual localisation experiments of the two isoforms, to determine conclusively whether both these isoforms were present within the same endosomal unit were not possible.

Figure 3.6. 7 DMT1a+ire demonstrated some localisation to the ER

DMT1a+ire transfected BeWo cells were stained for PDI. PDI demonstrated prominent staining of the perinuclear region and the cytoplasm (shown in red, a), DMT1a+ire also stained in the perinuclear region, however the cytoplasm demonstrated a punctate appearance (shown in green, b). Co-localisation of both proteins was evident in the perinuclear region, yellow staining image (c). DMT1 and PDI however did not overlap near the cell periphery. Original magnification x60.

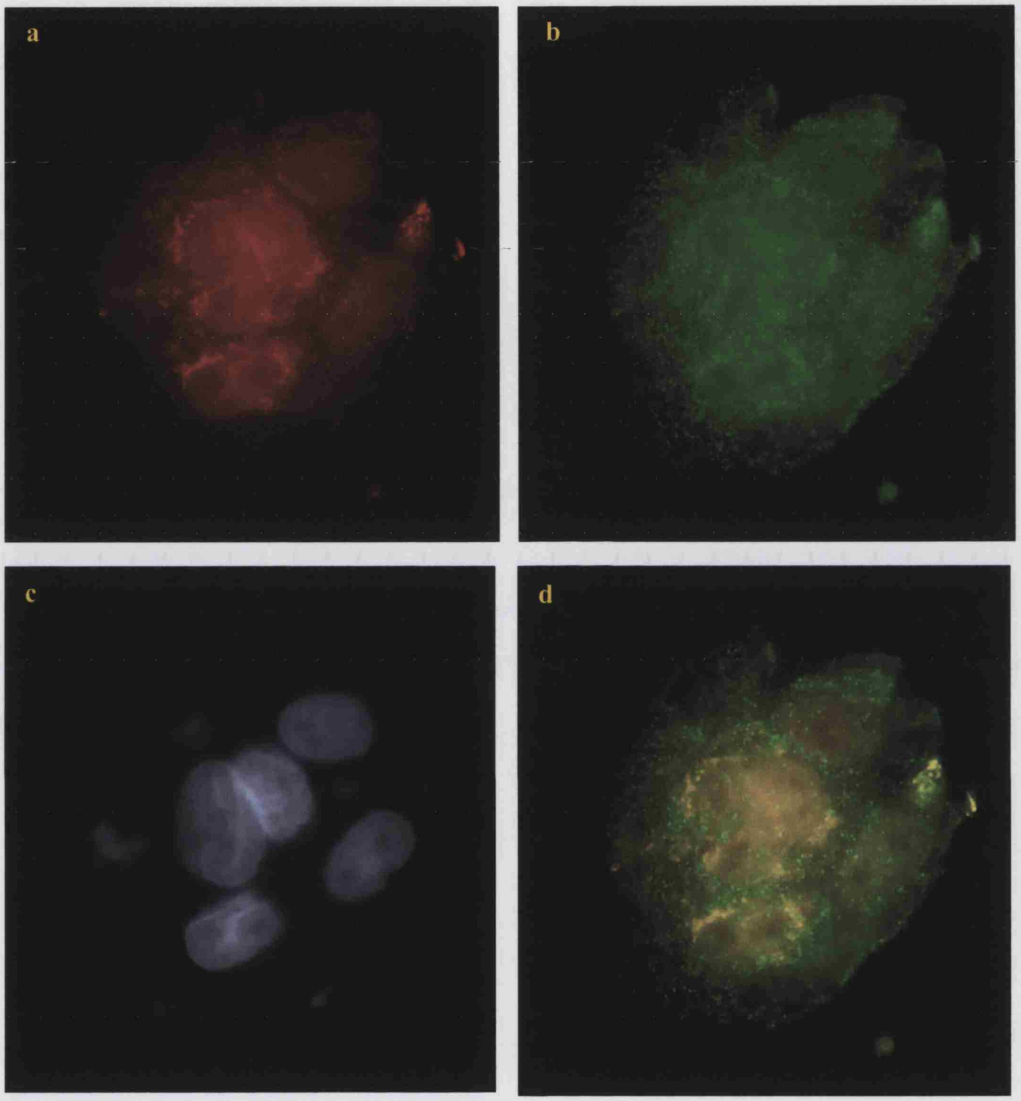

Figure 3.6. 8 DMT1a+ire did not co-localise with clathrin

DMT1a+ire *transfected cells were labelled with anti-clathrin antibody. Both DMT1a+ire (a) and clathrin (b), demonstrated punctate staining of the cytoplasm, especially towards the cell periphery. However, overlapping the images of both (d) revealed no localisation between these proteins. The position of nuclei was identified with DAPI staining shown in plate (c). Original image taken at x60.*

3.6.1.5 Loclisation of DMT1b

Transfected DMT1b-ire demonstrated extensive expression within the cytoplasm. The plasma membrane of cells transfected with DMT1b-ire was distinct (Figure 3.6.9). Dual labelling for PDI or adaptin (Figure 3.6.10) demonstrated incomplete localisation, and further highlighted the expression of the transfected protein to the plasma membrane. As no difference was demonstrated between the localisation of DMT1a isoforms with and without 3'IREs further localisation of both DMT1b+ and –ire was not pursued.

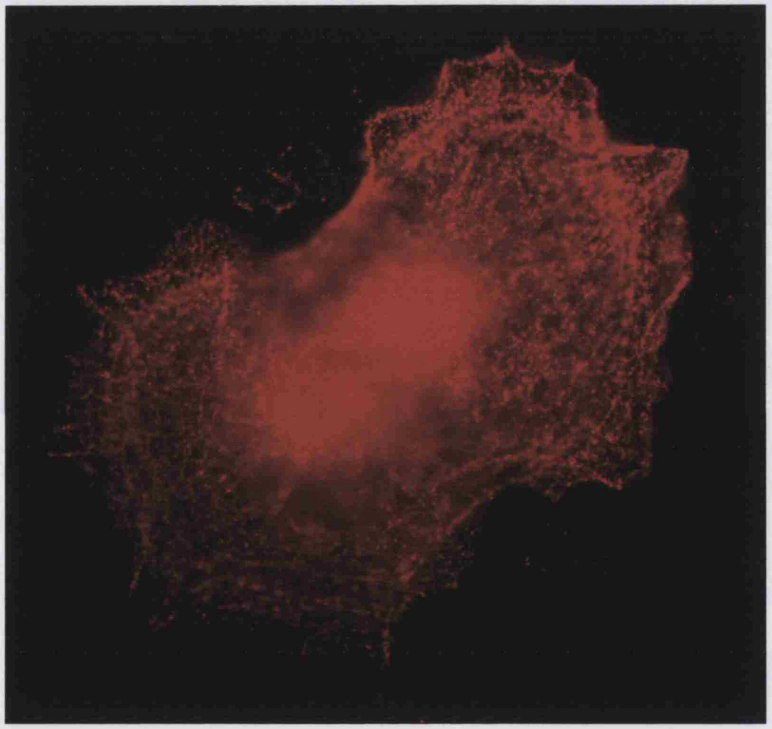

Figure 3.6. 9 DMT1b-ire was localised near the plasma membrane

BeWo cells were transfected with a tagged DMT1b-ire. *This was highly expressed in punctuate compartments in the cytoplasm and demonstrated staining to the plasma membrane. Original magnification x60.*

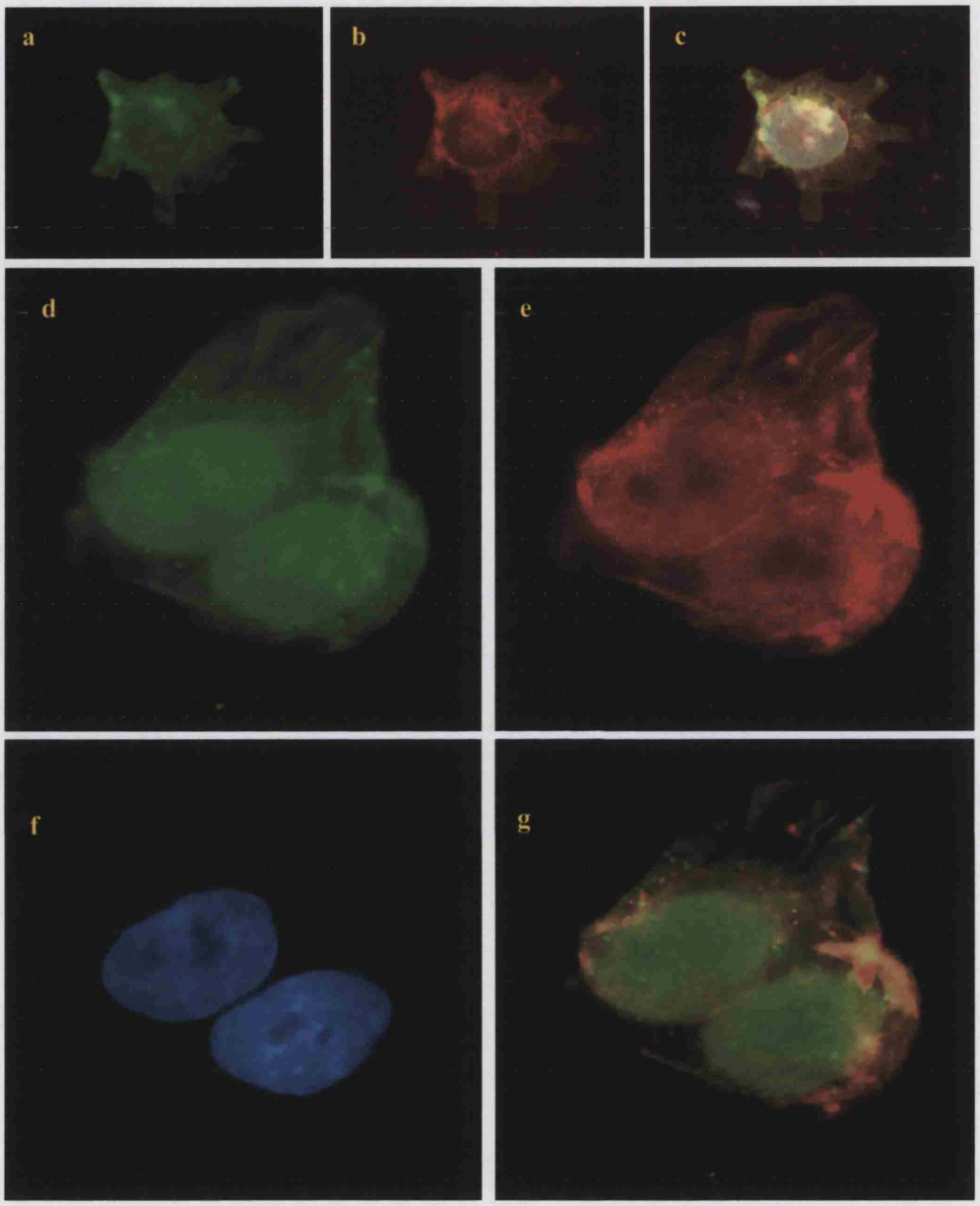

Figure 3.6. 10 DMT1b-ire localisation with PDI and α-adaptin

BeWo cells transfected with the DMT1b-ire construct were stained for PDI. DMT1b-ire, shown in green (a), demonstrated some but not full localisation with PDI (b). Original magnification x60.

DMT1b-ire transfected BeWo cells were also stained with a marker for early endosomes: α-adaptin. Both proteins, DMT1b-ire in red (e) and α-adaptin in green (d), demonstrated some degree of overlap in the cytoplasm, yellow regions (g). The position of the nucleus was identified with DAPI staining shown in plate (f). Original magnification x60.

3.6.1.6 DMT1-G185R localisation

The G185R isoform of DMT1 has been demonstrated to form aggregates within the golgi and reduce localisation to the plasma membrane (Touret *et al.*, 2004). The G185R-FLAG construct was therefore used as a control, to ensure that the FLAG tag itself did not cause localisation of the mature protein to the plasma membrane or endosomes. The DMT1-G185R mature protein localised predominantly to the nuclear region (Figure 3.6.11). Increasing the exposure time of the camera revealed very little localisation of DMT1-G185R to the cytoplasm and the plasma membrane.

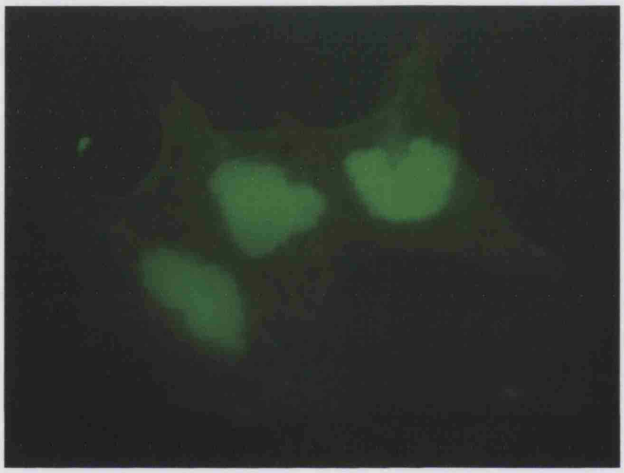

Figure 3.6. 11 G185R mutation in DMT1b-ire prevents localisation to endosomes

To demonstrate the specificity of DMT1 localisation, BeWo cells were transfected with a construct of DMT1b-ire which had an arginine residue in place of a glycine residue at position 185. This substitution was predicted to interfere with the correct localisation of the mature protein. DMT1-G185R localised extensively to the perinuclear region; staining in the cytoplasm was weak. Original magnification x60.

3.6.2 Ireg1 localisation

To identify the mechanism by which iron is effluxed from the syncytotrophoblast, the localisation of endogenous Ireg1 was determined by staining with anti-Ireg1 antibody. Expression was predominately nuclear (Figure 3.6.12a). Dual staining with classical endosomal markers: clathrin, Tfr1 and adaptin (Figure 3.6.12c-k) demonstrated little overlap, implying that Ireg1 was not present within early endosomal compartments. Cells were also stained with anti-ceruloplasmin and Ireg1 antibody (Figure 3.6.13). Little overlap was demonstrated between the localisation of the placental ceruloplasmin homologue and Ireg1.

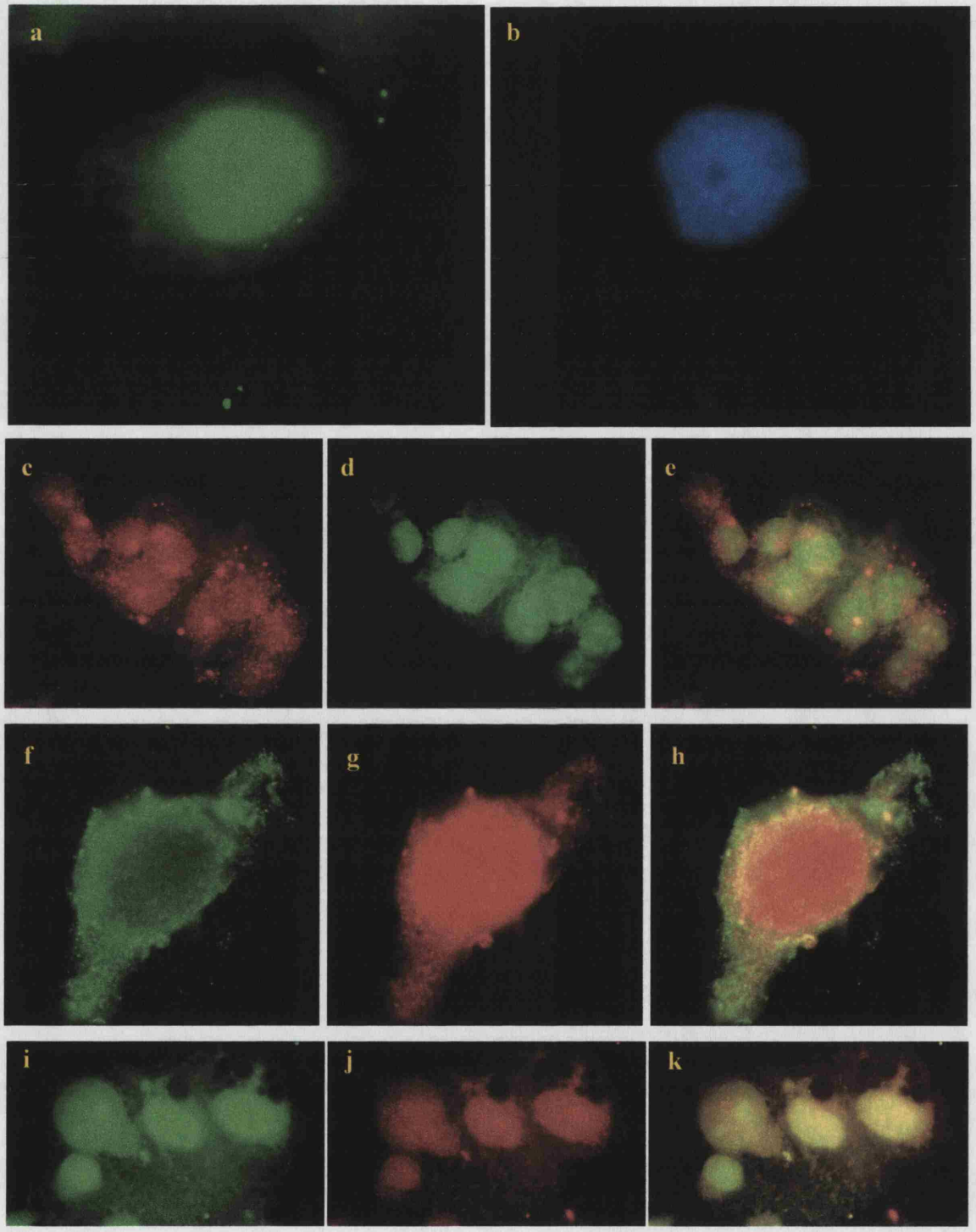

Figure 3.6. 12 Subcellular localisation of Ireg1.

Ireg1 staining was predominantly nuclear (a). Position of were identified nuclei with DAPI staining in plate (b). To demonstrate the subcellular localisation of Ireg1, cells were dual-labeled with markers of early endosomes: clathrin (d), Tfr1 (g) and α-adaptin (j) and Ireg1. Neither markers demonstrated any colocalisation with Ireg1 (e, h and k). Original magnification x60.

3.6.3 Copper oxidase localisation

Cells stained for Cp demonstrated a fine speckled appearance especially towards the cell periphery (Figure 3.6.13a), which demonstrated some localisation with α-adaptin in early endosomes (Figure 3.6.13c-e) and very little localisation with either endogenous DMT1 (Figure 3.6.15) or Ireg1 (Figure 3.6.14). Strong staining of the nuclear regoin was also evident (Figure 3.6.13a).

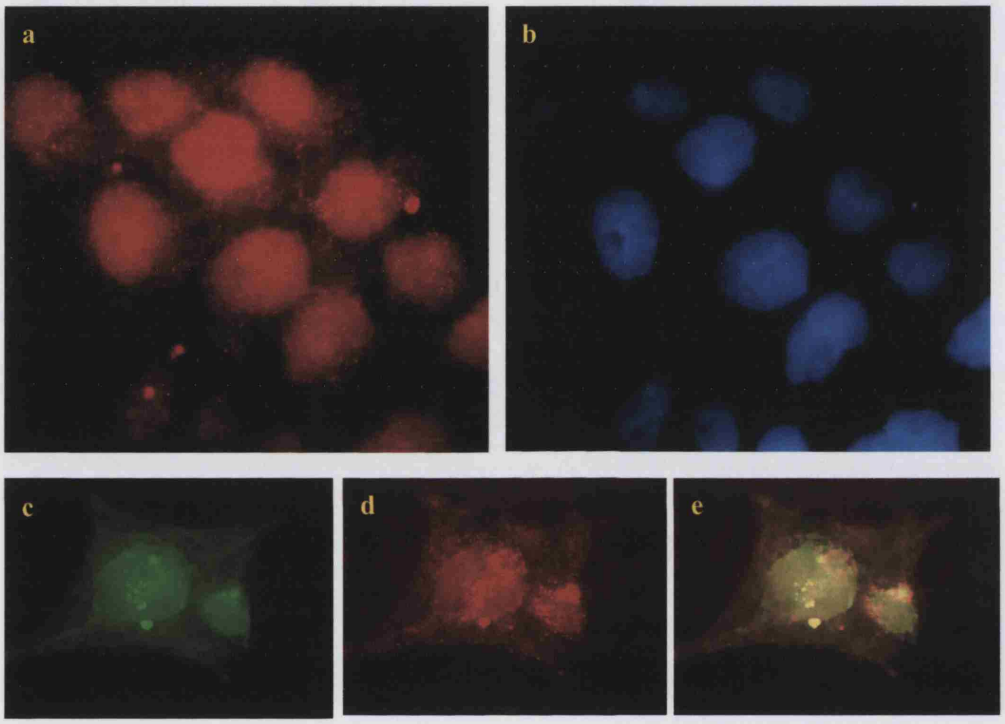

Figure 3.6. 13 Ceruloplasmin staining was speckled throughout the cytoplasm

BeWo cells were stained with anti-ceruloplasmin antibody. This demonstrated a very fine granular appearance of the cytoplasm (a). The position of cell nuclei were highlighted with DAPI staining (b).
BeWo cells were dual-labeled with anti-ceruloplasmin (d) and anti α-adaptin antibody (c). Some, although not total, colocalisation was identified in these cells, yellow staining in (e). Original magnification x60.

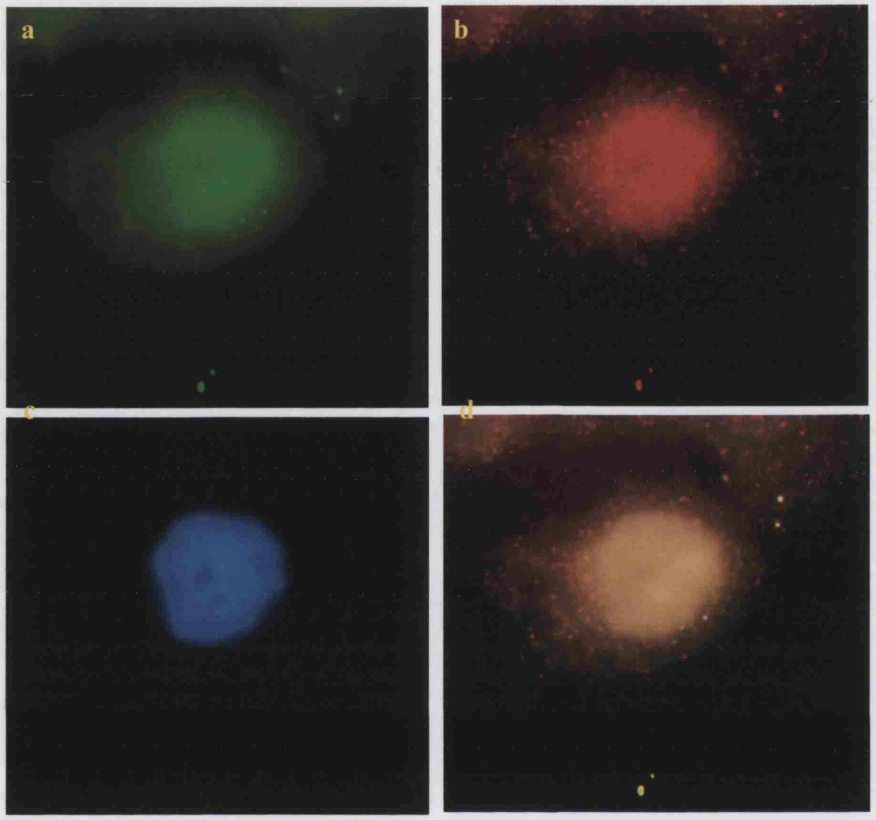

Figure 3.6. 14 Ireg1 localisation with the placental copper oxidase

BeWo cells were dual labelled with anti Ireg1 (a) and anti ceruloplasmin (b) antibodies. Little overlap was evident between the localisation of these two proteins demonstrated by the overlap of the two images except in the perinuclear regoins, yellow staining in figure (d). The position of the nucleus is demonstrated by DAPI staining in plate (c). Original magnification x60.

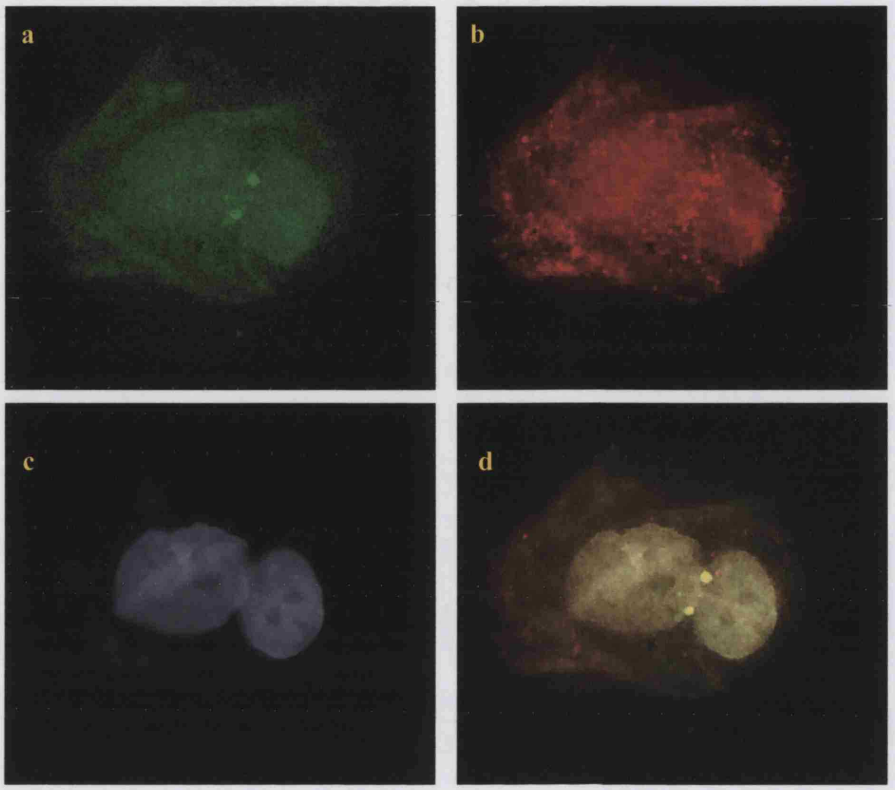

Figure 3.6. 15 DMT1 localisation with the placental copper oxidase

To demonstrate whether the placental copper oxidase localised with endogenously expressed DMT1, BeWo cells were dual-labelled with anti DMT1 (a) and anti ceruloplasmin (b) antibodies. Little overlap was evident between the localisation of these two proteins demonstrated by the overlap of the two images, yellow staining in figure (d). Original magnification x60.

3.6.4 Discussion

In the previous chapters *Tfr1, DMT1* and *Ireg1* mRNA expression was demonstrated in placental tissues, in this chapter the subcellular localisation of these gene products was determined and a mechanism by which iron is transferred across the syncytiotrophoblast membrane postulated.

The major findings presented here are: (1) DMT1 is localised predominately to late endosomes/lysosomes and does not colocalise with Tfr1; (2) IREs in the 3' UTR of DMT1 do not regulate subcellular localisation; (3) DMT1a is localised to late endosomes/lysosomes whereas DMT1b is localised to early endosomes; (4) Ireg1 has a perinuclear localisation and is not present in endosomes, and (5) Cp is present in early endosomes and does not localise with Ireg1.

Maternal Fe_2-Tf is taken up from the serum *via* Tfr1 (Faulk & Galbraith, 1979;Loh *et al.*, 1980;Vanderpuye *et al.*, 1986). Transferrin receptors were expressed on the plasma membrane and in the cytoplasm directly beneath in unpolarised BeWo cells. This is consistent with studies demonstrating the recycling of Tfr1 within early endosomes (Baker *et al.*, 1983). Once bound, Fe_2-Tf is internalised by membrane invagination and the formation of a clathrin-coated endosome. Low lumenal pH converts iron into its ferrous state; this reduces its affinity for Tf and is consequently released (Dautry-Varsat *et al.*, 1983;Dhungana *et al.*, 2004). The Tf-Tfr1 complex is then recycled back to the plasma membrane (Baker *et al.*, 1983).

The free iron is transported across the endosomal membrane presumably by DMT1 (Canonne-Hergaux *et al.*, 2001). The data presented here demonstrate that very little endogenous DMT1 is expressed on the plasma membrane; instead they demonstrate a punctate localisation throughout the cytoplasm, suggestive of a vesicular localisation. This is consistent with the role of DMT1 in the efflux of iron from endosomes and is also consistent with data from Georgieff *et al.* which localised DMT1 to the cytoplasm and the basal membrane of the syncytiotrophoblast in human placental biopsies (Georgieff *et al.*, 2000).

Consistent with the negligible staining observed on the plasma membrane, limited colocalisation of DMT1 was detected with either Tfr1 or clathrin. A similar finding was also noted in neuronal cells (Lis *et al.*, 2004), Cos-7, Hela and Hep-2 cells (Tabuchi *et al.*, 2000) and in human placental biopsies (Georgieff *et al.*, 2000). These data are contradictory to those published by Touret *et al.*, (2003), which demonstrated colocalisation and parallel trafficking of DMT1 with Tfr1, suggesting

that DMT1 may utilise coated pits for internalisation in CHO and LLC-PK_1 cells derived from the porcine proximal tubule.

Studies by Tabuchi *et al.* (2000) have identified the endosomal compartment containing DMT1 to be late endosomes; DMT1 also colocalised with the lysosomal marker LAMP-2 (Tabuchi *et al.*, 2000). Interestingly, this agrees with the role of DMT1 in macrophages where DMT1 is associated with the phagosomal membrane where it is required for the release of phagosomal free iron into the cytoplasm (Gruenheid *et al.*, 1995). The presence of DMT1 in lysosomal compartments suggests a role for DMT1 in the recycling of iron when cellular organelles, such as mitochondria, are broken down. However, to date there have been no studies demonstrating that iron derived from Fe_2-Tf endocytosis actually enters the lysosomal pathway. It is possible that early endosomes either fuse with late endosomes or that late endosomal constituents are inserted into the early endosomes' membrane leading to the maturation of the endosome. By this mechanism, iron released from Tf may be localised with lysosomal DMT1. It is also possible that the various splice variants of DMT1 have specific subcellular localisations, to either the plasma membrane as in duodenal enterocytes or to endosomal vesicles. To test this, the specific DMT1 isoforms were localised in BeWo cells.

Both DMT1b+ire and DMT1b-ire isoforms had a similar localisation to that of endogenous DMT1, showing strong punctate staining of the cytoplasm and perinuclear region, and a faint staining on the plasma membrane. Both isoforms also demonstrated little overlap with either Tfr1 or clathrin. These results indicate that the C-terminal IRE does not determine subcellular localisation in BeWo cells. These data support those from Cos-7 and HEK-293T which also demonstrate that the 3'IRE had no effect on the subcellular localisation of DMT1 (Zhang *et al.*, 2000).

In contrast to the localisation of DMT1b-ire, DMT1a-ire demonstrated extensive staining of the ER and possibly late endosomes with little staining of the plasma membrane. This is in agreement with localisation studies by Roth *et al.* (2000) which demonstrated a nuclear localisation of DMT1a in rat PC12 and sympathetic neuronal cells. However, these patterns for DMT1a and DMT1b staining contradict with studies by Hubert and Hentze (2002), which demonstrated a higher ratio of DMT1a expression compared to DMT1b in duodenal and kidney cells, which are polarised and in which DMT1 localises to the apical membrane; they therefore hypothesised that exon 1A may play a role in targeting DMT1 to the apical membrane of polarised cells. The

placental syncytiotrophblast is polarised and has many similarities to the duodenum. However in the model studied the cells were not polarised. Therefore it is possible that DMT1a is expressed on the brush border membrane *in vivo*.

Transfected DMT1 demonstrated stronger staining of the nuclear and perinuclear region compared to that of endogenous DMT1. Dual staining for transfected DMT1 with PDI demonstrated that this was due to accumulation of transfected DMT1 within the ER lumen. Although our observations suggest that DMT1 may be located here constitutively, it is possible that defective post-translational modification of DMT1 may have resulted in malfolded protein which was consequently retained by the ER.

It was hypothesied that iron was transported across the blm through Ireg1 as previous studies by two independent groups have demonstrated the localisation of Ireg1 on the basolateral side of the placental syncytiotrophoblast in human placental sections (Abboud & Haile, 2000;Donovan *et al.*, 2000). However, in this study Ireg1 expression was predominantly identified in the nucleus and cytoplasm. This is in agreement with studies in other unpolarised tissue culture models including RAW 267.4 monocytes and COS7 and in duodenal enterocytes under control diet conditions, strong basolateral localisation was only detected in iron deficient duodenal tissue (Abboud & Haile, 2000). The cytoplasmic localisation of Ireg1 suggests a role for Ireg1 in iron transport between the cytosol and organelles.

Interestingly, a perinuclear location was also been reflected in Cu oxidase activity in BeWo cells (Danzeisen *et al.*, 2000), placing the key components of the iron efflux pathway in the same subcellular location. However, in the present study cells stained with anti-ceruloplasmin antibody demonstrated a fine speckled appearance especially towards the cell periphery, which demonstrated very little localisation with either endogenous DMT1 or Ireg1. Dual staining of Cp with α-adaptin demonstrated some colocalisation. This is consistent with data shown by Kuo and colleagues which suggest that hephaestin, the duodenal homologue of ceruloplasmin, may be located in an intracellular compartment (Kuo *et al.*, 2004). In agreement with a study by Danzeisen *et al.* (2000), extensive staining by ceruloplasmin antibody to the nuclear region was also evident.

3.6.5 Conclusions

Iron transport across the placental syncytiotrophoblast can be divided into three steps.

(1) Iron uptake: The current data suggests that the placenta takes up plasma Tf-Fe^{3+} *via* Tfr1 receptors present in clathrin coated pits on the cell surface (Faulk & Galbraith, 1979; Loh *et al.*, 1980; Vanderpuye *et al.*, 1986). These attach to plasma Fe_2-Tf by an interaction not requiring temperature or energy (Cheng *et al.*, 2004). In a temperature- and energy-dependent manner, the Fe_2Tf·Tfr1 complexes are then internalised within clathrin-coated vesicles (Takahashi & Tavassoli, 1983). Once internalised the clathrin coat is shed and the vesicle fuses with early endosomes which lie beneath the plasma membrane. The endosomal lumen has an acidic environment (pH<6); this alters the affinity of Fe^{3+} for Tf, which subsequently releases it. Due to the low pH of the endosome apo-Tf remains attached to Tfr1 (Dautry-Varsat *et al.*, 1983;Dhungana *et al.*, 2004). The apo-Tf·Tfr1 complex is sorted to the recycling endosomes by pinching off of the endosomal membrane, reformation of a clathrin coat and eventual recycling back to the cell surface (Baker *et al.*, 1983).

(2) Iron efflux from the endosome: The early endosomes mature by gaining components specific for late endosomes; these include DMT1 and vacuolar H^+-ATPase, possibly by fusion to endolysosomes. These ATP-dependent proton pumps further acidify the endosome/lysosome. The free Fe^{3+} is reduced to Fe^{2+}, a process probably mediated by an oxidoreductase (Verrijt *et al.*, 1998). Fe^{2+} is finally released from the endosomal/lysosomal compartment by DMT1.

(3) Iron efflux from the cell: Iron is probably effluxed from the cytosol *via* Ireg1. This is predominantly located near the ER, which suggests a mechanism by which iron may be exported through a secretory pathway.

It is important to note that the current study is a localisation study and that iron transport was not assessed. Therefore we can only speculate as to the function of these proteins in each location. In addition, this study was carried out in unpolarised cells *in vitro*, therefore confirmation of these data in tissue sections will be necessary when antibodies specific to the proteins involved become available.

4 General Discussion

To define the molecular mechanism of duodenal and placental iron transfer this thesis posed the following questions:

(i) How is duodenal iron absorption increased during pregnancy?

(ii) How is duodenal iron absorption regulated?

(iii) What stimuli is duodenal iron absorption responsive to?

(iv) What is the molecular mechanism of placental iron transfer? And

(v) How is placental iron transfer regulated?

In light of the data presented here these are addressed below.

4.1 How is duodenal iron absorption increased during pregnancy?

How lumenal iron is transferred across the bbm of the duodenal enterocyte and transferred across the blm was understood prior to this thesis (outlined in Figure 4.1) but how this mechanism was modified during pregnancy was not known.

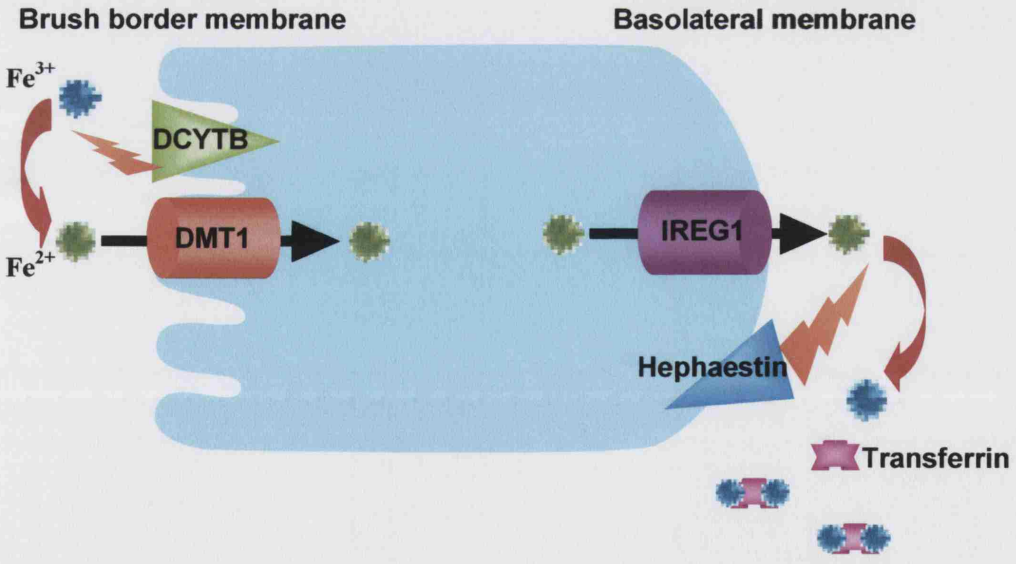

Figure 4. 1 Duodenal iron absorption

Dietary ferric iron is reduced by Dcytb. Ferrous iron is transported across the brush border membrane by DMT1. Transfer across the basolateral membrane is via Ireg1 as Fe^{2+}. Ferrous iron is oxidised by hephaestin prior to binding to serum apo-transferrin.

Lumenal ferric iron is reduced to ferrous iron before transportation across the bbm by DMT1. The importance of a reductase is highlighted in iron uptake experiments where the absorption of ferrous iron was found to be 1000 times greater than that of ferric iron (Chapter 3.4.2). The ferrireductase activity at the duodenal bbm is provided by Dcytb (McKie *et al.*, 2001). During pregnancy *Dcytb* mRNA expression did not increase significantly (Chapter 3.2.1.2), however studies in non-pregnant rats demonstrated an increase in Dcytb protein expression during iron deficiency (Chapter 3.1.4), whilst, in a similar study in mice, an increase at the mRNA level was not evident (Chapter 3.1.2). It is possible that Dcytb expression is regulated post-translationally, in support of this Millard *et al.*, (2004) have demonstrated an increase in Dcytb localisation to the duodenal bbm in late gestation rats.

During pregnancy, and during dietary iron deficiency in non-pregnant animals, duodenal and placental *DMT1* expression is increased (Chapter 3.2.1.2 and 3.1.2). Iron deficiency also causes an increase in DMT1 localisation to the duodenal bbm (Chapter 3.1.3). *DMT1* is regulated transcriptionally (by differential expression of exon 1a-1b), post-translationally (by IRE-IRP interaction) or by localisation of the mature protein to the site of iron uptake, usually the bbm. The studies in BeWo cells suggest that the localisation of DMT1 to the plasma membrane is regulated transcriptionally *via* the expression of either exon-1a, for plasma membrane localisation or exon-1b, for endosomal localisation (Chapter 3.5.10).

Ireg1 mRNA levels are not regulated by dietary or body iron status in mice (Chapter 3.1.2) or during pregnancy in rats (Chapter 3.2.1.2). However, Ireg1 protein levels fluctuate despite constant mRNA levels. Therefore, although not demonstrated in this study, it is possible that the basolateral iron transport mechanism is enhanced during pregnancy. Unfortunately we were unable to investigate this in the present study, however a subsequent study in rats has demonstrated an increase in duodenal Ireg1 protein from 15 gd until term (Millard *et al.*, 2004).

4.2 How is duodenal iron absorption regulated?

The work presented here highlights the link between the expression of *DMT1* in the duodenum and *hepcidin* in the liver:

- Iron deficiency in mice leads to decreased *hepcidin* and increased duodenal *DMT1* (Chapter 3.1.2).
- $Hfe^{-/-}$ mice have low *hepcidin* expression, and probably as a consequence of this, increased duodenal *DMT1* despite systemic iron loading (Chapter 3.1.2).
- During pregnancy, *hepcidin* expression is decreased (Chapter 3.2.1.3), whilst duodenal *DMT1* is increased (Chapter 3.2.1.2).
- Iron loading during pregnancy causes an increase in *hepcidin* expression (Chapter 3.4.1.2) and a decrease in duodenal *DMT1* (Chapter 3.4.1.1).

These findings suggest that the elevated iron absorption in $hfe^{-/-}$ mice was due to decreased *hepcidin* expression in the liver and shifted the emphasis away from regulation by hfe in the duodenal crypts. However, it is possible that hepcidin may act upon the duodenal crypt cells and program them in a mechanism analogous to that first hypothesised for hfe (see mucosal block theory in Figure 1.9). Although the study by Frazer *et al.* (2004), demonstrated that a reduction in *hepcidin* expression, following phenylhydrazine induced haemolysis, coincided with an increase in duodenal *DMT1* expression, without a 3-4 day delay, which would be required for crypt cell maturation if hepcidin regulated duodenal iron absorption from the crypt cells. This suggests that hepcidin targets the absorptive cells at the villus tips directly. In addition a study using fully differentiated Caco-2 cells, demonstrated a negative response to hepcidin treatment. Upon treatment these cells showed reduced DMT1 mRNA, protein and iron uptake (Yamaji *et al.*, 2004). These data highlight the role of hepcidin in the regulation of duodenal iron absorption.

4.3 How is hepcidin expression regulated?

During pregnancy various parameters are modified, these include Tf saturation, body iron stores, and hormonal balance. The relationship of these to *hepcidin* expression and duodenal iron absorption is discussed below.

4.3.1 Transferrin saturation

The increase in iron lost from the body (to the placenta and foetus) coupled with increased erythropoiesis which utilises iron, leads to a decrease in plasma Tf saturation during the final trimester (Figure 3.2.1). This reduces the iron supply to liver hepatocytes. It is possible that *hepcidin* expression is decreased due to cellular iron deficiency and/or an increase in IRE-IRP interactions in these cells.

Alternatively hfe may be involved in the monitoring of Tf saturation. Hfe is highly expressed in the liver sinusoidal membrane, the bbm of the placental syncytiotrophoblast and in duodenal crypt cells. In the latter two cell types hfe has been demonstrated to localise and competitively bind with Tfr1 (Waheed *et al.*, 1999). Binding is thought to reduce the affinity of the Tfr1 for Fe_2-Tf. Together, Tfr1 and hfe may monitor Tf saturation. Interestingly, the liver expresses very little Tfr1, instead the Tfr2 isoform is predominantly expressed. Studies localising hfe with Tfr2 have demonstrated negative results, therefore another mechanism by which hfe has a regulatory role must be appropriate at this site. Interestingly, $Tfr2^{-/-}$ patients display a phenotype identical to that of $hfe^{-/-}$ and $hepcdin^{-/-}$ individuals, suggesting all three proteins are part of the same signalling mechanism. This study demonstrates that *Tfr2* mRNA expression is not modulated by iron status (Chapter 3.1.2), although a study by Millard *et al.* (2004) demonstrated that hepatic *Tfr2* mRNA is decreased during pregnancy. Additionally studies by Johnson and Enns (2004) have demonstrated that Fe_2-Tf increases the half-life of Tfr2 protein. How Tfr2 levels regulate *hepcidin* expression, and the role of hfe in this, is not known.

Interestingly, Millard *et al.* (2004) recently demonstrated that hepatic *hfe* expression decreased during pregnancy. This is similar to the 'genotype' of $hfe^{-/-}$ mice, which also have functionally reduced hfe. As *hepcidin* expression is reduced during pregnancy and in $hfe^{-/-}$ individuals, this suggests that hfe enhances *hepcidin* expression.

However, iron supplementation during pregnancy raises *hepcidin* levels, although not to non-**pregnant** levels, and reduces duodenal *DMT1* without an increase in Tf saturation, suggesting that Tf saturation is not the sole factor contributing to the decrease in *hepcidin* expression during pregnancy.

4.3.2 Body iron stores

Body iron stores are a sink for excess iron within the body and form a buffer which compensates for fluctuations between the iron supply and demand. This iron is stored as ferritin mainly within the parenchymal tissue of the liver. How iron is taken up by these cells is not well understood. However, DMT1 is expressed here and is postulated to have a role in iron uptake. Indeed hepatic *DMT1* expression is decreased during pregnancy (Chapter 3.2.1.3), this coordinates with a decrease in iron stores (Chapter 3.2.1.4). The efflux of iron from hepatic stores is regulated by Cp and Ireg1 expression, which is increased during pregnancy (Chapter 3.2.1.3).

To test wether this decrease in iron stores contributes to the reduction in *hepcidin* expression during pregnancy, a rat model was utilised in which dams were supplemented with iron at gd 1. In this model iron supplementation compensated for the loss of iron stores during the first two trimesters, but was unable to compensate for loss during the final trimester (Chapter 3.4.1.2). However, due to the higher iron status at gd 14, iron supplemented dams had significantly higher iron stores during the final trimester, which was mirrored by an increase in *hepcidin* expression. This suggests that the decrease in maternal liver iron status contributes to the decrease in *hepcidin* expression during pregnancy.

4.3.4 Hormones

In non-pregnant animals Epo has been demonstrated to negatively correlate with hepcidin expression (Nicolas *et al.*, 2002a). At the onset of pregnancy Epo is decreased, and later shows a gradual increase until term (Bianco *et al.*, 2000;Akesson *et al.*, 2002). This is correlated to changes in sTfr, erythropoietic activity, the increase in red blood cell mass (Beguin *et al.*, 1991) and the decrease in hepcidin expression during the final trimester (Chapter 3.2).

Oestrogen levels increase during pregnancy, peaking at birth when duodenal and placental iron transfer is greatest. Interestingly a study in ovarirectomised rats administered oestrogen at levels similar to those found at term, demonstrated increased iron absorption (Haouari *et al.*, 1994). This suggests that oestrogen may promote the increase in iron absorption during pregnancy.

During pregnancy maternal cell-mediated immune responses are suppressed in order to maintain a physiologically compatible environment for the foetus (Raghupathy, 1997;Clark, 1999a;Clark, 1999b;Dealtry *et al.*, 2000; Mellor & Munn, 2000). The placenta also produces various proteins that aid the coexistence of the foetus and the mother. These include the secretion of PLIF (for placental immunomodulatory ferritin)(Moroz *et al.*, 2002). These proteins work on the local level by inhibiting T cell proliferation after activation (Weinberger *et al.*, 2003;Zahalka *et al.*, 2003). PLIF also initiates the secretion of IL-6 and decreased secretion of TNFα from spleenic macrophages (Nahum *et al.*, 2004). TNFα decreases, whereas IL-6 increases, hepcidin expression (Nemeth *et al.*, 2003). PLIF secretion may therefore regulate maternal hepcidin expression during pregnancy, although its effect would be to counterbalance that of decreased iron stores and Tf saturation.

4.3.5 Dilutary effect of increased plasma volume

In addition to the parameters discussed above, the increase in plasma volume, characteristic of pregnancy, may also stimulate iron absorption by having a dilutary effect not only on Hb but also on Fe_2-Tf and hepcidin concentration.

It is now generally accepted that hepcidin negatively regulates iron absorption in non-pregnant animal models. This study has demonstrated that this is also true during pregnancy. A mechanism by which *hepcidin* expression is regulated during pregnancy is summarised in figure 4.2.

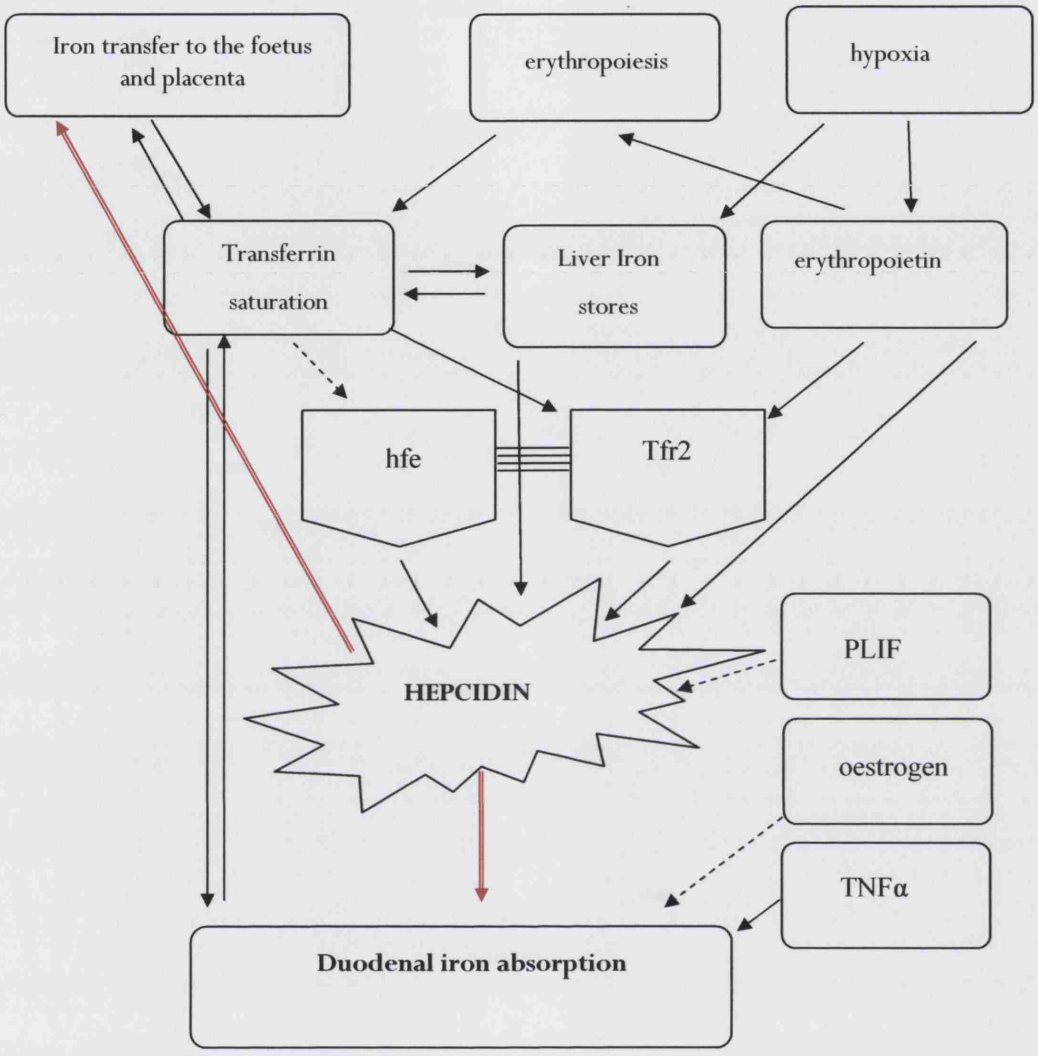

Figure 4. 2 Regulatory mechanism of iron homeostasis

Hepcidin is thought to be the central regulator of duodenal iron absorption. Hepcidin expression is regulated by transferrin saturation, body iron stores and erythropoiesis. How these are monitered is not known but may involve hfe and Tfr2. In turn hepcidin negatively regulates DMT1 expression in the duodenum and the placenta.

4.4 What is the molecular mechanism of placental iron transfer?

To understand the regulatory mechanism of placental iron transport it was necessary to determine the mechanism by which iron is transported across the placenta. This study demonstrated that Tfr1 is present in vesicles underlying the plasma membrane. DMT1 does not enter this endosomal compartment. This suggests that Tfr1 is recycled to the cell surface before DMT1 is inserted into the endosomal compartment. It is presumed that DMT1, present in vesicles and the perinuclear region, has a role in iron efflux out of the endosome (Georgieff *et al.*, 2000). Ireg1 also localises to the perinuclear region. It is possible that Ireg1 may be involved in the efflux of cytoplasmic free iron into secretory vesicles. Cp is localised to endosomes nearer the cell periphery and may be involved in the oxidation of iron prior to release into the foetal circulation (summarised in Figure 4.3).

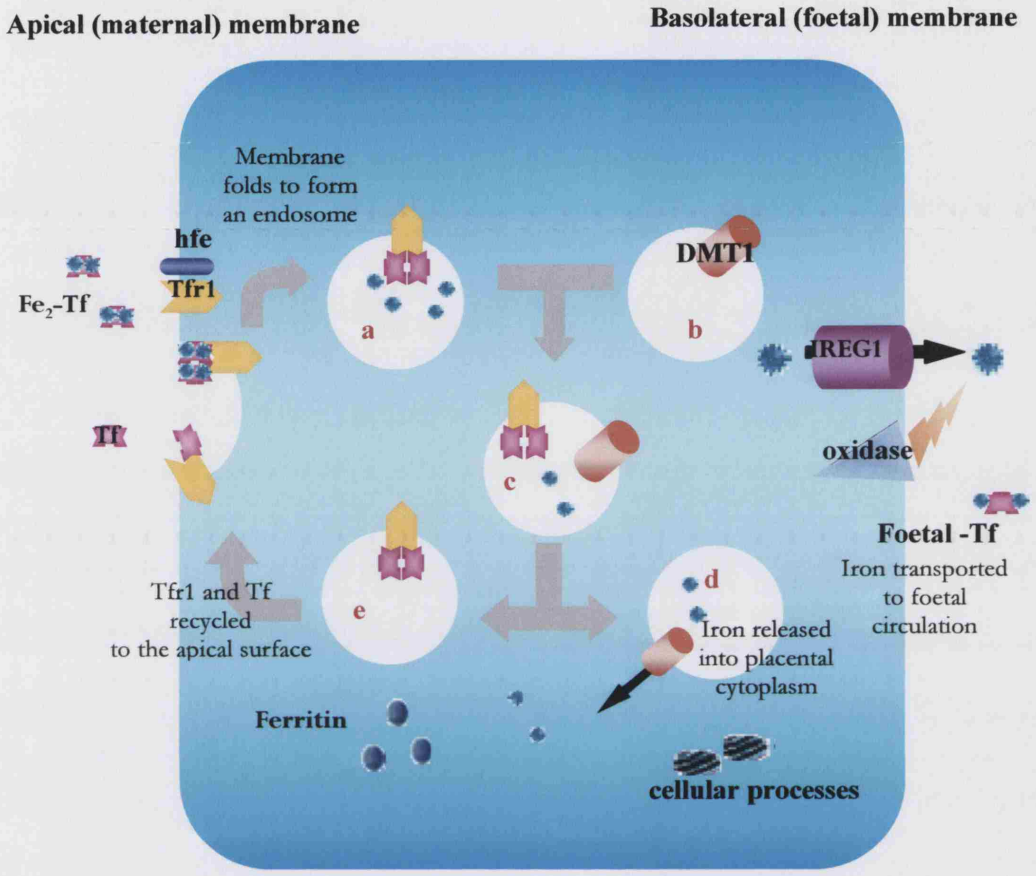

Figure 4. 3 Proposed mechanism of placental iron transport

Tfr1, in association with hfe, is present on the plasma membrane. Fe_2-Tf binding initiates membrane invagination and formation of a clathrin coated vesicle (a). The acidic lumen of this vesicle promotes the release of iron from transferrin. DMT1 is present in the cytoplasm within endosomes (b). These possibly merge with early endosomes containing Tf-Tfr1-Fe (c). These endosomes divide, Tf/Tfr1 recycles back to the plasma membrane (e), whilst DMT1 transports iron across the endosomal membrane (d). The iron efflux pathway is probably via Ireg1. The localisation of Ireg1 is probably to the blm. Iron is oxidised by the Cp homologue prior to loading onto foetal transferrin.

4.5 How is placental iron transfer regulated?

Placental iron transfer increases during the final trimester and is maximum at term. The gestational increase in iron transfer is not due to an increase in placental Tfr1 (Chapter 3.2.1.5), but is in part due to an increase in *DMT1* (Figure 3.2.6). An increase in DMT1 would result in an increase in iron uptake by the placenta if Tfr1 expression is adequate. An increase in placental *Ireg1* mRNA was not detected (Figure 3.2.6), suggesting that placental iron transfer is regulated by DMT1 levels, although it is important to note that Ireg1 protein levels, which were not quantified here, may be modified without a change in mRNA levels.

Placental iron uptake is regulated by cellular iron levels *via* IRE-IRP interactions. This is evident due to the coordinated increase in *DMT1* and *Tfr1* under iron deficient conditions (Chapter 3.3.1). If placental iron uptake is regulated by IRE-IRP interactions this suggests that placental transfer is ultimately responsive to basolateral iron transfer. If this increases, placental iron levels decrease, causing an increase in IRP activity, *DMT1* and *Tfr1* expression, and an increase in iron uptake (Figure 4.4). This method of regulation is physiologically sound as foetal iron requirements are not dictated by maternal iron status, and is supported by data which demonstrates that iron deficiency in the foetus is less severe then that of the mother (Appendix VI). Placental iron transfer is specifically enhanced to compensate for iron deficiency in the mother. Foetal iron requirements remain constant, reduced Tf saturation in maternal plasma reduces placental iron levels, which in turn increase the expression of *DMT1+ire* and *Tfr1* to effectively compete for maternal plasma Fe_2-Tf (Figure 4.4).

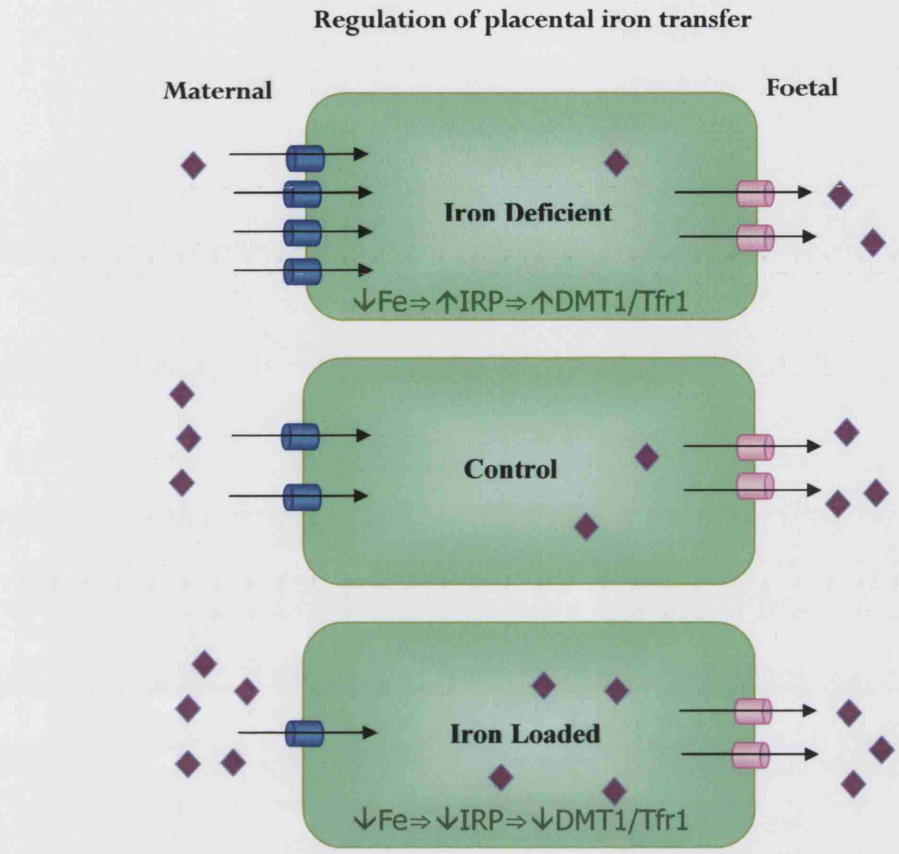

Figure 4. 4 Regulation of placental iron transfer

Iron deficiency in the mother reduces the availability of iron for placental iron uptake. As the iron efflux rate is not modified this causes a reduction in the placental iron concentration. IRP activity increases, causing an increase in Tfr1 and DMT1 expression. Under iron-loaded conditions, placental iron reserves are high. DMT1 and Tfr1 expression is reduced limiting bbm iron uptake. The iron requirements of the foetus are not modulated to maternal iron status therefore the efflux pathway is not increased or decreased due to placental or maternal iron deficiency or loading.

It was surprising to note that placental *DMT1-ire* decreased following iron supplementation, although *DMT1+ire* and *Tfr1* remained constant in humans (Chapter 3.4.3). *DMT1-ire* levels are not regulated by IRE-IRP interactions, therefore decreased *DMT1-ire* expression following iron supplementation suggests alternative regulatory mechanisms. The regulation of placental *DMT1* following iron supplementation is due to factors other then local iron levels, as it involved an increase in *DMT1-ire* and not *DMT1+ire* (Figure 3.4.11), and may therefore be due to the increase in circulating hepcidin in iron supplemented mothers. *In vitro* studies in placental BeWo cells demonstrated a negative effect of hepcidin on placental iron transport (Chapter 3.5.1.2). The negative regulation of placental iron transport by hepcidin is consistent with the decrease in *hepcidin* (Chapter 3.2.1.3), increased placental *DMT1* expression (Chapter 3.2.1.5) and increase in placental iron uptake during pregnancy (McArdle & Morgan, 1982). This suggests that duodenal and placental iron transport may be coordinately regulated. This is advantageous to the maintenance of maternal iron stores as it ensures that transfer to the foetus is in line with duodenal uptake.

4.2 Conclusions

Duodenal iron absorption increases during pregnancy as a consequence of increased *DMT1* expression. As with non-pregnant animals, this is negatively regulated by hepcidin which decreases during the final trimester. Reduced liver iron stores and a decrease in Tf saturation reduces *hepcidin* expression during the final trimester. This combined with the dilution effect of the increased plasma volume, results in increased duodenal iron absorption. Placental iron transfer also increases during the final trimester as a consequence of increased *DMT1* expression.

Iron deficiency during pregnancy causes a further increase in duodenal absorption as well as an increase in the placental iron uptake mechanism, consequently iron deficiency is less severe in the foetus then the mother. Iron supplementation during pregnancy maintains maternal liver iron stores and demonstrates that the reduction in maternal *hepcidin* expression during pregnancy is, in part, a consequence of reduced iron stores.

The placenta takes up Fe_2-Tf by binding and endocytosis with Tfr1. Once released from Tf, iron is thought to be transported across the endosomal membrane by DMT1. Surprisingly Tfr1 and DMT1 demonstrate very little co-localisation suggesting that the apoTf-Tfr1 complex is rapidly recycled to the apical membrane. Iron is most likely transported across the blm by Ireg1 linked with the Cp homologue.

Placental iron transfer increases during pregnancy due to the up-regulation of *DMT1*. This increase is concurrent with that in the duodenum and correlates with the decrease in *hepcidin* expression. Placental iron transfer is additionally responsive to maternal Tf saturation, which modifies cellular iron levels. This regulates IRP activity and the expression of *DMT1+ire* and *Tfr1*. Placental *DMT1-ire* is also regulated by maternal iron status, increasing with iron supplementation, and *in vitro* studies have demonstrated a negative effect of maternal hepcidin on placental iron uptake. This suggests an additional regulatory mechanism other then that by IRE-IRP interactions, possibly mediated by hepcidin. The foetal liver increases *hepcidin* expression during development, which is down-regulated following iron supplementation. However, this does not demonstrate a regulatory role on placental iron efflux, although a role on duodenal iron uptake in the neonate is postulated.

4.3 Future Studies

In this thesis the expression of iron transporter genes during pregnancy under iron deficient and iron loaded states was addressed. Messenger RNA levels do not necessarily correlate to protein expression levels. Therefore to confirm the mRNA data presented here quantification of the gene products by Western blotting is necessary as is the localisation of these gene products to their sites of action by immunocytochemistry on duodenal and placental biopsies. In addition we were unable to perform assays in which to quantitate iron transfer from the gut lumen into circulation (this is opposed to studies investigating iron uptake into the duodenal enterocyte, rather then subsequent transfer across the blm). Therefore the effect of the parameters studied here on blm transfer are not yet addressed. These can be studied using the 'tied loop' iron uptake assay as described in appendix VII (Laftah *et al.*, 2004).

Regulation of iron uptake by hepcidin

This study has demonstrated that hepcidin negatively regulates duodenal iron uptake by reducing *DMT1* expression. It was also demonstrated that hepcidin binds to the plasma membrane of placental cells in culture and in similarity to the duodenum reduces iron uptake. The mechanism by which hepcidin elicits this response is not known.

This study suggests that iron transfer in inhibited by hepcidin by reducing bbm uptake into the placental and duodenal epithelia, reducing the availably of iron for blm transfer. However, Nemeth *et al.* (2004) reversed this hypothesis in a study that demonstrated that hepcidin bound to Ireg1 and caused its internalisation, therefore reducing iron efflux. However this thesis demonstrated that in unpolarised BeWo cells, very little Ireg1 was present on the cell membrane (Chapter 3.6) and that hepcidin was bound but not taken up by these cells if incubated for 1 hour (Chapter 3.5.3). It is therefore necessary to determine the localisation of Ireg1 in polarised cells, and if present on the cellular membrane, to repeat the hepcidin localisation study in this polarised cell model.

Although hepcidin had no effect on iron efflux in BeWo cells a decrease in bbm iron uptake was observed. The study by Nemeth *et al.* (2004), suggests that a increase in hepcidin expression reduces iron uptake as reduced efflux increases cellular iron levels and reduces IRP activity/ *DMT1+ire/ Tfr1* expression and iron uptake. It is necessary to determine how hepcidin reduced placental iron uptake, DMT1/Tfr1 levels and localisation need to be quantified as do cellular iron levels.

DMT1, required for iron uptake is modulated by a number of factors. This study has demonstrated that DMT1a and DMT1b have specific subcellular localisations (Chapter 3.6) which may affect the activity of the mature protein. The regulation of these transcripts is not known. It will therefore be meaningful to quantitate these in cells treated with hepcidin and demonstrating decreased iron uptake, as it is possible that hepcidin may regulate the DMT1a:DMT1b ratio transcriptionally. In addition the localisation of the mature DMT1a/DMT1b proteins to the plasma membrane and to cytoplasmic vesicles may modulate the function of the epithelial for the uptake of Fe_2-Tf or NTBI.

The compartment to which DMT1 localised in BeWo cells was not identified in this study, neither was that of Ireg1, these could be identified using the techniques described in chapter 3.6. These studies also need to confirmed in placental biopsies. This would be additionally useful if tested throughout gestation and may reveal the optimisation mechanisms of placental iron transfer as pregnancy progresses.

5 Bibliography

Abboud, S. & Haile, D. J. (2000). A novel mammalian iron-regulated protein involved in intracellular iron metabolism. *J.Biol.Chem.* **275**, 19906-19912.

Adams, P. C., Barbin. , Y. P., Khan, Z. A., & Chakrabarti, S. (2003). Expression of ferroportin in hemochromatosis liver *Blood Cells Mol.Dis.* **31**, 256-261.

Aisen, P., Brown, E.B. (1975). Structure and function of trasferrin. Prog Hematol. **9**, 25-56.

Akesson, A., Bjellerup, P., Berglund, M., Bremme, K., & Vahter, M. (2002). Soluble transferrin receptor: longitudinal assessment from pregnancy to postlactation. *Obstet.Gynecol.* **99**, 260-266.

Alberts, B., Bray, D., Raff, M., Roberts, K., & Watson, J. D. (1989). Differentiated Cells and the Maintenance of Tissues. The Molecular Biology of the Cell pp. 961-961. Garland Publishing, Inc., New York

Aldieri, E., Ghigo, D., Tomatis, M., Prandi, L., Fenoglio, I., Costamagna, C., Pescarmona, G., Bosia, A., & Fubini, B. (2001). Iron inhibits the nitric oxide synthesis elicited by asbestos in murine macrophages. *Free Radic.Biol.Med.* **31**, 412-417.

Allen, L. H. (2000). Anemia and iron deficiency: effects on pregnancy outcome. *Am. J. Clin. Nutr.* **71**, 1280S-1284S.

American Institute of Nutrition (1980). Second report of the *ad hoc* committee on standards for nutritional studies. *J.Nutr.* **110**, 741-744.

Anaokar, S. G. & Garry, P. J. (1981). Effects of maternal iron nutrition during lactation on milk iron and rat neonatal iron status. *Am. J.Clin.Nutr.* **34**, 1505-1512.

Anderson, B. F., Baker, H. M., Norris, G. E., Rice, D. W., & Baker, E. N. (1989). Structure of human lactoferrin: crystallographic structure analysis and refinement at 2.8 A resolution. *J.Mol.Biol.* **209**, 711-734.

Anderson, G. J., Frazer, D. M., McKie, A. T., Wilkins, S. J., & Vulpe, C. D. (2002a). The expression and regulation of the iron transport molecules hephaestin and IREG1: implications for the control of iron export from the small intestine. *Cell Biochem.Biophys.* **36**, 137-146.

Anderson, G. J., Frazer, D. M., Wilkins, S. J., Becker, E. M., Millard, K. N., Murphy, T. L., McKie, A. T., & Vulpe, C. D. (2002b). Relationship between intestinal iron-transporter expression, hepatic hepcidin levels and the control of iron absorption. *Biochem.Soc.Trans.* **30**, 724-726.

Andreu, D. & Rivas, L. (1998). Animal antimicrobial peptides: an overview. *Biopolymers* **47**, 415-433.

Andrews, N. C. (1999). Disorders of iron metabolism. *N.Engl.J.Med.* **341**, 1986-1995.

Arden, K. E., Wallace, D. F., Dixon, J. L., Summerville, L., Searle, J. W., Anderson, G. J., Ramm, G. A., Powell, L. W., & Subramaniam, V. N. (2003). A novel mutation in ferroportin1 is associated with haemochromatosis in a Solomon Islands patient. *Gut* **52**, 1215-1217.

Arosio, P., Adelman, T. G., & Drysdale, J. W. (1978). On ferritin heterogeneity. Further evidence for heteropolymers. *J.Biol.Chem.* **253**, 4451-4458.

Bacon, B. R., Olynyk, J. K., Brunt, E. M., Britton, R. S., & Wolff, R. K. (1999). HFE genotype in patients with hemochromatosis and other liver diseases. *Ann.Intern.Med.* **130**, 953-962.

Bahram, S., Gilfillan, S., Kuhn, L. C., Moret, R., Schulze, J. B., Lebeau, A., & Schumann, K. (1999). Experimental hemochromatosis due to MHC class I HFE deficiency: Immune status and iron metabolism. *Proc. Nat. Acad. Sci.U.S.A.* **96**, 13312-13317.

Bailey, S., Evans, R. W., Garratt, R. C., Gorinsky, B., Hasnain, S., Horsburgh, C., Jhoti, H., Lindley, P. F., Mydin, A., Sarra, R., & *Watson J.* (1988). Molecular structure of serum transferrin at 3.3-A resolution. *Biochemistry* **27**, 5804-5812.

Baker, E., van Bockxmeer, F. M., & Morgan, E. H. (1983). Distribution of transferrin and transferrin receptors in the rabbit placenta. *Q.J.Exp.Physiol* **68**, 359-372.

Bannerman, R. M. (1976). Genetic defects of iron transport. *Fed.Proc.* **35**, 2281-2285.

Bany, B. M., Harvey, M. B., & Schultz, G. A. (2000). Expression of matrix metalloproteinases 2 and 9 in the mouse uterus during implantation and oil-induced decidualization. *J.Reprod.Fertil.* **120**, 125-134.

Barisani, D. & Conte, D. (2002). Transferrin receptor 1 (TfR1) and putative stimulator of Fe transport (SFT) expression in iron deficiency and overload: an overview. *Blood Cells Mol.Dis.* **29**, 498-505.

Batey, R. G. & Gallagher, N. D. (1977). Role of the placenta in intestinal absorption of iron in pregnant rats. *Gastroenterology* **72**, 255-259.

Bechensteen, A. G. & Halvorsen, S. (1996). Parenteral iron increases serum erythropoietin concentration during the "early anaemia' of 10-20-day-old mice. *Br.J.Haematol.* **94**, 529-532.

Beguin, Y., Lipscei, G., Thoumsin, H., & Fillet, G. (1991). Blunted erythropoietin production and decreased erythropoiesis in early pregnancy. *Blood* **78**, 89-93.

Beinert, H. & Kennedy, M. C. (1993). Aconitase, a two-faced protein: enzyme and iron regulatory factor. *FASEB J.* **7**, 1442-1449.

Benito, P., House, W., & Miller, D. (1998). Comparison of oral and intraperitoneal iron supplementation in anaemic rats: a re-evaluation of the mucosal block theory of iron absorption. *Br.J.Nutr.* **79**, 533-540.

Benyo, D. F., Miles, T. M., & Conrad, K. P. (1997). Hypoxia stimulates cytokine production by villous explants from the human placenta. *J.Clin.Endocrinol.Metab* **82**, 1582-1588.

Bergamaschi, G., Bergamaschi, P., Carlevati, S., & Cazzola, M. (1990). Transferrin receptor expression in the human placenta. *Haematologica* **75**, 220-223.

Bernstein, S. E. (1987). Hereditary hypotransferrinemia with hemosiderosis, a murine disorder resembling human atransferrinemia. *J.Lab Clin.Med.* **110**, 690-705.

Bianco, I., Mastropietro, F., D'Asero, C., Graziani, B., Piergrossi, P., Mezzabotta, M., & Modiano, G. (2000). Serum levels of erythropoietin and soluble transferrin receptor in the course of pregnancy in non beta thalassemic and beta thalassemic women. *Haematologica* **85**, 902-907.

Bierings, M. B., Baert, M. R., van Eijk, H. G., & van Dijk, J. P. (1991). Transferrin receptor expression and the regulation of placental iron uptake. *Mol.Cell Biochem.* **100**, 31-38.

Bingle, C. D., Kelly, F., Epstein, O., & Srai, S. K. (1992). Induction of hepatic and pulmonary caeruloplasmin gene expression in developing guinea pigs following premature delivery. *Biochim.Biophys.Acta* **1139**, 217-221.

Blanchard, K. L., Acquaviva, A. M., Galson, D. L., & Bunn, H. F. (1992). Hypoxic induction of the human erythropoietin gene: cooperation between the promoter and enhancer, each of which contains steroid receptor response elements. *Mol.Cell Biol.* **12**, 5373-5385.

Blot, I., Papiernik, E., Kaltwasser, J. P., Werner, E., & Tchernia, G. (1981). Influence of routine administration of folic acid and iron during pregnancy. *Gynecol.Obstet.Invest* **12**, 294-304.

Bomford, A. & Williams, R. (1976). Long term results of venesection therapy in idiopathic haemochromatosis. *Q.J.Med.* **45**, 611-623.

Bonnar, J. & Goldberg, A. (1969). The assessment of iron deficiency in pregnancy. *Scott.Med.J.* **14**, 209-214.

Boockfor, F. R., Harris, S. E., Barto, J. M., & Bonner, J. M. (1994). Placental cell release of transferrin: analysis by reverse haemolytic plaque assay. *Placenta* **15**, 501-509.

Bothwell, T. H., Charlton, R. W., Cook, J. E., & Finch, C. A. (1979b). Iron Metabolism in Man pp. 256-283. Blackwell Publishing, Oxford.

Bothwell, T. H. (2000). Iron requirements in pregnancy and strategies to meet them. *Am.J.Clin.Nutr.* **72**, 257S-264S.

Breuer, W., Ronson, A., Slotki, I. N., Abramov, A., Hershko, C., & Cabantchik, Z. I. (2000). The assessment of serum nontransferrin-bound iron in chelation therapy and iron supplementation. *Blood* **95**, 2975-2982.

Bridle, K. R., Frazer, D. M., Wilkins, S. J., Dixon, J. L., Purdie, D. M., Crawford, D. H., Subramaniam, V. N., Powell, L. W., Anderson, G. J., & Ramm, G. A. (2003). Disrupted hepcidin regulation in HFE-associated haemochromatosis and the liver as a regulator of body iron homoeostasis. *Lancet* **361**, 669-673.

Brown, P. J., Molloy, C. M., & Johnson, P. M. (1982). Transferrin receptor affinity and iron transport in the human placenta. *Placenta* **3**, 21-28.

Brune, M., Rossander-Hulten, L., Hallberg, L., Gleerup, A., & Sandberg, A. S. (1992). Iron absorption from bread in humans: inhibiting effects of cereal fiber, phytate and inositol phosphates with different numbers of phosphate groups. *J.Nutr.* **122**, 442-449.

Brune, M., Rossander, L., & Hallberg, L. (1989). Iron absorption and phenolic compounds: importance of different phenolic structures. *Eur.J.Clin.Nutr.* **43**, 547-557.

Burdett, K. & Reek, C. (1979). Adaptation of the small intestine during pregnancy and lactation in the rat. *Biochem.J.* **184**, 245-251.

Burns, J. & Paterson, C. R. (1993). Effect of iron-folate supplementation on serum copper concentration in late pregnancy. *Acta Obstet.Gynecol.Scand.* **72**, 616-618.

Butt, J., Kim, H. Y., Basilion, J. P., Cohen, S., Iwai, K., Philpott, C. C., Altschul, S., Klausner, R. D., & Rouault, T. A. (1996). Differences in the RNA binding sites of iron regulatory proteins and potential target diversity. *Proc.Natl.Acad.Sci.U.S.A* **93**, 4345-4349.

Buytaert, G., Wallenburg, H. C., van Eijck, H. G., & Buytaert, P. (1983). Iron supplementation during pregnancy. *Eur.J.Obstet.Gynecol.Reprod.Biol.* **15**, 11-16.

Byrnes, V., Barrett, S., Ryan, E., Kelleher, T., O'Keane, C., Coughlan, B., & Crowe, J. (2002). Increased duodenal DMT-1 expression and unchanged HFE mRNA levels in HFE-associated hereditary hemochromatosis and iron deficiency. *Blood Cells Mol.Dis.* **29**, 251-260.

Camaschella, C., Roetto, A., Cali, A., De Gobbi, M., Garozzo, G., Carella, M., Majorano, N., Totaro, A., & Gasparini, P. (2000). The gene TFR2 is mutated in a new type of haemochromatosis mapping to 7q22. *Nat.Genet.* **25**, 14-15.

Canonne-Hergaux, F., Fleming, M. D., Levy, J. E., Gauthier, S., Ralph, T., Picard, V., Andrews, N. C., & Gros, P. (2000). The Nramp2/DMT1 iron transporter is induced in the duodenum of microcytic anemia mk mice but is not properly targeted to the intestinal brush border. *Blood* **96**, 3964-3970.

Canonne-Hergaux, F., Gruenheid, S., Ponka, P., & Gros, P. (1999). Cellular and subcellular localisation of the Nramp2 iron transporter in the intestinal brush border and regulation by dietary iron. *Blood* **93**, 4406-4417.

Canonne-Hergaux, F., Zhang, A. S., Ponka, P., & Gros, P. (2001). Characterization of the iron transporter DMT1 (NRAMP2/DCT1) in red blood cells of normal and anemic mk/mk mice. *Blood* **98**, 3823-3830.

Casey, J. L., Hentze, M. W., Koeller, D. M., Caughman, S. W., Rouault, T. A., Klausner, R. D., & Harford, J. B. (1988). Iron-responsive elements: regulatory RNA sequences that control mRNA levels and translation. *Science* **240**, 924-928.

Casey, J. L., Koeller, D. M., Ramin, V. C., Klausner, R. D., & Harford, J. B. (1989). Iron regulation of transferrin receptor mRNA levels requires iron-responsive elements and a rapid turnover determinant in the 3' untranslated region of the mRNA. *EMBO J.* **8**, 3693-3699.

Cavell, P. A. & Widdowson, E. M. (1964). Intakes and Excretions of Iron, Copper, and Zinc in the neonatal period. *Arch.Dis.Child* **39**, 496-501.

Cazzola, M., Huebers, H. A., Sayers, M. H., MacPhail, A. P., Eng, M., & Finch, C. A. (1985). Transferrin saturation, plasma iron turnover, and transferrin uptake in normal humans. *Blood* **66**, 935-939.

Cerneus, D. P. & van der, E. A. (1991). Apical and basolateral transferrin receptors in polarized BeWo cells recycle through separate endosomes. *J.Cell Biol.* **114**, 1149-1158.

Cerneus, D. P., Strous, G. J., & van der, E. A. (1993). Bidirectional transcytosis determines the steady state distribution of the transferrin receptor at opposite plasma membrane domains of BeWo cells. *J.Cell Biol.* **122**, 1223-1230.

Chen, H., Su, T., Attieh, Z. K., Fox, T. C., McKie, A. T., Anderson, G. J., & Vulpe, C. D. (2003). Systemic regulation of Hephaestin and Ireg1 revealed in studies of genetic and nutritional iron deficiency. *Blood* **102**, 1893-1899.

Chen, H. L., Yang, Y. P., Hu, X. L., Yelavarthi, K. K., Fishback, J. L., & Hunt, J. S. (1991). Tumor necrosis factor alpha mRNA and protein are present in human placental and uterine cells at early and late stages of gestation. *Am.J.Pathol.* **139**, 327-335.

Cheng, H. & Leblond, C. P. (1974). Origin, differentiation and renewal of the four main epithelial cell types in the mouse small intestine. V. Unitarian Theory of the origin of the four epithelial cell types. *Am.J.Anat.* **141**, 537-561.

Cheng, Y., Zak, O., Aisen, P., Harrison, S. C., & Walz, T. (2004). Structure of the human transferrin receptor-transferrin complex. *Cell* **116**, 565-576.

Chmielnicka, J. & Sowa, B. (2000). Variations in metallothionein, Zn, Cu, and Fe concentrations and ceruloplasmin activity in pregnant rat dams and their fetuses. *Ecotoxicol.Environ.Saf* **46**, 130-136.

Chowrimootoo, G., Gillett, M., Debnam, E. S., Srai, S. K., & Epstein, O. (1992). Iron-transferrin binding to isolated guinea pig enterocytes and the regional localisation of intestinal iron transfer during ontogeny. *Biochim.Biophys.Acta* **1116**, 256-260.

Chua, A. C., Olynyk, J. K., Leedman, P. J., & Trinder, D. (2004). Nontransferrin-bound iron uptake by hepatocytes is increased in the Hfe knockout mouse model of hereditary hemochromatosis. *Blood* **104**, 1519-1525.

Clark, D. A. (1999b). Signaling at the fetomaternal interface. *Am J Reprod.Immunol.* **41**, 169-173.

Clark, D. A. (1999a). T cells in pregnancy: illusion and reality. *Am J Reprod.Immunol.* **41**, 233-238.

Collins, J. F., Franck, C. A., Kowdley, K. V., & Ghishan, F. K. (2005). Identification of Differentially Expressed Genes in Response to Dietary. *Am J Physiol Gastrointest.Liver Physiol.*

Conrad, K. P., Benyo, D. F., Westerhausen-Larsen, A., & Miles, T. M. (1996). Expression of erythropoietin by the human placenta. *FASEB J.* **10**, 760-768.

Conrad, M. E. & Barton, J. C. (1981). Factors affecting iron balance. *Am J Hematol.* **10**, 199-225.

Conrad, M. E. & Schade, S. G. (1968). Ascorbic acid chelates in iron absorption: a role for hydrochloric acid and bile. *Gastroenterology* **55**, 35-45.

Conrad, M. E., Umbreit, J. N., & Moore, E. G. (1991). A role for mucin in the absorption of inorganic iron and other metal cations. A study in rats. *Gastroenterology* **100**, 129-136.

Constable, A., Quick, S., Gray, N. K., & Hentze, M. W. (1992). Modulation of the RNA-binding activity of a regulatory protein by iron in vitro: switching between enzymatic and genetic function? *Proc.Natl.Acad.Sci.U.S.A* **89**, 4554-4558.

Contractor, S. F. & Eaton, B. M. (1986). Role of transferrin in iron transport between maternal and fetal circulations of a perfused lobule of human placenta. *Cell Biochem.Funct.* **4**, 69-74.

Cook, J. D., Barry, W. E., Hershko, C., Fillet, G., & Finch, C. A. (1973). Iron kinetics with emphasis on iron overload. *Am.J.Pathol.* **72**, 337-343.

Courselaud, B., Pigeon, C., Inoue, Y., Inoue, J., Gonzalez, F. J., Leroyer, P., Gilot, D., Boudjema, K., Guguen-Guillouzo, C., Brissot, P., Loreal, O., & Ilyin, G. (2002). C/EBPalpha regulates hepatic transcription of hepcidin, an antimicrobial peptide and regulator of iron metabolism. Cross-talk between C/EBP pathway and iron metabolism. *J.Biol.Chem.* **277**, 41163-41170.

Courselaud, B., Troadec, M. B., Fruchon, S., Ilyin, G., Borot, N., Leroyer, P., Coppin, H., Brissot, P., Roth, M. P., & Loreal, O. (2004). Strain and gender modulate hepatic hepcidin 1 and 2 mRNA expression in mice. *Blood Cells Mol.Dis.* **32**, 283-289.

Cox, T. C., Bawden, M. J., Martin, A., & May, B. K. (1991). Human erythroid 5-aminolevulinate synthase: promoter analysis and identification of an iron-responsive element in the mRNA. *EMBO J.* **10**, 1891-1902.

Cox, T. M. & Peters, T. J. (1978). Uptake of iron by duodenal biopsy specimens from patients with iron-deficiency anaemia and primary haemochromatosis. *Lancet* **1**, 123-124.

Cox, T. M. & Peters, T. J. (1979). The kinetics of iron uptake in vitro by human duodenal mucosa: studies in normal subjects. *J.Physiol.* **289**, 469-478.

Cranfield, L. M., Gollan, J. L., White, A. G., & Dormandy, T. L. (1979). Serum antioxidant activity in normal and abnormal subjects. *Ann.Clin.Biochem.* **16**, 299-306.

Cross, J. C. (2000). Genetic insights into trophoblast differentiation and placental morphogenesis. *Semin.Cell Dev.Biol.* **11**, 105-113.

Cross, J. C. (2003). The genetics of pre-eclampsia: a feto-placental or maternal problem? *Clin.Genet.* **64**, 96-103.

Crowe, C., Dandekar, P., Fox, M., Dhingra, K., Bennet, L., & Hanson, M. A. (1995). The effects of anaemia on heart, placenta and body weight, and blood pressure in fetal and neonatal rats. *J.Physiol.* **488**, 515-519.

Dallalio, G., Fleury, T., & Means, R. T. (2003). Serum hepcidin in clinical specimens. *Br.J.Haematol.* **122**, 996-1000.

Dandekar, T., Stripecke, R., Gray, N. K., Goossen, B., Constable, A., Johansson, H. E., & Hentze, M. W. (1991). Identification of a novel iron-responsive element in murine and human erythroid delta-aminolevulinic acid synthase mRNA. *EMBO J.* **10**, 1903-1909.

Daniel, W. A., Jr., Gaines, E. G., & Bennett, D. L. (1975). Iron intake and transferrin saturation in adolescents. *J.Pediatr.* **86**, 288-292.

Danzeisen, R., Fosset, C., Chariana, Z., Page, K., David, S., & McArdle, H. J. (2002). Placental ceruloplasmin homolog is regulated by iron and copper and is implicated in iron metabolism. *Am.J.Physiol. Cell Physiol.* **282**, C472-C478.

Danzeisen, R., Ponnambalam, S., Lea, R. G., Page, K., Gambling, L., & McArdle, H. J. (2000). The effect of ceruloplasmin on iron release from placental (BeWo) cells; evidence for an endogenous Cu oxidase. *Placenta* **21**, 805-812.

Dautry-Varsat, A., Ciechanover, A., & Lodish, H. F. (1983). pH and the recycling of transferrin during receptor-mediated endocytosis. *Proc.Natl.Acad.Sci.U.S.A* **80**, 2258-2262.

Davis, L. E., Widness, J. A., & Brace, R. A. (2003). Renal and placental secretion of erythropoietin during anemia or hypoxia in the ovine fetus. *Am.J.Obstet.Gynecol.* **189**, 1764-1770.

Dawson, E. B., Albers, J., & McGanity, W. J. (1989). Serum zinc changes due to iron supplementation in teen-age pregnancy. *Am. J.Clin. Nutr.* **50**, 848-852.

De Leeuw, N. K., Lowenstein, L., & Hsieh, Y. S. (1966). Iron deficiency and hydremia in normal pregnancy. *Medicine (Baltimore)* **45**, 291-315.

Dealtry, G. B., O'Farrell, M. K., & Fernandez, N. (2000). The Th2 cytokine environment of the placenta. *Int.Arch.Allergy Immunol.* **123**, 107-119.

Debnam, E. S., Srai, S. K., Chowrimootoo, G., & Epstein, O. (1991). Ontogeny of iron uptake across brush border membrane of guinea pig duodenum and its autoradiographic localisation. *Biol.Neonate* **59**, 30-36.

DeMaeyer, E. Preventing and controlling inron deficiency anaemia through primary health care. 1989. World Health Organisation, Geneva, Switzerland.

DeMaeyer, E. & Adiels-Tegman, M. (1985). The prevalence of anaemia in the world. *World Health Stat.Q.* **38**, 302-316.

Derman, D., Sayers, M., Lynch, S. R., Charlton, R. W., Bothwell, T. H., & Mayet, F. (1977). Iron absorption from a cereal-based meal containing cane sugar fortified with ascorbic acid. *Br.J.Nutr.* **38**, 261-269.

Dhungana, S., Taboy, C. H., Zak, O., Larvie, M., Crumbliss, A. L., & Aisen, P. (2004). Redox properties of human transferrin bound to its receptor. *Biochemistry* **43**, 205-209.

Disler, P. B., Lynch, S. R., Charlton, R. W., Torrance, J. D., Bothwell, T. H., Walker, R. B., & Mayet, F. (1975). The effect of tea on iron absorption. *Gut* **16**, 193-200.

Dommisse, J., Bell, D. J., Du Toit, E. D., Midgley, V., & Cohen, M. (1983). Iron-storage deficiency and iron supplementation in pregnancy. *S.Afr.Med.J.* **64**, 1047-1051.

Donovan, A., Brownlie, A., Zhou, Y., Shepard, J., Pratt, S. J., Moynihan, J., Paw, B. H., Drejer, A., Barut, B., Zapata, A., Law, T. C., Brugnara, C., Lux, S. E., Pinkus, G. S., Pinkus, J. L., Kingsley, P. D., Palis, J., Fleming, M. D., Andrews, N. C., & Zon, L. I. (2000). Positional cloning of zebrafish ferroportin1 identifies a conserved vertebrate iron exporter. *Nature* **403**, 776-781.

Downs, K. M. (2002). Early placental ontogeny in the mouse. *Placenta* **23**, 116-131.

Dube, S., Fisher, J. W., & Powell, J. S. (1988). Glycosylation at specific sites of erythropoietin is essential for biosynthesis, secretion, and biological function. *J.Biol.Chem.* **263**, 17516-17521.

Dupic, F., Fruchon, S., Bensaid, M., Borot, N., Radosavljevic, M., Loreal, O., Brissot, P., Gilfillan, S., Bahram, S., Coppin, H., & Roth, M. P. (2002). Inactivation of the hemochromatosis gene differentially regulates duodenal expression of iron-related mRNAs between mouse strains. *Gastroenterology* **122**, 745-751.

Duthie, H. L. (1964). The relative importance of the duodenum in the intestinal absorption of iron. *Br.J.Haematol.* **10**, 59-68.

Edwards, J. A., Hoke, J. E., Mattioli, M., & Reichlin, M. (1977). Ferritin distribution and synthesis in sex-linked anemia. *J.Lab Clin.Med.* **90**, 68-76.

Eide, D., Broderius, M., Fett, J., & Guerinot, M. L. (1996). A novel iron-regulated metal transporter from plants identified by functional expression in yeast. *Proc.Natl.Acad.Sci.U.S.A* **93**, 5624-5628.

Enns, C. A. (2002). In Molecular and Cellular Iron Transport, ed. Templeton, D. M., pp. 71-94. Marcel Dekker, New York.

European Communities. Nutrient and energy intakes for the European Community EG-report. Brussels Luxembourg: Commission of the European Communities. 1993.

Fairchild, B. D. & Conrad, K. P. (1999). Expression of the erythropoietin receptor by trophoblast cellsin the human placenta. *Biol.Reprod.* **60**, 861-870.

Faulk, W. P. & Galbraith, G. M. (1979). Trophoblast transferrin and transferrin receptors in the host--parasite relationship of human pregnancy. *Proc.R.Soc.Lond. Biol.Sci.* **204** , 83-97.

Feder, J. N., Gnirke, A., Thomas, W., Tsuchihashi, Z., Ruddy, D. A., Basava, A., Dormishian, F., Domingo, R., Jr., Ellis, M. C., Fullan, A., Hinton, L. M., Jones, N. L., Kimmel, B. E., Kronmal, G. S., Lauer, P., Lee, V. K., Loeb, D. B., Mapa, F. A., McClelland, E., Meyer, N. C., Mintier, G. A., Moeller, N., Moore, T., Morikang, E., Wolff, R. K., & . (1996). A novel MHC class I-like gene is mutated in patients with hereditary haemochromatosis. *Nat.Genet.* **13**, 399-408.

Feder, J. N., Penny, D. M., Irrinki, A., Lee, V. K., Lebron, J. A., Watson, N., Tsuchihashi, Z., Sigal, E., Bjorkman, P. J., & Schatzman, R. C. (1998). The hemochromatosis gene product complexes with the transferrin receptor and lowers its affinity for ligand binding. *Proc.Natl.Acad.Sci.U.S.A* **95**, 1472-1477.

Feder, J. N., Tsuchihashi, Z., Irrinki, A., Lee, V. K., Mapa, F. A., Morikang, E., Prass, C. E., Starnes, S. M., Wolff, R. K., Parkkila, S., Sly, W. S., & Schatzman, R. C. (1997). The hemochromatosis founder mutation in HLA-H disrupts beta2-microglobulin interaction and cell surface expression. *J.Biol.Chem.* **272**, 14025-14028.

Finch, C. (1994). Regulators of iron balance in humans. *Blood* **84**, 1697-1702.

Finch, C. A., Huebers, H. A., Miller, L. R., Josephson, B. M., Shepard, T. H., & Mackler, B. (1983). Fetal iron balance in the rat. *Am.J.Clin.Nutr.* **37**, 910-917.

Fitch, C. A., Song, Y., & Levenson, C. W. (1999). Developmental regulation of hepatic ceruloplasmin mRNA and serum activity by exogenous thyroxine and dexamethasone. *Proc.Soc.Exp.Biol.Med.* **221**, 27-31.

Fleming, M. D., Romano, M. A., Su, M. A., Garrick, L. M., Garrick, M. D., & Andrews, N. C. (1998). Nramp2 is mutated in the anemic Belgrade (b) rat: evidence of a role for Nramp2 in endosomal iron transport. *Proc.Natl.Acad.Sci.U.S.A* **95**, 1148-1153.

Fleming, M. D., Trenor, C. C., III, Su, M. A., Foernzler, D., Beier, D. R., Dietrich, W. F., & Andrews, N. C. (1997). Microcytic anaemia mice have a mutation in Nramp2, a candidate iron transporter gene. *Nat.Genet.* **16**, 383-386.

Fleming, P. J. & Kent, U. M. (1991). Cytochrome b561, ascorbic acid, and transmembrane electron transfer. *Am.J.Clin.Nutr.* **54**, 1173S-1178S.

Fleming, R. E., Ahmann, J. R., Migas, M. C., Waheed, A., Koeffler, H. P., Kawabata, H., Britton, R. S., Bacon, B. R., & Sly, W. S. (2002). Targeted mutagenesis of the murine transferrin receptor-2 gene produces hemochromatosis. *Proc.Natl.Acad.Sci.U.S.A* **99**, 10653-10658.

Fleming, R. E., Holden, C. C., Tomatsu, S., Waheed, A., Brunt, E. M., Britton, R. S., Bacon, B. R., Roopenian, D. C., & Sly, W. S. (2001). Mouse strain differences determine severity of iron accumulation in Hfe knockout model of hereditary hemochromatosis. *Proc.Natl.Acad.Sci.U.S.A* **98**, 2707-2711.

Fleming, R. E., Migas, M. C., Holden, C. C., Waheed, A., Britton, R. S., Tomatsu, S., Bacon, B. R., & Sly, W. S. (2000). Transferrin receptor 2: continued expression in mouse liver in the face of iron overload and in hereditary hemochromatosis. *Proc.Natl.Acad.Sci.U.S.A* **97**, 2214-2219.

Fleming, R. E., Migas, M. C., Zhou, X., Jiang, J., Britton, R. S., Brunt, E. M., Tomatsu, S., Waheed, A., Bacon, B. R., & Sly, W. S. (1999). Mechanism of increased iron absorption in murine model of hereditary hemochromatosis: increased duodenal expression of the iron transporter DMT1. *Proc.Natl.Acad.Sci.U.S.A* **96**, 3143-3148.

Frazer, D. M. & Anderson, G. J. (2003). The orchestration of body iron intake: how and where do enterocytes receive their cues? *Blood Cells Mol.Dis.* **30**, 288-297.

Frazer, D. M., Vulpe, C. D., McKie, A. T., Wilkins, S. J., Trinder, D., Cleghorn, G. J., & Anderson, G. J. (2001). Cloning and gastrointestinal expression of rat hephaestin: relationship to other iron transport proteins. *Am.J.Physiol Gastrointest.Liver Physiol* **281**, G931-G939.

Frazer, D. M., Wilkins, S. J., Becker, E. M., Murphy, T. L., Vulpe, C. D., McKie, A. T., & Anderson, G. J. (2003). A rapid decrease in the expression of DMT1 and Dcytb but not Ireg1 or hephaestin explains the mucosal block phenomenon of iron absorption. *Gut* **52**, 340-346.

Frazer, D. M., Wilkins, S. J., Becker, E. M., Vulpe, C. D., McKie, A. T., Trinder, D., & Anderson, G. J. (2002). Hepcidin expression inversely correlates with the expression of duodenal iron transporters and iron absorption in rats. *Gastroenterology* **123**, 835-844.

Frederiksen, M. C. (2001). Physiologic changes in pregnancy and their effect on drug disposition. *Semin.Perinatol.* **25**, 120-123.

Fridovich, I. (1979). Hypoxia and oxygen toxicity. *Adv.Neurol.* **26**, 255-259.

Frieden, E. & Hsieh, H. S. (1976). The biological role of ceruloplasmin and its oxidase activity. *Adv.Exp.Med.Biol.* **74**, 505-529.

Friedman, S. J. & Skehan, P. (1979). Morphological differentiation of human choriocarcinoma cells induced by methotrexate. *Cancer Res.* **39**, 1960-1967.

Galbraith, G. M., Galbraith, R. M., Temple, A., & Faulk, W. P. (1980). Demonstration of transferrin receptors on human placental trophoblast. *Blood* **55**, 240-242.

Galbraith, R. M. & Galbraith, G. M. (1981). Expression of transferrin receptors on mitogen-stimulated human peripheral blood lymphocytes: relation to cellular activation and related metabolic events. *Immunology* **44**, 703-710.

Gambling, L., Charania, Z., Hannah, L., Antipatis, C., Lea, R. G., & McArdle, H. J. (2002). Effect of iron deficiency on placental cytokine expression and fetal growth in the pregnant rat. *Biol.Reprod.* **66**, 516-523.

Gambling, L., Danzeisen, R., Gair, S., Lea, R. G., Charania, Z., Solanky, N., Joory, K. D., Srai, S. K., & McArdle, H. J. (2001). Effect of iron deficiency on placental transfer of iron and expression of iron transport proteins in vivo and in vitro. *Biochem.J* **356**, 883-889.

Gambling, L., Dunford, S., Wallace, D. I., Zuur, G., Solanky, N., Srai, S. K., & McArdle, H. J. (2003). Iron deficiency during pregnancy affects postnatal blood pressure in the rat. *J.Physiol.* **552**, 603-610.

Ganz, T. (1999). Defensins and host defense. *Science* **286**, 420-421.

Ganz, T. & Lehrer, R. I. (1995). Defensins. *Pharmacol.Ther.* **66**, 191-205.

Garn, S. M., Ridella, S. A., Petzold, A. S., & Falkner, F. (1981). Maternal hematologic levels and pregnancy outcomes. *Semin.Perinatol.* **5**, 155-162.

Gavrieli, Y., Sherman, Y., & Ben Sasson, S. A. (1992). Identification of programmed cell death in situ via specific labeling of nuclear DNA fragmentation. *J.Cell Biol.* **119**, 493-501.

Gehrke, S. G., Kulaksiz, H., Herrmann, T., Riedel, H. D., Bents, K., Veltkamp, C., & Stremmel, W. (2003). Expression of hepcidin in hereditary hemochromatosis: evidence for a regulation in response to the serum transferrin saturation and to non-transferrin-bound iron. *Blood* **102**, 371-376.

Georgieff, M. K., Berry, S. A., Wobken, J. D., & Leibold, E. A. (1999). Increased placental iron regulatory protein-1 expression in diabetic pregnancies complicated by fetal iron deficiency. *Placenta* **20**, 87-93.

Georgieff, M. K., Wobken, J. K., Welle, J., Burdo, J. R., & Connor, J. R. (2000). Identification and localisation of divalent metal transporter-1 (DMT-1) in term human placenta. *Placenta* **21**, 799-804.

Gillooly, M., Bothwell, T. H., Torrance, J. D., MacPhail, A. P., Derman, D. P., Bezwoda, W. R., Mills, W., Charlton, R. W., & Mayet, F. (1983). The effects of organic acids, phytates and polyphenols on the absorption of iron from vegetables. *Br.J.Nutr.* **49**, 331-342.

Godfrey, K., Robinson, S., Barker, D. J., Osmond, C., & Cox, V. (1996). Maternal nutrition in early and late pregnancy in relation to placental and fetal growth. *BMJ* **312**, 410-414.

Godfrey, K. M. & Barker, D. J. (1995). Maternal nutrition in relation to fetal and placental growth. *Eur.J.Obstet.Gynecol.Reprod.Biol.* **61**, 15-22.

Goya, N., Miyazaki, S., Kodate, S., & Ushio, B. (1972). A family of congenital atransferrinemia. *Blood* **40**, 239-245.

Griffiths, E. A., Duffy, L. C., Schanbacher, F. L., Dryja, D., Leavens, A., Neiswander, R. L., Qiao, H., DiRienzo, D., & Ogra, P. (2003). In vitro growth responses of bifidobacteria and enteropathogens to bovine and human lactoferrin. *Dig.Dis.Sci.* **48**, 1324-1332.

Griffiths, W. J., Kelly, A. L., Smith, S. J., & Cox, T. M. (2000). Localisation of iron transport and regulatory proteins in human cells. *QJM.* **93**, 575-587.

Gruenheid, S., Canonne-Hergaux, F., Gauthier, S., Hackam, D. J., Grinstein, S., & Gros, P. (1999). The iron transport protein NRAMP2 is an integral membrane glycoprotein that colocalises with transferrin in recycling endosomes. *J.Exp.Med.* **189**, 831-841.

Gruenheid, S., Cellier, M., Vidal, S., & Gros, P. (1995). Identification and characterization of a second mouse Nramp gene. *Genomics* **25**, 514-525.

Guillemot, F., Nagy, A., Auerbach, A., Rossant, J., & Joyner, A. L. (1994). Essential role of Mash-2 in extraembryonic development. *Nature* **371**, 333-336.

Gunshin, H., Allerson, C. R., Polycarpou-Schwarz, M., Rofts, A., Rogers, J. T., Kishi, F., Hentze, M. W., Rouault, T. A., Andrews, N. C., & Hediger, M. A. (2001). Iron-dependent regulation of the divalent metal ion transporter. *FEBS Lett.* **509**, 309-316.

Gunshin, H., Mackenzie, B., Berger, U. V., Gunshin, Y., Romero, M. F., Boron, W. F., Nussberger, S., Gollan, J. L., & Hediger, M. A. (1997). Cloning and characterization of a mammalian proton-coupled metal-ion transporter. *Nature* **388**, 482-488.

Guo, B., Phillips, J. D., Yu, Y., & Leibold, E. A. (1995). Iron regulates the intracellular degradation of iron regulatory protein 2 by the proteasome. *J.Biol.Chem.* **270**, 21645-21651.

Hallberg, L. (1992). Iron requirements. Comments on methods and some crucial concepts in iron nutrition. *Biol.Trace Elem.Res.* **35**, 25-45.

Hallberg, L. (1998). Does calcium interfere with iron absorption? *Am.J.Clin.Nutr.* **68**, 3-4.

Hallberg, L., Brune, M., & Rossander, L. (1989). Iron absorption in man: ascorbic acid and dose-dependent inhibition by phytate. *Am.J.Clin.Nutr.* **49**, 140-144.

Hallberg, L. & Rossander, L. (1982). Effect of different drinks on the absorption of non-heme iron from composite meals. *Hum.Nutr.Appl.Nutr.* **36**, 116-123.

Hallquist, N. A., McNeil, L. K., Lockwood, J. F., & Sherman, A. R. (1992). Maternal-iron-deficiency effects on peritoneal macrophage and peritoneal natural-killer-cell cytotoxicity in rat pups. *Am.J.Clin.Nutr.* **55**, 741-746.

Hammond, K. A. (1997). Adaptation of the maternal intestine during lactation. *J.Mammary.Gland.Biol.Neoplasia.* **2**, 243-252.

Hanashi, H., Shiokawa, S., Akimoto, Y., Sakai, K., Sakai, K., Suzuki, N., Kabir-Salmani, M., Nagamatsu, S., Iwashita, M., & Nakamura, Y. (2003). Physiologic role of decidual beta1 integrin and focal adhesion kinase in embryonic implantation. *Endocr.J.* **50**, 189-198.

Hancock, R. E. (1997). Peptide antibiotics. *Lancet* **349**, 418-422.

Hanson, E. S., Foot, L. M., & Leibold, E. A. (1999). Hypoxia post-translationally activates iron-regulatory protein 2. *J.Biol.Chem.* **274**, 5047-5052.

Hanson, E. S. & Leibold, E. A. (1998). Regulation of iron regulatory protein 1 during hypoxia and hypoxia/reoxygenation. *J.Biol.Chem.* **273**, 7588-7593.

Haouari, M., Haouari-Oukerro, F., Alguemi, C., Nagati, K., Zouaghi, H., & Kamoun, A. (1994). Effects of oestradiol-17 beta on small intestine iron absorption and iron uptake into blood and liver. *Horm.Metab.Res.* **26**, 53-54.

Harris, Z. L., Takahashi, Y., Miyajima, H., Serizawa, M., MacGillivray, R. T., & Gitlin, J. D. (1995). Aceruloplasminemia: molecular characterization of this disorder of iron metabolism. *Proc.Natl.Acad.Sci.U.S.A* **92**, 2539-2543.

Harrison, P. M. & Arosio, P. (1996). The ferritins: molecular properties, iron storage function and cellular regulation. *Biochim.Biophys.Acta* **1275**, 161-203.

Harthoorn-Lasthuizen, E. J., Lindemans, J., & Langenhuijsen, M. M. (2001). Does iron-deficient erythropoiesis in pregnancy influence fetal iron supply? *Acta Obstet.Gynecol.Scand.* **80**, 392-396.

Hayashi, A., Wada, Y., Suzuki, T., & Shimizu, A. (1993). Studies on familial hypotransferrinemia: unique clinical course and molecular pathology. *Am.J.Hum.Genet.* **53**, 201-213.

Heinrich, H. C. (1975). Deficiency and pathogenesis of iron deficiency. In Iron Metabolism and its Disorders, ed. Kief, H. Excerpta Medica., Amsterdam.

Hemberger, M. & Cross, J. C. (2001). Genes governing placental development. *Trends Endocrinol.Metab* **12**, 162-168.

Henderson, B. R., Seiser, C., & Kuhn, L. C. (1993). Characterization of a second RNA-binding protein in rodents with specificity for iron-responsive elements. *J.Biol.Chem.* **268**, 27327-27334.

Hentze, M. W., Caughman, S. W., Rouault, T. A., Barriocanal, J. G., Dancis, A., Harford, J. B., & Klausner, R. D. (1987). Identification of the iron-responsive element for the translational regulation of human ferritin mRNA. *Science* **238**, 1570-1573.

Herrmann, T., Muckenthaler, M., Van Der, H. F., Brennan, K., Gehrke, S. G., Hubert, N., Sergi, C., Grone, H. J., Kaiser, I., Gosch, I., Volkmann, M., Riedel, H. D., Hentze, M. W., Stewart, A. F., & Stremmel, W. (2004). Iron overload in adult Hfe-deficient mice independent of changes in the steady-state expression of the duodenal iron transporters DMT1 and Ireg1/ferroportin. *J.Mol.Med.* **82**, 39-48.

Hoffman, M. A., Ohh, M., Yang, H., Klco, J. M., Ivan, M., & Kaelin, W. G., Jr. (2001). von Hippel-Lindau protein mutants linked to type 2C VHL disease preserve the ability to downregulate HIF. *Hum.Mol.Genet.* **10**, 1019-1027.

Howells, M. R., Jones, S. E., Napier, J. A., Saunders, K., & Cavill, I. (1986). Erythropoiesis in pregnancy. *Br.J.Haematol.* **64**, 595-599.

Huang, A., Zhang, R., & Yang, Z. (2001). Quantitative (stereological) study of placental structures in women with pregnancy iron-deficiency anemia. *Eur.J.Obstet.Gynecol.Reprod.Biol.* **97**, 59-64.

Huang, L. E., Ho, V., Arany, Z., Krainc, D., Galson, D., Tendler, D., Livingston, D. M., & Bunn, H. F. (1997). Erythropoietin gene regulation depends on heme-dependent oxygen sensing and assembly of interacting transcription factors. *Kidney Int.* **51**, 548-552.

Huang, T. S., Melefors, O., Lind, M. I., & Soderhall, K. (1999). An atypical iron-responsive element (IRE) within crayfish ferritin mRNA and an iron regulatory protein 1 (IRP1)-like protein from crayfish hepatopancreas. *Insect Biochem.Mol.Biol.* **29**, 1-9.

Hubert, N. & Hentze, M. W. (2002). Previously uncharacterized isoforms of divalent metal transporter (DMT)-1: implications for regulation and cellular function. *Proc.Natl.Acad.Sci.U.S.A* **99**, 12345-12350.

Huebers, H., Huebers, E., Csiba, E., & Finch, C. A. (1978). Iron uptake from rat plasma transferrin by rat reticulocytes. *J.Clin.Invest* **62**, 944-951.

Hunter, H. N., Fulton, D. B., Ganz, T., & Vogel, H. J. (2002). The solution structure of human hepcidin, a peptide hormone with antimicrobial activity that is involved in iron uptake and hereditary hemochromatosis. *J.Biol.Chem.* **277**, 37597-37603.

Iacopetta, B. J., Morgan, E. H., & Yeoh, G. C. (1982). Transferrin receptors and iron uptake during erythroid cell development. *Biochim.Biophys.Acta* **687**, 204-210.

Ilyin, G., Courselaud, B., Troadec, M. B., Pigeon, C., Alizadeh, M., Leroyer, P., Brissot, P., & Loreal, O. (2003). Comparative analysis of mouse hepcidin 1 and 2 genes: evidence for different patterns of expression and co-inducibility during iron overload. *FEBS Lett.* **542**, 22-26.

Isaka, K., Usuda, S., Ito, H., Sagawa, Y., Nakamura, H., Nishi, H., Suzuki, Y., Li, Y. F., & Takayama, M. (2003). Expression and activity of matrix metalloproteinase 2 and 9 in human trophoblasts. *Placenta* **24**, 53-64.

Ito, E. & Terao, K. (1994). Injury and recovery process of intestine caused by okadaic acid and related compounds. *Nat.Toxins.* **2**, 371-377.

Ivan, M., Kondo, K., Yang, H., Kim, W., Valiando, J., Ohh, M., Salic, A., Asara, J. M., Lane, W. S., & Kaelin, W. G., Jr. (2001). HIFalpha targeted for VHL-mediated destruction by proline hydroxylation: implications for O2 sensing. *Science* **292**, 464-468.

Jacobson, L. O., Goldwasser, E., Fried, W., & Plzak, L. (1957). Role of the kidney in erythropoiesis. *Nature* **179**, 633-634.

Jameson, S. (1976). Refractory anaemia of pregnancy as an expression of zinc deficiency. *Acta Med.Scand.Suppl.* **593**, 65-76.

Johnson, D., Bayele, H., Johnston, K., Tennant, J., Srai, S. K., & Sharp, P. (2004). Tumour necrosis factor alpha regulates iron transport and transporter expression in human intestinal epithelial cells. *FEBS Lett.* **573**, 195-201.

Johnson, G., Jacobs, P., & Purves, L. R. (1983). Iron binding proteins of iron-absorbing rat intestinal mucosa. *J.Clin.Invest.* **71**, 1467-1476.

Johnson, M. B. & Enns, C. A. (2004). Diferric transferrin regulates transferrin receptor 2 protein stability. *Blood* **104**, 4287-4293.

Jordanov, J., Courtois-Verniquet, F., Neuburger, M., & Douce, R. (1992). Structural investigations by extended X-ray absorption fine structure spectroscopy of the iron center of mitochondrial aconitase in higher plant cells. *J.Biol.Chem.* **267**, 16775-16778.

Kameda, T., Matsuzaki, N., Sawai, K., Okada, T., Saji, F., Matsuda, T., Hirano, T., Kishimoto, T., & Tanizawa, O. (1990). Production of interleukin-6 by normal human trophoblast. *Placenta* **11**, 205-213.

Kanevsky, V. Y., Pozdnyakova, L. P., Katukov, V. Y., & Severin, S. E. (1997). Isolation of the transferrin receptor from human placenta. *Biochem.Mol.Biol.Int.* **42**, 309-314.

Kaptain, S., Downey, W. E., Tang, C., Philpott, C., Haile, D., Orloff, D. G., Harford, J. B., Rouault, T. A., & Klausner, R. D. (1991). A regulated RNA binding protein also possesses aconitase activity. *Proc.Natl.Acad.Sci.U.S.A.* **88**, 10109-10113.

Kawabata, H., Germain, R. S., Ikezoe, T., Tong, X., Green, E. M., Gombart, A. F., & Koeffler, H. P. (2001). Regulation of expression of murine transferrin receptor 2. *Blood* **98**, 1949-1954.

Kawabata, H., Germain, R. S., Vuong, P. T., Nakamaki, T., Said, J. W., & Koeffler, H. P. (2000). Transferrin receptor 2-alpha supports cell growth both in iron-chelated cultured cells and in vivo. *J.Biol.Chem.* **275**, 16618-16625.

Kawabata, H., Nakamaki, T., Ikonomi, P., Smith, R. D., Germain, R. S., & Koeffler, H. P. (2001b). Expression of transferrin receptor 2 in normal and neoplastic hematopoietic cells. *Blood* **98**, 2714-2719.

Kawabata, H., Yang, R., Hirama, T., Vuong, P. T., Kawano, S., Gombart, A. F., & Koeffler, H. P. (1999). Molecular cloning of transferrin receptor 2. A new member of the transferrin receptor-like family. *J.Biol.Chem.* **274**, 20826-20832.

Kelley-Loughnane, N., Sabla, G. E., Ley-Ebert, C., Aronow, B. J., & Bezerra, J. A. (2002). Independent and overlapping transcriptional activation during liver development and regeneration in mice. *Hepatology* **35**, 525-534.

Khatun, R., Wu, Y., Kanenishi, K., Ueno, M., Tanaka, S., Hata, T., & Sakamoto, H. (2003). Immunohistochemical study of transferrin receptor expression in the placenta of pre-eclamptic pregnancy. *Placenta* **24**, 870-876.

Killisch, I., Steinlein, P., Romisch, K., Hollinshead, R., Beug, H., & Griffiths, G. (1992). Characterization of early and late endocytic compartments of the transferrin cycle. Transferrin receptor antibody blocks erythroid differentiation by trapping the receptor in the early endosome. *J.Cell Sci.* **103**, 211-232.

Kim, M. J., Bogic, L., Cheung, C. Y., & Brace, R. A. (2001). Placental expression of erythropoietin mRNA, protein and receptor in sheep. *Placenta* **22**, 484-489.

King, B. F. (1976). Localisation of transferrin on the surface of the human placenta by electron microscopic immunocytochemistry. *Anat.Rec.* **186**, 151-159.

Knopfel, M. & Solioz, M. (2002). Characterization of a cytochrome b(558) ferric/cupric reductase from rabbit duodenal brush border membranes. *Biochem.Biophys.Res.Commun.* **291**, 220-225.

Kozma, M. M., Chowrimootoo, G., Debnam, E. S., Epstein, O., & Srai, S. K. (1994). Developmental changes in mucosal iron binding proteins in the guinea pig. Expression of transferrin, H and L ferritin and binding of iron to a low molecular weight protein. *Biochim.Biophys.Acta* **1201**, 229-234.

Kroos, M. J., Starreveld, J. S., Verrijt, C. E., van Eijk, H. G., & van Dijk, J. P. (1996). Regulation of transferrin receptor synthesis by human cytotrophoblast cells in culture. *Eur.J.Obstet.Gynecol.Reprod.Biol.* **65**, 231-234.

Kuhn, L. C. & Hentze, M. W. (1992). Coordination of cellular iron metabolism by post-transcriptional gene regulation. *J.Inorg.Biochem.* **47**, 183-195.

Kulaksiz, H., Gehrke, S. G., Janetzko, A., Rost, D., Bruckner, T., Kallinowski, B., & Stremmel, W. (2004). Pro-hepcidin: expression and cell specific localisation in the liver and its regulation in hereditary haemochromatosis, chronic renal insufficiency, and renal anaemia. *Gut* **53**, 735-743.

Kuo, Y. M., Su, T., Chen, H., Attieh, Z., Syed, B. A., McKie, A. T., Anderson, G. J., Gitschier, J., & Vulpe, C. D. (2004). Mislocalisation of hephaestin, a multicopper ferroxidase involved in basolateral intestinal iron transport, in the sex linked anaemia mouse. *Gut* **53**, 201-206.

Kvietikova, I., Wenger, R. H., Marti, H. H., & Gassmann, M. (1997). The hypoxia-inducible factor-1 DNA recognition site is cAMP-responsive. *Kidney Int.* **51**, 564-566.

Kwik-Uribe, C. L., Gietzen, D., German, J. B., Golub, M. S., & Keen, C. L. (2000). Chronic marginal iron intakes during early development in mice result in persistent changes in dopamine metabolism and myelin composition. *J.Nutr.* **130**, 2821-2830.

Laftah, A. H., Ramesh, B., Simpson, R. J., Solanky, N., Bahram, S., Schumann, K., Debnam, E. S., & Srai, S. K. (2004). Effect of hepcidin on intestinal iron absorption in mice. *Blood* **103**, 3940-3944.

Latunde-Dada, G. O., Van der, W. J., Vulpe, C. D., Anderson, G. J., Simpson, R. J., & McKie, A. T. (2002). Molecular and functional roles of duodenal cytochrome B (Dcytb) in iron metabolism. *Blood Cells Mol.Dis.* **29**, 356-360.

Latunde-Dada, G. O., Vulpe, C. D., Anderson, G. J., Simpson, R. J., & McKie, A. T. (2004). Tissue-specific changes in iron metabolism genes in mice following phenylhydrazine-induced haemolysis. *Biochim.Biophys.Acta* **1690**, 169-176.

Leazer, T. M., Liu, Y., & Klaassen, C. D. (2002). Cadmium absorption and its relationship to divalent metal transporter-1 in the pregnant rat. *Toxicol.Appl.Pharmacol.* **185**, 18-24.

Lebron, J. A., Bennett, M. J., Vaughn, D. E., Chirino, A. J., Snow, P. M., Mintier, G. A., Feder, J. N., & Bjorkman, P. J. (1998). Crystal structure of the hemochromatosis protein HFE and characterization of its interaction with transferrin receptor. *Cell* **93** , 111-123.

Lee, P. L., Gelbart, T., West, C., Halloran, C., & Beutler, E. (1998). The human Nramp2 gene: characterization of the gene structure, alternative splicing, promoter region and polymorphisms. *Blood Cells Mol.Dis.* **24**, 199-215.

Leitner, K., Ellinger, A., Zimmer, K. P., Ellinger, I., & Fuchs, R. (2002). Localisation of beta 2-microglobulin in the term villous syncytiotrophoblast. *Histochem.Cell Biol.* **117** , 187-193.

Leong, W. I., Bowlus, C. L., Tallkvist, J., & Lonnerdal, B. (2003). Iron supplementation during infancy--effects on expression of iron transporters, iron absorption, and iron utilisation in rat pups. *Am.J.Clin.Nutr.* **78**, 1203-1211.

Letendre, E. D. & Holbein, B. E. (1984). Ceruloplasmin and regulation of transferrin iron during Neisseria meningitidis infection in mice. *Infect.Immun.* **45**, 133-138.

Leventhal, B. & Stohlman, F., Jr. (1966). Regulation of erythropoiesis XVII: the determinants of red cell size in iron-deficiency states. *Pediatrics* **37**, 62-67.

Levi, S., Luzzago, A., Cesareni, G., Cozzi, A., Franceschinelli, F., Albertini, A., & Arosio, P. (1988). Mechanism of ferritin iron uptake: activity of the H-chain and deletion mapping of the ferro-oxidase site. A study of iron uptake and ferro-oxidase activity of human liver, recombinant H-chain ferritins, and of two H-chain deletion mutants. *J.Biol.Chem.* **263**, 18086-18092.

Levi, S., Santambrogio, P., Cozzi, A., Rovida, E., Corsi, B., Tamborini, E., Spada, S., Albertini, A., & Arosio, P. (1994). The role of the L-chain in ferritin iron incorporation. Studies of homo and heteropolymers. *J.Mol.Biol.* **238**, 649-654.

Levy, J. E., Jin, O., Fujiwara, Y., Kuo, F., & Andrews, N. C. (1999). Transferrin receptor is necessary for development of erythrocytes and the nervous system. *Nat.Genet.* **21**, 396-399.

Levy, J. E., Montross, L. K., & Andrews, N. C. (2000). Genes that modify the hemochromatosis phenotype in mice. *J.Clin.Invest* **105**, 1209-1216.

Lewis, R. M., Doherty, C. B., James, L. A., Burton, G. J., & Hales, C. N. (2001). Effects of maternal iron restriction on placental vascularization in the rat. *Placenta* **22**, 534-539.

Lieberman, E., Ryan, K. J., Monson, R. R., & Schoenbaum, S. C. (1988). Association of maternal hematocrit with premature labor. *Am.J.Obstet.Gynecol.* **159**, 107-114.

Liochev, S. I. & Fridovich, I. (1997). How does superoxide dismutase protect against tumor necrosis factor: a hypothesis informed by effect of superoxide on "free" iron. *Free Radic.Biol.Med.* **23**, 668-671.

Lioumi, M., Ferguson, C. A., Sharpe, P. T., Freeman, T., Marenholz, I., Mischke, D., Heizmann, C., & Ragoussis, J. (1999). Isolation and characterization of human and mouse ZIRTL, a member of the IRT1 family of transporters, mapping within the epidermal differentiation complex. *Genomics* **62**, 272-280.

Lis, A., Barone, T. A., Paradkar, P. N., Plunkett, R. J., & Roth, J. A. (2004). Expression and localisation of different forms of DMT1 in normal and tumor astroglial cells. *Brain Res.Mol.Brain Res.* **122**, 62-70.

Liu, X. B., Hill, P., & Haile, D. J. (2002). Role of the ferroportin iron-responsive element in iron and nitric oxide dependent gene regulation. *Blood Cells Mol.Dis.* **29**, 315-326.

Loh, T. T., Higuchi, D. A., van Bockxmeer, F. M., Smith, C. H., & Brown, E. B. (1980). Transferrin receptors on the human placental microvillous membrane. *J.Clin.Invest.* **65**, 1182-1191.

Loh, T. T. & Kaldor, I. (1971). Intestinal iron absorption in suckling rats. *Biol.Neonate* **17**, 173-186.

Lok, C. N. & Ponka, P. (1999). Identification of a hypoxia response element in the transferrin receptor gene. *J.Biol.Chem.* **274**, 24147-24152.

Loreal, O., Gosriwatana, I., Guyader, D., Porter, J., Brissot, P., & Hider, R. C. (2000). Determination of non-transferrin-bound iron in genetic hemochromatosis using a new HPLC-based method. *J.Hepatol.* **32**, 727-733.

Lou, D. Q., Nicolas, G., Lesbordes, J. C., Viatte, L., Grimber, G., Szajnert, M. F., Kahn, A., & Vaulont, S. (2003). Functional differences between hepcidin-1 and -2 in transgenic mice. *Blood* **103**, 2816-2821.

Louache, F., Testa, U., Pelicci, P., Thomopoulos, P., Titeux, M., & Rochant, H. (1984). Regulation of transferrin receptors in human hematopoietic cell lines. *J.Biol.Chem.* **259**, 11576-11582.

Lu, Z. M., Goldenberg, R. L., Cliver, S. P., Cutter, G., & Blankson, M. (1991). The relationship between maternal hematocrit and pregnancy outcome. *Obstet.Gynecol.* **77**, 190-194.

Lund, E. K., Fairweather-Tait, S. J., Wharf, S. G., & Johnson, I. T. (2001). Chronic exposure to high levels of dietary iron fortification increases lipid peroxidation in the mucosa of the rat large intestine. *J.Nutr.* **131**, 2928-2931.

Lymboussaki, A., Pignatti, E., Montosi, G., Garuti, C., Haile, D. J., & Pietrangelo, A. (2003). The role of the iron responsive element in the control of ferroportin1/IREG1/MTP1 gene expression. *J.Hepatol.* **39**, 710-715.

MacDonald, R. A. & Pechet, G. S. (1964). Liver and tissue iron, comparative studies and significance for hemochromatosis. *Arch.Pathol.* **77**, 348-353.

Makrides, M., Crowther, C. A., Gibson, R. A., Gibson, R. S., & Skeaff, C. M. (2003). Efficacy and tolerability of low-dose iron supplements during pregnancy: a randomised controlled trial. *Am.J.Clin.Nutr.* **78**, 145-153.

Manavalan, P., Swope, D. L., & Withy, R. M. (1992). Sequence and structural relationships in the cytokine family. *J.Protein Chem.* **11**, 321-331.

Mann, S., Bannister, J. V., & Williams, R. J. (1986). Structure and composition of ferritin cores isolated from human spleen, limpet (Patella vulgata) hemolymph and bacterial (Pseudomonas aeruginosa) cells. *J.Mol.Biol.* **188**, 225-232.

Martin, M. E., Nicolas, G., Hetet, G., Vaulont, S., Grandchamp, B., & Beaumont, C. (2004). Transferrin receptor 1 mRNA is downregulated in placenta of hepcidin transgenic embryos. *FEBS Lett.* **574**, 187-191.

Martini, L. A., Tchack, L., & Wood, R. J. (2002). Iron treatment downregulates DMT1 and IREG1 mRNA expression in Caco-2 cells. *J.Nutr.* **132**, 693-696.

Mattia, E., Rao, K., Shapiro, D. S., Sussman, H. H., & Klausner, R. D. (1984). Biosynthetic regulation of the human transferrin receptor by desferrioxamine in K562 cells. *J.Biol.Chem.* **259**, 2689-2692.

Mayeux, P., Dusanter-Fourt, I., Muller, O., Mauduit, P., Sabbah, M., Druker, B., Vainchenker, W., Fischer, S., Lacombe, C., & Gisselbrecht, S. (1993). Erythropoietin induces the association of phosphatidylinositol 3'-kinase with a tyrosine-phosphorylated protein complex containing the erythropoietin receptor. *Eur.J.Biochem.* **216**, 821-828.

Mazur, A., Feillet-Coudray, C., Romier, B., Bayle, D., Gueux, E., Ruivard, M., Coudray, C., & Rayssiguier, Y. (2003). Dietary iron regulates hepatic hepcidin 1 and 2 mRNAs in mice. *Metabolism* **52**, 1229-1231.

McArdle, H. J., Douglas, A. J., Bowen, B. J., & Morgan, E. H. (1985). The mechanism of iron uptake by the rat placenta. *J.Cell Physiol* **124**, 446-450.

McArdle, H. J., Douglas, A. J., & Morgan, E. H. (1984). Transferrin binding by microvillar vesicles isolated from rat placenta. *Placenta* **5**, 131-138.

McArdle, H. J. & Morgan, E. H. (1982b). Transferrin and iron movements in the rat conceptus during gestation. *J.Reprod.Fertil.* **66**, 529-536.

McArdle, H. J. & Morgan, E. H. (1984). The effect of monoclonal antibodies to the human transferrin receptor on transferrin and iron uptake by rat and rabbit reticulocytes. *J.Biol.Chem.* **259**, 1398-1400.

McKie, A. T. & Barlow, D. J. (2004). The SLC40 basolateral iron transporter family (IREG1/ferroportin/MTP1). *Pflugers Arch.* *447, 801-806.*

McKie, A. T., Barrow, D., Latunde-Dada, G. O., Rolfs, A., Sager, G., Mudaly, E., Mudaly, M., Richardson, C., Barlow, D., Bomford, A., Peters, T. J., Raja, K. B., Shirali, S., Hediger, M. A., Farzaneh, F., & Simpson, R. J. (2001). An iron-regulated ferric reductase associated with the absorption of dietary iron. *Science* **291**, 1755-1759.

McKie, A. T., Marciani, P., Rolfs, A., Brennan, K., Wehr, K., Barrow, D., Miret, S., Bomford, A., Peters, T. J., Farzaneh, F., Hediger, M. A., Hentze, M. W., & Simpson, R. J. (2000). A novel duodenal iron-regulated transporter, IREG1, implicated in the basolateral transfer of iron to the circulation. *Mol.Cell* **5**, 299-309.

McKnight, G. S., Lee, D. C., Hemmaplardh, D., Finch, C. A., & Palmiter, R. D. (1980b). Transferrin gene expression. Effects of nutritional iron deficiency. *J.Biol.Chem.* **255**, 144-147.

McKnight, G. S., Lee, D. C., & Palmiter, R. D. (1980a). Transferrin gene expression. Regulation of mRNA transcription in chick liver by steroid hormones and iron deficiency. *J.Biol.Chem.* **255**, 148-153.

McLaren, G. D., Nathanson, M. H., Jacobs, A., Trevett, D., & Thomson, W. (1991). Regulation of intestinal iron absorption and mucosal iron kinetics in hereditary hemochromatosis. *J.Lab Clin.Med.* **117**, 390-401.

Mellor, A. L. & Munn, D. H. (2000). Immunology at the maternal-fetal interface: lessons for T cell tolerance and suppression. *Annu.Rev.Immunol.* **18**, 367-391.

Mendel, G. A. (1961). Studies on iron absorption. I. The relationships between the rate of erythropoiesis, hypoxia and iron absorption. *Blood* **18**, 727-736.

Messier, B. & Leblond, C. P. (1960). Cell proliferation and migration as revealed by radioautography after injection of thymidine-H3 into male rats and mice. *Am.J.Anat.* **106**, 247-285.

Millard, K. N., Frazer, D. M., Wilkins, S. J., & Anderson, G. J. (2004). Changes in the expression of intestinal iron transport and hepatic regulatory molecules explain the enhanced iron absorption associated with pregnancy in the rat. *Gut* **53**, 655-660.

Mills, C. F. & Davies, N. T. (1979). Perinatal changes in the absorption of trace elements. *Ciba Found.Symp.* 247-266.

Miskimins, W. K., McClelland, A., Roberts, M. P., & Ruddle, F. H. (1986). Cell proliferation and expression of the transferrin receptor gene: promoter sequence homologies and protein interactions. *J.Cell Biol.* **103**, 1781-1788.

Moll, W. (2003). Structure adaptation and blood flow control in the uterine arterial system after hemochorial placentation. *Eur.J.Obstet.Gynecol.Reprod.Biol.* **110**, S19-S27.

Montosi, G., Donovan, A., Totaro, A., Garuti, C., Pignatti, E., Cassanelli, S., Trenor, C. C., Gasparini, P., Andrews, N. C., & Pietrangelo, A. (2001). Autosomal-dominant hemochromatosis is associated with a mutation in the ferroportin (SLC11A3) gene. *J.Clin.Invest.* **108**, 619-623.

Morck, T. A., Lynch, S. R., & Cook, J. D. (1983). Inhibition of food iron absorption by coffee. *Am.J.Clin.Nutr.* **37**, 416-420.

Morgan, E. H. & Oates, P. S. (2002). Mechanisms and regulation of intestinal iron absorption. *Blood Cells Mol.Dis.* **29**, 384-399.

Morita, H., Ikeda, S., Yamamoto, K., Morita, S., Yoshida, K., Nomoto, S., Kato, M., & Yanagisawa, N. (1995). Hereditary ceruloplasmin deficiency with hemosiderosis: a clinicopathological study of a Japanese family. *Ann.Neurol.* **37**, 646-656.

Moroz, C., Traub, L., Maymon, R., & Zahalka, M. A. (2002). PLIF, a novel human ferritin subunit from placenta with immunosuppressive activity. *J Biol.Chem.* **277**, 12901-12905.

Muckenthaler, M., Gray, N. K., & Hentze, M. W. (1998). IRP-1 binding to ferritin mRNA prevents the recruitment of the small ribosomal subunit by the cap-binding complex eIF4F. *Mol.Cell* **2**, 383-388.

Muir, A. & Hopfer, U. (1985). Regional specificity of iron uptake by small intestinal brush-border membranes from normal and iron-deficient mice. *Am.J.Physiol* **248**, G376-G379.

Mukhopadhyay, C. K., Mazumder, B., & Fox, P. L. (2000). Role of hypoxia-inducible factor-1 in transcriptional activation of ceruloplasmin by iron deficiency. *J.Biol.Chem.* **275**, 21048-21054.

Nahum, R., Brenner, O., Zahalka, M. A., Traub, L., Quintana, F., & Moroz, C. (2004). Blocking of the placental immune-modulatory ferritin activates Th1 type cytokines and affects placenta development, fetal growth and the pregnancy outcome. *Hum.Reprod.* **19**, 715-722.

Napier, J. A., Dunn, C. D., Ford, T. W., & Price, V. (1977). Pathophysiological changes in serum erythropoiesis stimulating activity. *Br.J.Haematol.* **35**, 403-409.

Nelson, R. L., Davis, F. G., Persky, V., & Becker, E. (1995). Risk of neoplastic and other diseases among people with heterozygosity for hereditary hemochromatosis. *Cancer* **76**, 875-879.

Nemeth, E., Tuttle, M. S., Powelson, J., Vaughn, M. B., Donovan, A., Ward, D. M., Ganz, T., & Kaplan, J. (2004). Hepcidin regulates cellular iron efflux by binding to ferroportin and inducing its internalisation. *Science* **306**, 2090-2093.

Nemeth, E., Valore, E. V., Territo, M., Schiller, G., Lichtenstein, A., & Ganz, T. (2003). Hepcidin, a putative mediator of anemia of inflammation, is a type II acute-phase protein. *Blood* **101**, 2461-2463.

Nicolas, G., Bennoun, M., Devaux, I., Beaumont, C., Grandchamp, B., Kahn, A., & Vaulont, S. (2001). Lack of hepcidin gene expression and severe tissue iron overload in upstream stimulatory factor 2 (USF2) knockout mice. *Proc.Natl.Acad.Sci.U.S.A* **98**, 8780-8785.

Nicolas, G., Bennoun, M., Porteu, A., Mativet, S., Beaumont, C., Grandchamp, B., Sirito, M., Sawadogo, M., Kahn, A., & Vaulont, S. (2002c). Severe iron deficiency anemia in transgenic mice expressing liver hepcidin. *Proc.Natl.Acad.Sci.U.S.A* **99**, 4596-4601.

Nicolas, G., Chauvet, C., Viatte, L., Danan, J. L., Bigard, X., Devaux, I., Beaumont, C., Kahn, A., & Vaulont, S. (2002b). The gene encoding the iron regulatory peptide hepcidin is regulated by anemia, hypoxia, and inflammation. *J.Clin.Invest.* **110**, 1037-1044.

Nicolas, G., Viatte, L., Bennoun, M., Beaumont, C., Kahn, A., & Vaulont, S. (2002a). Hepcidin, a new iron regulatory peptide. *Blood Cells Mol.Dis.* **29**, 327-335.

Njajou, O. T., de Jong, G., Berghuis, B., Vaessen, N., Snijders, P. J., Goossens, J. P., Wilson, J. H., Breuning, M. H., Oostra, B. A., Heutink, P., Sandkuijl, L. A., & van Duijn, C. M. (2002). Dominant hemochromatosis due to N144H mutation of SLC11A3: clinical and biological characteristics. *Blood Cells Mol.Dis.* **29**, 439-443.

Njajou, O. T., Vaessen, N., Joosse, M., Berghuis, B., van Dongen, J. W., Breuning, M. H., Snijders, P. J., Rutten, W. P., Sandkuijl, L. A., Oostra, B. A., van Duijn, C. M., & Heutink, P. (2001). A mutation in SLC11A3 is associated with autosomal dominant hemochromatosis. *Nat.Genet.* **28**, 213-214.

O'Brien, K. O., Zavaleta, N., Caulfield, L. E., Wen, J., & Abrams, S. A. (2000). Prenatal iron supplements impair zinc absorption in pregnant Peruvian women. *J.Nutr.* **130**, 2251-2255.

O'Connor, D. L., Picciano, M. F., & Sherman, A. R. (1988). Impact of maternal iron deficiency on quality and quantity of milk ingested by neonatal rats. *Br.J Nutr* **60**, 477-485.

O'Riordan, D. K., Debnam, E. S., Sharp, P. A., Simpson, R. J., Taylor, E. M., & Srai, S. K. (1997). Mechanisms involved in increased iron uptake across rat duodenal brush-border membrane during hypoxia. *J Physiol* **500**, 379-384.

Oates, P. S., Trinder, D., & Morgan, E. H. (2000). Gastrointestinal function, divalent metal transporter-1 expression and intestinal iron absorption. *Pflugers Arch.* **440**, 496-502.

Okuyama, T., Tawada, T., Furuya, H., & Villee, C. A. (1985). The role of transferrin and ferritin in the fetal-maternal-placental unit. *Am.J.Obstet.Gynecol.* **152**, 344-350.

Olynyk, J. K., Cullen, D. J., Aquilia, S., Rossi, E., Summerville, L., & Powell, L. W. (1999). A population-based study of the clinical expression of the hemochromatosis gene. *N.Engl.J.Med.* **341**, 718-724.

Osaki, S. & Johnson, D. A. (1969). Mobilisation of liver iron by ferroxidase (ceruloplasmin). *J Biol.Chem.* **244**, 5757-5758.

Park, C. H., Valore, E. V., Waring, A. J., & Ganz, T. (2001). Hepcidin, a urinary antimicrobial peptide synthesised in the liver. *J.Biol.Chem.* **276**, 7806-7810.

Parkkila, S., Waheed, A., Britton, R. S., Bacon, B. R., Zhou, X. Y., Tomatsu, S., Fleming, R. E., & Sly, W. S. (1997b). Association of the transferrin receptor in human placenta with HFE, the protein defective in hereditary hemochromatosis. *Proc.Natl.Acad.Sci.U.S.A* **94**, 13198-13202.

Parkkila, S., Waheed, A., Britton, R. S., Feder, J. N., Tsuchihashi, Z., Schatzman, R. C., Bacon, B. R., & Sly, W. S. (1997a). Immunohistochemistry of HLA-H, the protein defective in patients with hereditary hemochromatosis, reveals unique pattern of expression in gastrointestinal tract. *Proc.Natl.Acad.Sci.U.S.A* **94**, 2534-2539.

Parmley, R. T., Barton, J. C., Conrad, M. E., Austin, R. L., & Holland, R. M. (1981). Ultrastructural cytochemistry and radioautography of haemoglobin--iron absorption. *Exp.Mol.Pathol.* **34**, 131-144.

Pattillo, R. A. & Gey, G. O. (1968). The establishment of a cell line of human hormone-synthesizing trophoblastic cells in vitro. *Cancer Res.* **28**, 1231-1236.

Pharr, P. N., Hankins, D., Hofbauer, A., Lodish, H. F., & Longmore, G. D. (1993). Expression of a constitutively active erythropoietin receptor in primary hematopoietic progenitors abrogates

erythropoietin dependence and enhances erythroid colony-forming unit, erythroid burst-forming unit, and granulocyte/macrophage progenitor growth. *Proc.Natl.Acad.Sci.U.S.A* **90**, 938-942.

Philpott, C. C. (2002). Molecular aspects of iron absorption: Insights into the role of HFE in hemochromatosis. *Hepatology* **35**, 993-1001.

Philpott, C. C., Klausner, R. D., & Rouault, T. A. (1994). The bifunctional iron-responsive element binding protein/cytosolic aconitase: the role of active-site residues in ligand binding and regulation. *Proc.Natl.Acad.Sci.U.S.A* **91**, 7321-7325.

Pietrangelo, A. (2004). The ferroportin disease. *Blood Cells Mol.Dis.* **32**, 131-138.

Pigeon, C., Ilyin, G., Courselaud, B., Leroyer, P., Turlin, B., Brissot, P., & Loreal, O. (2001). A new mouse liver-specific gene, encoding a protein homologous to human antimicrobial peptide hepcidin, is overexpressed during iron overload. *J.Biol.Chem.* **276**, 7811-7819.

Potten, C. S. & Allen, T. D. (1977). Ultrastructure of cell loss in intestinal mucosa. *J.Ultrastruct.Res.* **60**, 272-277.

Potten, C. S. & Loeffler, M. (1990). Stem cells: attributes, cycles, spirals, pitfalls and uncertainties. Lessons for and from the crypt. *Development* **110**, 1001-1020.

Pountney, D. J., Raja, K. B., Simpson, R. J., & Wrigglesworth, J. M. (1999). The ferric-reducing activity of duodenal brush-border membrane vesicles is associated with a b-type haem. *Biometals* **12**, 53-62.

Qian, Y., Tiffany-Castiglioni, E., & Harris, E. D. (1996). Functional analysis of a genetic defect of copper transport (Menkes disease) in different cell lines. *Am.J.Physiol* **271**, C378-C384.

Raffin, S. B., Woo, C. H., Roost, K. T., Price, D. C., & Schmid, R. (1974). Intestinal absorption of hemoglobin iron-heme cleavage by mucosal heme oxygenase. *J.Clin.Invest* **54**, 1344-1352.

Raghupathy, R. (1997). Th1-type immunity is incompatible with successful pregnancy. *Immunol.Today* **18**, 478-482.

Raja, K. B., Bjarnason, I., Simpson, R. J., & Peters, T. J. (1987). In vitro measurement and adaptive response of Fe3+ uptake by mouse intestine. *Cell Biochem.Funct.* **5**, 69-76.

Raja, K. B., Simpson, R. J., & Peters, T. J. (1989). Membrane potential dependence of Fe(III) uptake by mouse duodenum. *Biochim.Biophys.Acta* **984**, 262-266.

Raja, K. B., Simpson, R. J., & Peters, T. J. (1992). Investigation of a role for reduction in ferric iron uptake by mouse duodenum. *Biochim.Biophys.Acta* **1135**, 141-146.

Rodriguez-Matas, M. C., Campos, M. S., Lopez-Aliaga, I., Gomez-Ayala, A. E., & Lisbona, F. (1998). Iron-manganese interactions in the evolution of iron deficiency. *Ann.Nutr.Metab.* **42**, 96-109.

Roetto, A., Alberti, F., Daraio, F., Cali, A., Cazzola, M., Totaro, A., Gasparini, P., & Camaschella, C. (2000). Exclusion of ZIRTL as candidate gene of juvenile hemochromatosis and refinement of the critical interval on 1q21. *Blood Cells Mol.Dis.* **26**, 205-210.

Roetto, A., Papanikolaou, G., Politou, M., Alberti, F., Girelli, D., Christakis, J., Loukopoulos, D., & Camaschella, C. (2003). Mutant antimicrobial peptide hepcidin is associated with severe juvenile hemochromatosis. *Nat.Genet.* **33**, 21-22.

Roetto, A., Totaro, A., Piperno, A., Piga, A., Longo, F., Garozzo, G., Cali, A., De Gobbi, M., Gasparini, P., & Camaschella, C. (2001). New mutations inactivating transferrin receptor 2 in hemochromatosis type 3. *Blood* **97**, 2555-2560.

Rolfs, A., Bonkovsky, H. L., Kohlroser, J. G., McNeal, K., Sharma, A., Berger, U. V., & Hediger, M. A. (2002). Intestinal expression of genes involved in iron absorption in humans. *Am.J.Physiol.Gastrointest.Liver Physiol.* **282**, G598-G607.

Rossant, J. & Cross, J. C. (2001). Placental development: lessons from mouse mutants. *Nat.Rev.Genet.* **2**, 538-548.

Roth, J. A., Horbinski, C., Feng, L., Dolan, K. G., Higgins, D., & Garrick, M. D. (2000). Differential localisation of divalent metal transporter 1 with and without iron response element in rat PC12 and sympathetic neuronal cells. *J.Neurosci.* **20**, 7595-7601.

Rouault, T. A., Haile, D. J., Downey, W. E., Philpott, C. C., Tang, C., Samaniego, F., Chin, J., Paul, I., Orloff, D., Harford, J. B., & . (1992). An iron-sulfur cluster plays a novel regulatory role in the iron-responsive element binding protein. *Biometals* **5**, 131-140.

Rouault, T. A., Stout, C. D., Kaptain, S., Harford, J. B., & Klausner, R. D. (1991). Structural relationship between an iron-regulated RNA-binding protein (IRE-BP) and aconitase: functional implications. *Cell* **64**, 881-883.

Rush, D. (2000). Nutrition and maternal mortality in the developing world. *Am.J.Clin.Nutr.* **72**, 212S-240S.

Sahlstedt, L., von Bonsdorff, L., Ebeling, F., Ruutu, T., & Parkkinen, J. (2002). Effective binding of free iron by a single intravenous dose of human apotransferrin in haematological stem cell transplant patients. *Br.J.Haematol.* **119**, 547-553.

Sakakibara, S. & Aoyama, Y. (2002). Dietary iron-deficiency up-regulates hephaestin mRNA level in small intestine of rats. *Life Sci.* **70**, 3123-3129.

Salonen, J. T., Nyyssonen, K., Korpela, H., Tuomilehto, J., Seppanen, R., & Salonen, R. (1992). High stored iron levels are associated with excess risk of myocardial infarction in eastern Finnish men. *Circulation* **86**, 803-811.

Samaniego, F., Chin, J., Iwai, K., Rouault, T. A., & Klausner, R. D. (1994). Molecular characterization of a second iron-responsive element binding protein, iron regulatory protein 2. Structure, function, and post-translational regulation. *J.Biol.Chem.* **269**, 30904-30910.

Sandstrom, B. (2001). Micronutrient interactions: effects on absorption and bioavailability. *Br.J.Nutr.* **85 Suppl 2**, S181-S185.

Santos, M., Schilham, M. W., Rademakers, L. H., Marx, J. J., de Sousa, M., & Clevers, H. (1996). Defective iron homeostasis in beta 2-microglobulin knockout mice recapitulates hereditary hemochromatosis in man. *J Exp.Med.* **184**, 1975-1985.

Sayers, M. H., Lynch, S. R., Jacobs, P., Charlton, R. W., Bothwell, T. H., Walker, R. B., & Mayet, F. (1973). The effects of ascorbic acid supplementation on the absorption of iron in maize, wheat and soya. *Br.J.Haematol.* **24**, 209-218.

Schalinske, K. L., Anderson, S. A., Tuazon, P. T., Chen, O. S., Kennedy, M. C., & Eisenstein, R. S. (1997). The iron-sulfur cluster of iron regulatory protein 1 modulates the accessibility of RNA binding and phosphorylation sites. *Biochemistry* **36**, 3950-3958.

Schneider, B. D. & Leibold, E. A. (2003). Effects of iron regulatory protein regulation on iron homeostasis during hypoxia. *Blood* **102**, 3404-3411.

Schrezenmeier, H., Noe, G., Raghavachar, A., Rich, I. N., Heimpel, H., & Kubanek, B. (1994). Serum erythropoietin and serum transferrin receptor levels in aplastic anaemia. *Br.J.Haematol.* **88**, 286-294.

Shike, H., Lauth, X., Westerman, M. E., Ostland, V. E., Carlberg, J. M., Van Olst, J. C., Shimizu, C., Bulet, P., & Burns, J. C. (2002). Bass hepcidin is a novel antimicrobial peptide induced by bacterial challenge. *Eur.J.Biochem.* **269**, 2232-2237.

Simmer, K. & Thompson, R. P. (1985). Zinc in the fetus and newborn. *Acta Paediatr.Scand.Suppl* **319**, 158-163.

Simpson, R. J., Debnam, E., Beaumont, N., Bahram, S., Schumann, K., & Srai, S. K. (2003a). Duodenal mucosal reductase in wild-type and Hfe knockout mice on iron adequate, iron deficient, and iron rich feeding. *Gut* **52**, 510-513.

Simpson, R. J., Debnam, E. S., Laftah, A. H., Solanky, N., Beaumont, N., Bahram, S., Schumann, K., & Srai, S. K. (2003b). Duodenal nonheme iron content correlates with iron stores in mice, but the relationship is altered by Hfe gene knock-out. *Blood* **101**, 3316-3318.

Singer-Sam, J., Robinson, M. O., Bellve, A. R., Simon, M. I., & Riggs, A. D. (1990). Measurement by quantitative PCR of changes in HPRT, PGK-1, PGK-2, APRT, MTase, and Zfy gene transcripts during mouse spermatogenesis. *Nucleic Acids Res.* **18**, 1255-1259.

Smith, C., Mitchinson, M. J., Aruoma, O. I., & Halliwell, B. (1992). Stimulation of lipid peroxidation and hydroxyl-radical generation by the contents of human atherosclerotic lesions. *Biochem.J.* **286 (Pt 3)**, 901-905.

Smith, M. W., Debnam, E. S., Dashwood, M. R., & Srai, S. K. (2000). Structural and cellular adaptation of duodenal iron uptake in rats maintained on an iron-deficient diet. *Pflugers Arch.* **439**, 449-454.

Sood, S. K., Ramachandran, K., Mathur, M., Gupta, K., Ramalingaswamy, V., Swarnabai, C., Ponniah, J., Mathan, V. I., & Baker, S. J. (1975). W.H.O. sponsored collaborative studies on nutritional anaemia in India. 1. The effects of supplemental oral iron administration to pregnant women. *QJM* **44**, 241-258.

Southon, S., Wright, A. J., & Fairweather-Tait, S. J. (1989). The effect of differences in dietary iron intake on 59Fe absorption and duodenal morphology in pregnant rats. *Br.J Nutr* **62**, 707-717.

Speeg, K. V., Jr., Azizkhan, J. C., & Stromberg, K. (1976). The stimulation by methotrexate of human chorionic gonadotropin and placental alkaline phosphatase in cultured choriocarcinoma cells. *Cancer Res.* **36**, 4570-4576.

Srai, S. K., Debnam, E. S., Boss, M., & Epstein, O. (1988). Age-related changes in the kinetics of iron absorption across the guinea pig proximal intestine in vivo. *Biol.Neonate* **53**, 53-59.

Srivastava, M., Duong, L. T., & Fleming, P. J. (1984). Cytochrome b561 catalyzes transmembrane electron transfer. *J.Biol.Chem.* **259**, 8072-8075.

Starreveld, J. S., Kroos, M. J., Van Suijlen, J. D., Verrijt, C. E., van Eijk, H. G., & van Dijk, J. P. (1995). Ferritin in cultured human cytotrophoblasts: synthesis and subunit distribution. *Placenta* **16**, 383-395.

Starreveld, J. S., van Denderen, J., Kroos, M. J., van Eijk, H. G., & van Dijk, J. P. (1996). Effects of iron supplementation on iron uptake by differentiating cytotrophoblasts. *Reprod.Fertil.Dev.* **8**, 417-422.

Starreveld, J. S., van Dijk, H. P., Kroos, M. J., & van Eijk, H. G. (1993). Regulation of transferrin receptor expression and distribution in in vitro cultured human cytotrophoblasts. *Clin.Chim.Acta* **220**, 47-60.

Stevens M.A. & D'Agostino R.B. (2005). *Goodness of Fit Techniques.* Marcel Dekker, New York.

Streu, A., Jeschke, U., Richter, D. U., Muller, H., Briese, V., & Friese, K. (2000). Human amniotic fluid transferrin stimulates progesterone production by human trophoblast cells in vitro. *Zentralbl.Gynakol.* **122**, 407-412.

Su, M. A., Trenor, C. C., Fleming, J. C., Fleming, M. D., & Andrews, N. C. (1998). The G185R mutation disrupts function of the iron transporter Nramp2. *Blood* **92**, 2157-2163.

Svanberg, B., Arvidsson, B., Bjorn-Rasmussen, E., Hallberg, L., Rossander, L., & Swolin, B. (1975). Dietary iron absorption in pregna. *Acta Obstet.Gynecol.Scand.Suppl* 43-68.

Syed, B. A., Beaumont, N. J., Patel, A., Naylor, C. E., Bayele, H. K., Joannou, C. L., Rowe, P. S., Evans, R. W., & Srai, S. K. (2002). Analysis of the human hephaestin gene and protein: comparative modelling of the N-terminus ecto-domain based upon ceruloplasmin. *Protein Eng.* **15**, 205-214.

Szabo, A., Perou, C. M., Karaca, M., Perreard, L., Quackenbush, J. F., & Bernard, P. S. (2004). Statistical modeling for selecting housekeeper genes. *Genome Biol.* **5**, R59.

Tabuchi, M., Tanaka, N., Nishida-Kitayama, J., Ohno, H., & Kishi, F. (2002). Alternative splicing regulates the subcellular localisation of divalent metal transporter 1 isoforms. *Mol.Biol.Cell* **13**, 4371-4387.

Tabuchi, M., Yoshida, T., Takegawa, K., & Kishi, F. (1999). Functional analysis of the human NRAMP family expressed in fission yeast. *Biochem.J.* **344**, 211-219.

Tabuchi, M., Yoshimori, T., Yamaguchi, K., Yoshida, T., & Kishi, F. (2000). Human NRAMP2/DMT1, which mediates iron transport across endosomal membranes, is localised to late endosomes and lysosomes in HEp-2 cells. *J.Biol.Chem.* **275**, 22220-22228.

Tacchini, L., Bianchi, L., Bernelli-Zazzera, A., & Cairo, G. (1999). Transferrin receptor induction by hypoxia. HIF-1-mediated transcriptional activation and cell-specific post-transcriptional regulation. *J.Biol.Chem.* **274**, 24142-24146.

Takahashi, K. & Tavassoli, M. (1983). Internalisation of iron-transferrin complex by murine L1210 leukemia cells and rat reticulocytes demonstrated by a minibead probe. *J.Ultrastruct.Res.* **82**, 314-321.

Takeichi, N., Umemura, T., Nishimura, J., Motomura, S., Kozuru, M., & Ibayashi, H. (1988). Regulation of erythropoietin and burst-promoting activity production in patients with aplastic anemia and iron deficiency anemia. *Acta Haematol.* **80**, 145-152.

Tandy, S., Williams, M., Leggett, A., Lopez-Jimenez, M., Dedes, M., Ramesh, B., Srai, S. K., & Sharp, P. (2000). Nramp2 expression is associated with pH-dependent iron uptake across the apical membrane of human intestinal Caco-2 cells. *J.Biol.Chem.* **275**, 1023-1029.

Taylor, D. J. & Lind, T. (1976). Haematological changes during normal pregnancy: iron induced macrocytosis. *Br.J.Obstet.Gynaecol.* **83**, 760-767.

Theil, E. C. (1987). Ferritin: structure, gene regulation, and cellular function in animals, plants, and microorganisms. *Annu.Rev.Biochem.* **56**, 289-315.

Touret, N., Furuya, W., Forbes, J., Gros, P., & Grinstein, S. (2003). Dynamic traffic through the recycling compartment couples the metal transporter Nramp2 (DMT1) with the transferrin receptor. *J.Biol.Chem.* **278**, 25548-25557.

Touret, N., Martin-Orozco, N., Paroutis, P., Furuya, W., Lam-Yuk-Tseung, S., Forbes, J., Gros, P., & Grinstein, S. (2004). Molecular and cellular mechanisms underlying iron transport deficiency in microcytic anemia. *Blood* **104**, 1526-1533.

Trenor, C. C., III, Campagna, D. R., Sellers, V. M., Andrews, N. C., & Fleming, M. D. (2000). The molecular defect in hypotransferrinemic mice. *Blood* **96**, 1113-1118.

Tribukait, B. (1963). The influence of chronic hypoxia corresponding to 1000-8000 m, altitude on erythropoiesis in the rat. *Acta Physiol.Scand.* **57**, 1-25.

Trinder, D., Oates, P. S., Thomas, C., Sadleir, J., & Morgan, E. H. (2000a). Localisation of divalent metal transporter 1 (DMT1) to the microvillus membrane of rat duodenal enterocytes in iron deficiency, but to hepatocytes in iron overload. *Gut* **46**, 270-276.

Trinder, D., Olynyk, J. K., Sly, W. S., & Morgan, E. H. (2002b). Iron uptake from plasma transferrin by the duodenum is impaired in the Hfe knockout mouse. *Proc.Natl.Acad.Sci.U.S.A* **99**, 5622-5626.

Trousseau, A. (1865). Glycosurie, diabete Sucre. *Clin.Med.Hotel Dieu Paris* 663-698.

Tsuji, Y., Miller, L. L., Miller, S. C., Torti, S. V., & Torti, F. M. (1991). Tumor necrosis factor-**alpha** and interleukin 1-alpha regulate transferrin receptor in human diploid fibroblasts. **Relationship** to the induction of ferritin heavy chain. *J.Biol.Chem.* **266**, 7257-7261.

Uppsten, M., Davis, J., Rubin, H., & Uhlin, U. (2004). Crystal structure of the biologically active form of class Ib ribonucleotide reductase small subunit from Mycobacterium tuberculosis. *FEBS Lett.* **569**, 117-122.

van Campen, D. (1972). Effect of histidine and ascorbic acid on the absorption and retention of 59 Fe by iron-depleted rats. *J.Nutr.* **102**, 165-170.

van der Ende, A., du Maine, A., Simmons, C. F., Schwartz, A. L., & Strous, G. J. (1987). Iron metabolism in BeWo chorion carcinoma cells. Transferrin-mediated uptake and release of iron. *J.Biol.Chem.* **262**, 8910-8916.

van der Ende, A., du Maine, A., Schwartz, A. L., & Strous, G. J. (1990). Modulation of transferrin-receptor activity and recycling after induced differentiation of BeWo choriocarcinoma cells. *Biochem.J.* **270**, 451-457.

van Dijk, J. P., van der Zande, F. G., Kroos, M. J., Starreveld, J. S., & van Eijk, H. G. (1993). Number and affinity of transferrin-receptors at the placental microvillous plasma membrane of the guinea pig: influence of gestational age and degree of transferrin glycan chain complexity. *J.Dev.Physiol* **19**, 221-226.

van Weert, A. W., Dunn, K. W., Gueze, H. J., Maxfield, F. R., & Stoorvogel, W. (1995). Transport from late endosomes to lysosomes, but not sorting of integral membrane proteins in endosomes, depends on the vacuolar proton pump. *J.Cell Biol.* **130**, 821-834.

Vanderpuye, O. A., Kelley, L. K., & Smith, C. H. (1986). Transferrin receptors in the basal plasma membrane of the human placental syncytiotrophoblast. *Placenta* **7**, 391-403.

Verrijt, C. E., Kroos, M. J., Huijskes-Heins, M. I., Cleton-Soeteman, M. I., van Run, P. R., van Eijk, H. G., & van Dijk, J. P. (1999). Accumulation and release of iron in polarly and non-polarly cultured trophoblast cells isolated from human term placentas. *Eur.J.Obstet.Gynecol.Reprod.Biol.* **86**, 73-81.

Verrijt, C. E., Kroos, M. J., Huijskes-Heins, M. I., van Eijk, H. G., & van Dijk, J. P. (1998). Non-transferrin iron uptake by trophoblast cells in culture. Significance of a NADH-dependent ferrireductase. *Placenta* **19**, 525-530.

Viteri, F. E. (1998). A new concept in the control of iron deficiency: community-based preventive supplementation of at-risk groups by the weekly intake of iron supplements. *Biomed.Environ.Sci.* **11**, 46-60.

Viteri, F. E., Liu, X., Tolomei, K., & Martin, A. (1995). True absorption and retention of supplemental iron is more efficient when iron is administered every three days rather than daily to iron-normal and iron-deficient rats. *J.Nutr.* **125**, 82-91.

Vulpe, C. D., Kuo, Y. M., Murphy, T. L., Cowley, L., Askwith, C., Libina, N., Gitschier, J., & Anderson, G. J. (1999). Hephaestin, a ceruloplasmin homologue implicated in intestinal iron transport, is defective in the sla mouse. *Nat.Genet.* **21**, 195-199.

Waheed, A., Grubb, J. H., Zhou, X. Y., Tomatsu, S., Fleming, R. E., Costaldi, M. E., Britton, R. S., Bacon, B. R., & Sly, W. S. (2002). Regulation of transferrin-mediated iron uptake by HFE, the protein defective in hereditary hemochromatosis. *Proc.Natl.Acad.Sci.U.S.A* **99**, 3117-3122.

Waheed, A., Parkkila, S., Saarnio, J., Fleming, R. E., Zhou, X. Y., Tomatsu, S., Britton, R. S., Bacon, B. R., & Sly, W. S. (1999). Association of HFE protein with transferrin receptor in crypt enterocytes of human duodenum. *Proc.Natl.Acad.Sci.U.S.A* **96**, 1579-1584.

Waheed, A., Parkkila, S., Zhou, X. Y., Tomatsu, S., Tsuchihashi, Z., Feder, J. N., Schatzman, R. C., Britton, R. S., Bacon, B. R., & Sly, W. S. (1997). Hereditary hemochromatosis: effects of C282Y and H63D mutations on association with beta2-microglobulin, intracellular processing, and cell surface expression of the HFE protein in COS-7 cells. *Proc.Natl.Acad.Sci.U.S.A* **94**, 12384-12389.

Wallace, D. F., Pedersen, P., Dixon, J. L., Stephenson, P., Searle, J. W., Powell, L. W., & Subramaniam, V. N. (2002). Novel mutation in ferroportin1 is associated with autosomal dominant hemochromatosis. *Blood* **100**, 692-694.

Wang, X., Manganaro, F., & Schipper, H. M. (1995). A cellular stress model for the sequestration of redox-active glial iron in the aging and degenerating nervous system. *J.Neurochem.* **64**, 1868-1877.

Wardrop, S. L. & Richardson, D. R. (1999). The effect of intracellular iron concentration and nitrogen monoxide on Nramp2 expression and non-transferrin-bound iron uptake. *Eur.J.Biochem.* **263**, 41-49.

Weinberg, E. D. (1985). Roles of iron in infection and neoplasia. *J.Pharmacol.* **16**, 358-364.

Weinberger, A., Halpern, M., Zahalka, M. A., Quintana, F., Traub, L., & Moroz, C. (2003). Placental immunomodulator ferritin, a novel immunoregulator, suppresses experimental arthritis. *Arthritis Rheum.* **48**, 846-853.

Weiss, G., Kastner, S., Brock, J., Thaler, J., & Grunewald, K. (1997). Modulation of transferrin receptor expression by dexrazoxane (ICRF-187) via activation of iron regulatory protein. *Biochem.Pharmacol.* **53**, 1419-1424.

Wessling-Resnick, M. (2000). Iron transport. *Annu.Rev.Nutr.* **20**, 129-151.

West, A. P., Jr., Bennett, M. J., Sellers, V. M., Andrews, N. C., Enns, C. A., & Bjorkman, P. J. (2000). Comparison of the interactions of transferrin receptor and transferrin receptor 2 with transferrin and the hereditary hemochromatosis protein HFE. *J.Biol.Chem.* **275**, 38135-38138.

Wheby, M. S. & Jones, L. G. (1963). Role of transferrin in iron absorption. *J.Clin.Invest.* **42**, 1007-1016.

Wheby, M. S., Jones, L. G., & Crosby, W. H. (1964). Studies on iron absorption. Intestinal regulatory mechanisms. *J.Clin.Invest.* **43**, 1433-1442.

Whittaker, P. G., Lind, T., & Williams, J. G. (1991). Iron absorption during normal human pregnancy: a study using stable isotopes. *Br.J.Nutr.* **65**, 457-463.

Wice, B., Menton, D., Geuze, H., & Schwartz, A. L. (1990). Modulators of cyclic AMP metabolism induce syncytiotrophoblast formation in vitro. *Exp.Cell Res.* **186**, 306-316.

Wigg, A. J., Harley, H., & Casey, G. (2003). Heterozygous recipient and donor HFE mutations associated with a hereditary haemochromatosis phenotype after liver transplantation. *Gut* **52**, 433-435.

Williams, R. B. & Mills, C. F. (1970). The experimental production of zinc deficiency in the rat. *Br.J.Nutr.* **24**, 989-1003.

Wilms, J. W. & Batey, R. G. (1983). Effect of iron stores on hepatic metabolism of transferrin-bound iron. *Am.J.Physiol.* **244**, G138-G144.

Winfield, M. E. (1965). Electron transfer within and between haemoprotein molecules. *J.Mol.Biol.* **12**, 600-611.

Wong, A. Y., Kulandavelu, S., Whiteley, K. J., Qu, D., Langille, B. L., & Adamson, S. L. (2002). Maternal cardiovascular changes during pregnancy and postpartum in mice. *Am.J.Physiol Heart Circ.Physiol.* **282**, H918-H925.

World Health Organisation. Micronutrient deficiencies: Battling iron deficiency anaemia. 2003.

Wyllie, J. C. & Kaufman, N. (1982). An electron microscopic study of heme uptake by rat duodenum. *Lab. Invest.* **47**, 471-476.

Yamaji, S., Sharp, P., Ramesh, B., & Srai, S. K. (2004). Inhibition of iron transport across human intestinal epithelial cells by hepcidin. *Blood* **104**, 2178-2180.

Yang, F., Liu, X. B., Quinones, M., Melby, P. C., Ghio, A., & Haile, D. J. (2002). Regulation of reticuloendothelial iron transporter MTP1 (Slc11a3) by inflammation. *J.Biol.Chem.* **277**, 39786-39791.

Zahalka, M. A., Barak, V., Traub, L., & Moroz, C. (2003). PLIF induces IL-10 production in monocytes: a calmodulin-p38 mitogen-activated protein kinase-dependent pathway. *FASEB J.* **17**, 955-957.

Zhang, A. S., Xiong, S., Tsukamoto, H., & Enns, C. A. (2004). Localisation of iron metabolism-related mRNAs in rat liver indicate that HFE is expressed predominantly in hepatocytes. *Blood* **103**, 1509-1514.

Zhang, L., Lee, T., Wang, Y., & Soong, T. W. (2000). Heterologous expression, functional characterization and localisation of two isoforms of the monkey iron transporter Nramp2. *Biochem.J.* **349**, 289-297.

Zhao, H. & Eide, D. (1996b). The yeast ZRT1 gene encodes the zinc transporter protein of a high-affinity uptake system induced by zinc limitation. *Proc.Natl.Acad.Sci.U.S.A* **93**, 2454-2458.

Zhao, H. & Eide, D. (1996a). The ZRT2 gene encodes the low affinity zinc transporter in Saccharomyces cerevisiae. *J Biol.Chem.* **271**, 23203-23210.

Zhou, X. Y., Tomatsu, S., Fleming, R. E., Parkkila, S., Waheed, A., Jiang, J., Fei, Y., Brunt, E. M., Ruddy, D. A., Prass, C. E., Schatzman, R. C., O'Neill, R., Britton, R. S., Bacon, B. R., & Sly, W. S. (1998). HFE gene knockout produces mouse model of hereditary hemochromatosis. *Proc.Natl.Acad.Sci.U.S.A* **95**, 2492-2497.

Zoller, H., Koch, R. O., Theurl, I., Obrist, P., Pietrangelo, A., Montosi, G., Haile, D. J., Vogel, W., & Weiss, G. (2001). Expression of the duodenal iron transporters divalent-metal transporter 1 and ferroportin 1 in iron deficiency and iron overload. *Gastroenterology* **120**, 1412-1419.

Zoller, H., Pietrangelo, A., Vogel, W., & Weiss, G. (1999). Duodenal metal-transporter (DMT-1, NRAMP-2) expression in patients with hereditary haemochromatosis. *Lancet* **353**, 2120-2123.

6 Appendices

Appendix I

Appendix I
Gene analysis data (mean ± S.E.M.)

	C57blk/6		$Hfe^{-/-}$		
Duodenum	mean	sem	mean	sem	P
DMT1	1.000	0.219	12.030	1.591	0.000
Tfr1	1.000	0.157	1.574	0.324	0.231
Ireg1	1.000	0.073	1.243	0.035	0.040
Dcytb	1.000	0.119	1.071	0.100	0.693
Hfe	1.000	0.071	2.260	0.279	0.073
Liver					
Hepc-1	1.000	0.369	0.130	0.061	0.034
Hepc-2	1.000	0.159	1.658	0.211	0.055
DMT1	1.000	0.801	0.201	0.079	0.276
Tfr2	1.000	0.573	0.695	0.130	0.204
Ireg1	1.000	0.015	0.879	0.056	0.197

Table A: Comparison of duodenal and hepatic gene expression in $hfe^{-/-}$ and C57blk/6 mice.

C57Blk/6	control		deficient			loaded		
duodenum	mean	sem	mean	Sem	P	mean	sem	P
DMT1	1.000	0.219	7.213	1.240	0.000	1.054	0.304	0.842
Ireg1	1.000	0.073	0.965	0.008	0.660	0.776	0.039	0.108
Dcytb	1.000	0.119	0.853	0.070	0.417	0.897	0.106	0.587
Tfr1	1.000	0.157	1.388	0.100	0.013	0.598	0.099	0.325
Hfe	1.000	0.071	1.432	0.110	0.255	2.494	0.573	0.194

C57Blk/6	control		deficient			loaded		
liver	mean	sem	mean	Sem	P	mean	sem	P
Hepc-1	1.000	0.369	0.018	0.011	0.067	0.905	0.336	0.605
Hepc-2	1.000	0.159	0.559	0.089	0.052	9.613	1.085	0.000
DMT1	1.000	0.801	0.082	0.031	0.489	0.231	0.215	0.374
Ireg1	1.000	0.015	0.938	0.039	0.316	1.039	0.051	
Tfr2	1.000	0.573	0.376	0.047	0.361	0.265	0.094	0.257

Table B: Comparison of duodenal and hepatic gene expression of C57blk/6 mice on control- iron-deficient and iron-loaded diets.

$Hfe^{-/-}$	control			deficient			loaded		
duodenum	mean	sem	P	mean	sem	P	mean	sem	P
DMT1	12.030	1.591	0.000	10.061	1.479	0.229	1.880	0.141	0.000
Ireg1	1.243	0.035	0.040	0.848	0.087	0.014	0.747	0.021	0.000
Dcytb	1.071	0.100	0.693	0.790	0.080	0.145	0.945	0.127	0.521
Tfr1	1.574	0.324	0.231	1.668	0.167	0.321	0.608	0.025	0.017
Hfe	2.260	0.279	0.073	1.796	0.299	0.321	2.513	0.238	0.350

$Hfe^{-/-}$	control			deficient			loaded		
liver	mean	sem	P	mean	sem	P	mean	sem	P
Hepc-1	0.130	0.061	0.034	0.094	0.033	0.651	0.990	0.211	0.000
Hepc-2	1.658	0.211	0.055	1.270	0.353	0.385	1.797	0.393	0.762
DMT1	0.201	0.079	0.276	1.363	0.544	0.040	0.147	0.109	0.686
Ireg1	0.879	0.056	0.197	0.918	0.078	0.739	1.095	0.032	0.065
Tfr2	0.695	0.130	0.204	0.844	0.177	0.503	0.547	0.117	0.411

Table C: Comparison of duodenal and hepatic gene expression of $hfe^{-/-}$ mice on control- iron-deficient and iron-loaded diets.

Appendix II

Appendix II

Gene analysis data (mean ± S.E.M)

Duodenum	*Dcytb*	*P*	*DMT1*	*P*	*Ireg1*	*P*
non-pregnant	1.00 ± 1.21		1.00 ± 0.38		1.00 ± 0.40	
2nd Trimester	1.64 ± 1.32	0.619	1.20 ± 0.24	0.647	1.67 ± 0.48	0.328
2nd Trimester +Fe	0.34 ± 0.20	0.475	1.09 ± 0.99			
Fe + 14 days	0.49 ± 0.06	0.570	3.25 ± 1.02	0.072	1.62 ± 0.43	0.328
3rd Trimester	4.42 ± 0.70	0.055	10.12 ± 2.44	0.006	4.78 ± 2.22	0.213
3rd Trimester +Fe	2.03 ± 0.72	0.359	0.31 ± 0.19	0.042	6.25 ± 2.49	0.058
Fe + 21 days	0.28 ± 0.10	0.428	0.12 ± 0.06	0.021	3.87 ± 1.06	0.045

Liver	*DMT1*	*P*	*Ireg1*	*P*	*Hepcidin*	*P*	*Tfr2*	*P*
non-pregnant	1.00 + 0.25		1.00 + 0.27		1.00 + 0.10		1.00 + 0.57	
2nd Trimester	0.16 + 0.05	0.043	1.20 + 1.03		1.12 + 0.37	0.126	1.18 + 0.73	0.414
2nd Trimester +Fe	0.11 + 0.03	0.013			1.01 + 0.50	0.985	0.27 + 0.13	
Fe + 14 days	1.03 + 0.34	0.945	0.28 + 0.14		1.61 + 0.15	0.027		
3rd Trimester	0.25 + 0.16	0.021	1.92 + 0.12	0.030	0.05 + 0.02	0.017	0.14 + 0.13	0.103
3rd Trimester +Fe	2.39 + 1.82	0.229	2.83 + 1.65	0.394	0.30 + 0.01	0.020	0.29 + 0.13	0.464
Fe + 21 days	0.97 + 0.29	0.948	0.76 + 0.35	0.613	0.63 + 0.18	0.177	1.86 + 0.87	0.153

Placenta	*DMT1*	*P*	Ireg1	*P*	Tfr1	*P*
2nd Trimester	1.00 ± 0.39		1.00 ± 0.46		1.00 ± 0.43	
3rd Trimester	3.01 ± 0.94	0.04	1.52 ± 0.33	0.374	0.64 ± 0.16	0.350
2nd Trimester +Fe	0.39 ± 0.15	0.324			1.35 ± 0.63	
3rd Trimester +Fe	4.40 ± 1.19	0.383	1.92 ± 0.70	0.626	0.71 ± 0.22	0.801

Foetal liver	*DMT1*	*P*	Ireg1	*P*	Hepcidin	*P*
2nd Trimester	1		1		1	
3rd Trimester	0.05 ± 0.02		1.64 ± 0.72		22.32 ± 6.79	
3rd Trimester +Fe	0.84 ± 0.29	0.03	2.66 ± 1.48	0.56	52.24 ± 6.04	0.05

Appendix III

Appendix III

BeWo cell efflux data

Figure 3.6.5 (mean± S.E.M)

Hepcidin in efflux buffer:
0 μM: 4.34 ± 0.24
1 μM: 4.11 ± 0.40 P=0.65
10 μM: 4.32 ± 0.17 P=0.93
100 μM: 4.33 ± 0.57 P=0.98

1 hour hepcidin pre-treatment:
0 μM: 4.24 ± 0.51
1 μM: 4.26 ± 0.28 P=0.97
10 μM: 5.28 ± 0.21 P=0.13
100 μM: 4.45 ± 0.62 P0.56

24 hour hepcidin pre-treatment:
0 μM 5.45 ± 0.70
1 μM: 5.25 ± 0.37 P=0.81
10 μM: 5.15 ± 1.08 P=0.83
100 μM: 5.83 ± 0.73 P=0.72

48 hour hepcidin pre-treatment:
0 μM 5.10 ± 0.74
1 μM: 5.16 ± 0.57 P=0.96
10 μM: 5.52 ± 0.76 P=0.71
100 μM: 6.38 ± 1.39 P=0.46

Figure 3.6.6 (mean ± S.E.M.)

hepcidin in efflux buffer only:
0 μM: 9.51 ± 0.93
1 μM: 9.31 ± 0.13 P=0.84
10 μM: 9.26 ± 0.16 P=0.81
100 μM: 8.14 ± 0.48 P=0.26

1 hour hepcidin pre-treatment:
0 μM: 8.98 ± 0.13
1 μM: 8.84 ± 0.84 P=0.88
10 μM: 11.79 ± 0.87 P=0.03
100 μM: 9.12 ± 1.02 P=0.89

24 hour hepcidin pre-treatment:
0 μM: 9.91 ± 0.44
1 μM: 8.50 ± 0.36 P=0.07
10 μM: 9.45 ± 0.75 P=0.62
100 μM 10.30 ± 0.38 P=0.53

48 hour hepcidin pre-treatment:
0 μM: 8.79 ± 0.18
1 μM: 8.23 ± 0.62 P=0.44
10 μM: 12.57 ± 3.11 P=0.29
100 μM: 8.96 ± 1.35 P=0.91

Appendix IV

Appendix V

Appendix VI

Appendix VII

Mining for iron